UNIVERSITÄT LEIPZIG

REPORT
Institute für Physik
The Physics Institutes

2005

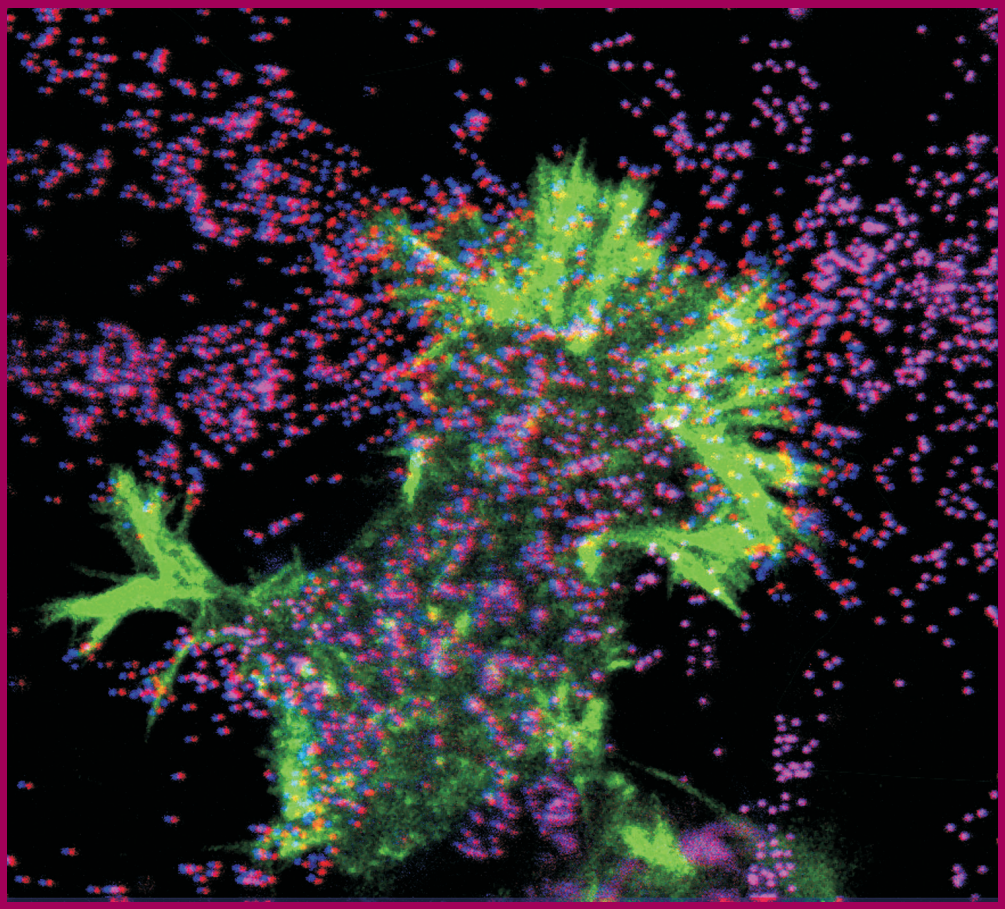

The Physics Institutes of Universität Leipzig, Report 2005
M. Grundmann (Ed.)

ISBN 3-934178-64-2

Technical Editor: Gregor Zimmermann

Printed in Germany by
MERKUR Druck und Kopierzentrum GmbH, Leipzig

online available at
http://www.uni-leipzig.de/~exph2/report_2005.pdf

Front cover
The actin cytoskeleton (*green*) of a moving neuronal cell exerts a force on an elastic polyacrylamide substrate. This force deforms the substrate, which can be detected by measuring the displacement of fluorescent particles (*blue*: relaxed substrate; *red*: deformed substrate). The measured displacement can then be used to determine the force of neuronal growth with pN precision.

Back covers
Recent book publications.

Institut für Experimentelle Physik I
Institut für Experimentelle Physik II
Institut für Theoretische Physik

Fakultät für
Physik und Geowissenschaften

Universität Leipzig

Institute for Experimental Physics I
Institute for Experimental Physics II
Institute for Theoretical Physics

Faculty of Physics and Geosciences

Universität Leipzig

Report 2005

Addresses

Institute for Experimental Physics I

Linnéstraße 5
D-04103 Leipzig, Germany
Phone: +49 341 97-32551
Fax: +49 341 97-32599
WWW: http://www.uni-leipzig.de/~gasse/nysid_a/inst/exp_1.htm

Institute for Experimental Physics II

Linnéstraße 5
D-04103 Leipzig, Germany
Phone: +49 341 97-32650
Fax: +49 341 97-32668
WWW: http://www.uni-leipzig.de/~exph2

Institute for Theoretical Physics

Vor dem Hospitaltore 1
D-04103 Leipzig, Germany
Phone: +49 341 97-32420
Fax: +49 341 97-32548
WWW: http://www.physik.uni-leipzig.de
Mailing address: Augustusplatz 10/11, 04109 Leipzig, Germany

Preface

We welcome you to read about the progress of research at the three Institutes of Physics of Universität Leipzig in our joint report covering 2005.

We have successfully finished our search to fill the vacant position of our retired colleague Dieter Michel. On April 1st 2006 Dr. Jürgen Haase, formerly at IFW, Dresden, took office and will strengthen our activities in solid-state physics, in particular with his studies of oxides with NMR methods also in high pulsed magnetic fields. In 2005, Dr. Petrik Galvosas was employed as assistant professor ('Juniorprofessor') and will strengthen the field of NMR diffusometry. In the Institute of Theoretical Physics (ITP) Rainer Verch, formerly at the Max Planck Institute for Mathematics in the Sciences (Leipzig), has started in October 2005. His focus is on the theory of gravity and quantum field theory. Moreover, Johannes Huebschmann (University of Lille), an expert in differential geometry and topology, holds a DFG–Mercator professor position at ITP from September 2005 until September 2006. Bernd A. Berg (Tallahassee, USA), a specialist in computer oriented quantum field theory, held the Leibniz professor position at ITP from May until August 2005.

The international conference 'Diffusion Fundamentals I', organized by the members of the workgroup 'Physics of Interfaces' was held in Leipzig from September 22nd to 24th, 2005. It was the contribution of Universität Leipzig to the festivities associated with the 'Einsteinjahr'. The conference was dedicated to the fundamental principles of theory, experiments and applications of diffusion to different branches of chemistry, physics and medicine. The response of the scientific community (250 participants for the scientific and the social program) was overwhelmingly positive.

Wolfhard Janke succeeded to manage the German site of the EU RTN-Network 'ENRAGE' *Random Geometry and Random Matrices: From Quantum Gravity to Econophysics* linking to 14 other teams throughout Europe.

The Theodor-Litt Prize 2005 was awarded to our colleague Jörg Kärger in recognition of his distinguished engagement in teaching at Universität Leipzig. Friedrich Kremer was awarded with the Karl-Heinz-Beckurts Prize for his achievements in the field of Broadband Dielectric Spectroscopy and its applications. For excellent contributions to gravity, Daniel Grumiller received the Erich-Schmid Award by the Austrian Academy of Sciences.

A 'HbfG' field-emission electron microscope equipped with a focused ion-beam source (FEM–FIB, FEI Nova 200 NanoLab) has been installed and is up and running since late 2005. It will be used by the DFG Research Groups ('Forscherguppen') 404 ('Oxidic Interfaces') and 522 ('Architecture of nano- and micro-dimensional building blocks'). Also the European Network of Excellence SANDiE will benefit from this versatile tool.

We are very grateful for the ongoing support of the university and many funding agencies. Third party funding is acknowledged in the topical reports and enables, together with the enthusiasm of our researchers and students, our work. Enjoy looking through our report!

Leipzig,
April 2006

M. Grundmann
F. Kremer
G. Rudolph
Directors

Contents

1

Structure and Staff of the Institutes

1.1 Institute for Experimental Physics I

1.1.1 Office of the Director

Prof. Dr. Friedrich Kremer (director)
Prof. Dr. Jörg Kärger (vice director)

1.1.2 Physics of Anisotropic Fluids, Physik anisotroper Fluide

Prof. Dr. Friedrich Kremer

Secretary

Karin Girke

Technical staff

PTA Ines Grünwald
Dipl.-Ing. Jörg Reinmuth
Dipl.-Phys. Wiktor Skokow
Dipl.-Phys. Uwe Weber

Academic staff

Dr. Patrick Kölsch
Dr. Jianjun Li
Dr. Rongbiao Wang

PhD candidates

Dipl.-Phys. Christof Gutsche
Julius Tsuwi Kazungu, M.Sc.
Dipl.-Phys. Kati Kegler

Dipl.-Biochem. Mathias Salomo
Dipl.-Phys. Anatoli Serghei
Michael Tammer, M.Sc.

1.1.3 Physics of Interfaces, Grenzflächenphysik

Prof. Dr. Jörg Kärger

Secretary

Katrin Kunze

Technical staff

Dipl.-Phys. Cordula Bärbel Krause
Dipl.-Ing. Bernd Knorr
Lutz Moschkowitz
Dagmar Prager

Academic staff

PD Dr. Horst Ernst
Prof. Dr. Dieter Freude
Dr. Karen Friedemann
Dr. Petrik Galvosas
PD Dr. Farida Grinberg
Dr. Pavel Kortunov
Dr. Margarita Krutyeva
Prof. (i.R.) Dr. Dr. h.c. Harry Pfeifer
Dr. Andreas Schüring
Dr. habil. Frank Stallmach
PD Dr. Sergey Vasenkov
Dr. Rustem Valiullin

PhD candidates

Dipl.-Phys. Constantijn Blondel
Dipl.-Phys. Andreas Brzank
Dipl.-Phys. Christian Chmelik
Dipl.-Phys. Muslim Dvoyashkin
Dipl.-Phys. Moisés Fernadez
Dipl.-Phys. Johanna Kanellopoulos
Dipl.-Phys. Aleksey Khokhlov
Dipl.-Phys. Sergej Naumov
Dipl.-Phys. Ekaterina Romanova
Dipl.-Phys. Denis Schneider

Dipl.-Geophys. Wiete Schönfelder
Dipl.-Ing. Despina Tzoulaki
Dipl.-Phys. Konstantin Ulrich

Students

Tomas Binder
Lars Heinke
Volker Künzel
Markus Wehring

1.1.4 Soft Matter Physics, Physik der weichen Materie

Prof. Dr. Josef A. Käs

Secretary

Claudia Honisch

Technical staff

Dipl.-Ing. Undine Dietrich
Dipl.-Phys. Bernd Kohlstrunk
Ing. Elke Westphal

Academic staff

Prof. Dr. M. Lösche (on leave of absence)
Prof. Dr. Herbert Schmiedel
Dr. Jochen Guck
Dr. Carsten Selle

PhD candidates

Vanessa Bell
Timo Betz
Claudia Brunner
Susanne Ebert
Allen Ehrlicher
Kristian Franze
Brian Gentry
Jens Gerdelmann
Michael Gögler
Daniel Koch
Bryan Lincoln
Karla Müller

Florian Rückerl
Frank Sauer
Stefan Schinkinger
Thomas Siegemund
David Smith
Björn Stuhrmann
Lydia Woiterski (ab 04/05)
Falk Wottawah

Students

Ann Falk
Cosima Koch
Daryl Lim
Steffen Lindert
Mireille Martin
Daniel Rings
Maren Romeyke
Frank Sauer
Dan Strehle
Stefan Surber
Lydia Woiterski (bis 03/05)
Cornel Wolf

1.2 Institute for Experimental Physics II

1.2.1 Office of the Director

Prof. Dr. Marius Grundmann (director)
Prof. Dr. Tilman Butz (vice director)

1.2.2 Nuclear Solid State Physics, Nukleare Festkörperphysik

Prof. Dr. Tilman Butz

Secretary

Annette Käthner

Technical staff

Dipl.-Ing. Bernd Krause
PTA Raimund Wipper

Academic staff

Dr. Thomas Agne
Dr. Dietmar Lehmann
Dr. Tilo Reinert
Dr. Jürgen Vogt

PhD candidates

Dipl.-Biol. Anja Fiedler
Dipl.-Phys. Frank Heinrich
Dipl.-Phys. Steffen Jankuhn
Dipl.-Phys. Frank Menzel
Dipl.-Phys. Christoph Meinecke
Charlotta Nilsson, M.Sc.
Dipl.-Phys. Daniel Spemann

Students

Philipp Eigmüller
Sven Friedemann
Jan Kohnert
Christian Ostwald
Silvio Petriconi
Martin Rothermel
Stephan Werner

1.2.3 Physics of Dielectric Solids, Physik Dielektrischer Festkörper

Prof. Dr. Dieter Michel / apl. Prof. Dr. Rolf Böttcher

Secretary

Ursula Seibt / Ursula Heinich

Technical staff

Dr. Winfried Böhlmann
Dipl.-Ing. Joachim Hoentsch
Dipl.-Phys. Gert Klotzsche

Academic staff

Dr. habil. Horst Braeter
Dr. André Pampel
apl. Prof. Dr. Andreas Pöppl

PhD candidates

Emre Erdem, M.Sc.
Özlen Ferruh Erdem, M.Sc.
Dipl.-Chem. Anke Matthes
Pavel Sedykh, M.Sc.
Nagarajan Vijayasarathi, M.Sc.

Students

Julia Köhler

External members

Maria Popova, M.Sc.
Dima Yaskov, M.Sc.
(PhD Students from St. Petersburg State University, Russia)

1.2.4 Semiconductor Physics, Halbleiterphysik

Prof. Dr. Marius Grundmann

Secretary

Anja Heck

SANDiE Network Office

Birgit Wendisch

Technical staff

Dipl.-Phys. Gabriele Benndorf
Dipl.-Ing. Giesela Biehne
Dipl.-Ing. Holger Hochmuth
Dipl.-Phys. Jörg Lenzner
Gabriele Ramm
Roswitha Riedel

Academic staff

Dr. Michael Lorenz
PD Dr. Rainer Pickenhain
Prof. Dr. Bernd Rheinländer
Dr. Heidemarie Schmidt
Dr. Alexander Weber
Dr. Qingyu Xu

PhD candidates

Dipl.-Phys. Jens Bauer
Mariana Diaconu, M.Sc.
Dipl.-Phys. Daniel Fritsch
Dipl.-Phys. Karsten Goede
Susanne Heitsch, M.Sc.
Dipl.-Ing. Stefan Jaensch
Dipl.-Phys. Thomas Nobis
Dipl.-Phys. Andreas Rahm
Dipl.-Phys. Rüdiger Schmidt-Grund
Dipl.-Phys. Holger von Wenckstern
Dipl.-Phys. Gregor Zimmermann

Students

Matthias Brandt
Christian Czekalla
Heiko Frenzel
Lars Hartmann
Christoph Henkel
Robert Johne
Maryam Khaksar
Alexander Müller
Hendrik Paetzelt
Abdelrahmen Raed
Matthias Schmidt
Christian Schulz
Chris Sturm
Yashwant Verma
Rao Voora, B.Sc.
Robin Weirauch

External Members

Dipl.-Phys. Amélia Ankiewicz
(PhD student at Universidade de Aveiro, Portugal)
Marc Schillgalies, M.Sc.
(PhD student at OSRAM OS, Regensburg)

1.2.5 Solid State Optics and Acoustics, Festkörperoptik und -akustik

Prof. Dr. Wolfgang Grill

1.2.6 Superconductivity and Magnetism, Supraleitung und Magnetismus

Prof. Dr. Pablo Esquinazi

Technical staff

Klaus Grünwald
Dipl.-Krist. Annette Setzer
Monika Steinhardt

Academic staff

Dr. YuanFu Chen
Dr. Roland Höhne
Dr. Hans-Christoph Semmelhack
Dr. Michael Ziese

PhD candidates

Dipl.-Phys. Kristian Schindler

Students

Roland Salzer
Norman Leps
Katharina Fritsch

1.3 Institute for Theoretical Physics

1.3.1 Office of the Director

Prof. Dr. Gerd Rudolph (director)
Prof. Dr. Klaus Kroy (vice director)

1.3.2 Computational Quantum Field Theory, Computerorientierte Quantenfeldtheorie

Prof. Dr. Wolfhard Janke

Secretary

Gabriele Menge
Gloria Salzer
Lea Voigt

Academic staff

Dr. Michael Bachmann
Dr. Elmar Bittner
Dr. Leszek Bogacz
Dr. Peter Crompton
Dr. habil. Adriaan Schakel

PhD candidates

Dipl.-Phys. Andreas Nußbaumer
Dipl.-Phys. Stefan Schnabel
Dipl.-Phys. Thomas Vogel
Sandro Wenzel, M.Sc.

Students

Rainer Bischof
Thomas Haase
Christoph Junghans
Goetz Kähler
Anna Kallias
Axel Krinner
Eric Lorenz
Rodrigo Megaides
Reinhard Schiemann
Jakob Schluttig

1.3.3 Molecular Dynamics / Computer Simulation, Moleküldynamik / Computersimulation

Speaker: PD Dr. Horst L. Vörtler (PD Dr. Siegfried Fritzsche)

Academic staff

PD Dr. Horst L. Vörtler
PD Dr. Siegfried Fritzsche
Prof. Dr. Reinhold Haberlandt
Dr. Andreas Schüring
Dr. Partha Biswas

PhD candidates

Arthorn Loisruangsin, B.Sc.
Oraphan Saengsawang, M.Sc.

Students

Katja Schaefer

1.3.4 Quantum Field Theory and Gravity, Quantenfeldtheorie und Gravitation

Prof. Dr. Gerd Rudolph

Academic staff

PD Dr. Michael Bordag
Dr. Daniel Grumiller
Prof. Dr. Johannes Huebschmann
Dr. Pjotr Marecki
Dr. Matthias Schmidt
Dr. Dmitri V. Vassilevich
Prof. Dr. Rainer Verch

Retired

Prof. em. Bodo Geyer
Prof. em. Armin Uhlmann
Prof. em. Wolfgang Weller

Permanent Guests

Doz. Dr. Peter Alberti
Dr. Bernd Crell
Dr. Rainer Matthes

PhD candidates

Dipl.-Phys. Alexander Hertsch
Dipl.-Phys. Stefan Neumeier
Alexei Strelchenko, M.Sc.

Students

Carsten Balleier
Friederike Danneil
Stefan Funkner
Nadine Große
Diana Kaminski
René Meyer
Gilbert Spiegel
Sandra Stephan
Hedwig Wilhelm

1.3.5 Statistical Physics, Statistische Physik

Prof. Dr. Manfred Salmhofer

Academic staff

Dr. Oliver Lauscher

PhD candidates

Dipl-Ing. Walter Pedra
Dipl-Phys. Christoph Husemann

Students

Friedmar Schütze
Kay–Uwe Giering
Thomas Kahle

1.3.6 Theory of Condensed Matter, Festkörpertheorie

Prof. Dr. Ulrich Behn (Speaker)
Prof. Dr. Dieter Ihle (retired October 2005)
Prof. Dr. Klaus Kroy
Prof. Dr. Adolf Kühnel (retired)

Academic staff

PD Dr. Winfried Kolley (retired October 2005)

PhD candidates

Dipl.-Phys. Dipl.-Math. Steffen Arnrich
Dipl.-Phys. Iren Juhász Junger
Dipl.-Phys. Micaela Krieger-Hauwede
Dipl.-Phys. Benedikt Obermayer

Students

Christian Brettschneider
Jens Glaser
Daniel Rings
Fabian Senf
Holger Schmidtchen
Reinhard Vogel

External members

Dr. Oskar Hallatschek
(Academic staff, Hahn-Meitner-Institut Berlin)
Sebastian Fischer
(Student, Hahn-Meitner-Institut Berlin and FU Berlin)
Jörg Menche
(Student, Institut für Physik, Humboldt-Universität Berlin)

1.3.7 Theory of Elementary Particles, Theorie der Elementarteilchen

Prof. Dr. Klaus Sibold

Academic staff

PD Dr. Roland Kirschner
Dr. Yi Liao
PD Dr. Holger Perlt
PD Dr. Arwed Schiller

PhD candidates

Dipl.-Phys. Christoph Dehne

I

Institute for Experimental Physics I

2

Physics of Anisotropic Fluids

2.1 Introduction

In the central research topics of our group i.e. Broadband Dielectric Spectroscopy, time-resolved FTIR-spectroscopy and experiments with optical tweezers good progress could be achieved: (i) Evidence could be found that in thin polymer films the glasstransition temperatures as measured with different (microscopic and macroscopic) techniques do not coincide - in contrast to the bulk. (ii) refined experiments were carried out concerning structure, order and dynamics in self-supporting nematic liquid crystalline elastomers [J. Li, D. Geschke: Polym. Adv. Technol. 16, 11 (2005)] and (iii) with optical tweezers novel experiments were carried out dealing with protein/DNA interaction but as well with microfluidics. In December 2005 I was awarded with the Karl Heinz Beckurts-prize for my contributions to dielectric spectroscopy and it's applications. I take this as a great encouragement.

Friedrich Kremer

2.2 Molecular Dynamics in Thin Films of Polymers with Special Architecture

A. Serghei, F. Kremer

This projects aims to investigate confinement effects on the dynamic glass transition of polymers having special architectures. Thin films of hyper-branched polymers (Fig. 2.1a) and star-branched polymers are prepared and their molecular dynamics is investigated in dependence on the confinement size (film thickness). Two questions are addressed. The first one, what role plays the architecture of the macromolecular systems in the deviations of the dynamic glass transition from the bulk behaviour observed in thin films. For example, thin layers of hyper-branched polyesters show an increase of the average alpha relaxation rate with decreasing films thickness. This effect appears at much larger thicknesses (Fig. 2.1b) that those reported for linear polymers and therefore must be assigned to the special architecture of these dendritic macromolecules.

The second question, to what extent different methods to investigate the glass transition provide comparable results when applied to thin films. For that, complementary measurements by Broadband Dielectric Spectroscopy, capacitive dilatometry and

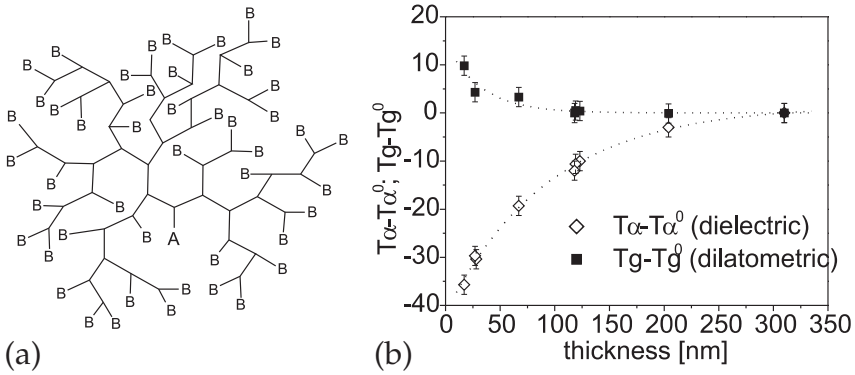

Figure 2.1: (**a**) scheme showing the architecture of hyper-branched polymers, (**b**) the maximum temperature position of the alpha relaxation peak (by Broadband Dielectric Spectroscopy, at 0.6 Hz) and the glass transition temperature (by capacitive dilatometry), both normalized in respect to the values corresponding to 310 nm, as a function of film thickness.)

AC-calorimetry are employed. In the case of hyper-branched polyesters, the dielectric measurements show a faster dynamic glass transition with decreasing film thickness while simultaneous dilatometric determinations reveal a slight increase of T_g. Such an apparent controversy, reported for the first time for polymers in confinement, indicates that microscopic and macroscropic experimental techniques do not necessarily deliver similar results.

[1] Y.H. Kim: J. Polym. Sci. A **36**, 1685 (1998)
[2] A. Serghei et al.: Eur. Phys. J. E **17**, 199 (2005)

2.3 Novel Developments in the Preparation of Thin Polymer Films

A. Serghei, F. Kremer

In this work novel methods for the preparation of thin polymer films are developed. One approach is schematically described in Fig. 2.2. Silica nano-colloids are used as spacers between two ultra-flat highly conductive silicon wafers. On one of the two wafers a thin polymer film was previously deposited by spin-coating from solution. This preparation procedure enables one – for the first time – the investigation of the dynamic glass transition in thin films having a free upper interface.

This method is sensitive down to film thicknesses as small as 10 nm or even lower, depending on the size of the colloids used as spacers and on the dielectric strength of the investigated materials. Its advantages, over the standard preparation procedure for dielectric measurements on thin films, are: 1) one avoids the evaporation of metal electrodes; 2) the samples have a free upper interface; 3) the samples are spin-coated on silicon wafers, resulting in an identical sample geometry and interfacial interactions as in the case of ellipsometric studies.

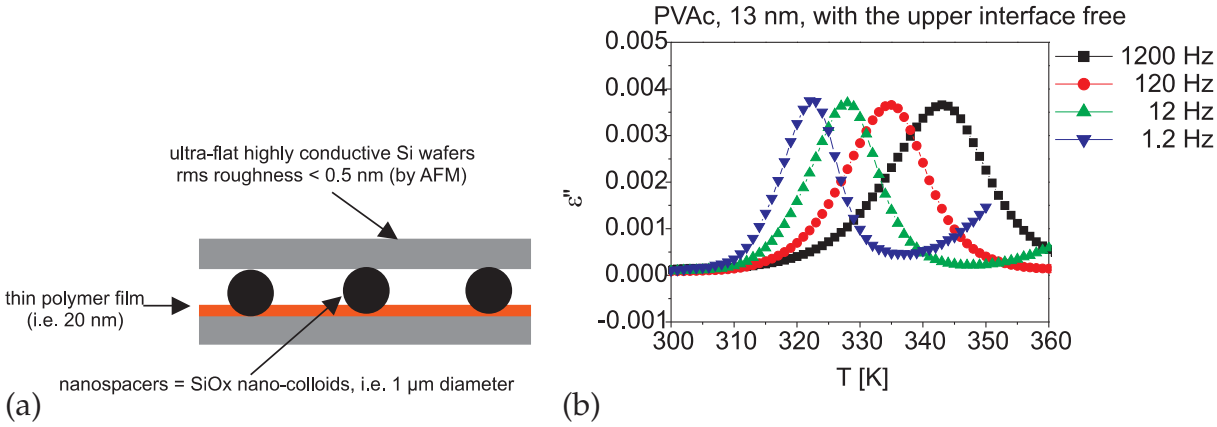

Figure 2.2: (**a**) schematic representation of the sample preparation; (**b**) dielectric loss vs. temperature at different frequencies, as indicated, for a thin film of PVAc having a thickness of 13 nm.

2.4 Dielectric Properties of Ionic Liquids

A. Serghei, F. Kremer

The chemical reactions which take place in ionic solvents exhibit - in comparison to those in molecular solvents - modified properties. They lead to better yields and higher conversion rates, and the regio- and enantioselectivity are improved. Although a variety of reactions, as enzymatic, transition metal catalysed and non-catalized reactions have been optimised in ionic solvents, only a little is known about the mechanisms underlying these "ionic liquid effects". The aim of this project is to investigate whether and how the reactivity and regioselectivity correlate with the permitivitty of the ionic solvents. For that, dielectric measurements are performed by means of Broadband Dielectric Spectroscopy in a wide frequency range covering ten decades (0.1 Hz – 1 GHz). Due to the high conductivity of these materials, the geometry of the sample cell has to be optimised. A first approach is schematically illustrated in Fig. 2.3a. Preliminary measurements on tetrafluoroborate using this sample geometry (Fig. 2.3b) show an excellent agreement between the low and the high frequency experimental curves.

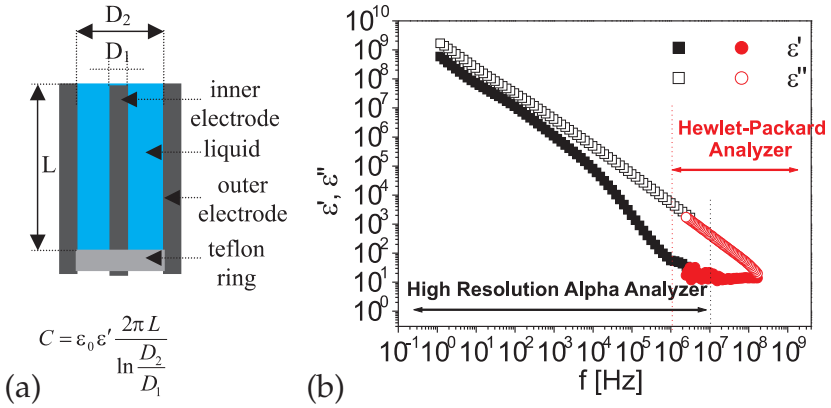

Figure 2.3: (**a**) schematic illustration of the sample cell; (**b**) real ε' and imaginary part ε'' of the complex permitivitty vs. frequency at room temperature for tetrafluoroborate (BF4).

2.5 Molecular Dynamics in Semifluorinated Side-Chain Polyesters as Studied by Broadband Dielectric Spectroscopy

J. Tsuwi, F. Kremer

Structural segments consisting of alkyl and perfluoroalkyl groups covalently linked by a C−C bond are well known for their microphase separation resulting in highly ordered bulk structures. The use of such materials for surface modification is numerous because of the resulting low surface free energy. We are employing Broadband Dielectric Spectroscopy to study the molecular dynamics in fluorinated side-chain polyesters.

The polymers comprise of non-substituted main chain polyesters and polyesters with semifluorinated (oxydecylperfluorodecyl) side chains. Combining temperature-dependent small angle X-ray scattering (T-SAXS), differential scanning calorimetry (DSC) and BDS it can be shown that the microphase separated semifluorinated polymers exhibit independent dynamic glass transition relaxations taking place in the separate microphases. Additionally in the glassy state, the non-substituted polymers show an Arrhenius type relaxation whose activation energy decreases gradually from 52 kJ/mol to 40 kJ/mol with increasing main chain flexibility. The semifluorinated polymers exhibit a relaxation assigned to fluctuations of the perpendicular component of the fluoroalkyl end group with activation energies between 38 − 40 kJ/mol. With increasing flexibility of the main chain, the dynamics of the backbone becomes faster for the non-substituted polymers while an opposite trend is observed in the oxydecylperfluorodecyl substituted side chain materials. The dielectric results are analyzed in the context of micro-phase separated layered structures, supported by DSC and T-SAXS studies (Fig. 2.4).

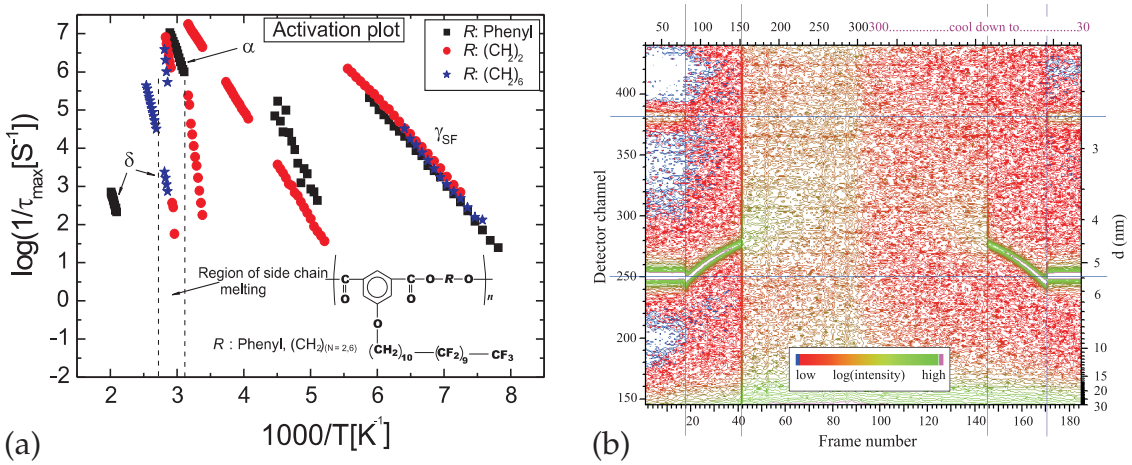

Figure 2.4: (**a**) Activation plot showing four relaxation processes $\gamma_{SF}\beta$, α and δ in order of their mean relaxation times. (**b**) Temperature dependent small angle X-ray (T-SAXS).

[1] J. Tsuwi et al.: J. Polym. Sci. B (2006), in preparation
[2] J. Tsuwi et al.: Coll. Polym. Sci. **283**, 1321 (2005)
[3] J. Tsuwi et al.: Macromol. **37**, 6050 (2004)
[4] A. Gottwald et al.: Macromol. Chem. Phys. **203**, 854 (2002)

2.6 The Microwave Absorption of Emulsions Containing Aqueous Micro- and Nanodroplets: A Means to Optimize Microwave Heating

J. Tsuwi, F. Kremer

The microwave absorption of frequencies between 10 MHz – 4 GHz is measured for aqueous brine droplets dispersed in a dielectric medium ($\varepsilon' = 2.0$), cf. Fig. 2.5. By varying the size of the droplets, ion type and ion concentration, it is found that the absorption goes through a maximum which depends as well on the type of ions and their concentration. The absorption process is attributed to the polarization of the microdroplets through surface charges. Means to optimize microwave heating in these systems is discussed.

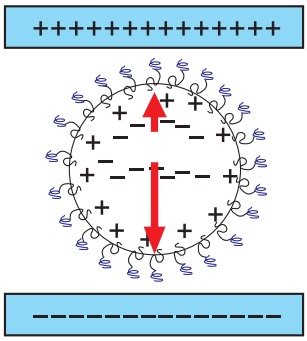

Figure 2.5: A droplet containing aqueous solution placed between two charged electrodes.

[1] C. Holtze et al.: submitted to Langmuir
[2] M. Antonietti, K. Landfester: Prog. Polym. Sci. **27**, 689 (2002)
[3] J. Sjöblom et al.: Disp. Sci. Technol. **20**, 921 (1999)
[4] T. Hanai: in *Emulsion Science*, ed. by P. Sherman (Academic Press, London 1968)

2.7 Spacer Length Dependent Mesogen Main Chain Alignment in Liquid Crystalline Elastomer Films

M. Tammer, P. Kölsch, F. Kremer

There are multiple ways of embedding liquid crystalline molecules into a polymer network. One of the most common techniques is a connection between one end of the mesogens and the main chain with an alkyl spacer chain, so called side chain liquid crystalline elastomers (SC-LCE). Polarized Fourier transform infrared (FTIR) spectroscopy is a powerful tool to determine the mean orientation and the order for the various molecular segments [1]. We applied this method to investigate the reorientation of the mesogens and spacer groups upon mechanically stretching the polymer network of thin nematic and cholesteric SC-LCE films. For both systems the mesogens are found

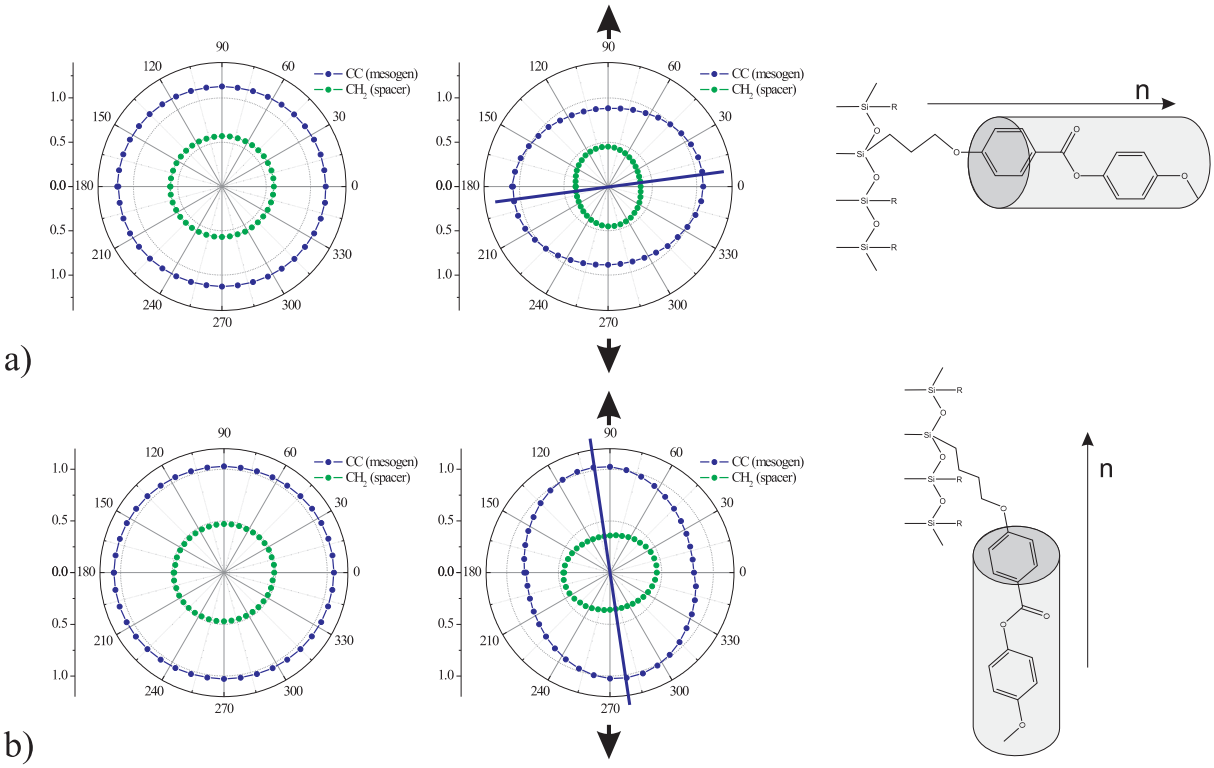

Figure 2.6: Polar plot of the absorbance for cholesteric films with (**a**) an even and (**b**) an odd number of aliphatic units in the spacer chain. *Left*: initial state; *Middle*: stretched; *Right*: molecular picture.

to form an oblate (director perpendicular to the main chain) or prolate (director parallel to the main chain) preferred orientation depending on whether the number of atoms in the spacer chain is even or odd. For the cholesteric films with no initial preferred orientation of the mesogens in the film plane, the strength of the coupling between the liquid crystal molecules and the polymer chain was compared for different spacer length (Fig. 2.6). The shortest spacer with a length of four atoms revealed the highest coupling. Additionally for films with equally mixed spacer lengths (even and odd), the results after stretching showed an oblate conformation due to the stronger influence of the shorter spacer chains [2].

[1] J. Li et al.: Eur. Phys. J. E **17**, 423 (2005)
[2] M. Tammer et al.: in preparation

2.8 Time Resolved FTIR-Spectroscopy on Segmental Reorientation of Nematic Elastomers under External Mechanical Fields

J. Li, M. Tammer, F. Kremer

Fourier transform infrared (FTIR) spectroscopy [1, 2, 3] is an especially suitable method for obtaining molecular level information for liquid crystalline networks. Time resolved

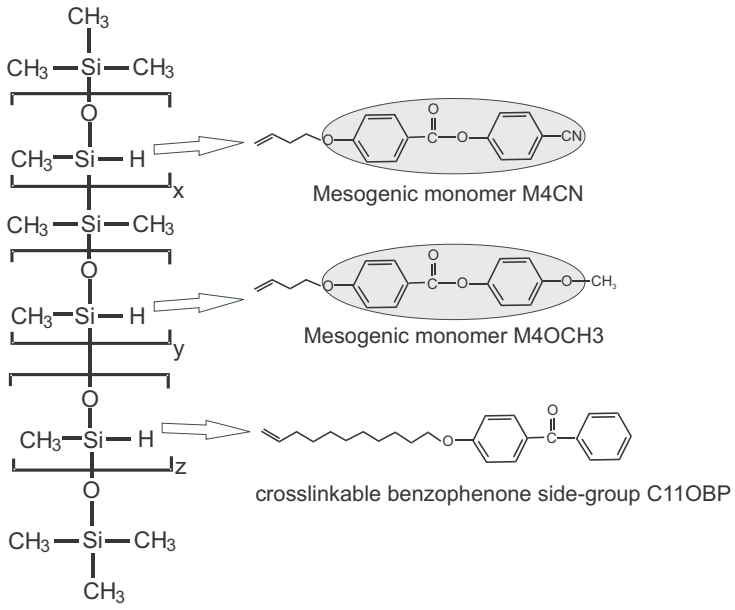

Figure 2.7: NLCE material.

FTIR spectroscopy with polarized light is employed to study the segmental orientation and the order parameters of nematic liquid crystalline elastomers (NLCEs, (Fig. 2.7) with a monodomain structure in response to an external mechanical field [4, 5]. Detailed results about the reorientation of the mesogens, the spacer molecules and the main chain are obtained due to the specifity of the FTIR measurements.

Mechanical strain is applied to thin NLCE films parallel and perpendicular to the initial mesogen orientation and the evolution of the orientation and the molecular order parameter with time is obtained for the different molecular moieties after each increase of the elongation ratio. While at parallel strain neither a reorientation nor a significant chage of the order parameters takes place for all groups, the molecular units react

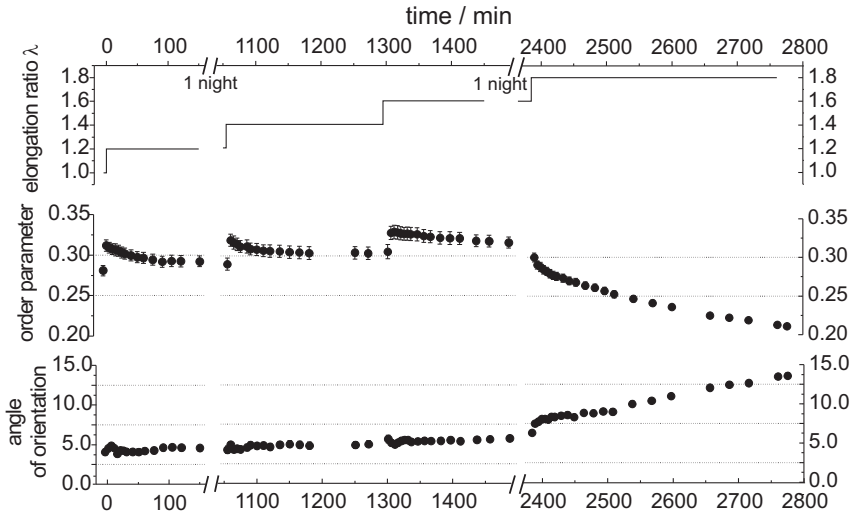

Figure 2.8: Orientation and order parameters for the CC group (mesogens) at perpendicular strain.

differently to a strain apllied perpendicular to the initial mesogen orientation (Fig. 2.8). Below a threshold value of the elongation ratio the orientation and order parameters remain nearly constant. Above this value a continuous reorientation is found for all molecular segments while the order parameters decrease. The network is not stable anymore and flows until the film breaks.

[1] H.W. Siesler, K. Holland-Moritz: *Infrared and Raman Spectroscopy of Polymers, Practical Spectroscopy Volume 4* (Marcel Dekker, New York 1980)
[2] S.V. Shilov et al.: Appl. Spectrosc. Rev. **31**, 125 (1996)
[3] H. Skupin et al.: Macromolecules **32**, 3746 (1999)
[4] M. Tammer et al.: Macromol. Chem. Phys. **206**, 709 (2005)
[5] J. Li, M. Tammer et al.: Eur. Phys. J. E **17**, 423 (2005)

2.9 Structural Analysis of Films Cast from Recombinant Spider Silk Proteins

M. Tammer, P. Kölsch, F. Kremer

Silks are one of natures best performing protein fibers. Spiders produce silk with outstanding mechanical properties, getting spidersilk in the focus of possible technical applications. Silk proteins can not only be processed into threads as found in nature, but can also be cast artificially into films in vitro. We investigated films of bacterially produced proteins mimicking the two dragline silkcomponents ADF-3 and ADF-4 of the garden cross spider Araneus diadematus [1] in cooperation with Thomas Scheibel at the TU-Munich. The secondary structure for such silk films can be analyzed using FTIR spectroscopy to measure the absorbance spectra. A deconvolution of the amide I absorbance band between 1600 cm^{-1} and 1700 cm^{-1}, representing primarily the C=O

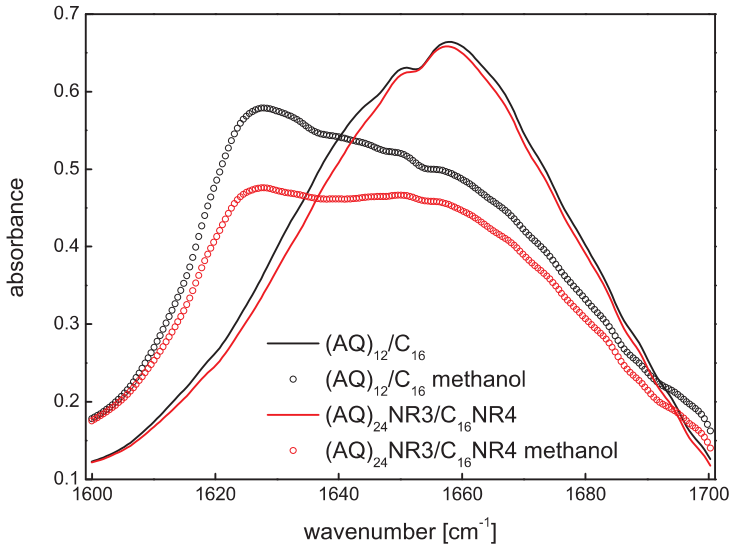

Figure 2.9: IR spectra of untreated samples without $(AQ)_{12}C_{16}$ and with NR-regions $(AQ)_{24}NR3/C_{16}NR4$ and of the same material treated with methanol.

Table 2.1: Resulted content of secondary structure for the films as derived by deconvoluting the amide I band.

	α-helix	β-sheet	β-turn	random coil
$(AQ)_{12}/C_{16}$ [as cast]	20.5	20.5	35.7	23.3
$(AQ)_{12}/C_{16}$ [mathanol]	8.2	46.4	19.9	25.5
$(AQ)_{24}$NR3/C_{16}NR4 [as cast]	22.5	17.7	33.7	26.1
$(AQ)_{24}$NR3/C_{16}NR4 [methanol]	9.9	38.8	30.3	21.0

stretching vibrations, with Lorentzian oscillators is used for determining the ratio of e.g. α-helical or β-sheet structure.

ADF-2 and ADF-3 consist mainly of repetitive sequences with characteristic polyalanine and glycine-rich motifs as well as non-repetitive (NR) regions at their carboxyl-terminus. We investigated whether the NR-regions play a decisive role in assembly, structure and stability of films cast therefrom. There had been no significant difference between the spectra of the proteins with or without NR-regions (Fig. 2.9). Furthermore, the influence of methanol and potassium phosphate treatment on the secondary structure has been studied. A shift of the maximum of the absorbance to lower wavenumbers ($\sim 1630\,\mathrm{cm}^{-1}$) indicating the formation of β-sheet structures at the expense of α-helices ($\sim 1660\,\mathrm{cm}^{-1}$) was found in all treated samples (Tab. 2.1) [2].

[1] T. Scheibel: Microbial Cell Factories **3**, 14 (2004)
[2] U. Slotta et al.: (2006), submitted to Supramol. Chem.

2.10 The Flow Resistance of Single DNA-Grafted Colloids as Measured by Optical Tweezers

C. Gutsche, M. Salomo, Y.W. Kim, R.R. Netz, F. Kremer

In rheological experiments the flow resistance of single blank or DNA-grafted colloids is determined and compared (Fig. 2.10). The length of the double-stranded (ds)-DNA varies between 1000 base pairs (bp), 4000 bp and 6000 bp corresponding to contour lengths between 340 nm and 2040 nm at a grafting density of $(0.03 \pm 0.01)\,\mu\mathrm{m}^2$/chain. The degree of swelling of the grafted DNA is adjusted by exchanging the ion concentration of the surrounding medium. For all examined flow velocities ranging between 100 µm/s to 1200 µm/s one observes an interesting deviation from Stokes law which

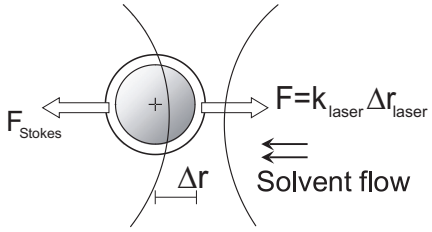

Figure 2.10: Forces acting on a grafted colloid in flow.

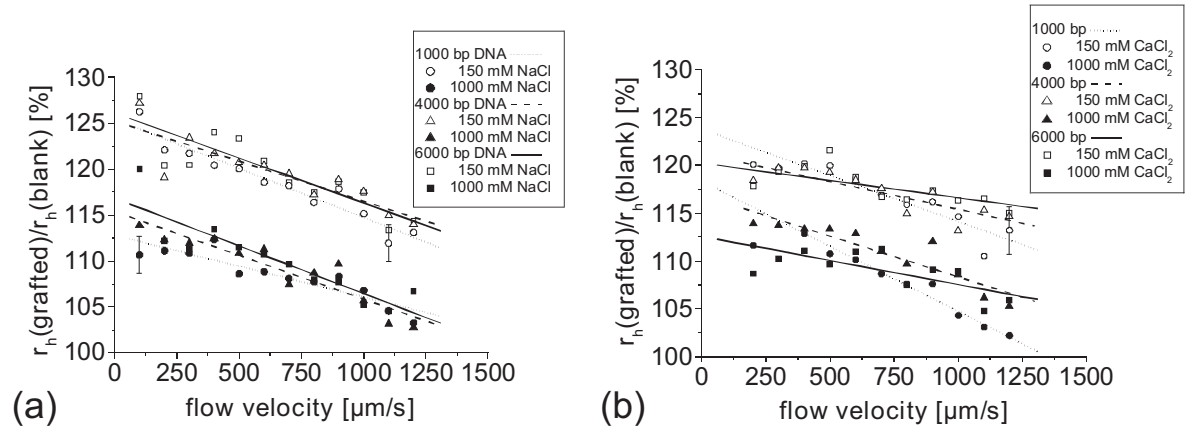

Figure 2.11: Ratio of the effective hydrodynamic radii for DNA-grafted and blank colloids versus flow velocity. Three single colloids with different DNA-grafting (1000 bp, 4000 bp and 6000 bp, same grafting density) are measured in two NaCl/$CaCl_2$-media ((**a**): 1000-bp DNA chains: *open circle* 150 mM NaCl, *filled circle* 1000 mM NaCl, 4000-bp DNA chains: *open triangle* 150 mM NaCl, *filled triangle* 1000 mM NaCl, 6000-bp DNA chains: *open square* 150 mM NaCl, *filled square* 1000 mM NaCl, (**b**) as (**a**) but for $CaCl_2$ solutions).

can be traced back to a shear-dependent conformational change of the brush layer. The ratio of the effective hydrodynamic radii of DNA-grafted and blank colloids shows a pronounced dependence on the flow velocity, but as well on the length of the grafted DNA and the ionic strength of the solvent (Fig. 2.11). The experimental findings are in qualitative agreement with hydrodynamic simulations based on an elastically-jointed chain model.

[1] C. Gutsche et al.: Microfluid. Nanofluid., in press (2006)
[2] C. Baumann et al.: Proc. Natl. Acad. Sci. **97**, 6185 (1997)
[3] F. Brochard-Wyart: Europhys. Lett. **23**, 105 (1993)
[4] F. Brochard-Wyart et al.: Europhys. Lett. **26**, 511 (1994)
[5] X. Schlagberger, R.R. Netz, Europhys. Lett. **70**, 129 (2005)
[6] Y.W. Kim, R.R. Netz: Europhys. Lett. in press (2005)

2.11 The Flow Resistance of *one* Blank Colloid in a Polymer Solution

C. Gutsche, M. Krüger, M. Rauscher, F. Kremer

The flow resistance of one *blank* colloid in a solution of λ-DNA (48 000 bp, contour length of $L_0 = 16\,\mu$m, radius of gyration $R_g = 500$ nm) was measured for concentrations between 0 to 30 µg/ml (Figs. 2.12, 2.13).

A dependence according to the Stoke's law is found with a flow resistance which increases by more than 100 % in going from 0 µg/ml to 50 µg/ml (Fig. 2.14). This pronounced effect cannot be explained on the basis of measurements of the macroscopic viscosity as determined with the flow viscosimeter.

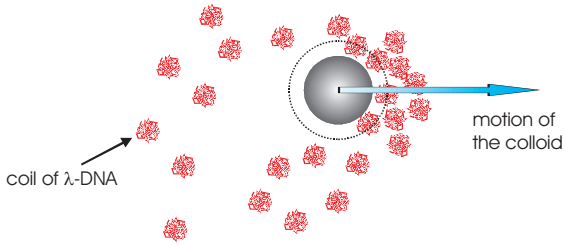

Figure 2.12: Assumed distribution of DNA coils with respect to a colloid in motion.

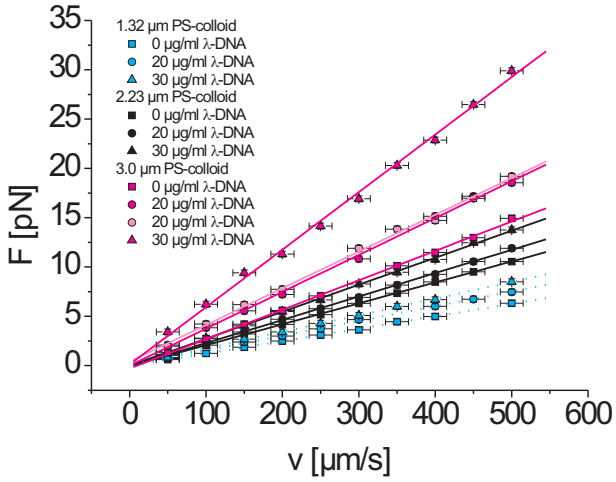

Figure 2.13: Force acting on *single* colloids (1.32 µm, 2.23 µm and 3.00 µm diameter) in solutions with different λ-phage-DNA concentrations as indicated. The measurements were carried out at 25 °C.

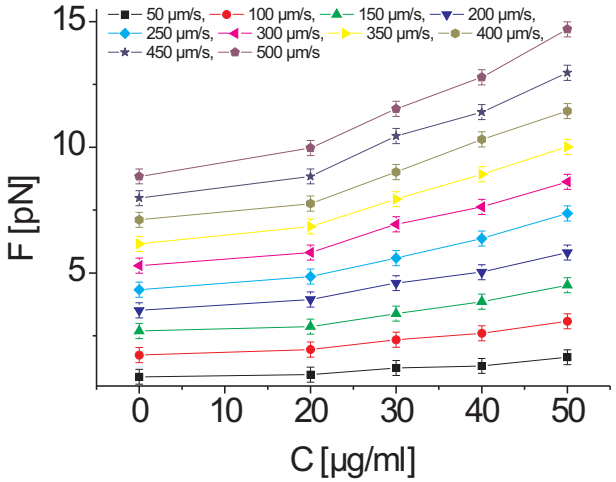

Figure 2.14: Force acting on a *single* colloids (2.23 µm diameter) in dependence of different λ-phage-DNA concentrations at different flow velocities.

It is assumed that this finding has its molecular origin in the heterogeneous nature of the DNA solution [1, 2, 3, 4]. The DNA-coils are in size not negligible compared to the colloids. Furthermore absorption of DNA on the colloid might play a role and must be ruled out.

[1] C. Bustamante et al.: Science **265**, 1599 (1994)
[2] T.R. Strick et al.: Science **271**, 1835 (1996)
[3] C: Bustamante et al.: Nature **421**, 423 (2003)
[4] J.-C. Meiners, S.R. Quake: Phys. Rev. Lett. **84**, 5014 (2000)

2.12 The Interaction Between Colloids (Diameter 2.2 µm) Grafted with DNA of Varying Length

K. Kegler, F. Kremer

The forces of interaction between two colloids grafted with DNA varying in length between 1000 base pairs (bp) and 6000 bp is measured for a grafting density of 450 ± 50 chains per colloid corresponding to $0.03\,\mu m^2$/chain. One colloid is hold by a micropipette which the other is kept in the optical trap. The separation between the colloids can be adjusted in nm-steps. It is possible to exchange the medium and to measure the interaction with *one* single pair of DNA-grafted colloids in different media e.g. for different ionic strengths. Furthermore the forces in x- and y- direction (Fig. 2.15) can be measured separately.

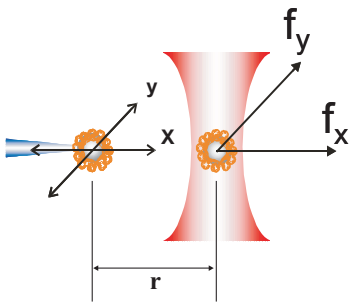

Figure 2.15: Scheme of two colloid grafted with DNA of varying length. One colloid is fixed by a micropipette, the other is kept in the optical trap. The former can be moved in x- and y-direction and resulting forces f_x and f_y are measured separately.

The following results were obtained:

1. Measuring the forces in a salt free medium one finds pure repulsive interactions and no attraction if the colloids are withdrawn from each other. This changes in the presence of salts (e.g. in a medium of 150 mM NaCl): After contact between the colloids one has an attractive interaction which is caused by counter-ion condensation.

2. Moving the colloids in y-direction perpendicular to the x-axis delivers for colloids in contact for the forces in x-direction a smooth response while in y-direction stick-slip phenomena are observed (Fig. 2.16a). Exchanging the medium from 150 mM to 1 M NaCl results in strongly reduced forces of interaction (Fig. 2.16b).

3. Comparing the frictional forces for grafted colloids having a length of 1000 bp and 4000 bp it is shown that the interaction sets in a correspondingly shorter separation.

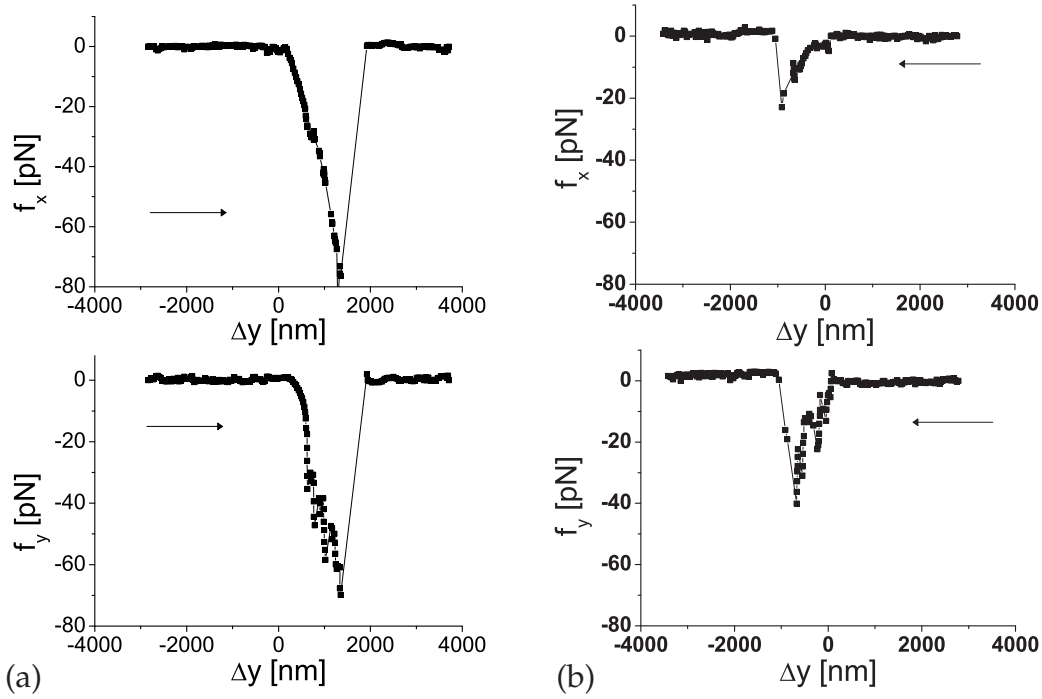

Figure 2.16: Forces of interaction f_x in x-direction and f_y in y-direction between two DNA(4000 bp)-grafted colloids in NaCl-solution of different ionic strength as indicated. In (**a**) the separation between the solid surface of the colloid is $l = 61$ nm in (**b**) it is $l = 63$ nm. It is shown that for the measurement at 150 mM NaCl where the DNA is more swollen than at 1 M NaCl the forces are much stronger. In x-direction a smooth response is found while in y-direction stick-slip phenomena take place. The arrow indicates from which side in y-direction the colloids are approached to each other.

2.13 Investigation of the DNA-Binding Protein TmHU with Optical Tweezers

M. Salomo, K. Kegler, M. Struhalla, J. Reinmuth, V. Skokow, F. Kremer

We applied the advantages of optical tweezers to study the TmHU/DNA complex formation kinetics and the disruption of the protein from the DNA chain by mechanical forces. The histone-like protein TmHU from the hyperthermophilic eubacterium *Thermotoga maritima* belongs to the group of HU proteins that are small basic proteins occurring in all prokaryotes. Its major function consists in binding and compacting DNA into structures similar to eukaryotic chromatin. The functional form of TmHU contents two identical subunits having a monomeric molecular mass of 9.993 kDa and contents 90 amino acids. TmHU binds the DNA tightly ($K_D = 73$ nM) without detectable sequence specificity. It bends the DNA very ($\sim 160^\circ$) and simultaneously increases its flexibility.

For our experiments we developed a special flow cell which enables us to immobilize a single DNA molecule between two functionalized polystyrene beads of which one is fixed at a micropipette and the other one is held by the optical trap. Further more it is possible to flush the cell with buffers or protein solution. After establishing a single DNA chain between two beads the force extension dependence of naked DNA was

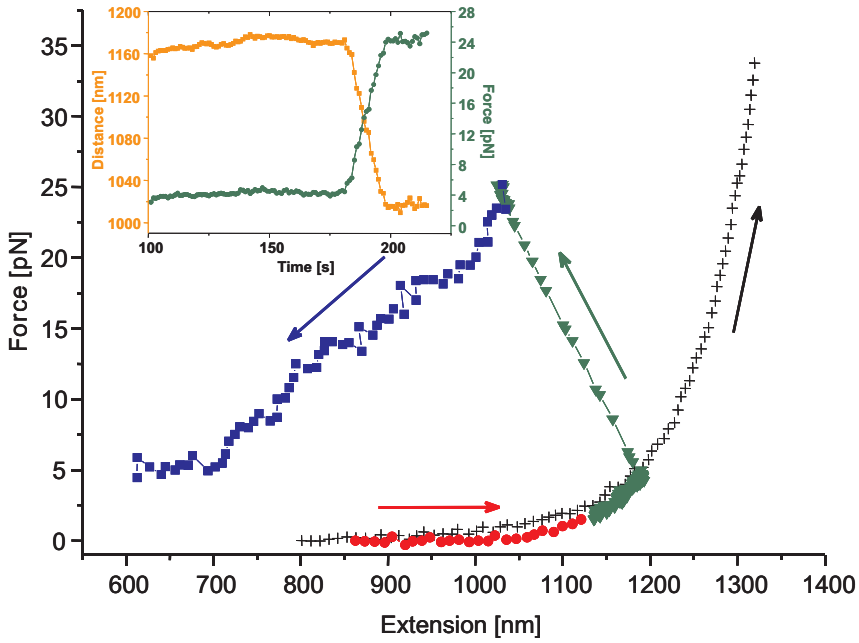

Figure 2.17: Prior to incubation of the DNA with protein a force extension dependence of naked DNA is recorded (*black crosses*). Afterwards the DNA is stretched to a definite force level between 1 – 3 pN (*full red circles*). Flushing the sample cell with TmHU solution takes ~ 129 s and causes a slight drift of the bead on top of the micropipette (*full green triangles*, see as well *inset*). The action of the protein shows up as a rapid shortening of the DNA and an increase of its tension (see *inset*). At forces of about 20 – 25 pN the reaction is halted. Afterwards the protein/DNA complex is relaxed (*blue squares*).

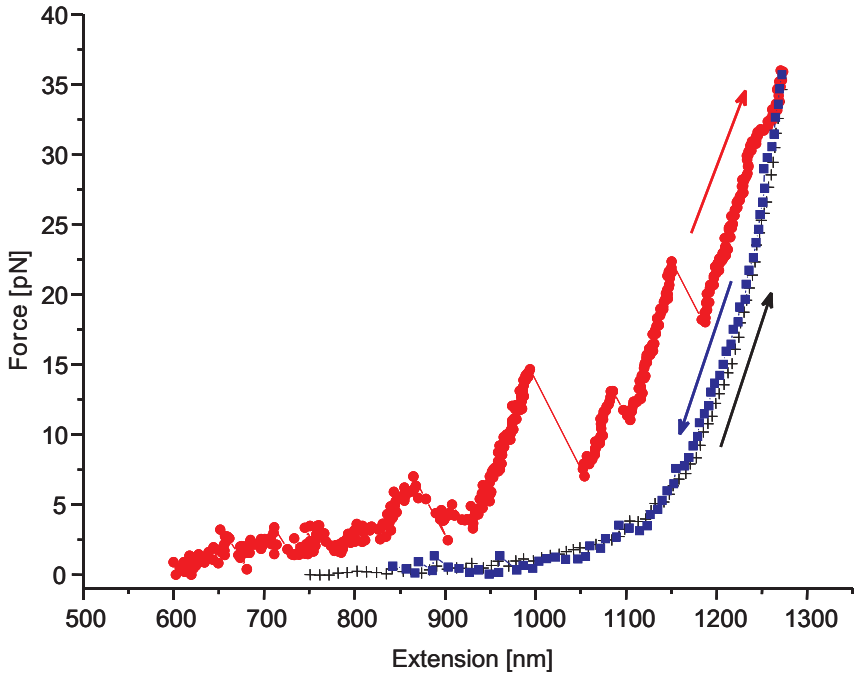

Figure 2.18: When the TmHU/DNA complex is stretched distinct disruption events can be observed (*full red circles*). Subsequent relaxation (*blue squares*) of the chain delivers a force-extension dependence well comparable to that of naked DNA (*black crosses*). Repeated stretching cycles in the protein solution result in fully comparable disruption events as shown above.

measured. After flushing the sample cell with TmHU solution of 5 nM concentration (in 10 mM Na_2HPO_4/NaH_2PO_4 pH 7.5), a rapid decrease in the length of DNA is observed. Subsequent to the assembling of the TmHU/DNA complex, it was relaxed (Fig. 2.17). Afterwards the formed TmHU/DNA complex is stretched and relaxed again (Fig. 2.18). A distinct saw tooth pattern is observed being characterized by well defined disruption events. At higher force levels the length of naked DNA is recovered.

Binding and disruption of TmHU to and from DNA are found to take place in discrete steps of 4 5nm length and 5×10^{-20} J energy. This is in reasonable agreement with a microscopic model which estimates the extension of the binding-sites of the protein and evaluates the energetic mainly of the bending of DNA in the course of interaction.

2.14 Funding

Optische Pinzette als mikroskopische Sensoren und Aktuatoren zum Studium der Wechselwirkung zwischen einzelnen Biomolekülen
Prof. Dr. F. Kremer
SMWK-Projekt 7531.50-02-0361-01/11 (2001–2006)

Nano- und Mikrofluidik: Von der molekularen Bewegung zur kontinuierlichen Strömung
Prof. Dr. F. Kremer
Teilprojekt im Rahmen des "DFG-Schwerpunktprogrammes SPP 1164", KR 1138/14-1 (2004–2006)

2.15 Organizational Duties

Friedrich Kremer

- Director of the Institute of Experimental Physics I
- Fachgutachter für die Deutsche Forschungsgemeinschaft für das Fachgebiet "Chemie und Physik der Polymere"
- Herausgeber der internationalen Zeitschrift *Journal of Colloid and Polymer Science*
- Mitglied des Editorial Boards der Zeitschriften: *Macromolecular Rapid Communication*, *Macromolecular Chemistry and Physics* and *Polymers for Advanced Technologies*

2.16 External Cooperations

Academic

- Rostock University
  C. Schick
- Institute of Polymer Research, Dresden
  B. Voit, D. Pospiech, M. Stamm, P. Uhlmann

- Martin Luther University, Halle
  F. Bordusa, C. Wespe
- Max Planck Institute of Colloids and Interfaces, Golm
  M. Antonietti
- Experimental Soft Condensed Matter Group, Harvard University, USA
  C. Holze
- University of Freiburg
  H. Finkelmann
- Technical University Munich
  T. Scheibel, R.R. Netz
- Max Planck Institute for Metals Research, Stuttgart
  M. Rauscher
- University of Technology, Dresden
  A. Pich

Industry

- Novocontrol Hundsangen, Germany
  Dr. G. Schaumburg, G. den Dulk
- Comtech GmbH München, Germany
  Dr. A. Hussain
- Freudenberg Dichtungs- und Schwingungstechnik KG Weinheim, Germany
  Dr. E. Bock, Dr. T. Klenk

2.17 Publications

Journals

J. Li, D. Geschke: *Pyroelectric inverstigations of a hydrogen bonded ferroelectric liquid crystal gel by LIMM*, Polym. Adv. Technol. **16**, 11 (2005)

N.A. Nikonorova, E.B. Barmatov, D.A. Pebalk, R. Diaz-Calleja, F. Kremer: *Dielectric relaxation of side-chain liquid crystalline ionomers containing alkaline metal ions*, Macromol. Chem. Phys. **206**, 1630 (2005)

M. Tammer, J. Li, A. Komp, H. Finkelmann, F. Kremer: *FTIR-spectroscopy on segmental reorientation of a nematic elastomer under external mechanical fields*, Macromol. Chem. Phys. **206**, 709 (2005)

J. Li, M. Tammer, F. Kremer, A. Komp, H. Finkelmann: *Strain-induced reorientation and mobility in nematic liquid crystalline elastomers as studied by time-resolved FTIR spectroscopy*, Europ. J. Phys. E **17**, 423 (2005)

A. Serghei, H. Huth, M. Schellenberger, C. Schick, F. Kremer: *Pattern formation in thin polystyrene films induced by an enhanced mobility in ambient air*, Phys. Rev. E **71**, 061 801 (2005)

A. Serghei, Y. Mikhailova, K.-J. Eichhorn, B. Voit, F. Kremer: *Molecular dynamics of hyper-branched polyesters in the confinement of thin films* Eur. Phys. J. E **17**, 199 (2005)

J. Tsuwi, D. Appelhans, S. Zschoche, R-C. Zhuang, P. Friedel, L. Häußler, B. Voit, F. Kremer: *Molecular dynamics in fluorinated side-chain MI copolymers as studied by Broadband Dielectric Spectroscopy* Coll. Polym. Sci. **283**, 1321 (2005)

W. Weissflog, U. Dunemann, M.W. Schröder, R.A. Reddy; H. Kresse, S. Diele, S. Grande, G. Pelzl: *Field-induced inversion of chirality in antiferroelectric and ferroelectric smectic phases formed by bent-core mesogens*, J. Mater. Chem. **15**, 939 (2005)

W. Weissflog, U. Dunemann, M.W. Schröder, S. Diele, G. Pelzl, H. Kresse, S. Grande: *Field-induced inversion of chirality in SmCPA phases of a new achiral bent-core mesogens*, J. Mater. Chem. **15**, 939 (2005)

Books

F. Kremer: *Broadband Dielectric Spectroscopy to study the molecular dynamics of polymers having different molecular architectures*, in *Physical properties of polymer handbook*, ed. by J.E. Mark (Springer, Berlin 2005)

A. Serghei, F. Kremer: *Molecular dynamics in thin polymer films*, in *Fractals, diffusion and relaxation in disordered complex systems*, Advances in Chemical Physics ACP, ed. by S.A. Rice, W.T. Coffey, Y.P. Kalmykov (Wiley, Weinheim 2005)

in press

A. Serghei, F. Kremer: *Unexpected preparative effects on the properties of thin polymer films*, Progress Coll. Polym. Sci. (2005)

C. Gutsche, M. Salomo, Y.W. Kim, R.R. Netz, F. Kremer: *The flow resistance of single DNA-grafted colloids as measured by Optical Tweezers*, J. Microfluid. Nanofluid. (2005)

2.18 Graduations

Doctorate

- Dipl.-Phys. Anatoli Serghei
  Confinement-effects on the molecular dynamics in thin polymer films
  12/2005

3

Physics of Interfaces

3.1 Introduction

In the year 2005, the “Physics of Interfaces” Department achieved greater success in teaching and research. Research on diffusion, particularly the methodical enhancements of PFG NMR, interference microscopy, and IR microscopy was in the center of the scientific activities. The investigations in the field of NMR diffusometry and NMR spectroscopy form an integral part of the activities of the Center of Magnetic Resonance (MRZ) of our university.

Scientists in the group were awarded seventeen externally funded research projects. In particular, we would like to mention our activities in international research associations coordinated by us. These are: the International Research Training Group “Diffusion in Porous Media” in collaboration with the Dutch colleagues from the universities of Amsterdam, Delft, and Eindhoven, the International Research Group “Diffusion in Zeolites” jointly sponsored by EPSRC, CNRS and DPG, our work within the framework of the EU project (Network of Excellence) “In Situ Study and Development of Processes Involving Nanoporous Materials” (INSIDE PORES) started in the current year; and the completion of our work in the framework of the EU project TROCAT.

The crowning success of the activities of the “Physics of Interfaces” Department was the international conference “Diffusion Fundamentals I”, organized by the members of the Department and held in Leipzig from September 22^{nd} to 24^{th}, 2005. The conference represented the city of Leipzig’s and the University of Leipzig’s contribution to the festivities associated with the “Einsteinjahr”. The conference was dedicated to the fundamental principles of theory, experiments and applications of diffusion to different branches of chemistry, physics and medicine. The response of the scientific community (250 participants for the scientific and the social program) was overwhelmingly positive. This encouraged us to continue publication of our online journal that is devoted to the publication of scientific results as well as presentations at the regularly held conferences such as "Diffusion Fundamentals".

In 2005, Dr. Petrik Galvosas returned to our group as an assistant professor (Juniorprofessor) after several years abroad. The establishment of this professorship is a significant milestone for the Department which has not only to defend but enhance its reputation as a leading center of NMR diffusometry.

Even the departure of our longtime colleague Sergey Vasenkov had one positive aspect. He was appointed to a faculty position at the fourth largest university in the US

(University of Florida, Gainesville, Florida). The most prominent guest of our department this year is Professor Dr. Dhananjai B. Shah from Cleveland State University, Ohio, USA. He came to us as a "Gast-Mercator Professor" in summer 2005 for a twelve month stay. Professor Shah's research is dedicated to the transport of different components in zeolites and zeolite membranes.

Jörg Kärger

3.2 *In situ* ^{1}H and ^{13}C MAS NMR Kinetic Study of the Mechanism of Hydrogen Exchange for Propane on Zeolite HZSM-5

A.G. Stepanov*, S.S. Arzumanov*, H. Ernst, D. Freude

*Boreskov Institute of Catalysis, Novosibirsk, Russia

A simple reaction of hydrogen exchange between the Brönsted sites of zeolites and a small alkane molecule provides a pathway for claryfing the mechanism of alkane activation on solid acid catalysts. The existing data on the mechanism of the exchange for propane on acidic zeolites are contradictive [1, 2, 3]. Two mechanisms are mainly suggested. The first one implies intermediacy of propene in equlibrium with isopropyl cation to provide the exchange first into the methyl groups and then into methylene group by intramolecular hydrogen scrambling (consecutive scheme of the exchange) [1, 2]. The second mechanism suggests that both methyl and methylene groups are equally involved in the exchange via a direct proton/deuteron transfer between the

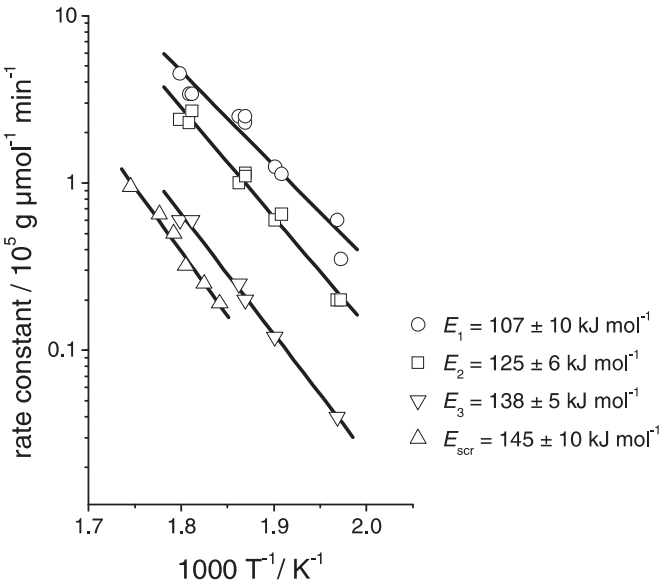

Figure 3.1: Arrhenius plot and activation energies for the H/D exchange reaction in deuterated propane on H-ZSM-5 and the ^{13}C-scrambling in propane-2-^{13}C on H-ZSM-5. k_1(○), k_2(□), k_3(▽), and k_{scr}(△).

catalyst acid sites and the alkane in a concerted step involving a pentacoordinated carbon atom (parallel scheme of the exchange) [3].

The kinetics of hydrogen (H/D) exchange between Bronsted acid sites of zeolite H-ZSM-5 and variously deuterated propane (propane-d_8, propane-1,1,1,3,3,3-d_6, propane-2,2-d_2) have been monitored *in situ* by ^{1}H MAS NMR spectroscopy within the temperature range of 503 – 556 K. The contribution of intramolecular hydrogen transfer to the H/D exchange in the adsorbed propane was estimated by monitoring the kinetics of ^{13}C-label scrambling in propane-2–^{13}C *in situ* with ^{13}C MAS NMR at 543 – 573 K. The rate constant (k_3) for intramolecular H/D exchange between the methyl and the methylene groups is 4 – 5 times lower compared to the direct exchange of both the methyl (k_1) and the methylene (k_2) groups with Bronsted acid sites of the zeolite, the k_1 being *ca.* 1.5 times higher than k_2 (Fig. 3.1). At lower temperature (473 K) the exchange is slower, and the expected difference between k_1 and k_2 is more essential, $k_1 \approx 3k_2$. This accounts for earlier observed regioselectivity of the exchange for propane on H-ZSM-5 at 473 K [1]. Faster direct exchange with the methyl groups compared to that with the methylene groups was attributed to a possible more spatial accessibility of the methyl groups for the exchange. Similar activation energies for H- and C-scramblings with two times more rapid rate of H-scrambling was rationalization by proceeding of these two processes through the intermediacy of isopropyl cation as in classical carbenium ion chemistry.

[1] J. Sommer et al.: J. Am. Soc. **117**, 1135 (1995)
[2] M. Haouas et al.: J. Am. Soc. **117**, 599 (2004)
[3] A.G. Stepanov: Catal. Lett. **54**, 1 (1998)

3.3 Internal Post-Curing of Concretes Studied by NMR

K. Friedemann, W. Schönfelder, F. Stallmach, J. Kärger

In the ongoing project "Water balance in high-performance concretes during internal post-curing with innovative additives" supported by the DFG (Ka 953/17-1), the water balance, the pore water self-diffusion and the transverse relaxation time T_2 in hardening cements of different compositions are investigated using non-destructive NMR methods [1, 2]. In particular, the transition of water from gel-like water-saturated alginate spheres to hydrating cement pasts of low initial water/cement (w/c)-ratios was studied.

The relaxation time distributions measured by low-field NMR relaxometry allow to distinguish between physically-bound water in the cement paste region, which appears at short transverse relaxation times, and the gel water in the alginate at much longer relaxation times. Following the changes in the relaxation time distribution with hydration time allows changes in the pore size of the hydrating cement to be assessed and the water transition from the alginate to the cement paste to be monitored (Fig. 3.2).

By analysing these relaxation time distributions, we found that the cement paste starts to uptake water from the alginate spheres with the onset of the accelerated period in the cement hydration. Small amounts of water added via the alginate spheres (e.g. 20 g per kilogram dry cement for an initial w/c-ratio of 0.3 as in Fig. 3.2) are completely transferred to the cement paste and consumed in the hydration reaction. If too much

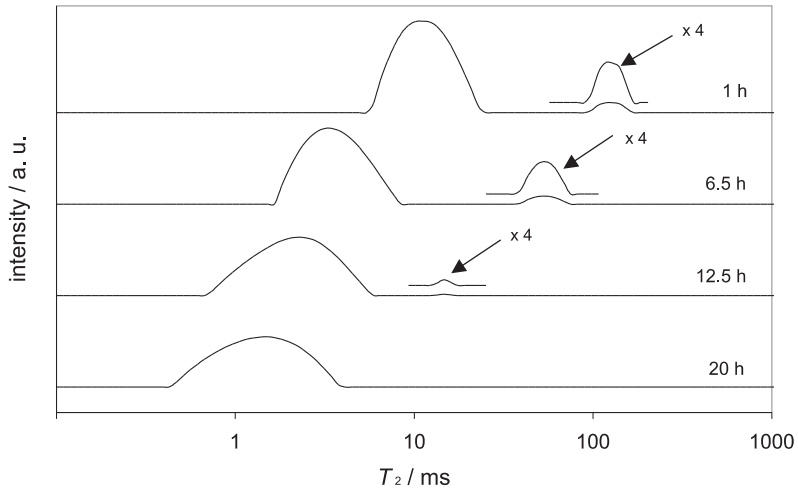

Figure 3.2: Transverse relaxation time distribution of water during cement hydration as studied by low-field NMR relaxometry. The two peeks correspond to physically-bound water in the hydrating cement (*left*) and gel-like water in the alginate (*right*) added for internal post curing (see [2] for more information).

alginate is added, the excess water remains in the alginate spheres. With this approach, we investigate the water requirement for internal post curing of different cement pastes.

[1] K. Friedemann et al.: LACER **10**, Universität Leipzig (2005) p 375
[2] K. Friedemann et al.: Cem. Concr. Res., in press

3.4 PFG NMR Investigations of Diffusion in MOF-5

F. Stallmach, V. Künzel, M. Wehring, J. Kärger, U. Müller*

*BASF AG, Ludwigshafen, Germany

Within our long-lasting co-operation with the BASF AG, we performed NMR studies of hydrocarbons adsorbed on metal-organic framework (MOF) coordination polymers. MOF represent a new class of nanoporous materials with prospective application in catalysis and gas processing [1]. Its most prominent representative MOF-5 [2] consists of a porous, cubic network of zinc acetate clusters linked by theraphtalic acid.

For the NMR studies, we obtained MOF-5 synthesized on a kilogram-scale in an optimized procedure at BASF AG [1] and studied the diffusion of methane, ethane, *n*-hexane and benzene. The results, which were published as "Hot Paper" in *Angew. Chemie Int. Ed.* [3], represent the very first experimental data on diffusion available for a MOF material.

These studies benefited from (and continue to require) methodological developments in FT PFG NMR (DFG project Ka 953/16-1) since ^{1}H or ^{13}C NMR signal contributions from the organic linkers and residual solvents of the MOF's must be separated from those of the adsorbed molecules. E.g., this is achieved by employing magic-angle spinning (MAS) for improved spectral resolution in combination with an optimized relaxation time-weighting in the spin echo MAS PFG NMR sequences (see Fig. 3.3).

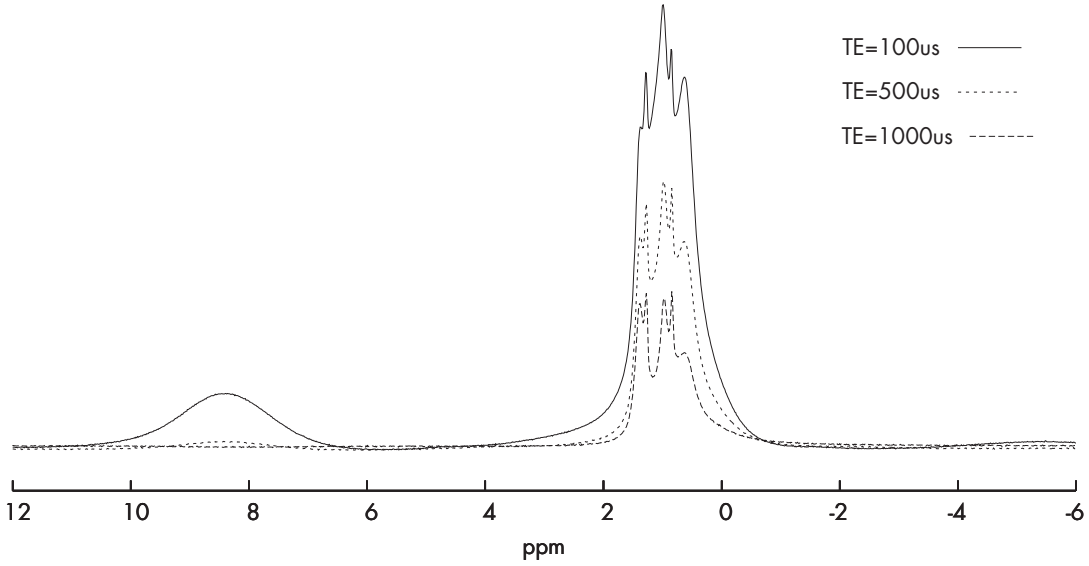

Figure 3.3: ^{1}H MAS NMR spectrum of *n*-hexane adsorbed in MOF-5 measuered with a primary spin echo sequence. At long echo times (*TE*), the signal from the MOF matrix at about 8 ppm vanishes while the typical NMR lines from the *n*-hexane remain observable.

[1] U. Müller et al.: J. Mater. Chem. **16**, 626 (2006)
[2] M. Eddaoudi et al.: Science **295**, 469 (2002)
[3] F. Stallmach et al.: Angew. Chemie Int. Ed. **45** in press

3.5 NMR Studies of Pore Size Distribution and Diffusion in Aquifer Rocks

W. Schönfelder, F. Stallmach, K. Kopinga*, H.-R. Gläser†

*Department of Biomedical Engineering, Eindhoven University of Technology, The Netherlands

†Department Hydrogeology, Umweltforschungszentrum Leipzig-Halle, Halle

This project aims at the advanced characterization of pore structure and water transport of aquifer rocks from an industrial effluent polluted aquifer in Central Germany about 50 km south-west of Leipzig. It is performed within the International Research Training Group (IRTG) "Diffusion in Porous Materials".

The investigated samples are natural dolomite rocks from a Zechstein formation. They were cut from 10 cm diameter core samples obtained during well drilling through an aquifer in the vicinity of the former sub-surface liquid waste disposal site. For non-destructive studies of pore size distribution, water-saturated plugs of 2 cm diameter and roughly 3 cm length were investigated by low-field ^{1}H NMR relaxometry with a new home-built 9.1 MHz NMR sensor. The transverse (T_2) relaxation decays of the pore water were recorded using the CPMG NMR sequence and analyzed by regularized inverse Laplace transformation.

Examples for the obtained T_2 relaxation time distribution are shown in the Fig. 3.4. Generally, in order to transfer the T_2 values into a pore size (R), the surface-relaxivity

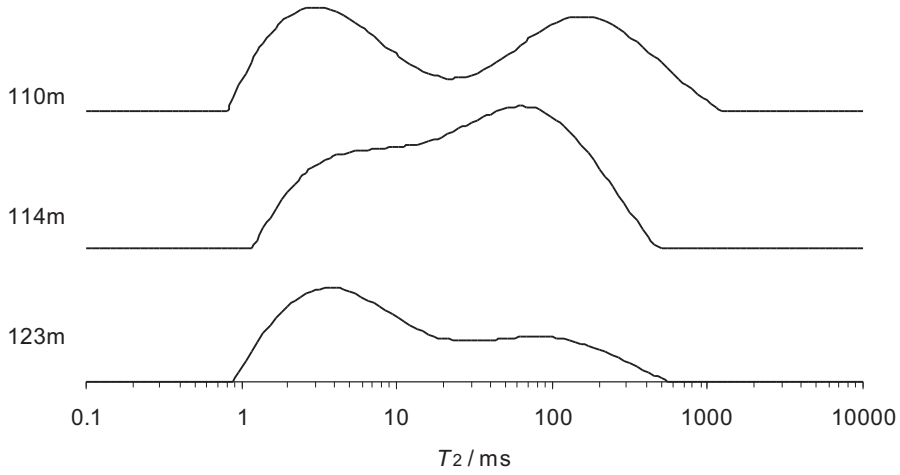

Figure 3.4: T_2 relaxation time distributions of dolomite rocks from different depth.

parameter ρ is required ($R = \rho \times T_2$) [1]. However, ρ, which depends on chemical composition of the pore-matrix interface, is not known for the natural dolomite rocks investigated. Additionally, T_2 is influenced by internal magnetic field gradients induced by iron-bearing minerals in these dolomites [2]. Therefore, the present work focuses on methods which might be able to relate the T_2 relaxation time distributions to pore size and pore types of the dolomite rocks. For this purpose, we investigate low-field NMR relaxometry in combination with cryoporometry and NMR diffusometry, but also with analysis of thin sections and studies at different water-saturation levels.

[1] A.T. Watson et al.: Ann. Rep. NMR Spectr. **48**, 113 (2003)
[2] W. Schönfelder et al.: in *Diffusion Fundamentals*, ed. by J. Kärger et al. (Leipziger Universitätsverlag, Leipzig 2005) p 470

3.6 New Options for Measuring Molecular Diffusion in Zeolites by MAS PFG NMR

M. Fernandez, A. Pampel, J. Kärger, D. Freude

Combination of pulsed field gradient (PFG) NMR with magic-angle spinning (MAS) NMR is demonstrated to have remarkable advantages in comparison with conventional PFG NMR [1], if applied to diffusion measurements in beds of nanoporous particles, notably zeolites [2].

The contribution describes investigations that mainly profit from the elimination of the disturbing influence of the inhomogeneity of the sample susceptibility [3] playing a decisive role for PFG NMR diffusion measurements of molecules in beds of zeolites.

In general, NMR spectra of polycrystalline materials are broadened by anisotropic interactions such as dipolar coupling, chemical shift anisotropy, quadrupolar coupling, and susceptibility effects. Depending on their strength and the achievable rotation frequency, MAS can reduce or even completely suppress these effects during the time course of an NMR experiment, see Fig. 3.5.

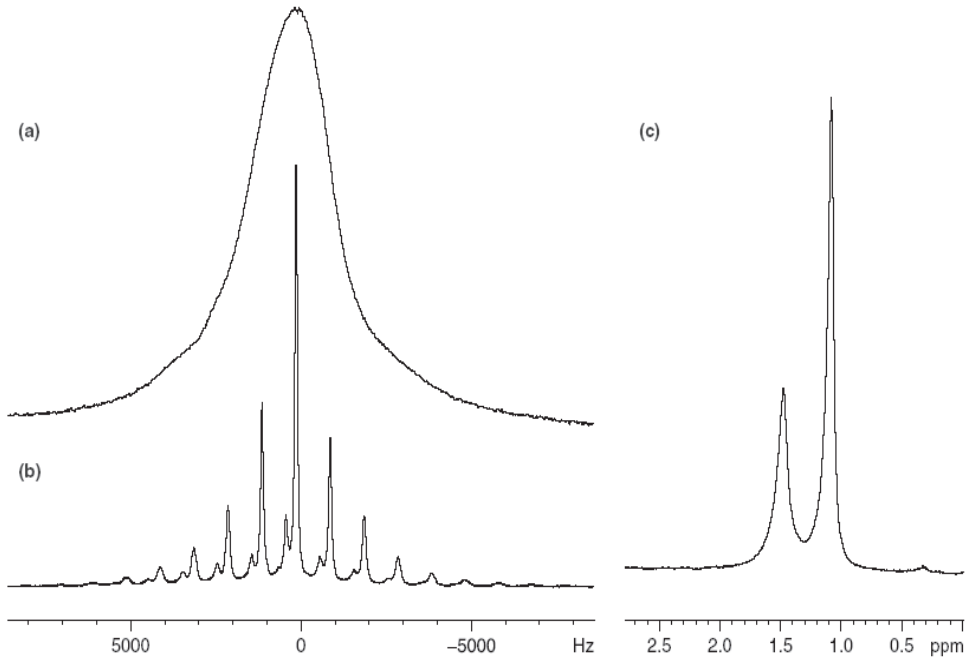

Figure 3.5: ^{1}H MAS NMR (observation frequency 749.98 MHz) spectra of *n*-butane adsorbed in silicalite-1 observed at room temperature. (**a**) Spectrum observed without sample spinning. **b**) Spectrum observed using MAS at 1 kHz rotation frequency. (**c**) Spectrum observed using MAS at 10 kHz rotation frequency.

Using a 750 MHz spectrometer, at a rotation frequency of 10 kHz, the spectrum of *n*-butane is observed with a residual line width of 44 Hz and 73 Hz of the signals of the CH_3- and CH_2-groups, respectively. The performance of the PFG NMR diffusion experiment is straightforward under these conditions. The diffusion coefficient calculated from the decay of integrals of the signal of the CH_3 peak is $3.17\times10^{-10}\,m^2s^{-1}$.

MAS PFG NMR is able to provide spectral resolution that is suitable for the spectroscopic separation of signals from different components. Under these conditions diffusion experiment with binary mixtures absorbed in zeolites were carried out. Samples under study are mixtures of *n*-butane and isobutene absorbed in NaX and silicalite-1. The measurements show how it is possible to distinguish the diffusivities of both isomers. The diffusivities obtained for the binary mixture absorbed in NaX are $1.37\times10^{-10}\,m^2s^{-1}$ and $1.12\times10^{-10}\,m^2s^{-1}$ for *n*-butane and isobutene, respectively.

PFG NMR and MAS NMR have been combined to measure intracrystalline zeolitic diffusion. It has been demonstrated that in this way line broadening due to the susceptibility heterogeneities inevitable in such systems may be dramatically reduced. Thus, the bad resolution, one of the most decisive limitations of the application of PFG NMR to zeolitic host-guest systems, may be overcome. This opens broad application concerning intra-cristalline diffusion measurements for multicomponent mixtures in zeolitic host systems.

[1] A. Pampel et al.: Chem Phys Lett **407**, 53 (2005)
[2] J. Kärger: in *Encyclopedia of Nuclear Magnetic Resonance, Vol. 3*, ed. by R.K. Harris et al. (Wiley, Chichester 1996) p 1656
[3] D. Michel et al.: J Chem Phys **119**, 9242 (2003)

3.7 High Temperature ^{1}H MAS NMR Studies of the Proton Mobility in Zeolites

J. Kanellopoulos, H. Ernst, D. Freude

Bridging hydroxyl groups capable of donating protons to molecules in the cages of zeolites are Bronsted-acid sites in heterogeneous catalysis. ^{1}H NMR studies of the acid protons in dehydrated zeolites gave some insight into the proton mobility [1, 2, 3]. The proton mobility in hydrogen zeolites was observed from 160 K to 550 K by conventional heating of the bearing gas and to 790 K by means of the laser heating of dehydrated and fused samples. ^{1}H MAS NMR spectra of the bare Bronsted sites of zeolites were monitored in this temperature range. The full width at half maximum of the ^{1}H MAS NMR spectrum of the dehydrated unloaded samples narrows by a factor of 24 for zeolite H-ZSM-5 and a factor of 55 for zeolite 85 H-Y. For the latter, the activation energy of 78 kJ mol^{-1} has been determined. Figure. 3.6 shows the ^{1}H MAS NMR spectra of the dehydrated zeolite 85 H-Y with a rotation frequency of 1 kHz. There are two reasons for choosing such a low rotation frequency. First, the envelope of many sidebands gives a good picture of the static (without sample rotation) line width. Second, the condition $\omega_{rot}\tau_c \ll 1$ giving the line widths as a linear function of the correlation time is fulfilled at lower temperature for a lower rotation frequency. The narrowing onset takes place between 298 and 420 K, see Fig. 3.6. Independent of the line narrowing model it can be concluded that the correlation time τ_c which is given by the mean residence time τ of a proton at an oxygen atom is in order of magnitude of the reciprocal low temperature line width ($\sim 100\,\mu$s) at the temperature of the narrowing onset.

Now the question arises whether the proton mobility is caused by jumps of hydrogen atoms over the oxygen framework of the zeolites or rather by a proton vehicle mechanism using residual water or ammonia molecules, which could not be removed from the zeolite by the activation procedure. Therefore, slightly reammoniated or rehydrated zeolites were investigated. One-dimensional exchange spectroscopy was performed by means of the NOESY pulse group, see Fig. 3.7.

In conclusion, zeolites H-Y and H-ZSM-5 were investigated by ^{1}H MAS NMR spectroscopy in the temperature range from 160 K to 790 K. We found that the hydrogen

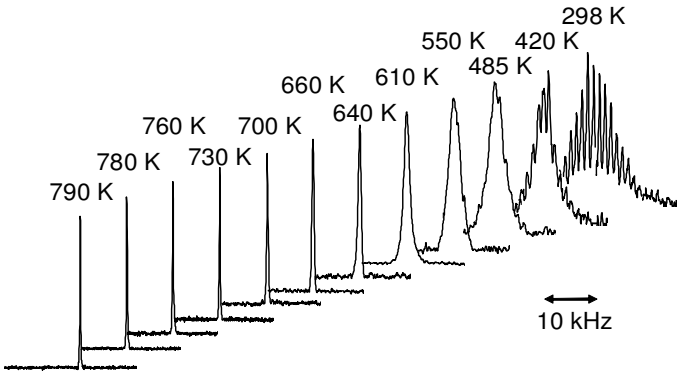

Figure 3.6: ^{1}H MAS NMR spectra of the dehydrated zeolite 85 H-Y for measuring temperatures from 298 K to 790 K. The rotation frequency is 1 kHz. No spinning sidebands can be observed at temperatures above 500 K, whereas at room temperature they are well-resolved.

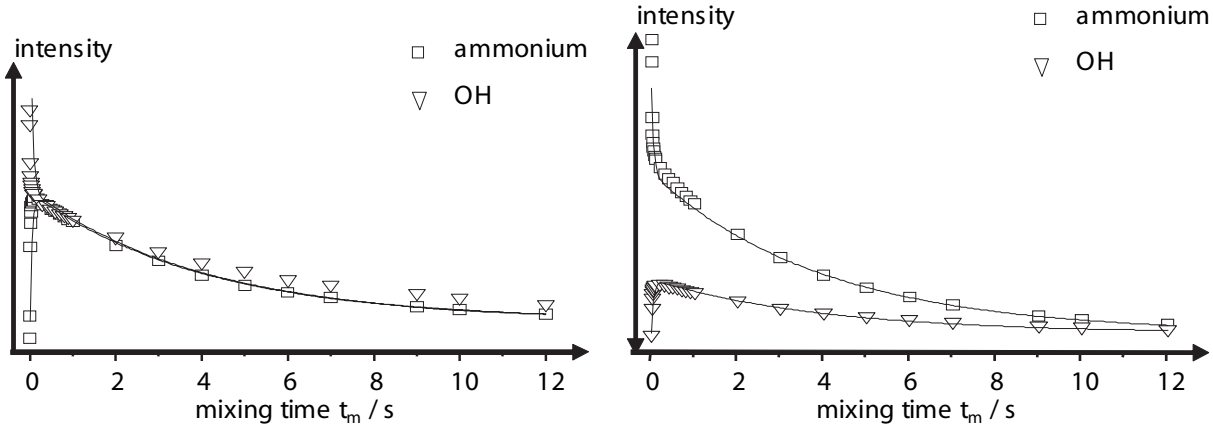

Figure 3.7: Amplitudes of the ^{1}H MAS NMR signal of ammonium ions and structural OH-groups as a function of the mixing time t_m. The zeolite H-Y was loaded with 1.5 ammonia molecules per supercage. For the *left panel*, the offset is shifted by the frequency difference between both signals from the left hand side of the left signal (ammonium ions). For the *right panel*, the offset is shifted by the same value to the right hand side from the right signal (bridging hydroxyl groups).

form of a zeolite, which contains almost residual ammonium ions, represents an ammonium conducting material for which the proton mobility is dominated by the high mobility of the ammonium ions in the zeolite. Thus, the proton vehicle mechanism by means of residual atoms in the zeolite seems to be responsible for the proton mobility at high temperatures.

[1] J. Kanellopoulos: PhD thesis, University of Leipzig 2006
[2] J. Kanellopoulos et al.: J. Catal. **237**, 416 (2006)
[3] D. Freude et al.: J. Catal. **49**, 123 (1977)

3.8 Progress of ^{17}O NMR for Zeolite Characterization

D. Schneider, D. Prochnow, H. Ernst, D. Freude

$AlPO_4$-14 and several zeolites of type A, X, Y, ZSM-5 isotopically enriched in ^{17}O were analysed by means of ^{17}O NMR in the field of 17.6 T using several solid-state NMR techniques for quadrupole nuclei. The influence of molecule adsorption is discussed including the question how the ^{17}O NMR shift reflects the basicity of the oxygen framework.

^{17}O MQ MAS (multi-quantum) experiments and ^{17}O DOR (double rotation) experiments were performed in the external magnetic field of 17.6 T (Bruker AVANCE 750 with wide-bore magnet) at 101.7 MHz. Probes constructed at the Institute of Chemical Physics in Tallinn and Bruker MAS probes were used for the DOR (double rotation) and MQ (multi-quantum) MAS experiments, respectively. The repetition time was in the range from 200 ms to 1 s corresponding to the measured longitudinal relaxation times T_1, which vary from 100 ms to 500 ms for the various zeolite samples under study. The time step t_1 in the multiple-quantum dimension was increased in steps of the reciprocal spinning frequency, in order to avoid spinning sidebands. DOR experiments were

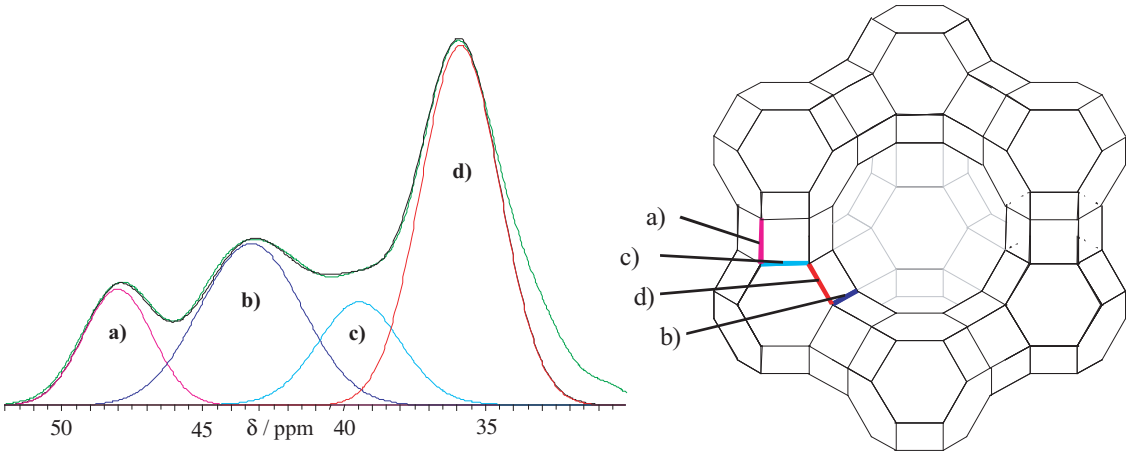

Figure 3.8: ^{17}O DOR NMR spectra of the dehydrated Na-LSX. The fit uses the fact that O_4-positions occur twice as much as the othe crystallographic positions in the material.

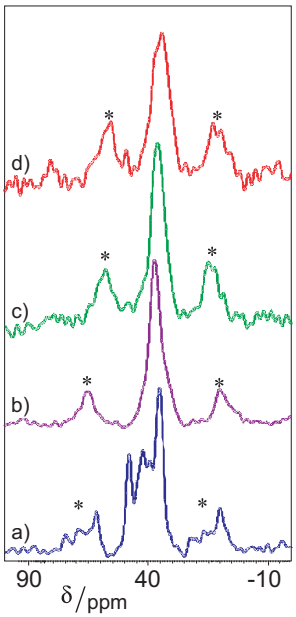

Figure 3.9: ^{17}O DOR NMR spectra of pure ^{17}O enriched Na-LSX (**a**), Na-LSX loaded with pyrrole (**b**), Na-LSX loaded with formic acid (**c**) and Na-LSX loaded with acetic acid (**d**). All samples were also immersed in octane to avoid hydration during the filling of the rotor. The spectra were measured in a magnetic field of B_0 = 17.6 T and at a spinning frequency of 1.2 to 1.4 kHz.

performed typically in a synchronized manner [1] with an outer rotor speed of about 1.4 kHz and an inner rotor speed of 6.0 – 6.5 kHz.

Our studies confirm that the quadrupole coupling constant increases with increasing ionic character of the bonds T_α-O and O-T_β. Considering the values of C_{qcc} obtained from ^{17}O atoms in bridging positions in barium pyrophosphate (P-O-P) [2], in $AlPO_4$-14 (Al-O-P) [2], in zeolites LSX [3] (Si-O-Al), see also Fig. 3.8, and in the layer silicate ilerit [2] (Si-O-Si) we obtain the relation

$$C_{qcc}(\mathrm{P-O-P}) > C_{qcc}(\mathrm{Al-O-P}) > C_{qcc}(\mathrm{Si-O-Si}) > C_{qcc}(\mathrm{Si-O-Al})\ .$$

A similar connection can be found for the isotropic chemical shift of the ^{17}O NMR:

$$\delta_{qcc}(P-O-P) > \delta_{qcc}(Al-O-P) > \delta_{qcc}(Si-O-Si) > \delta_{qcc}(Si-O-Al)\ .$$

New experimental results claim that the ^{17}O-signals of the oxygen framework are shifted and also moved together due to adsorption of acid molecules, see Fig 3.9.

[1] A. Samoson, E. Lippmaa: J. Magn. Reson. **84**, 410 (1989)
[2] D. Prochnow: PhD thesis, Universität Leipzig, 2003
[3] D. Freude et al.: Solid. State. Nucl. Magn. Reson. **20**, 46 (2001)

3.9 Long-Time Scale Molecular Dynamics of Constrained Fluids Studied by NMR

F. Grinberg

Soft matter systems like liquid crystals, polymers, colloids or biomembranes are characteristic of the orientational molecular order on the meso- and macroscopic length scales. Individual or collective molecular motions in these substances tend to range over many time decades. This in turn gives rise to extremely slow spin relaxation mechanisms in the range of milliseconds and longer. The most illustrative examples can be found with the confined liquid crystals [1] widely used in the electro-optical devices. Another example is given by elastomers in which ultra-slow chain relaxation modes are associated with the presence of chemical cross-links [2].

Addressing molecular dynamics of complex fluids by the NMR techniques raise a problem of decomposing numerous overlapping stochastic processes contributing to spin relaxation in the same frequency or time ranges. In our work we investigate the effects produced by nano- to micrometer scale constraints on dynamical and structural properties of organised fluids using a combination of several NMR techniques: stimulated echo studies [1], 2D-exchange spectroscopy [3], temperature and frequency dependent measurements of the relaxation rates [3, 4] and diffusion studies with help of Pulsed Field Gradient NMR [5]. Experimental data are supported by the Monte-Carlo simulations.

In confined liquid crystals, the cavity constraints are found to strongly affect molecular collective and non-collective orientational fluctuations both below and above the nematic-isotropic transition. The correlation length of the surface-induced order is determined. In elastomers, ultraslow chain relaxation modes with correlation times of the order of a few milliseconds were monitored by measuring the dipolar-correlation effect on the stimulated echo [2]. The mean squared fluctuation of the residual dipolar coupling constant shows a strong dependence on the cross-link density of rubber materials and suggests a new contrast parameter for NMR mapping [6].

Acknowledgements: I cordially thank Prof. R. Kimmich and Prof. M. Vilfan for fruitful multi-year co-operation. Financial support by the Deutsche Forschungsgemeinshaft (DFG) and the Ministerium für Wissenschaft, Forschung und Kunst Baden-Württemberg is gratefully acknowledged.

[1] F. Grinberg et al.: in *NMR of Ordered Liquids* ed. by E.E. Burnell, C.A. de Lange (Kluver Academic, Dordrecht 2003)

[2] F. Grinberg: in *Handbook of Modern Magnetic Resonance* ed. by G. Webb (Kluwer Academic, Dordrecht 2005)
[3] F. Grinberg: in *Nato Science Series "Magnetic Resonance in Colloid and Interface Science"* ed. by J. Fraissard, O. Lapina (Kluver, Dordrecht 2002)
[4] R. Kimmich: *MR: Tomography, Diffusometry, Relaxometry* (Springer, Heidelberg 1997)
[5] J. Kärger: Diffusion Fundamentals **1**, 5.1 (2005)
[6] F. Grinberg et al.: J. Magn. Reson. **159**, 87 (2002)

3.10 2D Correlation and Exchange NMR Spectroscopy in Organic Microporous Materials

P. Galvosas, Y. Qiao*, M. Schönhoff†, P.T. Callaghan*

*MacDiarmid Institute for Advanced Materials and Nanotechnology,
Victoria University of Wellington, New Zealand
†Institut für Physikalische Chemie, Westfälische Wilhelms-Universität Münster

Two-dimensional (2D) NMR methods for the investigation of correlation and exchange have been introduced recently [1] and applied to a wide range of different systems. Here we report on the use of diffusion-diffusion correlation spectroscopy (DDCOSY), diffusion-relaxation correlation spectroscopy (DRCOSY) and diffusion-diffusion exchange spectroscopy (DEXSY) for two different samples.

Diffusion exchange of dextran with a molecular weight of 77 kDa through polyelectrolyte multilayer (PEM) hollow capsules consisting of four bilayers of polystyrene sulfonate/polydiallyldimethylammonium chloride (PSS/PDADMAC) has been investigated using DEXSY and DRCOSY [2]. Results obtained in DRCOSY experiments show that the diffusion process of dextran 77 kDa exhibits an observation time dependence suggesting a diffusion behavior restricted by confinement. Results from DEXSY experiments show around 1.5 % of dextran 77 kDa diffuse exchange through the capsules at a mixing time of 200 ms (Fig. 3.10a) but no exchange process could be observed at a mixing time of 20 ms. This quantitative information may be used in designing PEM capsules as drug carriers.

Anisotropic diffusion of water in chive (Allium Schoenoprasum) tissue has been investigated using DDCOSY and DRCOSY [3]. Corresponding 1D measurements confirm independently the results of the two-dimensional investigations and reveal separate distributions of T_2 and D values. The challenge is to understand how these components relate to the various forms of water compartmentalization associated with the different chive cells. One means of making such assignments is via diffusion anisotropy. The 1D diffusion measurements made both parallel and perpendicular to the chive axis, reveal the anisotropy properties. We are able to correlate these compartments with the result of the DRCOSY using the values of the diffusion coefficient, relaxation time and peak intensity. On the other hand the DDCOSY method resolves the different components of the diffusion tensor (Fig. 3.10b) and the experiment can be used to show how these various water peaks are related to cell shape and orientation.

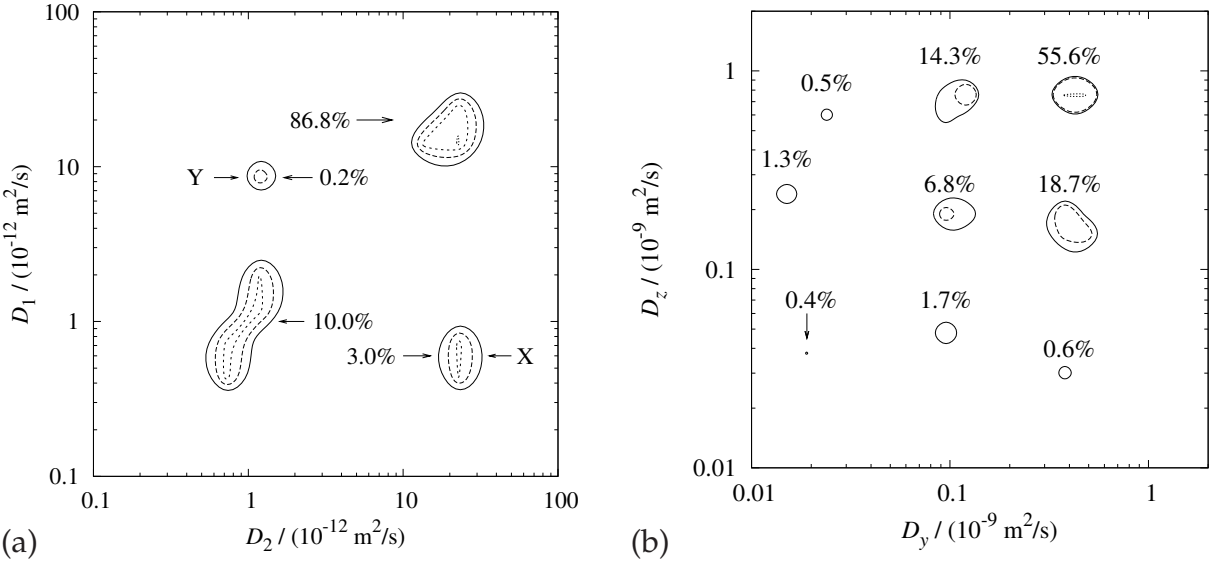

Figure 3.10: Diffusion exchange marked with X and Y of dextran in PSS/PDADMAC capsules (**a**) and diffusion-diffusion correlation in chive in z and y direction respectively (**b**).

[1] Y.-Q. Song et al.: J. Magn. Reson. **154**, 261 (2002)
[2] Y. Qiao et al.: J. Chem. Phys. **122**, 214 912 (2005)
[3] Y. Qiao et al.: Biophys. J. **89**, 2899 (2005)

3.11 Influence of the Surface of Zeolite Crystals on Molecular Transport: PFG NMR Measurements and Computer Simulations

M. Krutyeva, S. Vasenkov*, J. Kärger

*Department of Chemical Engineering, University of Florida, Gainesville, USA

One of the main applications of nanoporous materials is in mass separations. Sorption kinetics in such systems is strongly influenced by surface properties of building blocks (crystals). For a quantitation of the sorption process one may introduce, in complete analogy to its classical definition, a sticking coefficient. The sticking coefficient represents the probability that, on encountering the particle surface, a molecule will be captured by the particle and will enter its intraparticle space, rather than being rejected to continue its trajectory in the space between the particles [1, 2]. In addition to its practical relevance for the performance of nanoporous materials in separation and catalysis, the sticking coefficient represents a fundamental quantity of molecular dynamics on interfaces.

The influence of the surface of zeolite crystals on molecular exchange between the inter- and intracrystallin volumes was studied. The studies were performed by using pulsed field gradient (PFG) NMR in combination with dynamic Monte Carlo simulations.

Zeolite NaCaA, whose surface was modified by TEOS treatment, was used as a model system. Diffusion of CH_4 and C_2H_8 in that system was studied by using PFG NMR. The PFG NMR data show large surface barriers in the CaNaA zeolite treated by TEOS. This behavior represents the limiting case when the sticking coefficient is small. Non-treated samples show small surface barriers. In this case the fraction of guests leaving the intracrystalline volume during the observation time and the effective intracrystallin diffusion coefficient can be estimated by using the tracer desorption technique [3]. However, the sticking coefficient can not be obtained directly from this type of PFG NMR experiment.

It was demonstrated that Monte Carlo simulations can be applied to estimate a sticking coefficient from the PFG NMR data. Monte Carlo simulations were performed by using a two-dimensional lattice model. As simulation parameters, the elementary diffusion step and the probability of crossing the boundary of a zeolite crystal were chosen. Dependencies of the effective diffusion coefficient D and of the fraction of the particle N_{rem} that remained in crystals after a certain tracer-exchange time on this time have been studied in detail.

It was shown that D and N_{rem} do not depend on the diffusion step length. It implies that the simulation results do not depend on the generally unknown diffusion step length.

This work demonstrates that combined application of dynamic (lattice) MC simulations and PFG NMR measurements can lead to new insights into the details of translational dynamics of guest molecules in interaction with the external surface of microporous materials.

[1] P.G. Ashmore: *Catalysis and Inhibition of Chemical Reactions* (Butterworth, London 1963)
[2] J.-M. Simon et al.: J. Phys. Chem. B. **109**, 13 523 (2005)
[3] J. Kärger et al.: *Diffusion in Zeolites*, (Wiley & Sons, New York 1992)

3.12 Phase Transitions and Dynamics in Nanoporous Materials

R. Valiullin, A. Khokhlov, S. Naumov, M. Dvoyashkin, J. Kärger

Exploration of physical phenomena on nanoscalic length-scale is one of the hot topics of the modern science. Phase transitions and molecular dynamics under mesoscalic confinement are among these topics. The present studies were aimed in a deeper understanding of the condensation/evaporation and the melting/freezing transitions with a particular goal focused on the clarification of internal dynamics leading to the hysteresis phenomenon.

Our previous experimental studies revealed the occurrence of diffusivity hysteresis in line with adsorption hysteresis in various mesoporous materials[1]. Here, this phenomenon has been further explored on the basis of a comparative study of molecular transport characteristics in mesopores using microscopic (pulsed field gradient NMR) and macroscopic (NMR-based uptake measurements) techniques. The obtained self-consistent set of experimental data unequivocally points out that (i) out of the

adsorption hysteresis region the uptake is well described by the diffusion-controlled model; (ii) in the hysteresis region a slowing down of the uptake is observed. The latter is discussed within the activated-dynamics scenario [2], inherent to the random-field Ising systems [3]. Series of experiments where desorption was initiated by changing temperature have been performed and used to make conclusions about the character of the evaporation transition in random nanoporous materials (Fig. 3.11).

The origin of the melting/freezing hysteresis in porous materials is also far from beeing understood [4]. There exist three frequently used approaches relating the hysteresis phenomenon (i) to nucleation delay for freezing, (ii) to geometrical hindrance of the solid-front propagation, and (iii) to the existence of free-energy barriers separating non-equilibrium phases in pores from the equilibrium ones. In the present work, this issue is

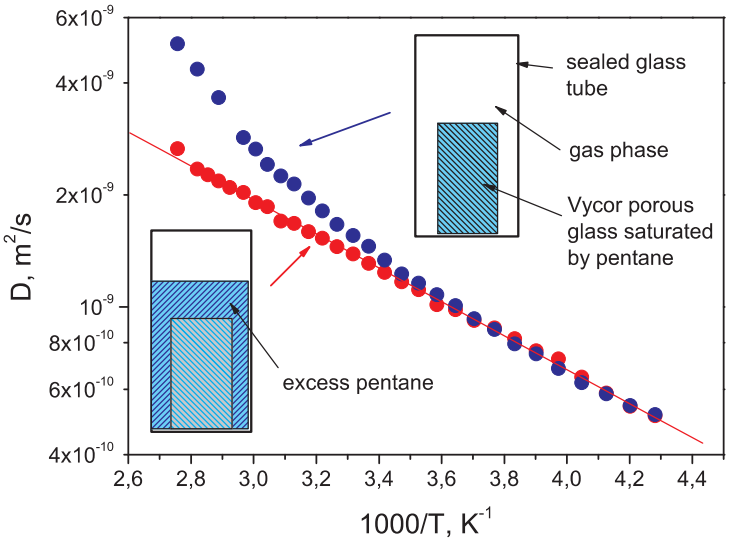

Figure 3.11: Temperature dependencies of the self-diffusion coefficient D of pentane in Vycor porous glass. By the blue and red points the diffusivities measured without and with excess bulk pentane phase are shown, respectively.

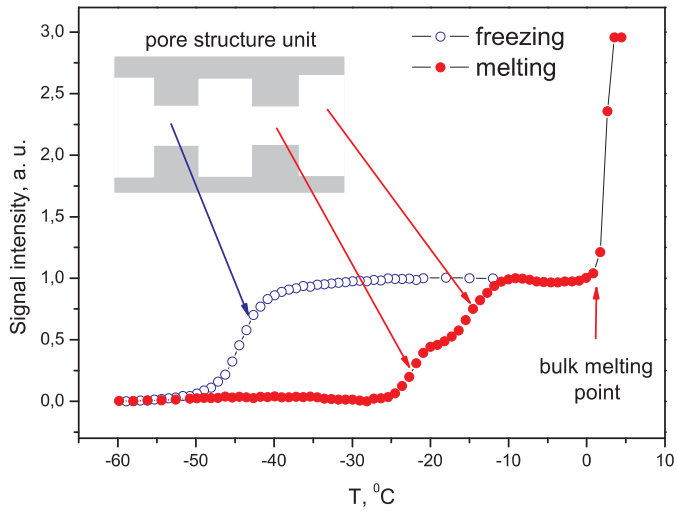

Figure 3.12: Freezing and melting transitions of nitrobenzene in porous silicon with modulated structure.

addressed by using porous silicon with a well defined porous structure. Moreover, use of specific preparation conditions allowed us to obtain channel-like pores with alternating cross-section. Using the NMR-cryoporometry method, two melting transitions corresponding to different pore size has been established. However, only one freezing transition has been located at the temperature expected for freezing of the smaller pores (Fig. 3.12). Thus, this finding unveils the significance of a pore-blocking effect for, at least, materials with the characteristic dimensions of the pore units used in this work.

[1] J. Kärger et al.: New J. Phys. **7**, 1 (2005)
[2] H.J. Woo, P.A. Monson: Phys. Rev. E **67**, 041 207 (2003)
[3] D.S. Fisher: Phys. Rev. Lett. **56**, 416 (1986)
[4] O. Petrov, I. Furó: Phys. Rev. E **73**, 011 608 (2006)

3.13 Computer Simulations and Analytical Calculations on the Influence of the Crystal Boundaries on the Exchange of Molecules between Zeolite Nanocrystals and their Surroundings

A. Schüring, J. Gulín-González*, S. Vasenkov†, S. Fritzsche, J. Kärger

*Department of Mathematics, University of Informatics Sciences, La Habana, Cuba
†Department of Chemical Engineering, University of Florida, Gainesville, USA

Molecular dynamics simulations are applied to study the influence of crystal boundaries on the overall diffusional transport of molecules in nanoporous crystals. Boundary effects are expected to be of importance if the crystals are small, i.e. if the ratio of surface to volume is high. This is the case e.g. in heterogeneous catalysis, where relatively small catalyst particles are used, and, furthermore, in currently developed hierarchically ordered porous materials [1] which enable a fast transport of molecules to the catalytically active zones of microporosity through a mesoporous channel system.

The investigations follow two main lines, where we distinguish between the cases of normal diffusion and single-file diffusion. In the latter case, the particles in the channel are too large to mutually exchange their positions. Therefore, the order of the particles is conserved as long as they stay in the channel.

A novel boundary effect, reported in [2, 3] for single-file systems, is verified by MD simulations [4] and quantified by analytical calculations [5]. An example for the observed boundary effect in single-file systems is shown in Fig. 3.13a. The concentration profiles of particles obeying single-file diffusion are flat near the boundaries. Two diffusion mechanisms occuring in parallel were found to be responsible for the boundary effect. On the one hand, the exchange of the particles in the center of the channel is possible only by a collective movement of the whole "chain" of particles (center-of-mass diffusion), because the order of the particles within the channel is conserved. On the other hand, each particle can move within a certain range relative to the center of mass of all particles in the channel. Therefore, particles near the boundaries can escape

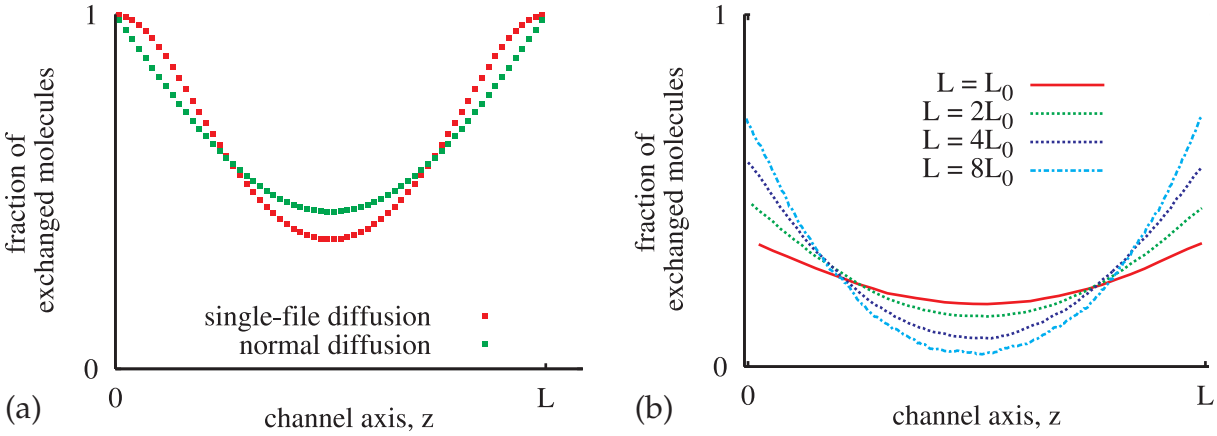

Figure 3.13: Boundary effects occuring im the cases of single-file diffusion (**a**) and normal diffusion (**b**). In the case of single-file diffusion, the concentration profiles have a shape that deviates from those of normal diffusion. In the case of normal diffusion, the influence of the permeability of the surface was studied. Flat concentration profiles indicate a low permeability and limitation of the overall transport by the surface.

the channel on a time scale shorter than expected by the diffusion coefficient of the center-of-mass of the chain of particles.

In the second line of the project, the passage of molecules through the crystal margins is studied for the case of normal diffusion. The quantity describing the ability of molecules to overcome the boundary region between gas phase and crystal is referred in [6] to as permeability, α, and is defined by specifying the boundary condition for Fick's law,

$$J(t) = \alpha(C_0 - C(t)) \ ,$$

where it is assumed that the flux $J(t)$ through the surface is proportional to the difference between the concentration C_0 necessary to maintain equilibrium with the surrounding gas phase and the actual concentration $C(t)$ in the crystal margin. If the ratio $\alpha L/D$ (L is the length of the crystal and D the intracrystalline diffusion coefficient) is low, flat profiles may be observed as can be seen in Fig. 3.13b. In this case the transport is limited by the surface. With increasing crystal length L, the influence of the surface becomes less important and the intracrystalline diffusion coefficient limits the transport. This can be deduced from the bowed shape of the profiles. The analytical investigations have revealed a fundamental dependence of α on the energy difference between the inner part of the crystal and the gas phase [7].

[1] Y. Tao, H. Kanoh: J. Am. Chem. Soc. **125**, 6044 (2003)
[2] P.H. Nelson, S.M. Auerbach: J. Chem. Phys. **110**, 9235 (1999)
[3] S. Vasenkov, J. Kärger: Phys. Rev. E **66**, 0526011 (2002)
[4] A. Schüring et al.: J. Phys. Chem. B, **109**, 16711 (2005)
[5] S. Vasenkov et al.: Langmuir submitted
[6] J. Crank: *The Mathematics of Diffusion* (Clarendon Press, Oxford 1956)
[7] J. Gulín-González et al.: in preparation

3.14 Transport Properties of Guest Molecules in Modified SBA-15 Materials Studied by Pulsed Field Gradient NMR

P. Kortunov, F. Grinberg, J. Kärger, E. Vansant*

*Laboratory of Adsorption and Catalysis, University of Antwerp, Belgium

Catalysts are one of the most important materials in the modern industry, accelerating required chemical reactions and conversion of initial substances to final products. Efficiency of catalysts often strongly depends on the relation between the intrinsic reaction rates and the adsorption and/or desorption rates of the reactants. Understanding molecular diffusion in nano- and mesoporous solids is crucial for developing materials with improved chemical and optimized transport properties.

The porous SBA-15 materials (Fig. 3.14) attract an increasing interest in catalytic applications owing to their specific internal structure. The straight non-intersecting channels with diameters of several nanometres build up a favourable porous space facilitating an enhanced transfer of substances towards chemically active centres and an easy removal of the reaction products. This work represents a comprehensive study of guest diffusion in a series of SBA-15 materials using the pulsed field gradient nuclear magnetic resonance (PFG NMR) technique [1]. The investigated samples include reference SBA-15 and samples modified by vanadium silicalite (VS) [2].

Diffusion of guest molecules was monitored at two different lengths scales ($1-2\,\mu m$ and $50\,\mu m$) using appropriate experimental conditions. In the first group of experiments, diffusivities of molecules (*n*-hexane) were measured as a function of the external gas pressure (Fig. 3.15). The molecular displacements were much larger than the mean size of the particles providing conditions for a (potential) fast exchange between the meso- and macropores. In the second group of experiments, the liquid (benzene) in the macropores was frozen so that molecular diffusion was restricted to mesopores only. Crucial effects produced by the presence of VS on molecular diffusivities were observed

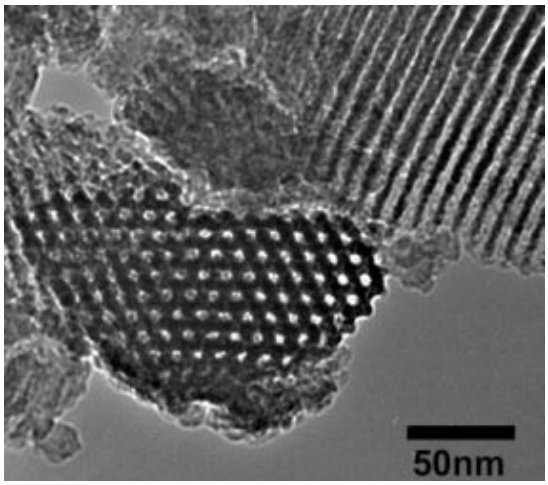

Figure 3.14: View on the hexagonally ordered channels in SBA-15

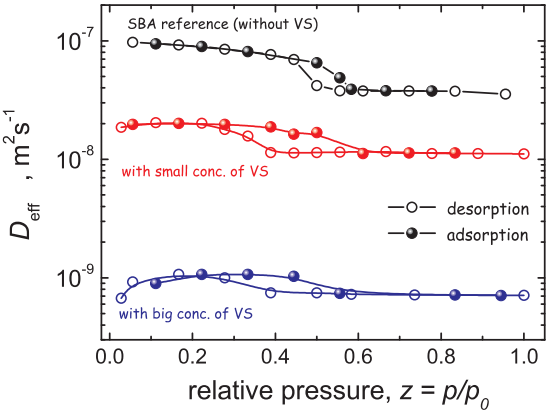

Figure 3.15: Self-diffusivities of *n*-hexane in SBA-15 with various contents of vanadium silicalite (VS) at room temperature as a function ot the applied *n*-hexane pressure

in both groups of experiments. The results are discussed in terms of structural changes occurring in modified samples and barriers to diffusion arising at the particle surface.

[1] J. Kärger et al.: Adv. Magn. Reson. **12**, 2 (1988)
[2] V. Meynen et al.: Chem. Commun. **117**, 898 (2004)

3.15 Time- and Space-Resolved Study of Methanol Sorption on Ferrierite Crystals Using Interference and IR Microscopy

P. Kortunov, C. Chmelik, J. Kärger, R.A. Rakoczy*, D.M. Ruthven†, Y. Traa*, S. Vasenkov‡, J. Weitkamp*

*Institute of Technical Chemistry, University of Stuttgart
†Department of Chemical and Biological Engineering, University of Maine, USA
‡Department of Chemical Engineering, University of Florida, Gainesville, USA

The present work is devoted to the study of sorption kinetics of methanol in Ferrierite crystals using the Interference Microscopy (IFM) and the IR Microscopy (IRM) techniques. These techniques provide the possibility to image the adsorbate distribution within a single crystal during the sorption process: Transient intracrystalline profiles reflect the distribution of molecular concentration inside the crystal at a certain time. The integration of such profiles over the entire crystal dimension provides the information identical to that of conventional uptake and release measurements. In the present work, we illustrate the benefit of our spatially resolved experiments in comparison with the conventional way of uptake measurement.

The two-dimensional concentration profiles inside the Ferrierite crystal (Fig. 3.16c) with a high spatial resolution (of about 0.5 μm) were measured using IFM [1]. Gaseous methanol was used as an adsorbate, which at different vapor pressures was brought into contact with the Ferrierite crystals [2]. The data for more than twenty single Ferrierite crystals were obtained and used for the data analysis. It is worth noting that the local

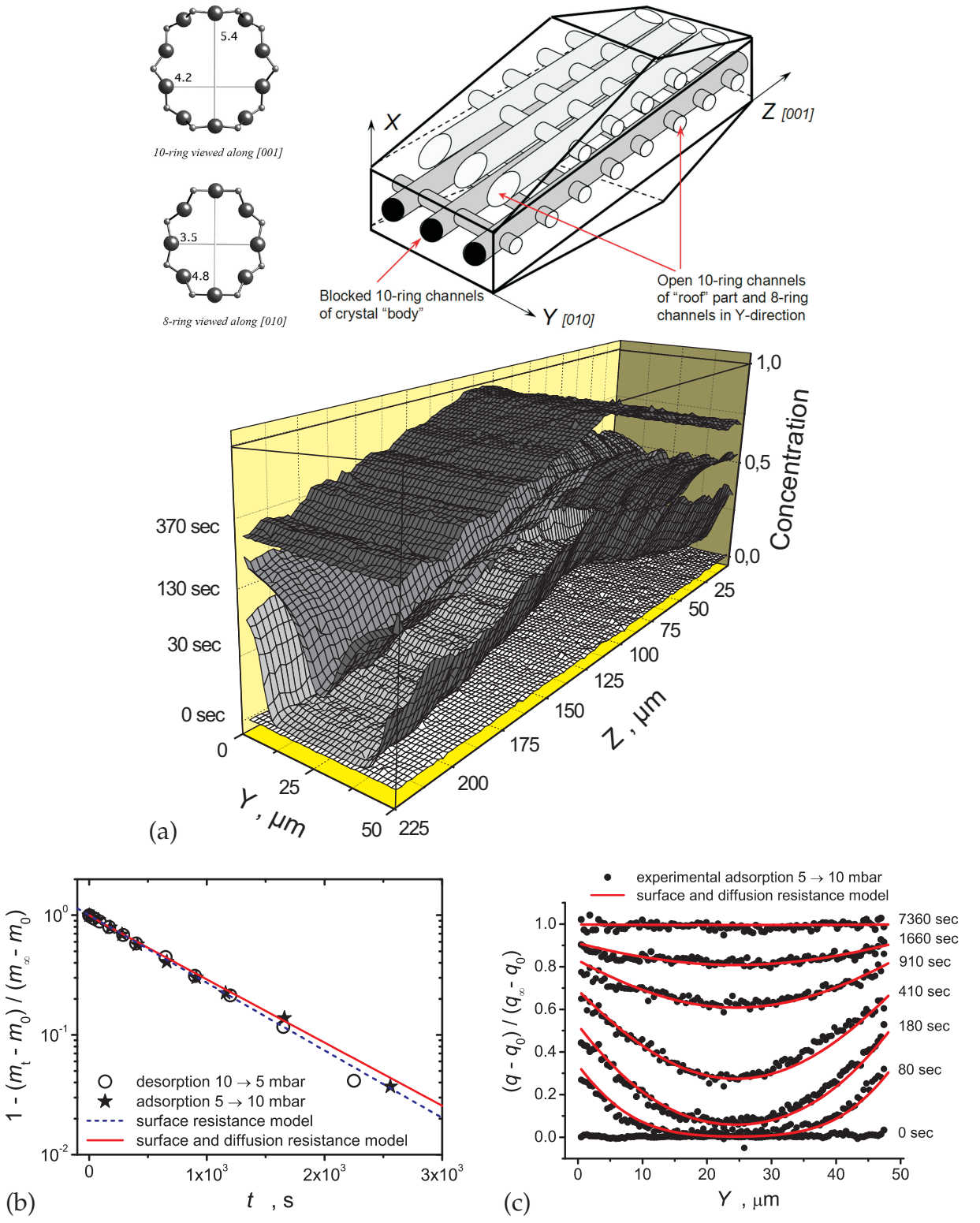

Figure 3.16: Shape of the ferrierite crystal and 2D-concentration profiles for the entire crystal for a large pressure step (0 – 80 mbar) (**a**), experimental adsorption and desorption curves plotted in semi-logarithmic scales (**b**) and adsorption concentration profiles in the y-direction near the edge of the crystal ($z = 2\,\mu$m) for the pressure step 5 – 10 mbar at different times (**c**). Also the theoretical curves calculated using the surface-resistance model and the surface- and diffusion-resistance model, respectively, are shown.

concentration of adsorbate molecules in the crystal can also be measured using IR microscopy [3].

Adsorption/desorption concentration profiles and kinetics were analyzed in the frame of three theoretical models: the surface-resistance model, the diffusion-resistance model and the surface- and diffusion-resistance model [4]. It was found that the data on sorption kinetics (Fig. 3.16b) can be well described by both models within the given experimental precision. At the same time, the spatially resolved data (the concentration profiles in (Fig. 3.16c) are satisfactorily described only within the surface- and diffusion-resistance model. The diffusion coefficient D of methanol in the 8-ring channels of the Ferrierite crystals and the surface mass-transfer coefficient α were determined according to this model.

[1] J. Kärger et al.: *Adsorption Science and Technology, Proc. 2nd Pacific Conf. Adsorpt.*, ed. by D.D. Do (World Scientific, Singapore 2000) p 324
[2] W.M. Meier, D.H. Olson: *Atlas of Zeolite Structure Types*, 3rd Edition (Butterworth-Heinemann, 1992) p 98
[3] M. Hermann et al.: Stud. Surf. Sci. Catal. **94**, 131 (1995)
[4] J. Crank: *Mathematics of Diffusion* (Oxford University Press, London 1956)

3.16 The New Options of Interference Microscopy for Evaluating the Local Molecular Diffusivities inside Porous Crystals

P. Kortunov, L. Heinke, J. Kärger, R.A. Rakoczy*, Y. Traa*, S. Vasenkov†, J. Weitkamp*

*Institute of Technical Chemistry, University of Stuttgart
†Department of Chemical Engineering, University of Florida, Gainesville, USA

The information about the molecular mobility in porous crystals is highly interesting from both practical and fundamental points of view. There are a number of techniques providing the opportunity to directly measure molecular mobility on different displacement scales. In contrast to such techniques, the local diffusivity can be also estimated from the concentration distribution inside a chosen crystal by using Fick's Second Law of Diffusion:

$$\frac{\partial c}{\partial t} = \frac{\partial}{\partial x}\left[D\,(c,x)\,\frac{\partial c}{\partial x}\right] = D\,(c,x)\,\frac{\partial^2 c}{\partial x^2} + \frac{\partial D\,(c,x)}{\partial c}\cdot\left(\frac{\partial c}{\partial x}\right)^2 .$$

In the present work we have demonstrated the application of this idea by using the unique benefit of the Interference Microscopy technique to measure the local molecular concentrations with a high spatial und temporal resolution (Fig. 3.17). The local molecular diffusivities have been estimated in the 8-ring channels of Ferrierite crystals in dependence on the molecular concentration of the chosen crystal. The surface resistance can be estimated by considering the flux through the surface. We have checked the estimated values of diffusivity and surface permeability by comparison of the experimentally determined molecular concentration profiles with the concentration profiles

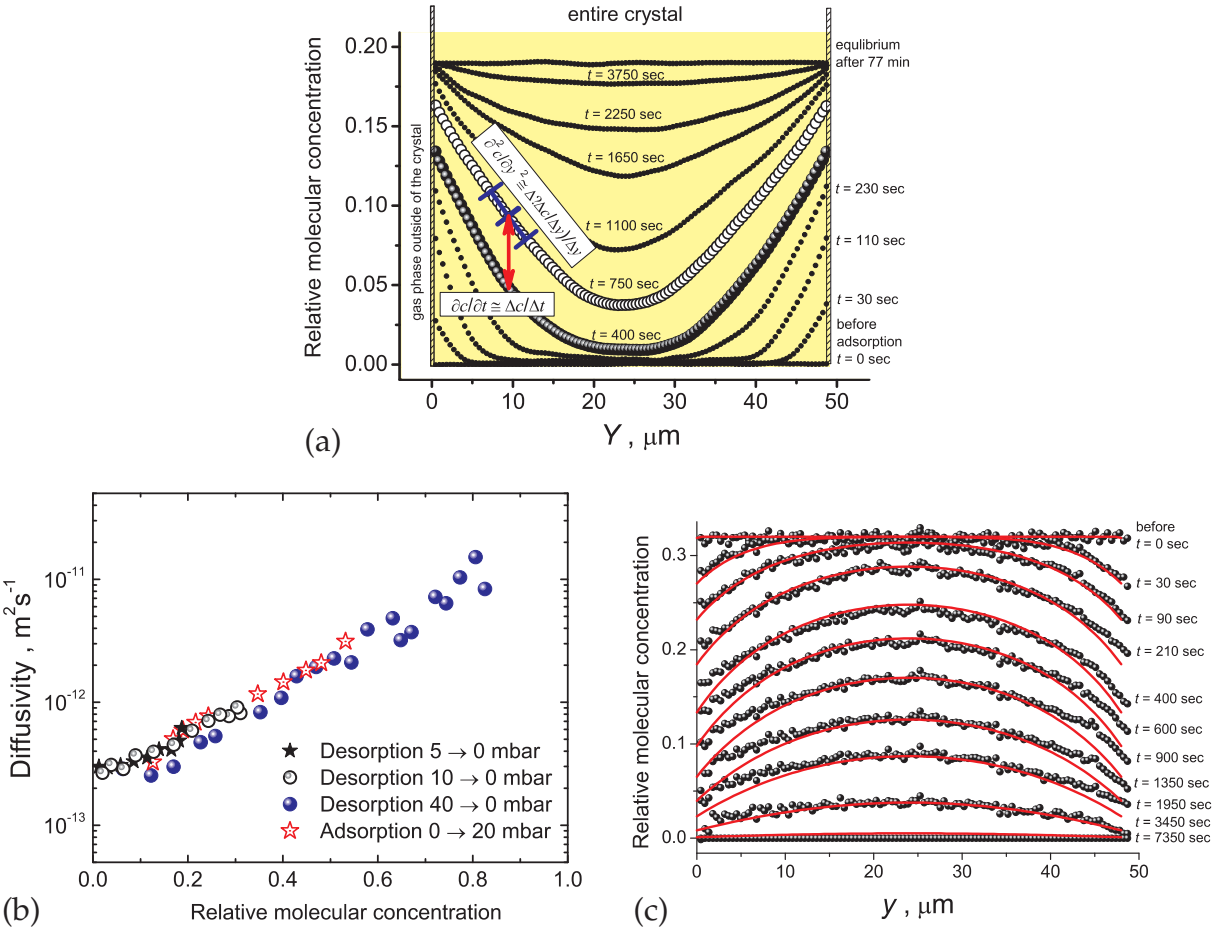

Figure 3.17: (**a**) The way of evaluation of a local molecular diffusivity by using Fick's Second Law from one-dimensional intracrystalline concentration profiles measured by Interference Microscopy during uptake. (**c**) The experimentally measured concentration profiles (*points*) and calculated profiles (*lines*) by using estimated concentration dependence of molecular diffusivity of methanol in the 8-ring channels of Ferrierite (**b**).

calculated using the estimated functions $D(c)$ and $\alpha(c)$. It turned out that the intracrystalline concentration profiles can in fact be satisfactorily fitted by using the calculated values of diffusivity and permeability.

3.17 Interference Microscopy Study of Molecular Diffusion in the One-Dimensional Channels of a Novel MOF Material

P. Kortunov, M. Arnold*, J. Kärger, J. Caro*

*Institute of Physical Chemistry and Electrochemistry, University of Hannover

For many applications in catalysis or separation ordered (ultra)-microporous materials are of crucial importance. During the last few years extensive research was done in the field of metal-organic frameworks (MOFs) [1, 2]. The potential use of MOFs is

characterised by their unique properties of high stability, specific structure and organic functionality.

In the present work for the first time patterns of intracrystalline concentration profiles of guest molecules in porous $Mn(HCO_2)_2$ are reported, proving the accessibility and orientation of the one-dimensional channels. The uptake rates and intracrystalline concentration profiles were measured by interference microscopy.

The 2D intracrystalline concentration profiles for adsorption and desorption of methanol at different pressure steps (Fig. 3.18) indicate uptake along x direction only. Local transport diffusivity within the crystal channels and permeability of barriers on the crystal surface were estimated. The molecular diffusivity evaluated in the middle part of the chosen crystal from the Fick's Second Law does not depend on molecular

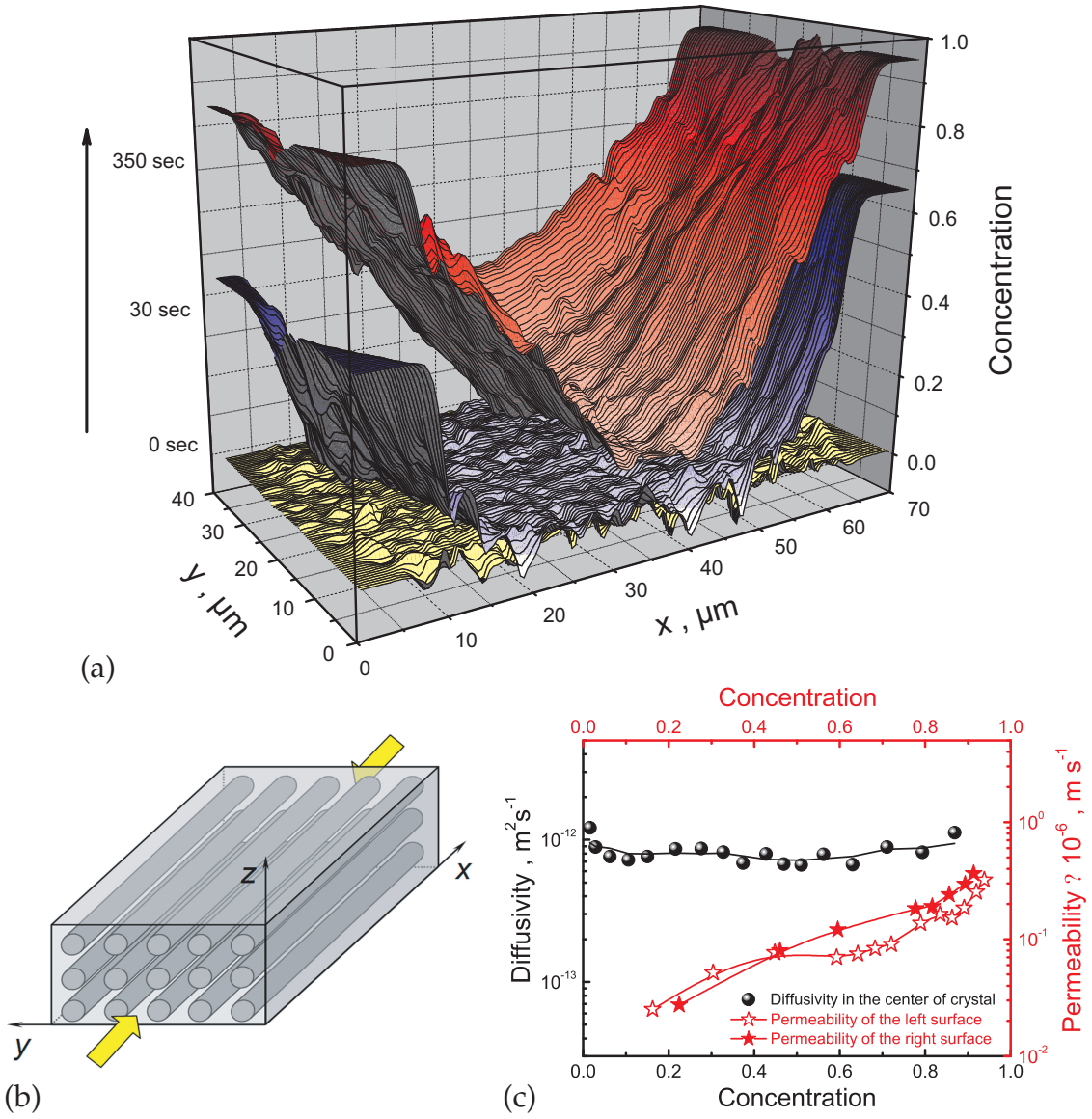

Figure 3.18: Intracrystalline concentration profiles for adsorption of methanol into MOF crystal measured by IFM (**a**). One dimensional pore structure of the MOF crystals (**b**). Estimated diffusivity of methanol molecules inside pores of MOF crystal and surface permeability as function of molecular concentration (**c**).

concentration and its average value ($9.15\times10^{-13}\,m^2s^{-1}$) is in good agreement with data obtained from the uptake rate ($1.05\times10^{-12}\,m^2s^{-1}$). We are surprised to obtain a concentration dependence of the surface permeability (Fig. 3.18c). This result requires further investigations.

[1] O.M. Yaghi et al.: Nature **423**, 705 (2003)
[2] D.N. Dybtsev et al.: J. Am. Chem. Soc **126**, 32 (2004)

3.18 Molecular Diffusion in the Three-dimensional Pore Structure of SAPO STA-7 Materials. An Interference Microscopy Study

P. Kortunov, M.J. Castro*, D. Tzoulaki, J. Kärger, P.A. Wright*

*University of St. Andrews, Scotland, UK

Molecular separation in pores of crystals plays a very important role in catalytic industry. Molecules of various reactants can use their own, specific crystal channel to reach the place where they meet. The product molecules may leave the crystal by again different channels. In this way, a minimum of mutual interference between the reactant and product molecules is ensured. In order to control such a complex diffusion processes one should know the transport properties of each system of crystal pores.

In the present work, one kind of crystals was studied, namely SAPO STA-7, which contains a three-dimensional channel network, (Fig. 3.19b). Interference microscopy (IFM) was used for these experiments. It allows to monitor the intracrystalline concentration distribution for a selected crystal during molecular adsorption/desorption with an unprecedented spatial resolution.

The obtained two-dimensional intracrystalline concentration profiles (Fig. 3.19a) for adsorption of the guest molecules (methanol) reveal that intracrystalline diffusion is the rate-determining process. Owing to the ability of Interference Microscopy to measure spatially resolved molecular concentrations inside a crystal, we can separate molecular uptake in different direction. 1D concentration profiles measured in the centre of the crystal along y-direction show that the concentration front in y-direction reaches the centre after approximately 70 seconds from the beginning of adsorption. It means that, for sufficiently shorter times, we can separate and detect adsorption in each direction. This is achieved by subtracting the integral concentration in x-direction from the total concentration profiles. Molecular diffusivity in each system of pores can be estimated by using the formula for diffusion-limited uptake.

The estimated diffusivities show almost identical values in x- and y-direction ($D_x = 4.5\times10^{-14}\,m^2s^{-1}$ and $D_y = 4.2\times10^{-14}\,m^2s^{-1}$) while the transport diffusivity in z-direction is two times larger ($D_z = 8.5\times10^{-14}\,m^2s^{-1}$). Most likely, it is related to the larger size of pores in this direction. The average diffusivity estimated from uptake curve for the whole crystal ($D_{whole} = 6.9\times10^{-14}\,m^2s^{-1}$) may be reconstructed from the data for different directions, but it is clearly insufficent to provide the exact information about molecular mobilities in different directions.

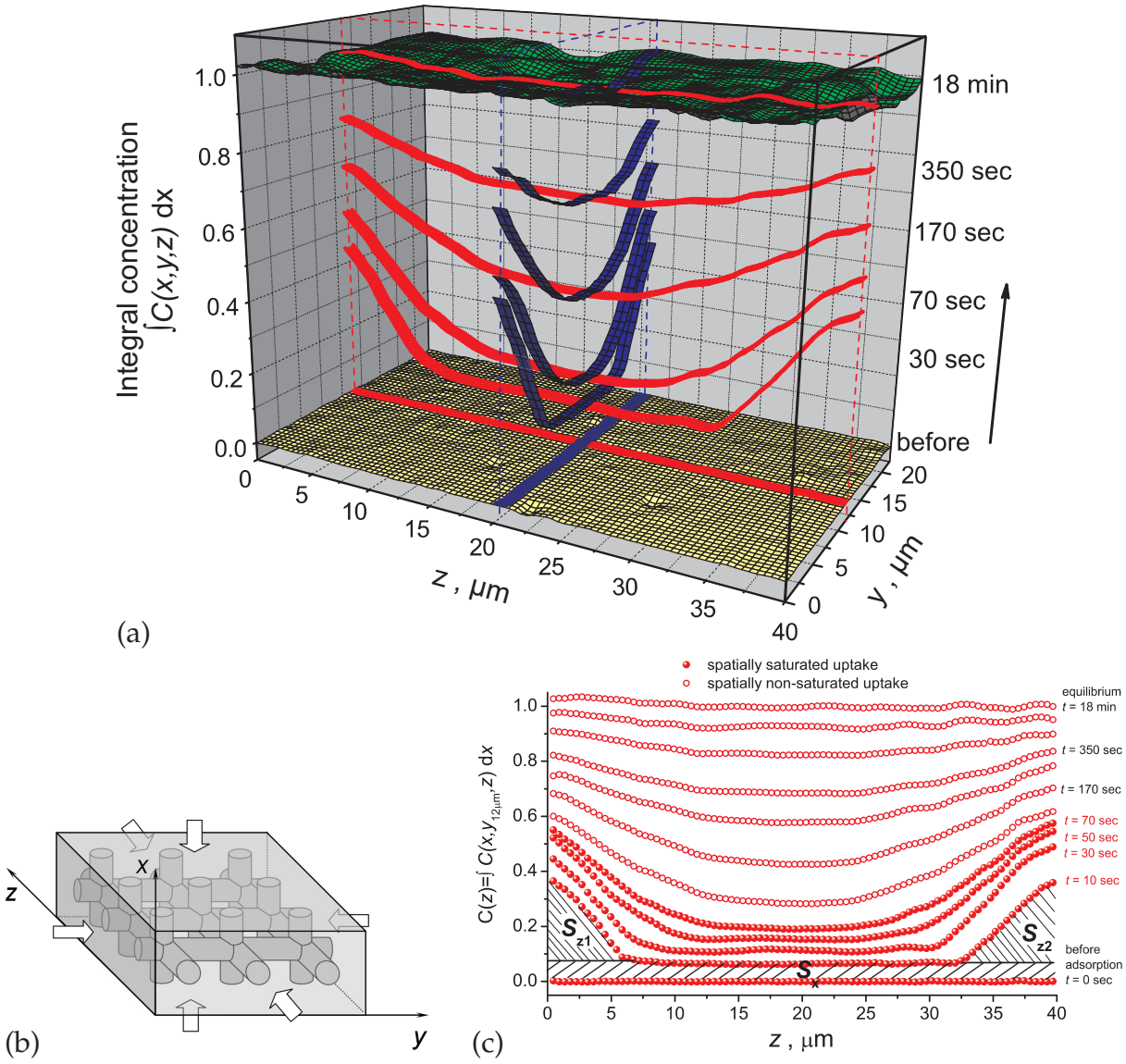

Figure 3.19: Schematical description of SAPO STA-7 crystal (**b**), evolution of concentration profiles in the center of the crystal along *y*- and *z*-direction at different time of adsorption (**a**), 1D profiles along *z*-direction in the center of the crystal (**c**) and the relative amount of molecules adsorbed in the channels in *z*-direction (shown by *areas* S_{z1} and S_{z2}), and in *x*-direction (*area* S_x).

3.19 Funding

Alkan- und Alken-Aktivierung in der heterogenen Säurekatalyse. In situ-^{13}C und ^{1}H MAS NMR-Untersuchungen der Kinetik des Isotopen-Scramblings (^{13}C, ^{2}H) im Reaktionsverlauf
Prof. Dr. D. Freude
DFG-Project FR 902 / 15-1

Combined NMR Studies of Diffusion and Reaction
Prof. Dr. D. Freude
DFG-Project GRK 1056/1

Anwendungen der Doppelrotations- und Multiquanten-Messtechnik für Hochfeld-NMR-Untersuchungen an O-17-Kernen in porösen Festkörpern
Prof. Dr. D. Freude, Dr. H. Ernst
DFG-Project FR 902/16-1

Untersuchung der Protonen-Beweglichkeit in H-Zeolithen mit SFG NMR und MAS NMR im Temperaturbereich bis 800 K
Prof. Dr. D. Freude, Dr. H. Ernst
DFG-Project FR 902 / 12-1

Computersimulation und analytische Untersuchungen zum Einfluss der Kristallgrenze auf den Austausch von Gastmolekülen zwischen Zeolith-Nanokristallen und der Umgebung
Dr. S. Fritzsche, Prof. Dr. S. Vasenkov
DFG-Project FR 1486/2-1, SPP 1155

Reaktion und Diffusion in Single-File Netzwerken: Computersimulationen und statistisch-thermodynamische Untersuchungen.
Prof. Dr. J. Kärger
DFG-Project KA 953/15-2

Studying Zeolitic Diffusion by Interference and IR Microscopy.
Prof. Dr. J. Kärger
DFG-Project KA 953/18-1, International Research Group "Diffusion in Zeolites"

Bestimmung mikroskopischer Kenngrößen der Molekültranslation in Schüttungen nanoporöser Partikel mittels PFG NMR und Monte-Carlo-Simulation.
Prof. Dr. J. Kärger, Prof. Dr. S. Vasenkov
DFG-Project KA 953/19-1

Confinement Effects on Diffusion and Reaction in Zeolites, Studied by Dynamic MC Simulations, PFG NMR and Interference/IR Microscopy.
Prof. Dr. J. Kärger
DFG-Projekt GRK 1056/1, International Research Training Group “Diffusion in Porous Materials”

In situ study and development of processes involving nanoporous solids
Prof. Dr. J. Kärger
EU-Project NMP3-CT-2004-500895

Molecular diffusion in nanoporous materials
Prof. Dr. J. Kärger, Prof. Dr. H. Jobic
DFG-CNRS-Project KA 953/14-1

PFG NMR investigations on formulated catalysts; Bestimmung von Diffusionskoeffizienten an Katalysatoren
Prof. Dr. J. Kärger, Dr. F. Stallmach
BASF AG

Fourier-Transform-PFG-NMR mit starken Feldgradientenimpulsen zur selektiven Selbstdiffusionsmessung.
Prof. Dr. J. Kärger, Dr. F. Stallmach
DFG-Projekt KA 953/16-1

Innovative Zugabestoffe für die Innere Nachbehandlung von Hochleistungsbeton unter Berücksichtigung der räumlichen und zeitlichen Wasserbilanz.
Prof. Dr. J. Kärger, Dr. F. Stallmach
DFG-Project KA 953/17-1

Intelligent design of nanoporous sorbents
Prof. Dr. J. Kärger, Prof. Dr. S. Vasenkov
EU-Projekt CT-2004-005503

Fluid transport in porous rocks and sediments from near-surface aquifers studied by NMR and MRI
Dr. F. Stallmach
DFG-Projekt GRK 1056/1, International Research Training Group "Diffusion in Porous Materials"

NMR and MRI studies of aquifer rocks; NMR- and MRI-Untersuchungen an Aquifergesteinen
Dr. F. Stallmach, Prof. Dr. J. Kärger
UFZ Halle/Leipzig GmbH

3.20 Organizational Duties

Jörg Kärger

- Ombudsman of Leipzig University
- Membership in the Programme Committee "Magnetic Resonance in Porous Media" (Bologna 2006), "Fundamentals of Adsorption" (Giardini Naxos, Sicily, Italy 2007), International Zeolite Conference (Peking 2007) and in the permanent DECHEMA committees Zeolites and Adsorption
- Membership in Editorial Boards: Microporous and Mesoporous Materials (European Editor); Diffusion Fundamentals (Online Journal, Editor); Adsorption
- Referee: Phys. Rev., Phys. Rev. Lett., Europhys. Lett., J. Chem. Phys., J. Phys. Chem., Langmuir, Micropor. Mesopor. Mat., PCCP, J. Magn. Res.
- Project Reviewer: Deutsche Forschungsgemeinschaft, National Science Foundation (USA)

Dieter Freude

- Director of the Magnetic Resonance Centre (MRZ) of Leipzig University
- Membership in Editorial Boards: Solid State NMR; Diffusion Fundamentals (Online Journal)
- Referee: Chem. Phys. Lett., J. Chem. Phys., J. Phys. Chem., J. Magn. Res., Solid State NMR

Farida Grinberg
- Membership in "AMPERE Division of Spatially Resolved Magnetic Resonance" Polish German Radiospectroscopy Group (PGRG)
- Membership in Editorial Boards: Diffusion Fundamentals (Online Journal, Editor)

Brigitte Staudte
- Referee: Micropor. Mesopor. Mat.

Sergey Vasenkov
- Referee: J. Am. Chem. Soc., Micropor. Mesopor. Mat.

Frank Stallmach
- Referee: J. Magn. Res., Micropor. Mesopor. Mat., Phys. Rev. Lett.

3.21 External Cooperations

Academic

- Acad. Sci. Czech. Republ., Heyrovsky-Inst. Phys. Chem., Czech Republic
  Dr. Kocirik, Dr. Zikanova
- Delft University, Inst.Chem. Tech., Delft, The Netherlands
  Prof. Kapteijn
- Institut de Recherches sur la Catalyse, CNRS, Villeurbanne, France
  Dr. Jobic
- Institut Francais du Petrole, Malmaison, France
  Dr. Methivier
- Max Planck Institut für Kohlenforschung, Mülheim
  Dr. Schmidt, Prof. Schüth
- Max Planck Institut für Metallforschung, Stuttgart
  Dr. Majer
- Russian Acad. Sci., Boreskov Inst. Catalysis, Siberian Branch, Novosibirsk, Russia
  Dr. Stepanov
- TU München, Lehrstuhl Technische Chemie 2
  Prof. Lercher
- Università di Sassari, Dipartimento Chimica, Sassari, Italy
  Prof. Demontis, Prof. Suffritti
- Universiät Eindhoven, Schuit Institute, Eindhoven, The Netherlands
  Prof. van Santen
- Universität Erlangen Nürnberg, Dept. Chem. Engin., Erlangen
  Prof. Emig, Prof. Schwieger
- Universität Hannover, Dept. Phys. Chem., Hannover
  Prof. Caro, Prof. Heitjans

- Universität Leipzig, Institut für Analytische Chemie, Leipzig
  Prof. Berger
- Universität Leipzig, Institut für Technische Chemie, Leipzig
  Prof. Einicke, Prof. Papp
- Universität Leipzig, Institut für Medizinische Physik und Biophysik, Leipzig
  Prof. Arnold, Prof. Gründer
- Universität Regensburg, Inst. Biophysik & Physikalische Biochemie, Regensburg
  Prof. Brunner
- Universität Stuttgart, Institut für Technische Chemie, Stuttgart
  Prof. Hunger, Prof. Weitkamp
- University Athens, Dept Chem. Engn., Athens, Greece
  Prof. Theodorou
- University of Amterdam, The Netherlands
  Prof. Krishna
- University of Maine, Dept. Chem. Engin., USA
  Prof. Ruthven
- University College London, UK
  Prof. Brandani
- Westfälische Wilhelms-Universität Münster, Institut für Physikalische Chemie
  Dr. Schönhof
- Victoria University of Wellington, MacDiarmid Institute for Advanced Materials and Nanotechnology, School of Chemical and Physical Sciences, New Zealand
  Prof. Callaghan

Industry

- Air Prod & Chem Inc, Allentown, USA
  Dr. Coe, Dr. Zielinski
- BASF, Ludwigshafen, Germany
  Dr. Müller, Dr. Nestle, Dr. Rittig
- Cepsa, Madrid, Spain
  Dr. Perez
- Grace, Worms, Germany
  Dr. McElhiney
- Resonance Instruments Ltd., Witney, UK
  J. McKendry
- SINTEF, Oslo, Norway
  Prof. Stöcker
- Tricat, Berlin, Germany
  Dr. Tufar, Dr. Lutz

3.22 Publications

Journals

S. Vasenkov, P. Kortunov: Diff. Fundam. **1**, 2.1 (2005)

A. Brzank, S. Kwon, G. Schütz: Diff. Fundam. **1**, 4.1 (2005)

J. Kärger: Diff. Fundam. **1**, 5.1 (2005)

S. Vasenkov, J. Kärger: Magn. Reson. Imag. **23**, 139 (2005)

Y. Qiao, P. Galvosas, T. Adalsteinsson, M. Schönhoff, P.T. Callaghan: J. Chem Phys **122**, 214 912 (2005)

Y. Qiao, P. Galvosas, P.T. Callaghan: Biophys J. **89**, 2899 (2005)

A. Schüring, S. Vasenkov, S. Fritzsche: J. Phys. Chem. B **109**, 16 711 (2005)

T. Selvam, V.R.R. Marthala, R. Herrmann, W. Schwieger, N. Pfänder, R. Schlögl, H. Ernst, D. Freude: Stud. Surf. Sci. Catal. **158**, 501 (2005)

P. Kortunov, C. Cmelik, J. Kärger, R.A. Rakozy, D.M. Ruthven, Y. Traa, S. Vasenkov, J. Weitkamp: Adsorption **11**, 235 (2005)

A. Brzank, G. Schütz: Appl. Catal. A **288**, 194 (2005)

J. Kärger, S. Vasenkov: Micropor. Mesopor. Mater. **85**, 195 (2005)

S.S. Arzumanov, S.I. Reshetnikov, A.G. Stepanov, V.N. Parmon, D. Freude: J. Phys. Chem. B **109**, 19 748 (2005)

S. Russ, S. Zschiegner, A. Bunde, J. Kärger: Phys. Rev. E. **72**, 030 101 (2005)

E.E.T.E.A. Mohamed, S. Gröger, J. Schiller, F. Stallmach, J. Kärger, K. Arnold: Phys. Medica **21**, 69 (2005)

P. Kortunov, S. Vasenkov, J. Karger, R. Valiullin, P. Gottschalk, M.F. Elia, M. Perez, M. Stocker, B. Drescher, G. McElhiney, C. Berger, R. Glaser, J. Weitkamp: J. Am. Chem. Soc. **127**, 13 055 (2005)

H. Jobic, J. Kärger, C. Krause, S. Brandani, A. Gunadi, A. Methivier, G. Ehlers, B. Farago, W. Haeussler, D.M. Ruthven: Adsorption **11**, 403 (2005)

C. Chmelik, P. Kortunov, S. Vasenkov, J. Kärger: Adsorption **11**, 455 (2005)

D. Ruthven, F. Brandani: Adsorption **11**, 31 (2005)

A.G. Stepanov, S.S. Arzumanov, M.V. Luzgin, H. Ernst, D. Freude, V.N. Parmon: J. Catal. **235**, 221 (2005)

S. Fritzsche, T. Osotchan, A. Schüring, S. Hannongbua, J. Kärger: Chem. Phys. Lett. **411**, 423 (2005)

J.M. Simon, J.P. Bellat, S. Vasenkov, J. Kärger: J. Phys. Chem. B **109**, 13 523 (2005)

J. Jiao, J. Kanellopoulos, W. Wang, S.S. Ray, H. Foerster, D. Freude, M. Hunger: Phys. Chem. Chem. Phys. **7**, 3221 (2005)

F. Bauer, U. Decker, A. Dierdorf, H. Ernst, R. Heller, H. Liebe, R. Mehnert: Prog. Org. Coat. **53**, 183 (2005)

S. Haufe, D. Prochnow, D. Schneider, O. Geier, D. Freude, D. Stimming: Solid State Ionics **176**, 955 (2005)

A. Pampel, M. Fernandez, D. Freude, J. Kärger: Chem. Phys. Lett. **407**, 53 (2005)

R. Valiullin, P. Kortunov, J. Kärger, V. Timoshenko: Magn. Reson. Imag. **23**, 209 (2005)

K. Banas, F. Brandani, D.M. Ruthven, F. Stallmach, J. Kärger.: Magn. Reson. Imaging. **23**, 227 (2005)

P. Kortunov, S. Vasenkov, J. Kärger, MF. Elia, M. Perez, M. Stocker, G.K. Papadopoulos, D. Theodorou, B. Drescher, G. McElhiney, B. Bernauer, V. Krystl, M. Kocirik, A. Zikanova, H. Jirglova, C. Berger, R. Glaser, J. Weitkamp, E.W. Hansen: Magn. Reson. Imag. **23**, 233 (2005)

P. Kortunov, S. Vasenkov, J. Kärger, M.F. Elia, M. Perez, M. Stöcker, G.K. Papadopoulos, D. Theodorou, B. Drescher, G. McElhiney, B. Bernauer, V. Krystl, M. Kocirik, A. Zikanova, H. Jirglova, C. Berger, R. Glaser, J. Weitkamp, E.W. Hansen: Chem. Mater. **17**, 2466 (2005)

J. Kärger, R. Valiullin, S. Vasenkov: New J. Phys. **7**, 1 (2005)

A.G. Stepanov, S.S. Arzumanov, M.V. Luzgin, H. Ernst, D. Freude: J. Catal. **229**, 243 (2005)

T. Uma, H.Y. Tu, D. Freude, D. Schneider, U. Stimming: J. Mater. Sci. **40**, 227 (2005)

T. Uma, H.Y. Tu, S. Warth, D. Schneider, D. Freude, U. Stimming: J. Mater. Sci. **40**, 181 (2005)

Books

J. Kärger, P. Heitjans: *Diffusion in Condensed Matter* (Springer, Berlin Heidelberg 2005)

J. Kärger, F. Stallmach: *PFG NMR Studies of Anomalous Diffusion*, in *Diffusion in Condensed Matter*, ed. by J. Kärger, P. Heitjans (Springer, Berlin Heidelberg 2005) p 417

J. Kärger, F. Grinberg, P. Heitjans: *Diffusion Fundamentals*, (Leipziger Universitätsverlag, Leipzig 2005)

A. Bunde, J. Kärger, S. Russ, S. Zschiegner: *Correlating Self- and Transport Diffusion in the Knudsen Regime*, in *Diffusion Fundamentals*, ed. by J. Kärger, F. Grinberg, P. Heitjans (Leipziger Universitätsverlag, Leipzig 2005) p 68

J. Kärger: *Molecular Diffusion under Confinement*, in *Diffusion Fundamentals* ed. by J. Kärger, F. Grinberg, P. Heitjans (Leipziger Universitätsverlag, Leipzig 2005) p 389

3.23 Graduations

Doctorate

- Pavel Kortunov
  Rate Controlling Processes of Diffusion in Nanoporous Materials
- Michael von Mengershausen
  3D Diffusion Tensor Imaging of the Human Brain with Nuclear Magnetic Resonance

Diploma

- Volker Künzel
  NMR-Untersuchungen zum diffusiven Stofftransport in mikroporösen metallorganischen Festkörpern (MOF)
- Sergej Naumov
  NMR Study of Adsorption and Desorption Phenomena in Porous Media
- Stefan Hetzer
  Entwicklung einer Labelspule zur Diffusionsmessung beider Hirnhemisphären

3.24 Guests

- Jorge Gulin-Gonzalez (Alexander von Humdoldt awardee)
  University of Habana
  January – July 2005
- Dhananjai Shah (Mercator guest professor)
  Cleveland State University/Ohio
  since August 2005
- Alexander Stepanov
  Novosibirsk
  January – March and July – August 2005

4

Soft Matter Physics

4.1 General Scientific Goals – Polymers and Membranes in Cells

In his book "What is Life?", Schrödinger raised the question of how cellular processes can be understood through their basic physics and chemistry. Commencing with Watson and Crick, science has gained tremendous insight into the molecular basis of biological cells. Over 25 000 genes encode the information of human life, and their subsequent transcription and translation add to the complexity of molecular interactions resulting in an insurmountable combinatorial number of relations. By identifying cellular subunits acting as independent functional modules this complexity becomes tractable and the fundamental physical principles of these modules can be studied. A prototypical example for such a module is the intracellular scaffold known as the cytoskeleton. The cytoskeleton is the key structural element in cellular organization and is an indicator of pathological changes in cell function. It is a compound of highly dynamic polymers and active nano-elements inside biological cells that mechanically and chemically senses a cell's environment. The cytoskeleton generates cellular motion and forces sufficiently strong to push rigid AFM cantilevers out of the way. These forces are generated by molecular motor-based nano-muscles and by polymerization through mechanisms similar to Feynman's hypothetical thermal ratchet. Further, the nano-sized motors overcome the inherently slow, often glass-like Brownian polymer dynamics resulting in novel self-organization and rapid switching through dynamical instabilities. This active, soft condensed matter, with structures on nanometer and micron scales representative of individual proteins and cells, calls forth new biological and polymer physics. Our research group's specific goals center on unraveling this new physics of the cytoskeleton. One of the most appealing aspects of such interdisciplinary research is that it simultaneously provides fundamental advances in science as well as novel applications in medical fields such as oncology, neurology, and regenerative medicine. Furthermore, the insight into this active biological matter will cross-fertilize with nano-sciences by providing the blue prints for the assembly of nano-constituents into complex molecular machines. Our current and future goals are summarized in the following sections.

4.2 Reconstituted Active Polymer Networks

V. Bell, B. Gentry, D. Smith, B. Stuhrmann, D. Strehle

It is inherent to independent intracellular functional modules that their elements can be reconstituted and studied in detail *ex vivo*. This research lays the basis to explain the physics of active filamentous scaffolds in cells combining polymer physics, nonlinear dynamics, and field theoretical approaches. Considering the nonlinear dynamics aspect, Turing's ideas about self-organization and dynamic instabilities in nonequilibrium biological systems encounter a renaissance. Our recent work has demonstrated that molecular motor-induced filament sliding supersedes Brownian-driven polymer dynamics, allowing motor activity to fluidize otherwise elastic polymer networks and rapidly switch the degree of these networks' self-organization. The current focus of our *in vitro* work is on self-sustaining, thin, active polymeric films which move by polymerization and depolymerization, and on nano-muscles created from polymers and molecular motors (Fig. 4.1). As a further intracellular active element, we investigate the extent to which the protein Formin may be considered a molecular motor which parasitically harnesses the energy from actin polymerization to generate motile forces.

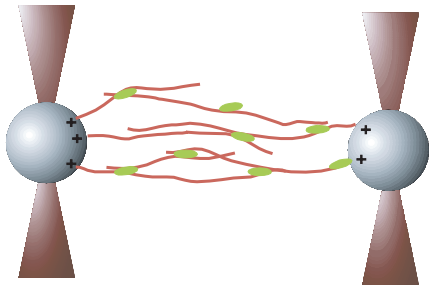

Figure 4.1: Nanomuscle between two optical tweezers.

[1] D. Humphrey et al.: Nature **416**, 413 (2002)
[2] D. Smith et al.: Science, resubmitted
[3] J. Käs et al.: Nature **368**, 226 (1994)
[4] F.J. Nedelec et al.: Nature **389**, 305 (1997)

4.3 Mechanics of the Cytoskeleton

S. Ebert, K. Franze, B. Lincoln, F. Sauer, S. Schinkinger, F. Wottawah, M. Romeyke, F. Sauer, M. Martin, J. Guck

Theory and experiments on reconstituted cytoskeletal elements provided the basis for the quantitative description of the viscoelastic behavior of semiflexible cytoskeletal filaments. For the knowledge transfer to cells we combine cell rheology performed with our novel optical trap, the optical stretcher, with genetic modification of the cytoskeletal composition. Even minute alterations in the cytoskeleton result in significant changes in a cell's elastic strength since the cytoskeletal mechanics nonlinearly amplify these alterations. The combination of the optical stretcher's sensitivity and high

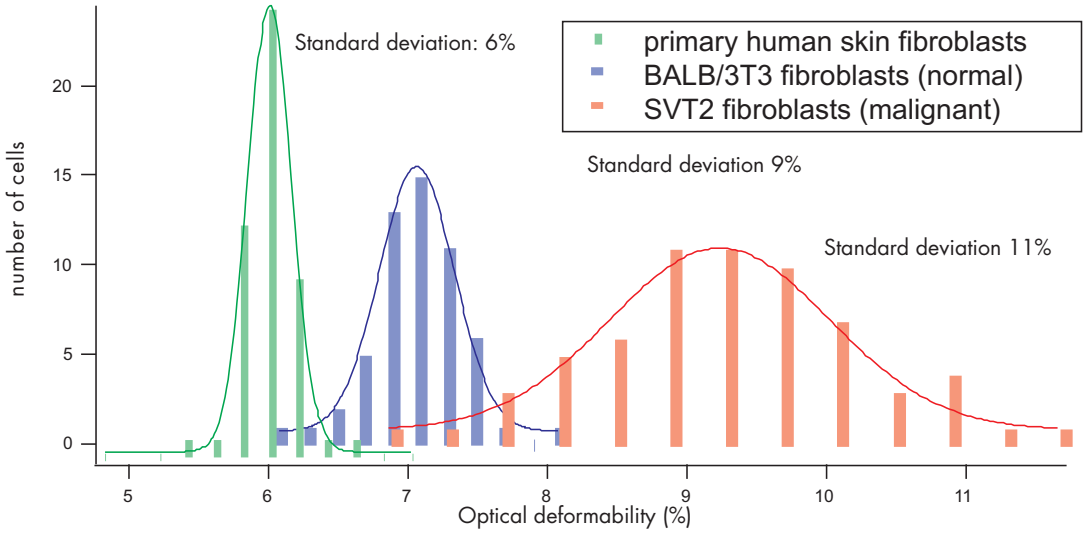

Figure 4.2: Small cell populations (< 100 cells) are sufficient to distinguish cells by their optical stretchiness. Dedifferentiated cells such as malignant cell are softer and show a broader distribution than mature cells. Primary cells are particularly well defined in their viscoelastic properties.

throughput capacity make a cell's "optical stretchiness" an extremely precise parameter to distinguish different cell types. This avoids the use of expensive, often unspecific molecular cell markers. This technique applies particularly well to cells with dissimilar degrees of differentiation, as a cell's maturation correlates with an increase in cytoskeletal strength. Because malignant cells gradually dedifferentiate during the progression of cancer, the optical stretcher allows, for the first time, the direct staging from early dysplasia to metastasis of a tumor sample obtained by fine needle aspirations or cytobrushes (Fig. 4.2). With a prototype of a microfluidic optical stretcher at our hands, we prepare preclinical trials to study its potential in resolving breast tumors' progression towards metastasis and to explore to what extent the optical stretcher can serve as dentists' screen for oral cancer. Moreover, the stretcher is tested to identify stem cell-like undifferentiated adult cells such as pluripotent hematopoetic precursors of white blood cells. Here, we collaborate with two companies to isolate adult stem cells for tissue engineering and for regenerative therapies in connection with Parkinson's disease. In the later case, we explore to what extent we can separate in a population of neural stem cells the desirable neuronal precursor cells from cells that will differentiate into unwanted Glia cells. We are additionally in touch with cord blood banks to minimize the amount of cells in storage by separating stem cells from blood. Since the optical stretcher represents a basic technology for cell recognition and sorting, an abundance of further biomedical applications can be envisioned.

[1] F. Wottawah et al.: Phys. Rev. Lett. **94**, 98 103 (2005)
[2] J. Guck et al.: Biophys. J. **88**, 3689 (2005)
[3] R. Ananthakrishnan et al.: Curr. Sci. India **88**, 1434 (2005)
[4] F. Wottawah et al.: Acta Biomat. **1**, 263, (2005)
[5] F.-U. Gast et al.: Mircofluid. Nanofluid. **2**, 21 (2005)
[6] J. Guck et al.: Phys. Rev. Lett. **84**, 5451 (2000)

4.4 Force Generation by the Cytoskeleton

C. Brunner, A. Ehrlicher, J. Gerdelmann, M. Gögler, K. Müller, C. Koch, D. Rings

The cytoskeleton's static structural properties are the basis for its active behavior. For example, malignant cells with a softer actin cytoskeleton show increased motility and higher metastatic aggressiveness. Cell motility is a fundamental process of many phenomena in nature, such as immune response, wound healing, and metastasis. Mechanisms of force generation for cell migration have been described in various hypotheses requiring actin polymerization and/or molecular motors, but to date quantitative force measurements to date have focused only on traction forces. We have started with direct measurements of the forward force generated at the leading edge of the lamellipodium and at the cell body of a translocating fish keratocyte. To elucidate the sub-cellular force generation machinery, we additionally determined the forward force of locomoting lamellar fragments, which lack their nuclei but remain motile. We positioned an elastic spring, the cantilever of an atomic force microscope (AFM), in front of a moving cell, which subsequently pushes this spring out of the way. The forward force was calculated using the detected vertical deflection of the cantilever in an "elastic wedge model", which takes into account cellular deformation. Our measurements of the propulsive forces, which are in the expected lower nN range, provide quantitative insight into how a polymeric network of active and passive molecular components acts in concert as an active locomoting machine (Fig. 4.3). Our future research will focus particularly on the characterization of malignant cells' increase in motility during metastasis and on the role of cell biomechanics during tumor growth.

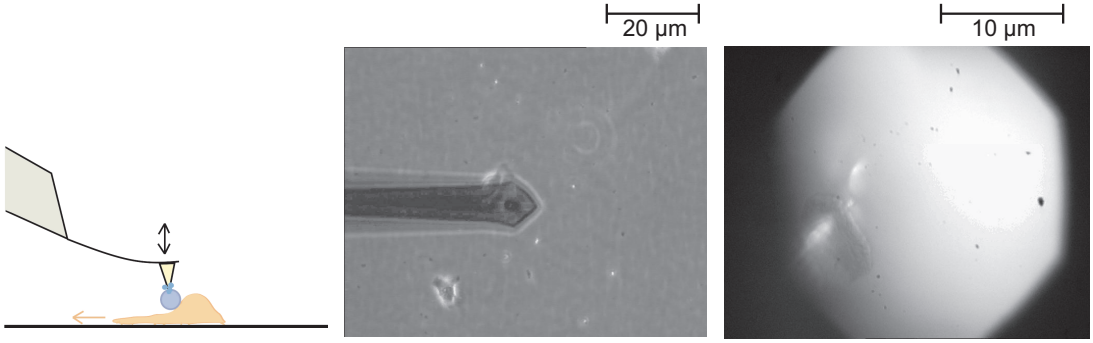

Figure 4.3: Cellular forces probed by an AFM. Schematic view (*left*), phase contrast image (*middle*), and interference reflection image (*right*).

[1] S. Park et al.: Biophys. J. **89**, 4330 (2005)
[2] R. Mahaffy et al.: Phys. Rev. Lett. **85**, 880 (2000)

4.5 Optomolecular Control of Cytoskeletal Activity

A. Ehrlicher, T. Betz, M. Gögler, D. Koch, D. Lim

Besides quantitative description of cellular motion, strategies for the controlled influence of this process are also desirable. This is clearly seen in the case of neuronal

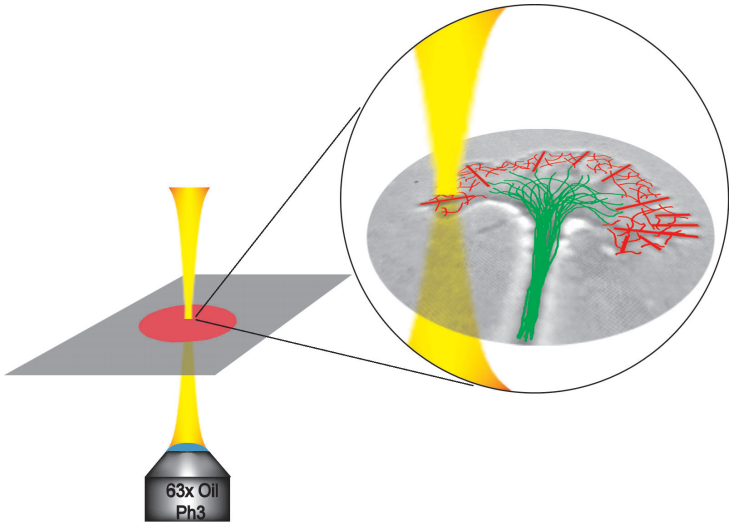

Figure 4.4: Optical cell guidance of a neuronal growth cone.

growth. Fundamental knowledge about neuronal growth and the ability to control it are invaluable in solving the enigma of nerve regeneration and the challenge of *in vitro* formation of neuronal circuits with defined architectures. These circuits interfaced with semiconductor devices could be an important technique in pharmacological drug screens. The growth cone, a highly motile, sensory structure at the tip of an advancing neurite, is regulated through a complicated network of gene expression and signal transduction mechanisms. These molecular commands address the cytoskeleton, which is responsible for the forces and contour changes that allow a growth cone to mechanically advance. Due to the dielectric nature of proteins, lasers potentially affect macromolecular ensembles such as those found in the cytoskeleton. Our current results show that we can use laser-induced forces to influence the movement of a growth cone (Fig. 4.4). The laser affects four active constituents relevant to neuronal growth: the growth speed, the direction taken by a growth cone, the splitting of a growth cone, and the contact of a growth cone to other nerve cells. Our efforts will identify the underlying optomolecular interactions of laser controlled neuronal growth by experimentally resolving different possible cellular mechanisms. These investigations will have the added benefit of deepening the general understanding of growth cone motility. The obtained insight will yield new strategies to shape neuronal networks, providing fundamental knowledge essential for optically controlled biomimetic machines.

[1] B. Stuhrmann et al.: Rev. Sci. Instrum. **76**, 035 105 (2005)
[2] A. Ehrlicher et al.: P. Natl. Acad. Sci. USA **99**, 16 024 (2002)

4.6 Intracellular Transport and Signaling

F. Rückerl, L. Woiterski, A. Falk, S. Surber, C. Selle

Cells cannot modulate diffusive transport by the parameters found in the Einstein equation (temperature, viscosity, molecular size) and thus developed rich multifaceted

transport mechanisms including ballistic transport by motors and anomalous diffusion. Molecular motors carry loads such as ribosomes, transport vesicles, or lipid tethers (originating from the endoplasmic reticulum) through the cytoskeleton. This motor-based transport is essential for a cell's metabolism and the arrangement of its organelles. In the cytoplasm a molecular motor spends a certain fraction of its time, depending upon its degree of processivity, walking along a cytoskeletal filament towards one of its polar ends. The rest of the time the motor diffuses until it encounters another filament. Although the directed motion of a molecular motor along a filament is well understood, the transport of a molecular motor in a cytoskeletal network as an alternating series of ballistic motion and diffusion has not yet been studied in depth. Using fluorescence techniques we will visualize the motion of individual motors of the myosin family in actin networks. We will study how network architecture, motor density ("traffic jams"), cross-linking of the network, and actin polymerization and depolymerization affects the transport. The above mentioned limitation to diffusive transport is also reflected in cellular signaling. The cell membrane plays a quintessential role in signal transduction acting as a delay line for the diffusive transport of second messengers and thus controlling intracellular signaling speed. It is clear that the underlying cytoskeleton and the inhomogeneous membrane structure generated by lipid rafts and membrane proteins create a complex energy landscape for diffusive transport. For instance, changes in lipid raft size and structure are implicated in the occurrence and progression of Alzheimer's disease.

Nevertheless, the resulting physical mechanisms that affect diffusive transport of individual membrane components remain unclear. We have developed a method to follow the motion of nanoprobes (quantum dots and gold nanocolloids, see Fig. 4.5) in Langmuir monolayers to understand and quantitatively describe the fundamental interactions that control the Brownian motion of a particle in a lipid matrix. We found that dipole-dipole interactions between the probe particle and lipid domains influence the diffusive transport by inducing attractive interactions. These interactions can be

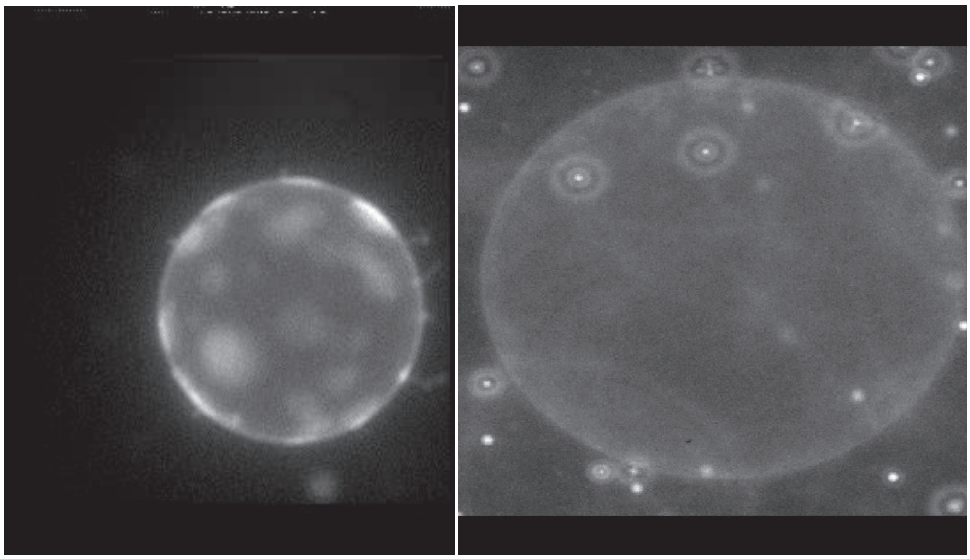

Figure 4.5: Fluorescent image of the domain structure of giant vesicles (*left*). Fluorescent nanoprobes diffusing in a vesicle membrane (*right*).

drastically modulated in strength and range resulting in transitions between events of localized 1-dimensional diffusion along the domain boundaries and occurrences of extensive 2-dimensional diffusion in the fluid lipid matrix. Thus, it is conceivable that changes in dipole-dipole interactions through alterations in lipid domain size and shape modulate the signalling speed in cell membranes.

[1] C. Selle et al.: Phys. Chem. Chem. Phys. **6**, 5535 (2004)
[2] M.B. Forstner et al.: Langmuir **19**, 4876 (2003)
[3] M.B. Forstner et al.: Langmuir **17**, 567 (2001)

4.7 Biophotonics for Cells

T. Betz, M. Gögler, D. Koch

The quantitative study of biological systems, which have not been previously studied in terms of physics, naturally requires the development of novel experimental techniques. Innovative optical techniques, such as novel imaging approaches, play a central role for this purpose. In this spirit, we have built an optical microscope integrated in a film balance, which allows for the first time single-particle tracking for nano-probes in Langmuir monolayers. Confocal and multiphoton microscopy are established tools in modern life sciences. Both techniques rely on lasers as excitation sources, and the current practice of using monochromatic radiation allows only a limited number of simultaneously usable dyes. By replacing all excitation lasers in a confocal microscope with pulsed white-light ranging from 430 to 1300 nm generated in a tapered silica fiber (a well-known device in nonlinear optics), we are exploring to what extent this limitation can be overcome (Fig. 4.6). Light has been used to observe cells since Leeuwenhoek's times and novel techniques in optical microscopy are frequently developed in biological physics. In contrast, with the optical stretcher we use the forces caused by light described by Maxwell's surface tensor to feel cells. Thus, the stretcher

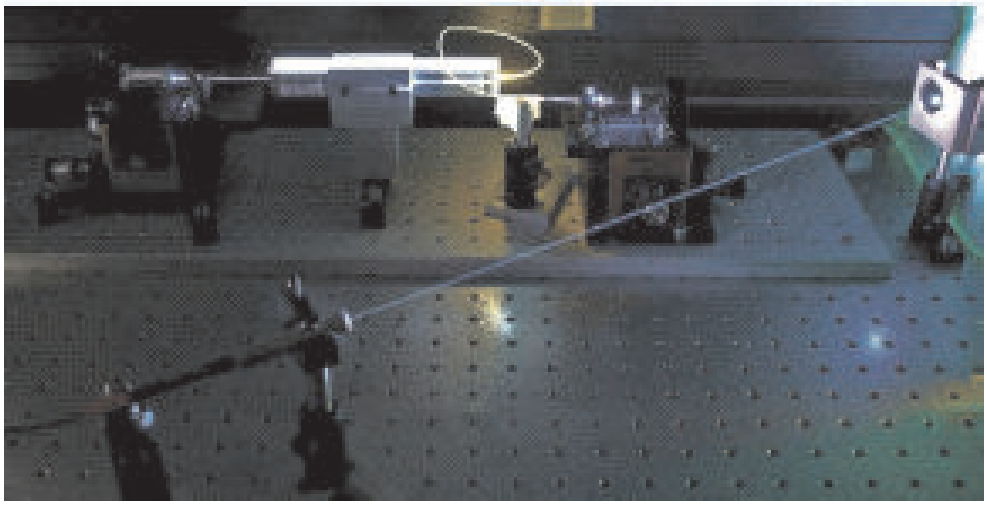

Figure 4.6: White light laser source based on a tapered optical fiber.

exemplifies the other type of biophotonic devices that do not image but manipulate cells. The optical stretcher uses optical surface forces to deform cells, while optical gradient forces, which are used in optical tweezers, play a minor role and only contribute to a stable trapping configuration. For the second optical micromanipulation technique we have developed, an optical tweezers configuration is used to induce intracellular optomolecular interactions for the optical control of neuronal growth. Here the gradient forces are used to bias cytoskeletal activity, not to hold cellular structures. The optical neuronal guidance has been fully automated and can control the growth activity in a neuronal network for a duration of days. As a spin-off of this technique, we have developed a laser scalpel to isolate individual cells for single-cell PCR from cell layers. For optimal use, these laser-based cell manipulation techniques must be combined with sophisticated microfluidics. Here, we particularly focus on high throughput cell sorting, exploring combinations of microfluidics and laser manipulation in parallel. Besides, biophotonic approaches scanning probe techniques are also significant factor in biological physics. AFM measurements of cell elasticity have been only of a qualitative nature due to the complex, nonlinear deformation by standard AFM tips, hydrodynamic contributions of the cantilever, and deviations from the Hertz model caused by finite sample thickness. Our AFM-based microrheology allows us precise quantitative measurements of the spatial distribution of a cell's viscoelastic behavior (i.e. complex shear modulus and Poisson ratio) and adhesive state.

[1] B. Stuhrmann et al.: Rev. Sci. Instrum. **76**, 035 105 (2005)
[2] T. Betz et al.: J. Biomed. Optics **10**, 054 009 (2005)

4.8 Interaction of Functionalized Nanoparticles with β-Amyloid Peptides

H. Schmiedel, W. Härtig, T. Siegemund

The general purpose of the project is the explanation of the structure and the physicochemical properties of nanoparticles acting as carriers of active ingredients in the treatment of neurodegenerative deseases such as Alzheimer disease (AD). One hallmark of brains in AD is the appearance of extracellular plaques consisting of amyloid-beta-peptide aggregates (Aβ, usually comprising 40 – 42 amino acids). Polymer nanoparticles with different size, surface and hydrophobicity (see e.g. [1]) were shown to penetrate the blood-brain barrier and might interact with the Aβ plaques. Coated nanoparticles will be chosen for the in vitro interactions between Aβ-aggregates and some of their specific ligands. This study includes nanoparticles surface-labelled with: 1. β-sheet breaking low-molecular-mass substances, 2. Aβ-specific antibodies and 3. Aβ itself (with appropriate spacers). Due to the interdisciplinary character of the project largely different methods are applied to study the interaction of functionalized nanoparticles with Aβ-aggregates. SANS (Small Angle Neutron Scattering) [2] measurements are performed to derive the structure of the active layers coating the nanoparticles. QELS (Quasi Elastic Light Scattering) and ITC (Isothermic Titration Calorimetry) measurements are used to support the SANS results. The distribution of the nanoparticles and

their released model drugs targeting fibrillar Aβ in the brains of transgenic mice with age-dependent β-amyloidoses are studied by light and electron microscopy including multiple fluorescence labelling and confocal laser scanning. First electron microscopic data on the delivery of the Aβ-binding model compound thioflavin-T after injection of nanoparticles with encapsulated thioflavin into the hippocampus of wild-type mice were published [3]. Nanoparticles optimized by the physico-chemical methods mentioned above are tested for drug targeting in animal models and might result in carriers for medical applications.

[1] B.-R. Paulke et al.: Acta Polym. **43**, 288 (1992)
[2] H. Schmiedel et al.: J. Phys. Chem. B **105**, 111 (2001)
[3] W. Härtig et al.: Neurosci. Lett. **338**, 174 (2003)

4.9 Publications

Journals

B. Stuhrmann, M. Gögler, T. Betz, A. Ehrlicher, D. Koch, J. Käs: *Automated tracking and laser micromanipulation of motile cells*, Rev. Sci. Instrum. **76**, 035 105 (2005)

F. Wottawah, S. Schinkinger, B. Lincoln, R. Ananthakrishnan, M. Romeyke, J. Guck, J. Käs: *Optical rheology of biological cells*, Phys. Rev. Lett. **94**, 98 103 (2005)

J. Guck, H. Erickson, R. Ananthakrishnan, D. Mitchell, M. Romeyke, S. Schinkinger, F. Wottawah, B. Lincoln, J. Käs, S. Ulvick, C. Bilby: *Optical Deformability as Inherent Cell Marker for Malignant Transformation and Metastatic Competence*, Biophys. J. **88**, 3689 (2005)

R. Ananthakrishnan, J. Guck, F. Wottawah, S. Schinkinger, B. Lincoln, M. Romeyke, J. Käs: *Modelling the structural response of an eukaryotic cell in the optical stretcher*, Curr. Sci. India **88**, 1434 (2005)

S. Park, D. Koch, R. Cardenas, J. Käs, C.K. Shih: *Cell motility and local viscoelasticity of fibroblasts*, Biophys. J. **89**, 4330 (2005)

T. Betz, J. Teipel, D. Koch, W. Härtig, J. Guck, J. Käs, H. Giessen: *Excitation beyond the monochromatic laser limit: Simultaneous 3-D confocal and multiphoton microscopy with a tapered fiber as white-light laser source*, J. Biomed. Optics **10**, 054 009 (2005)

F. Wottawah, S. Schinkinger, B. Lincoln, S. Ebert. K. Müller, F. Sauer, K. Travis, J. Guck: *Characterizing Single Suspended Cells by Optorheology*, Acta Biomat. **1**, 263 (2005)

F. Wottawah, S. Schinkinger, B. Lincoln, R. Ananthakrishnan, M. Romeyke, J. Guck, J. Käs: *Optical rheology of biological cells*, Phys. Rev. Lett. **94**, 98 103 (2005)

in press

K. Travis, K. Sokolov, J. Guck: *Scattering from Single Nanoparticles: Mie theory revisited*, Lect. Notes Phys. (2005)

Talks

J. Käs: DPG - Spring Conference, Berlin March 2005

J. Käs: Seminar at Cavendish Laboratory of Cambridge University, GB May 2005 (invited)

J. Käs: Seminar at Carl-Zeiss Jena GmbH, Jena May 2005 (invited)

J. Käs: *Dynamics of Cell and Tissue Structure*, 347nd WE-Heraeus-seminar, Bad Honnef May 2005 (invited)

J. Käs: Munich Physics Kolloquium, Technische Universität Munich May 2005 (invited)

J. Käs: Meeting "Cell Biomechanics", Institute Matiére et Systèmes Complexes, Université Paris, France, June 2005 (invited)

J. Käs: Seminar at Dept. for Biomedical Physics of Innsbruck Medical University, Austria, June 2005 (invited)

J. Käs: Seminar at Dept. Chemistry and Biochemistry, LMU Munich, July 2005 (invited)

J. Käs: Workshop "Mathematical Biology of the Cell", Banff, Canada July 2005 (invited)

J. Käs: Workshop "Dynamics Days 2005", Berlin, July 2005 (invited)

J. Käs: Conference "Nonlinear Dynamics of Complex Continue", Bayreuth, October 2005 (invited)

J. Käs: Workshop "EAMNET Imaging", Institute Pasteur, Paris, France, September 2005 (invited)

J. Käs: Seminar at Labor für Biophysik, Westfälische Universität Münster, November 2005 (invited)

J. Käs: Seminar at Institute for Applied Physics, Universität Duisburg-Essen, December 2005 (invited)

J. Käs: Dutch Physical Society Meeting "12th FOM - Decemberdagen", Veldhoven, Netherlands, December 2005 (invited)

J. Guck: DPG - Spring Conference, Berlin, March 2005

J. Guck: SPIE-conference "Optics & Photonics 2005", San Diego, USA, August 2005

J. Guck: Seminar at Labor für Biophysik, Westfälische Universität Münster, November 2005 (invited)

C. Selle: DPG - Spring Conference, Berlin, March 2005

Posters

C. Selle: Conference "Liposomes 2005", Dept. of Biochemistry, University of Alberta, Canada, July 2005

4.10 Graduations

Diploma

- Mireille Martin
  Biomechanik menschlicher Hautzellen
  April 2005

Master

- Allen Ehrlicher
  Laser Manipulation of Extending Neurites
  February 2005
- Daryl Lim
  Low Concentration of Cytochalasin D Triggers Phase Transition-Like Collapse of Lamellipodium in Growth Cones
  August 2005
- Lydia Woiterski
  Infrared spectroscopic study on the water/lipid interface organization within cationic model membranes
  July 2005

4.11 Guests

- Yunbi Lu
  School of Medicine Zhejiang/Hangzhol
  since October 2004
- Cosima Koch
  Technische Universität Wien
  since September 2004

II

Institute for Experimental Physics II

5

Nuclear Solid State Physics

5.1 Introduction

The working horse in the nuclear solid state physics division is the LIPSION accelerator laboratory. Our research interest focuses on ion beam analysis and modification (e.g. proton beam writing) in the fields of material and life sciences. In addition, time differential perturbed angular correlation (TDPAC) experiments are carried out with emphasis on material science at the TDPAC-laboratory and at the isotope separator ISOLDE at CERN, Geneva.

Tilman Butz

5.2 The High-Energy Ion Nanoprobe LIPSION

T. Butz, D. Lehmann, A. Fiedler, S. Jankuhn, C. Meinecke, F. Menzel, C. Nilsson, S. Petriconi, T. Reinert, M. Rothermel, D. Spemann, Y. Tong, J. Vogt

The high-energy ion nanoprobe LIPSION at the University of Leipzig has been operational since October 1998. Its magnetic quadrupole lens system, arranged as a separated Russian quadruplet, was developed by the Microanalytical Research Centre (MARC), Melbourne and has a symmetrical demagnification factor of about 130. The single-ended 3 MV SINGLETRON^{TM} accelerator (High Voltage Engineering Europe B.V.) supplies H^+ and He^+ ion beams with a beam brightness of approximately $20\,A\,rad^{-2}m^{-2}eV^{-1}$. Due to this high brightness, the excellent optical properties of the focusing system of the nanoprobe and the suppression of mechanical vibrations by founding the bed-plates of accelerator and probe in greater depths separately from the surroundings, lateral resolutions below 100 nm for the low current mode (STIM) and 300 nm at a current of 50 pA (PIXE) were achieved routinely. A beam diameter of 41 nm was achieved. The UHV experimental chamber is equipped with electron, X-Ray, and particle detectors to detect simultaneously the emitted secondary electrons (Ion Induced Secondary Electron Emission, SE), the characteristic X-rays (Particle Induced X-Ray Emission, PIXE), as well as the backscattered ions (Rutherford Backscattering Spectrometry, RBS) and – in case of thin samples – the transmitted ions (Scanning Transmission Ion Microscopy, STIM, and Scanning Transmission

Ion Micro-Tomography, STIM-T). A newly installed optical microscope allows sample positioning and inspection during measurement. The magnetic scanning system moves the focused beam across the sample within a scan field of adjustable extent. The data collection system MPSYS (MARC Melbourne) collects and stores the spectra of the several techniques at any beam position (Total Quantitative Analysis, TQA). In addition, optional windows can be set in the spectra for real-time elemental mapping. The pictures are viewed and printed as two-dimensional colour-coded intensity distributions.

The installation of an irradiation platform designed for single ion bombardment of living cells allows first patterned irradiations and hit verification tests.

Current work in nuclear nanoprobe performance is focused on:

1. A new target chamber with a UHV-x,y,z-translation stage and eucentric goniometer was developed and built; the chamber can also be converted into a new irradiation platform for living cells with microscope access from the rear.
2. A real time scan and data acquisition system with lithography capabilities was installed.
3. Installation of faceted RBS-detector foreseen for middle of 2006.

Accelerator Statistics 2005:

- operating hours: 2178 h
- maintenance and conditioning: 20 h

5.3 Quantitative Trace Element Analysis with Sub-Micron Resolution

T. Reinert, D. Spemann, T. Butz

Quantitative trace element analysis with sub-micron spatial resolution is still a developing field with manifold challenges. Studies of elemental distributions with nanometer resolution and low detections limits are already known from synchrotron X-ray fluorescent microprobes (μSXRF) [1] and from SIMS, especially NanoSIMS [2]. The beam spots that are available for these two techniques are well below 100 nm due to nanotechnological developments in this field over the last two decades.

Several high-energy ion microprobe laboratories have reached the sub-micron scale with low beam currents (< 1 pA) for analytical techniques like scanning transmission ion microscopy (STIM) or for proton beam writing (PBW). The Singapore and Leipzig groups have achieved beam spots below 50 nm [3, 4]. Many other groups are currently also taking efforts to break the sub-500-nm frontiers.

For a 500 pA, 2.25 MeV proton beam the resolution is slightly less than 1 μm (0.9 μm diameter beam spot measured on a 2000 mesh Cu-rid). This is achieved with 100 μm object and 200 μm aperture diaphragms. By reducing the object to 50 μm the beam spot reduces to slightly less than 0.5 μm (460 nm × 495 nm) at 120 pA. With the 20 μm object the beam current is further reduced to 20 pA. The resulting beam spot of

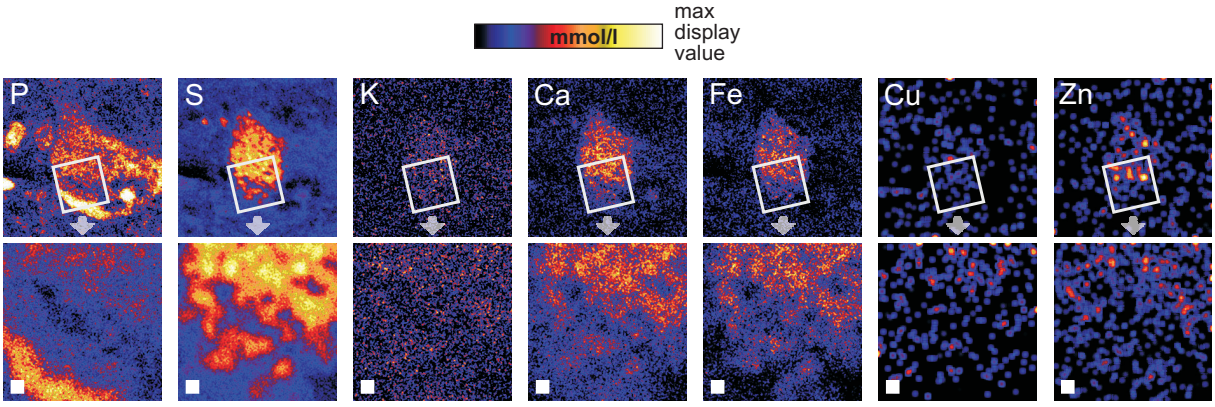

Figure 5.1: Elemental maps (50×50 μm^2, *top row*) and a zoom-in (12.5×12.5 μm^2) of neuromelanin inside a neuron of the *substantia nigra* (healthy control). The spatial resolution is about 0.5 µm (*white square* in the *bottom row* is 1 μm^2). The maximum display values are (mmol/l): P: 420; S: 880; K: 44; Ca: 105; Fe: 145; Cu: 8; Zn: 14.

less than 300 nm (260 nm × 280 nm), however, could only be achieved using the second pair of anti-scattering slits, which left a beam current of 10 pA. The acquisition time for the 100 pA beam was five minutes and for the 10 pA beam was about 15 minutes.

Occasionally, we have observed longterm drifts (hours) with an amplitude of almost 1 µm. The 15 minutes resolution of 300 nm deteriorated to 500 nm after 45 minutes acquisition time. The reason of this occasional longterm drift is presently unknown, but may be caused by the sample holder stage that is located outside the chamber with a bellow-coupled feed-through and is therefore susceptible even for air convection. A new in-vacuum stage is currently being tested and intended for the newly designed analysis chamber.

Application to biological samples In the last years we have undertaken several quantitative studies on elemental distributions on biological material, especially on rat and human brain [5, 6]. These studies led to new demands from the neuroscience department regarding higher lateral resolution and lower detection limits. Here, we give as an example the trace element analysis with sub-micron lateral resolution on Neuromelanin. Neuromelanin is a dark coloured intracellular pigment that appears in a specific population of neurons (dopaminergic and noradrenergic) predominantly in the *substantia nigra* and in the *locus coeruleus*.

Our aim is to study the content and distribution of trace elements in neuromelanin in situ of Parkinsonian and healthy brain tissue in order to reveal any possible differences. Since the ultrastructure of neuromelanin shows different binding capacities a sub-micron elemental analysis is needed. Figure 5.1 shows in the upper row the distribution of the elements P, S, K, Ca, Fe, Cu, Zn in a human neuron (non PD). The phosphorous map mainly represents the cytosolic phosphorous, thus giving an image of the cell body. Within the cell body the melanin appears due to its high sulphur content in the S-map. The ultrastructural granular shape with pigment associated lipids (cavities in the S-map) is well resolved. The elements K, Ca, Fe, (Cu) and Zn are clearly co-localized with the neuromelanin. The minimum detection limit of these elements was about 50 µmol/l (2 µg/g) in the total scan area. The lower row in the figure reveals in higher magnification the distributions of these ele-

ments in the pigment itself. The concentrations of K, Ca, Fe, Cu and Zn are higher in the sulphur containing granules of the pigment. Currently we are launching a study to investigate the change in trace element contents of neuromelanin in Parkinsonian disease.

[1] C. Mérigoux et al.: Biochim. Biophys. Acta **1619**, 53 (2003)
[2] P. Hoppe et al.: N. Astron. Rev. **48**, 171 (2004)
[3] F. Watt et al.: Nucl. Instr. Meth. B **210**, 14 (2003)
[4] D. Spemann et al.: Nucl. Instr. Meth. B **190**, 312 (2002)
[5] T. Reinert et al.: Nucl. Instr. Meth. B **210**, 395 (2003)
[6] M. Morawski et al.: Nucl. Instr. Meth. B **231**, 224 (2005)

5.4 The New Irradiation Platform at LIPSION

C. Nilsson, T. Reinert, S. Petriconi, T. Butz

Within the framework of the EU funded Marie Curie Research & Training Network CELLION, studies on cellular response to targeted single ions are carried out. To facilitate these experiments, a new cell irradiation platform is under development at the LIPSION nanoprobe. This platform is one part in the major rebuild of the irradiation end station that is currently being carried out. The rebuild includes a new target chamber, that will replace the old system of cylinders and flanges, a new custom manufactured 7 axis translation stage with goniometer and the new cell irradiation platform. The new target chamber will increase the accessibility and versatility during experiments and the new translation stage is needed in order to reduce the previously experienced, undesired vibration of the sample during an experiment to a minimum. The goniometer part is needed for performing e.g. channeling and STIM-Tomography work. The linear part of the translation stage consists of three piezo motors (in the x, z and q-directions) and one stepper motor (y-direction), and the goniometer of three piezo motors (x', y' and j-directions). The linear piezo axes have values of resolution, accuracy and repeatability in the range of 0.1 μm, which ensures precise positioning. The accuracy and repeatability of the stepper motor has been shown to be in the range of 1 μm. To accompany these technical developments, extensive improvements regarding the beam control and the stage control are also under way. The scan system has already undergone substantial revision, and runs now in a hard real-time environment under LINUX/RTAI. The new chamber will be taken into use around the middle of 2006.

5.5 Cellular Distribution and Localisation of Iron in Adult Rat Brain *(substantia nigra)*

C. Meinecke, M. Morawski*, T. Reinert, T. Arendt*, T. Butz

*Paul-Flechsig-Institute for Brain Research, University of Leipzig

Iron is essential for nearly all living organisms since it is involved in a variety of physiological processes, e.g. oxygen transport and electron transfer, redox/non-redox

reactions as well as other cell functions. In the brain, iron is an important co-factor for the generation of dopamine and several cellular and intra-cellular processes, e.g. tyrosine hydroxylase. In recent years many investigations account for the iron metabolism in brain tissue due to its link to neurodegenerative diseases [1]. According to a well established theory [2, 3] a dysfunction in the iron-homeostasis can result in an increased production of free radicals (Fenton reaction) which can lead to oxidative stress and finally to cell death [2]. This is discussed to be one of the major causes for the neuronal cell-death in the *substantia nigra pars compacta* (*SN pc*) in Parkinson's disease (PD).

The quantitative analysis shows that the relation between the integral iron content in the *SN pars compacta* and the *SN pars reticulata* is app. 1:2 (see Tab. 5.1). This relation is corroborated by different studies [4]. The intracellular (neuronal and glia cell related) iron content as well as the extracellular iron content in the *pars reticulata* is twice as high as in the *pars compacta* (see Tab. 5.1). These results corroborate other experiments which investigated the human *substantia nigra* [5]. The investigations of the cellular iron content revealed that neurons and glia cells do not differ significantly in their iron

Table 5.1: Quantitative results of the integral, neuronal, glial and extracellular iron content of the *SN pc* and the *SN pr*. Data are mean values ± standard deviation. (Significance test - students *t*-test with a significance level of $p < 0.05$).

iron concentration [mmol/l]	*PC*	*PR*	difference significant	number (n) of measurements
integral	0.4 ± 0.1	0.86 ± 0.22	yes	13
neuronal	0.58 ± 0.25	0.84 ± 0.36	no	10
glial	0.5 ± 0.2	1.13 ± 0.57	yes	22
extracellular	0.44 ± 0.07	0.95 ± 0.25	yes	13

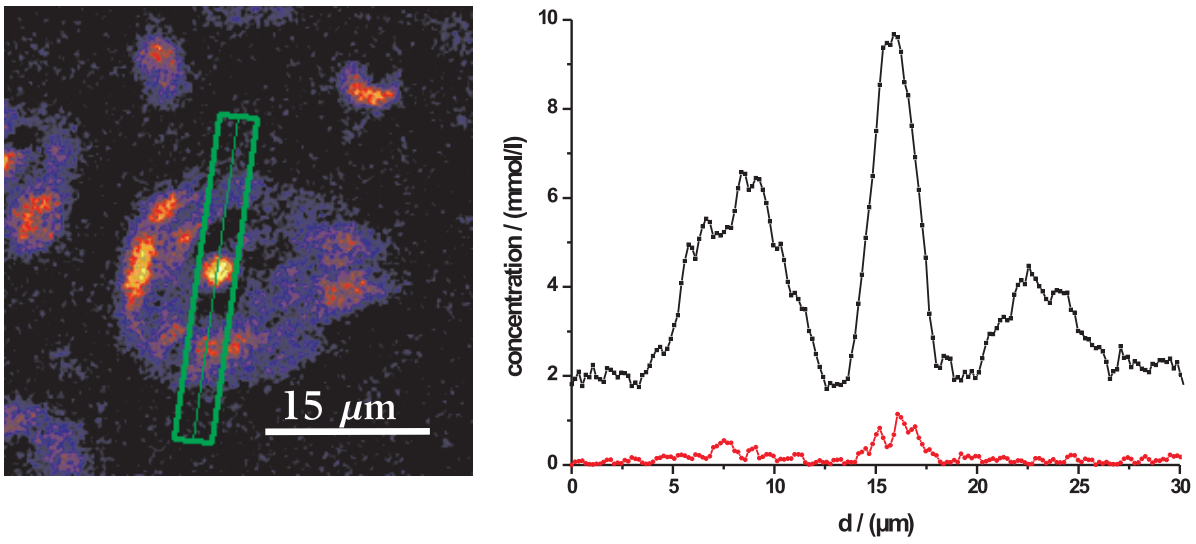

Figure 5.2: *Left*: Phosphorous map of a scan of a neuron (phosphorous used as indicator for the cell). The iron and phosphorous concentration profiles were determined along the traverse (*green box*). *Right*: Elemental concentration profile of a neuron (*black line*: iron concentration, *red line*: phosphorous concentration).

concentrations. This is in contrast to numerous histochemical studies which explain the increased iron content in the *SN pr* as non-neuronal iron [4, 6]. We could show that neurons and glia cells acquire nearly the same amount of iron. Also we could show that in the nucleolus a high iron content is located (see Fig. 5.2), but the intraneuronal iron concentration (averaged over the entire cell) is equal to the extraneuronal (non-somatic) iron concentration.

[1] D. Berg et al.: Neuroscience **79**, 225 (2001)
[2] M. Gerlach et al.: J. Neurochem. **63**, 793 (1994)
[3] M.B.H. Youdim, P. Riederer: Sci. Am. **276**, 52 (1997)
[4] J.R. Connor, S.A. Benkovic: J. Comp. Neurol. **338**, 97 (1993)
[5] M. Morawski et al.: Nucl. Instr. Meth. B **231**, 224 (2005)
[6] J.M. Hill, R.C. Switzer III: Neuroscience **111**, 595 (1984)

5.6 DNA-DSB and Hsp70 Induction in Living Cells by Proton Irradiation

A. Fiedler*, T. Reinert, T. Butz, J. Tanner†

*also at Faculty of Biology, Pharmacy and Psychology
†Clinic and Polyclinic for Radiation Oncology, University of Halle-Wittenberg

TDNA-double strand breaks (DNA-DSBs) in living cells can be directly provoked by ionising radiation. A repair process at the damaged DNA site is triggered including the phosphorylation of the histone H2AX (phosphorylated form γH2AX). The immunostaining of γH2AX visualizes the DNA-DSB in the form of a focus. Our concern was to test the feasibility of γH2AX staining for a direct visualization of single proton hits. If single protons would produce detectable foci, DNA-DSBs could be used as "biological track detectors" for protons replacing the solid state track detector CR-39 for hit verification tests. Ionising radiation can also damage proteins indirectly by inducing free radicals. The proteins then can either get refolded into a functional structure or even degraded by heat shock protecting proteins (Hsp). The most famous heat shock protein, Hsp70, is upregulated by ionising radiation, which is reported for heavy ions, γ- and X-Rays, but hardly ever for proton irradiation. Besides the DSBs, we also investigated the expression of the cellular stress response protein after patterned proton beam irradiation. The irradiation was done in cross and line patterns with counted numbers of 2.25 MeV protons on primary human skin fibroblasts. The experiments were carried out at 21 ℃, but for DSBs analysis the cells and the sample holder were later on cooled on ice before irradiation. Additional a Hsp70 control was done by heat shocking the cells at 42 ℃ for 30 min.

The proton induced DSBs appear more delocalised than it was expected by the ion hit accuracy. Possibly, due to the less dense ionising processes the DSBs are induced predominantly by indirect, secondary effects after proton irradiation. This assumption is based on the observation that the cooling reduces the delocalisation of DNA-DSBs which is probably caused by the reduced diffusion of DNA damaging agents (see Fig. 5.3). For DSBs based proton hit verification cell cooling is mandatory.

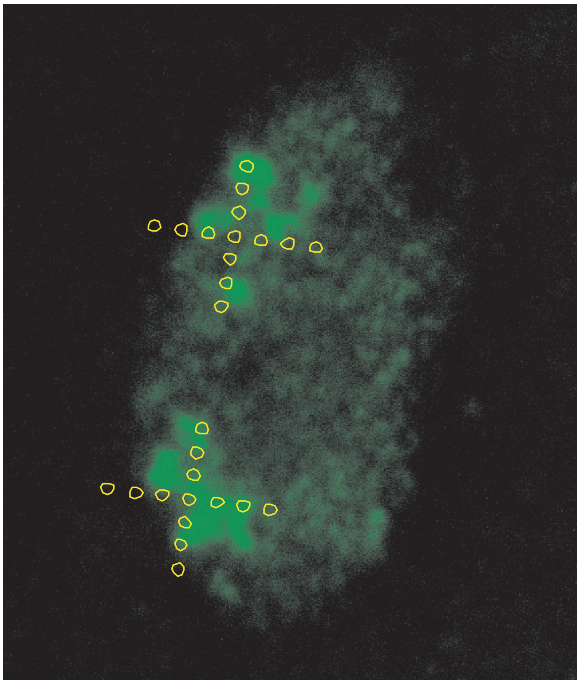

Figure 5.3: Induction of DNA-DSB-crosses by proton irradiation at low temperatures. Cross pattern with 7 × 7 pixel, 1 μm distance and intercross distance of 5 μm. DSBs stained by γH2AX antibody.

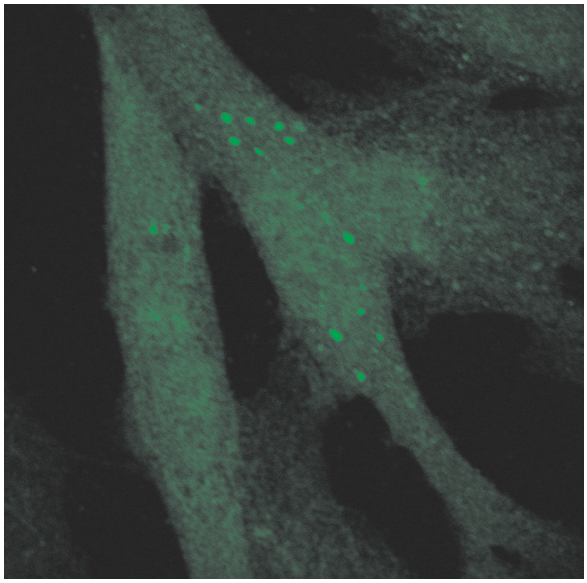

Figure 5.4: Hsp70 expression in fibroblasts after an irradiation with 10 protons/pixel in lined irradiation pattern (pixel distance 4 μm × 2 μm). Bright cytoplasmic Hsp70 aggregates were observed.

The localisation of Hsp70 after heat shock dominantly in the cell nucleus assumes that Hsp70 mainly induces gene expressions to avert damages caused by heat and even participate in DNA repair. Proton irradiation, contrary to the heat shock, seems to provoke protein damages mainly in the cytoplasm indicated by cytoplasmic Hsp70 aggregates (see Fig. 5.4). The different expression patterns after heat shock and proton irradiation lead to the assumption that the Hsp70 pathways depend on the type of the stressor and its damages. However, the irradiated area could not be recognized, all cells on the Si_3N_4 window showed a homogenous expression pattern. Might this probably remind of the bystander effect? These are preliminary results that remain to be investigated in more detail.

5.7 Quantitative Elemental Microanalysis of Perineuronal Net-Ensheathed Neurons

A. Fiedler*, T. Reinert, M. Morawski*, G. Brückner*, T. Arendt*, T. Butz

*Paul Flechsig Institute of Brain Research, University of Leipzig

Iron is assumed to contribute to oxidative stress in Parkinson's disease (PD) and therefore to neuronal degeneration by catalysing hydroxyl radical generation. Interestingly, perineuronal nets (PNs) appear in close vincinity to the regions affected in PD and are able to bind large amounts of iron (postmortem studies) due to their negatively

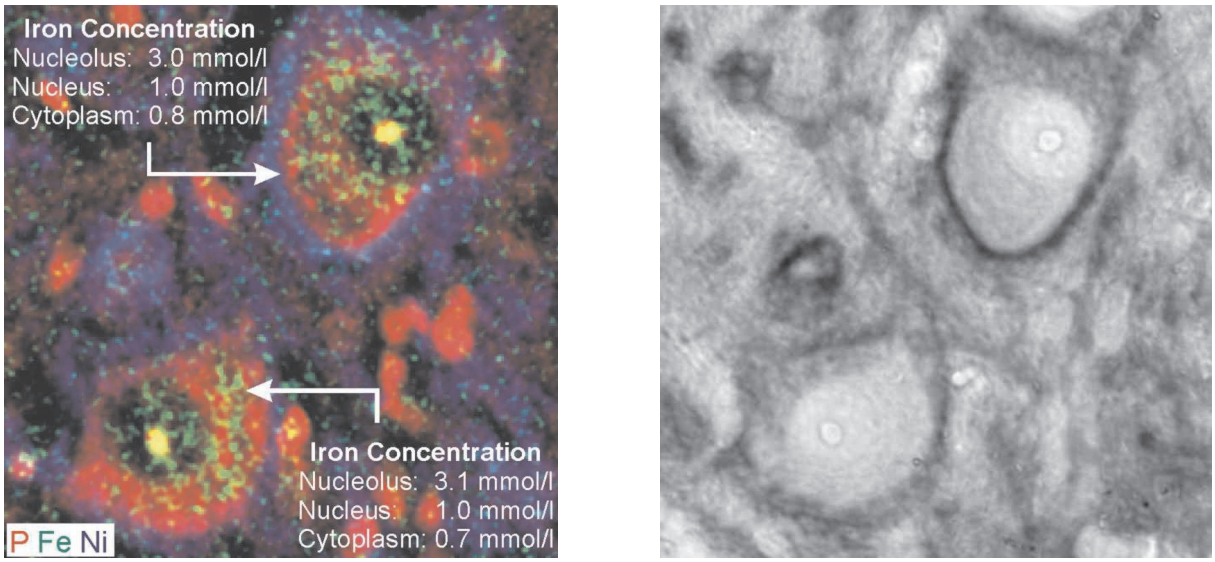

Figure 5.5: *Left*: Nuclear microscopic elemental map (100 μm × 100 μm) of two neurons in the nuc. ruber, the upper neuron is enclosed with a perineuronal net (PN), the lower one enclosed by a faintly outlined PN. PNs are marked by nickel-enhanced staining (Ni: *blue*). Cytoplasm can be recognized by intense phosphorus concentration (P: *red*). Elemental iron is shown in green (Fe: *green*). The yellow areas indicate a co-localization of phosphorus and iron, especially in the nucleoli. *Right*: Light microscopy image of the same area as in the left image showing the nickel enhancement of the PN (*dark*).

charged chondroitin sulfate proteoglycans [1]. According to the polyanionic character of the PNs, they potentially have a neuroprotective effect by scavenging iron ions and therefore reducing the oxidative stress [2].

Utilizing ion beam microscopy, the intraneuronal concentration of iron and other relevant elements (P, S, Ca, Ni, Cu, Zn) can be quantitatively analysed with a spatial resolution of less than 1 μm and detection limits well below 1 μg/g (e.g. for Fe about 10 μmol/l). We analyzed the elemental concentration in rat brain sections including the regions of the substantia nigra, nucleus ruber, subiculum, parietal cortex, brain stem, and cerebellum. PNs were immunohistochemically marked with lectin WFA and intensified by DAB-Ni to facilitate the PN visualization by ion beam microscopy (see Fig. 5.5) [3].

A slightly higher intraneuronal iron concentration was observed in PN-ensheathed neurons than in neurons devoid of PNs. Thus, the selective vulnerability of PNs might be explained on the basis that the PNs protect the neurons against degeneration by scavenging free iron ions with the possible conversion to non-toxic iron (Fe^{3+}) which can be stored inside the cell. This could probably delay functional changes as well as metabolic imbalances in the course of PD.

[1] T. Reinert et al.: Nucl. Inst. Meth. B **210**, 395 (2003)
[2] M. Morawski et al.: Nucl. Inst. Meth. B **231**, 229 (2004)
[3] M. Morawski et al.: Exp. Neurol. **188**, 309 (2004)

5.8 Ion Beam Analysis of Bragg-reflectors, Synthetic Cylindrite-Microstructures and GaAs/AlAs Heterostructures

C. Meinecke, F. Menzel, J. Bauer*, R. Kaden†, J. Vogt, T. Butz

*Institute for Experimental Physics II
†Institute for Mineralogy, Crystallography and Material Research

In the framework of the research group "Architecture of nano- and microdimensional building blocks"(FOR 522) we investigated different micro-structures (wires) consiting of glass (radii: 6.5 µm, 5 µm) which were coated with Bragg-reflectors using PECVD. The homogeneity of the layer thickness and composition of the Bragg-layers were analysed using the spatially resolved Micro-Rutherford Backscattering Spectrometry (µRBS). The PIXE analysis of these Bragg-reflectors shows no contaminations (trace element analysis) due to the producing process. The aim of these investigations was the improvement of the production to get optimal Bragg-reflectors [1].

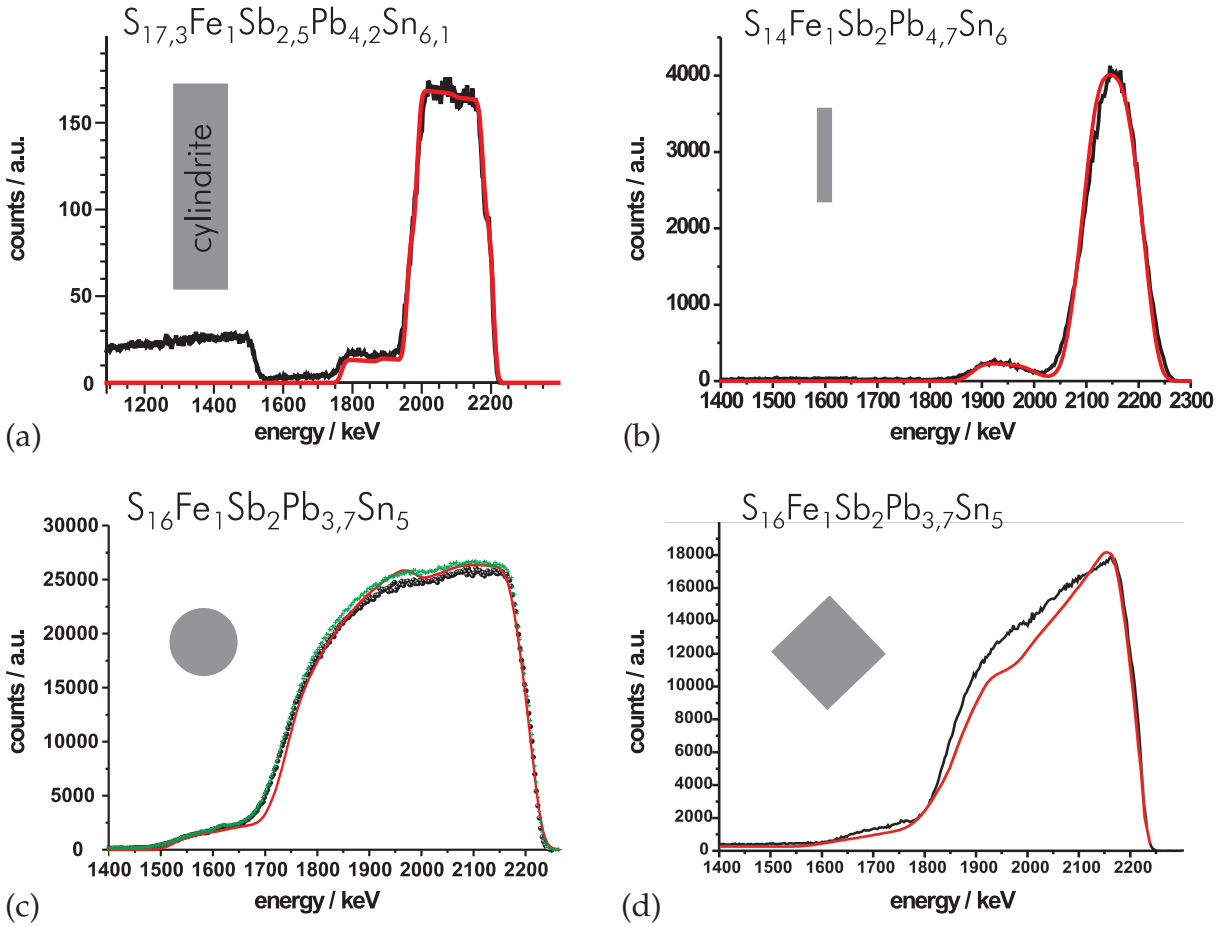

Figure 5.6: Influence of the sample morphology to the RBS-spectra. (**a**): cylindrite plate (thickness (6 µm); (**b**): thin cylindrite plate (thickness 2 µm); (**c**): cylindrite cylinder (radius 6 µm); (**d**): cylindrite rod with a square cross-section (thickness 4 µm)

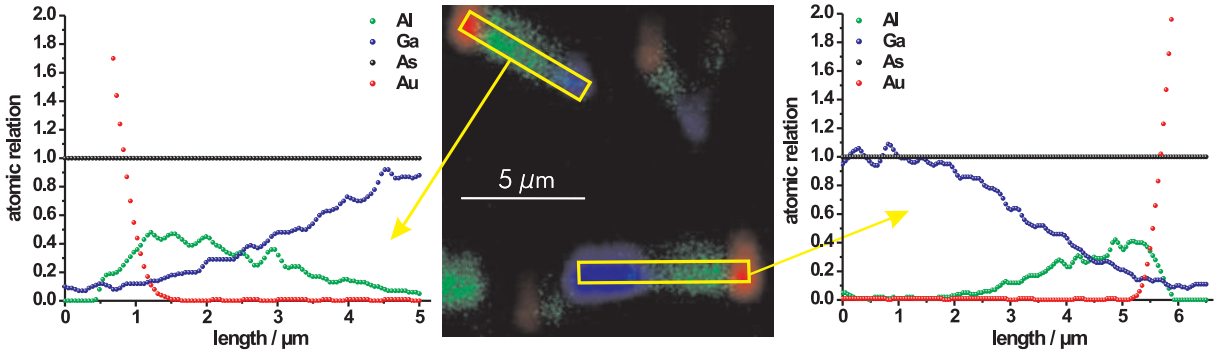

Figure 5.7: Elemental composition along the traverse of 2 different GaAs/AlAs-hetero-structures. The figure in the middle shows an element map of the GaAs/AlAs-hetero-structures (*red*: gold; *green*: aluminum; *blue*: gallium)

Furthermore, the stoichiometry of cylindrite-microstructures was analysed to gain more information about the production of synthetic cylindrite. Different Microstructures like thin plates [2] and cylinders with different cross-sections (round, squared) with a size of some µm were analysed. For the determination of the physical properties it was necessary that the determination of the stoichiometry does not destroy the sample. Therefore we improved the analysis technique of ion beam analysis so that we do not need any thin cuts of the sample. Now we can investigate 3-dimensional samples taking the morphology into account (see Fig. 5.6). These investigations shows that the synthetic cylindrite microstructures have the same stoichiometry despite of different cross-sections.

Using these technique we also investigated the stoichiometry of micro-dimensional hetero-structures consisting of gallium arsenide and aluminum arsenide in order to gain more information about the growing procedure and physical properties of the micro-structures in comparison to bulk material AlAs/GaAs heterostructures. These columnar, longitudinal heterostructures which were grown by metal-organic vapor phase epitaxy (MOVPE) had a diameter of approx. 1 µm and a length of approx. 6 µm. Due to the size of the sample the beam spot size had to be focused below 500 nm to obtain information about the mixed crystal system of these longitudinal hetero-structures. From the RBS- and PIXE-measurements of the GaAs/AlAs longitudinal hetero-structures we obtained the laterally resolved stoichiometry along the symmetry axis (see Fig. 5.7). Apparently, there is a massive interdiffusion at the interface.

[1] C. Meinecke et al.: T. Butz: Nucl. Instr. Meth. B, in press
[2] F. Menzel et al.: T. Butz: Nucl. Instr. Meth. B, in press

5.9 Proton Beam Writing

F. Menzel, D. Spemann, S. Petriconi, J. Lenzner*, T. Butz

*Institute for Experimental Physics II

Within the framework of the research group "Architecture of nano- and microdimensional building blocks" (FOR 522) the technique of proton beam writing (PBW) was

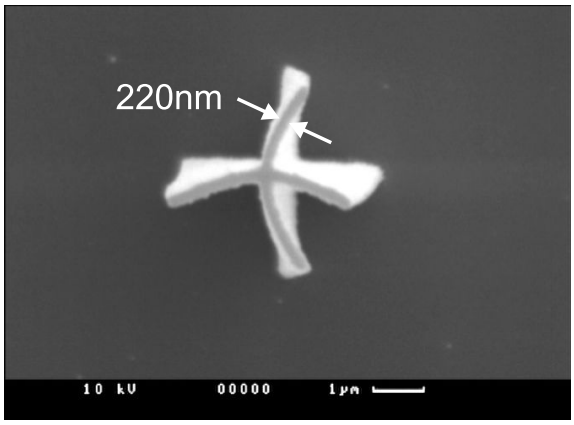

Figure 5.8: Cross written in 10 µm thick SU-8. The small walls with a thickness of 220 nm were produced with a low current beam of 2.25 MeV protons. Due to the high aspect ratio of 45 the structure is unstable.

developed further at the LIPSION nanoprobe. The dimensions of the structures created in the photo resist layers were reduced dramatically by using a low current (1 pA) beam of 2.25 MeV protons. Due to the small beam diameter of about 100 nm under these conditions we were able to produce structures with feature sizes down to 220 nm in the negative photo resist SU-8 (see Fig. 5.8). Structures for different applications within the research group were produced. For example, cubes and cylinders were written in SU-8, which were used for the investigation of Bragg reflector layers. Furthermore, we succeeded to embed cylindrite wires in SU-8 walls in order to fix them for further investigations. In addition, templates for the creation of metal structures were written in the positive resist PMMA. By this way, templates for contact loops were written, which were vapourised with a gold layer. After removing of the unirradiated PMMA a gold contact loop remains on the Si substrate which is required in the division Superconductivity and Magnetism (SUM). Furthermore, first Ni grids were produced by electro-plating using a PMMA template. However, the height of the Ni structure is irregular and due to bad adhesion between the PMMA and the Cu contact layer the PMMA template was partly shifted by some µm which led to an irregular Ni pattern. Therefore, further tests have to be carried out in order to improve the quality of the Ni structures.

5.10 TDPAC-Laboratory

T. Agne, S.K. Das, F. Heinrich, T. Butz

Nuclear probes were used to study the nuclear quadrupole interaction in macromolecules and various compounds which are of current use in material science. We used the highly sensitive spectroscopic method Time Differential Perturbed Angular Correlation (TDPAC). Two modern 6-detector-TDPAC spectrometer are installed permanently at the Solid State Physics Lab of the ISOLDE on-line isotope separator at CERN. This outstation of the Leipzig TDPAC Laboratory is dedicated for TDPAC experiments with rather short-lived TDPAC isotopes, like ^{111m}Cd or ^{199m}Hg or ^{204m}Pb with half-lifes less than 70 minutes. Three further spectrometer are at Leipzig.

5.11 The Nuclear Quadrupole Interaction of ^{99}Tc in Ammoniumparamolybdate

S.K. Das, T. Butz

Ammoniumparamolybdate (APM) is widely used in molybdenum-based heterogeneous catalysis as a starting material. It is prototypic for polymolybdates which consist of Mo-oxygen octahedra sharing edges and corners. With drastically improved statistical accuracy using ^{99}Tc-TDPAC it was possible to identify three classes of deformed octahedra with population 4:2:1, in perfect agreement with the proposed crystal structure of APM. The derived nuclear quadrupole interaction can serve as fingerprints for other polymolybdates.

5.12 A New Isomeric TDPAC-Probe: ^{180m}Hf

S.K. Das, T. Agne, T. Butz

TDPAC usually employs unstable nuclei which decay to the neighboring daughter isotope via β^+/EC- or β^--decay. Three situations can occur:

1. The mother isotope is a constituent of the sample under investigation. Here, no doping problems occur but the spectroscopy is carried out at a foreign element For β^+/EC decays electronic after-effects due to the rearrangement of the electric shell may play a role.
2. The mother isotope is a foreign element but the daughter is not. Here doping problems have to be solved. Otherwise the interpretation of the data is not complicated by impurities effects.
3. Neither mother or daughter are constituents of the sample under investigation, a rather common situation which renders the interpretation of data difficult, especially for nuclear quadrupole interactions.

Yet there are a few isotopes with longlived isomeric states like ^{111m}Cd, ^{199m}Hg and ^{204m}Pb. We have shown for the first time that ^{180m}Hf with a first excited state halflife of 1.5 ns can be used successfully in $HfF_4 \cdot 3H_2O$. This new TDPAC-probe will help to clarify to what extent the broad signals in the group IVb tetrafluorides observed at ^{181}Ta on Hf-lattice sites are of dynamic origin or rather associated with valence fluctuations of the impurity probe. The stretched cascade in ^{180m}Hf poses problems with conventional spectrometers but can be fully exploited with digital spectrometers.

5.13 ESRF: Development of a Spectrometer for SRPAC for ^{61}Ni Spectroscopy in Biomolecules

T. Agne, S.K. Das, T. Butz

Synchrotron-based Perturbed Angular Correlation (SRPAC) spectroscopy is a rapidly growing field because it complements nuclear forward scattering. Thus far, first exper-

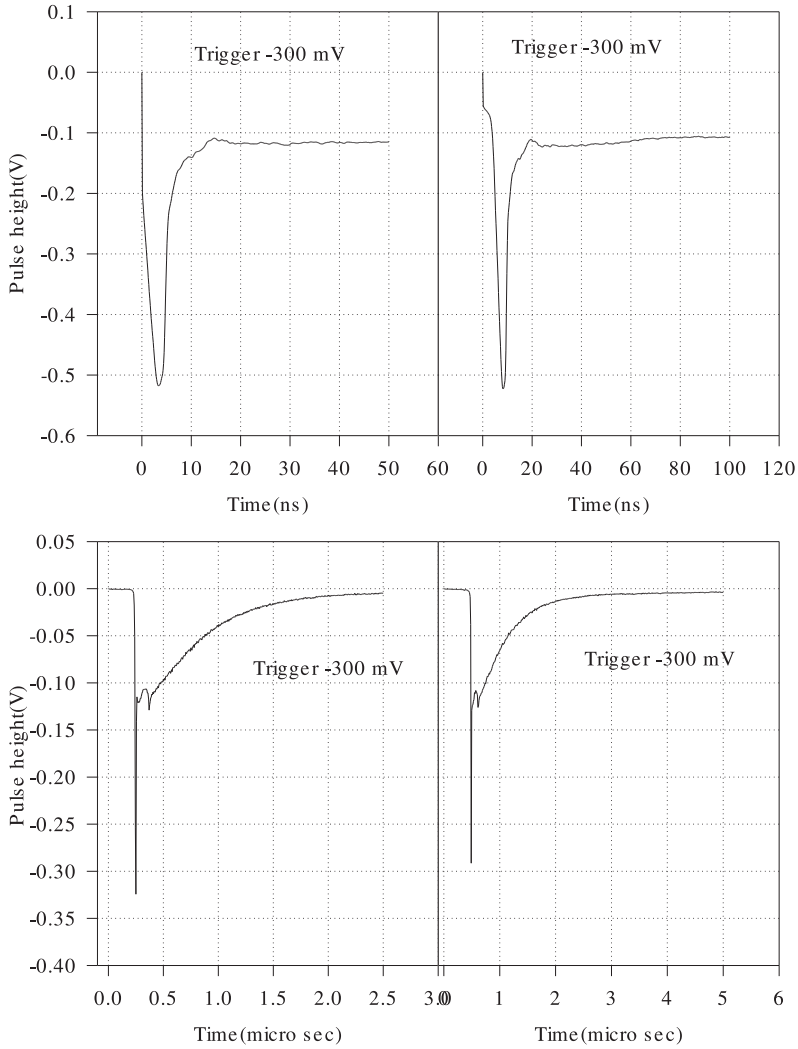

Figure 5.9: Anode pulses with 511 keV photons. *Top*: BaF_2(La) on XP2020Q. *Bottom*: BaF_2 on XP2020Q.

iments with ^{57}Fe and ^{61}Ni were successfully carried out at the European Synchrotron Radiation Facility (ESRF) at Grenoble by various groups. For ^{61}Ni spectroscopy, efficient detectors for photon energies around 60 keV are required which yield ultrashort pulses. BaF_2 doped with La in order to suppress the 600 ns fluorescence mounted on photomultipliers, are very promising. A typical signal, averaged over a few thousend pulses, is shown in Fig. 5.9.

5.14 ISOLDE: Development of a Fully-Digital, User-Friendly PAC-Spectrometer

T. Agne, S.K. Das, T. Butz

The new generation of PAC-spectrometers developed at Leipzig consists of fast digitizers with 1 GSample/s and massive data reduction on board using field programmable gated arrays (FPGA). A timing signal is generated, the pulse area is determined and selected,

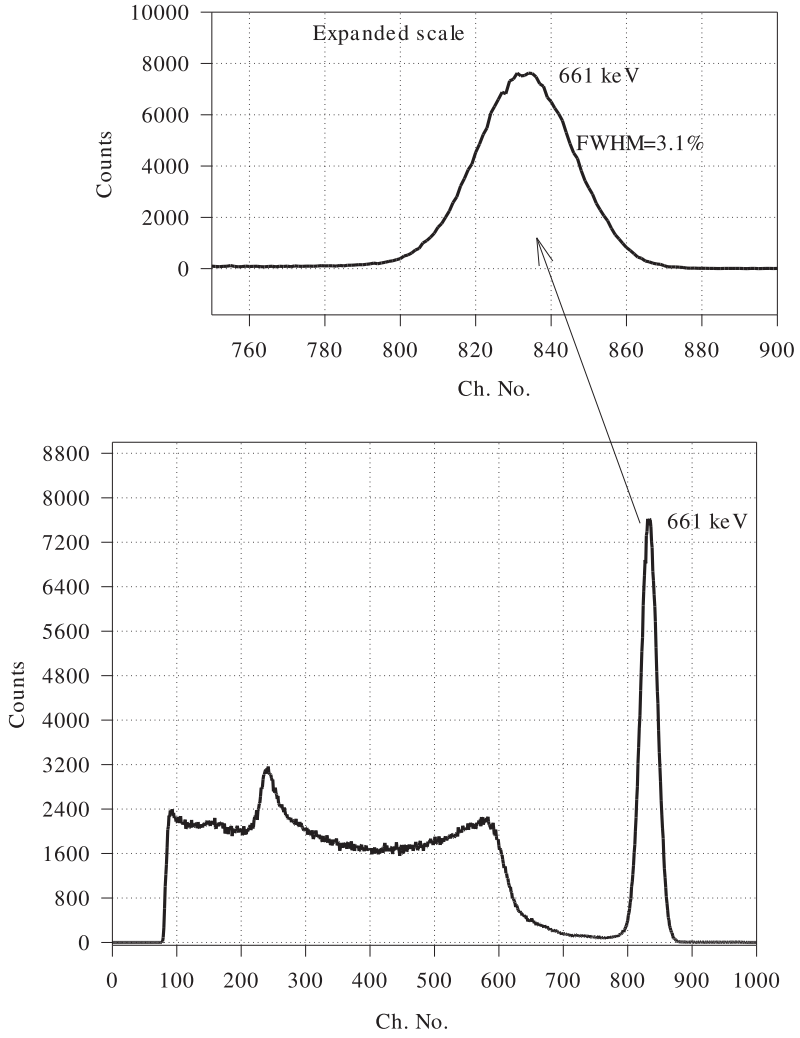

Figure 5.10: Energy spectrum of ^{137}Cs on $LaBr_3$-(Ce) (*dia* = 12 mm × 18 mm).

and the detector number is added as a tag to the data stream to the PC where the coincidences are detected and stored for real-time processing. The FPGA-programming is completed. The new spectrometer will use brand-new $LaBr_2$-(Ce)-scintillators which give excellent energy resolution (see Fig. 5.10).

5.15 The Nuclear Quadrupole Interaction of ^{181}Ta in Group IVb Tetrafluorides

S.K. Das, T. Butz

The nuclear quadrupole interaction of ^{181}Ta in $HfF_4 \cdot 3H_2O$, $ZrF_4 \cdot nH_2O$ and $TiF_4 \cdot nH_2O$ was measured by TDPAC (Fig. 5.11). The results are intriguing in several respects:

1. Our results of $HfF_4 \cdot 3H_2O$ are in disagreement with literature data whereas the unhydrous HfF_4-data agree. We assume, that the discrepancy is due to different hydration states.

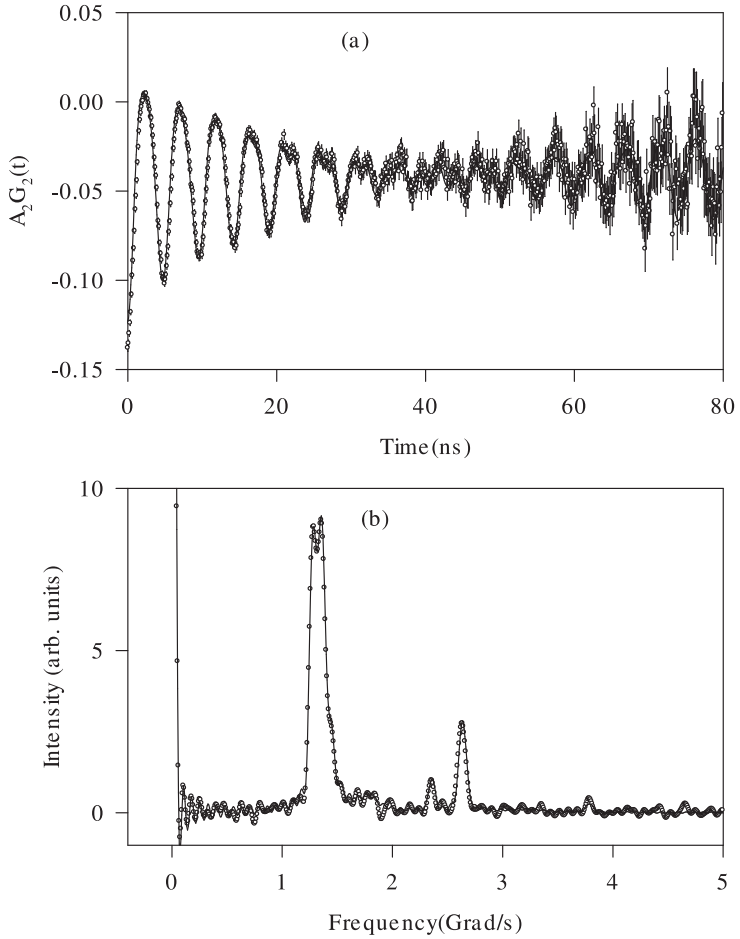

Figure 5.11: TDPAC spectrum for $HfF_4 \cdot 3H_2O$ (**a**) A_2G_2 spectrum and (**b**) Fourier spectrum.

2. More intriguing is the fact that unique sharp frequencies are observed for $HfF_4 \cdot 3H_2O$ (with a small broad contribution), whereas for $ZrF_4 \cdot nH_2O$ the sharp and broad components have about equal population and for $TiF_4 \cdot nH_2O$ only the broad component prevails. This is reminiscent of internal dynamics, maybe associated with H_2O mobility.

5.16 Ab Initio Calculations of the Electric Field Gradient in Simple Molecules

F. Heinrich, T. Butz

Electric field gradients (EFG) at the nucleus of a nuclear probe can be measured via the nuclear quadrupole interaction by various methods, e.g. NMR or time differential perturbed angular correlation spectroscopy (TDPAC). Usually, the interpretation of the experimental data is done by comparison of the experimental EFG with well-known EFGs of model compounds. Ab initio calculations of the EFG represent an alternative to validate proposed chemical geometries of metal binding sites.

In order to provide a deeper understanding of the origin of EFGs, a series of calculations were performed using the Amsterdam-Density-Functional code for simple molecules like H_2 and $H_3/H_3^+/H_3^{2+}$ versus bond angle. There is a considerable variation of the charge associated with the central/peripheral atoms when the bond angle is varied despite the fact that contributions from p-orbitals are absent or negligible.

5.17 Funding

3D-Ionenstrahlanalytik zur morphologischen und stofflichen Charakterisierung nano- und mikrodimensionaler Strukturbauelemente und "Ionenstrahl-Micromachining"
Prof. Dr. T.Butz
DFG Bu 594/19-1 within Forschergruppe FOR 522

CELLION: Studies of cellular response to targeted single ions using nanotechnology
Prof. Dr. T. Butz
EU-Project: MRTN-CT-2003-503923

ESRF: Aufbau eines SRPAC Spektrometers zur Untersuchung der Koordination und Dynamik von Nickel-Zentren in biologischen Systemen
PD Dr. W. Tröger, Prof. T. Butz
BMBF, 05KS40LA/3

NANODERM – Quality of Skin as a barrier to ultra-fine particles
Prof. Dr. T. Butz
EU-Project, QLK4-CT-02678

Radioactive Metal Probes as Diagnostic Tools in Biomolecules
PD Dr. W. Tröger, Prof. T. Butz
DFG, Tr327/8-1

ISOLDE: Aufbau eines volldigitalen, nutzerfreundlichen PAC-Spektrometers
PD Dr. W. Tröger, Prof. T. Butz
BMBF, 05KK4OL1/4

5.18 Organizational Duties

T. Butz

- Member of the ISOLDE and Neutron Time of Flight Committee, CERN
- Vertrauensdozent der Studienstiftung des deutschen Volkes
- Sprecher der Ortsgruppe Leipzig des deutschen Hochschulverbandes
- Co-tutor for students of Tautenburg (astrophysics), LMU München (astrophysics), DESY/Zeuthen (particle physics)
- Reviewer: DFG, Studienstiftung des deutschen Volkes, Israeli Science Foundation, Alexander von Humboldt Foundation, US Immigration Service, CNRS (France)
- Referee: J. Phys. C, Phys. Rev. B, Chem. Rev., Phys. Rev. Lett., J. Biol. Inorg. Chem., Nucl. Instr. Meth. B, Hyperfine Interactions

T. Reinert
- Referee: Nucl. Instr. Meth. B

D. Spemann
- Referee: Nucl. Instr. Meth. B

F. Menzel
- Referee: Nucl. Instr. Meth. B

C. Meinecke
- Referee: Nucl. Instr. Meth. B

C. Nilsson
- Referee: Nucl. Instr. Meth. B

5.19 External Cooperations

Academic

- Centre d'Etudes Nucléaires de Bordeaux Gradignan, Bordeaux, France
  Prof. PH. Moretto
- European Organization for Nuclear Research (CERN), Genf, Switzerland
  ISOLDE Collaboration
- Commonwealth Scientific and Industrial Research Organisation (CSIRO), Exploration and Mining, Sydney, Australia
  Dr. C. Ryan
- European Molecular Biology Laboratory (EMBL), Outstation Hamburg
  Dr. W. Meyer-Klauke, Dr. A. Vogel, O. Schilling
- FRM, Garching
  Prof. E. Wagner, Dr. U. Wagner
- FU Berlin
  Prof. U. Abram
- Gray Cancer Institute, London, UK
  Prof. B.Michael
- Gesellschaft für Schwerionenforschung (GSI), Darmstadt
  Dr. D. Dobrev, Dr. B. Fischer
- Hahn-Meitner Institut (HMI), Berlin
  Dr. D. Alber, Dr. H. Haas, Dr. W.-D. Zeitz
- Institut für Interdisziplinäre Isotopenforschung (IIF), Leipzig
  K. Franke
- Institute of Physics, Kraków, Poland
  Dr. Z. Stachura
- Institute of Nuclear Technology, Sacavém, Portugal
  Dr. T. Pinheiro

- Leibniz-Institut für Oberflächenmodifizierung (IOM), Leipzig
  Dr. K. Zimmer, Dr. J. Gerlach
- Royal Veterinary and Agricultural University (KVL), Kopenhagen, Denmark
  Dr. L. Hemmingsen
- Martin-Luther-Universität Halle-Wittenberg
  Dr. J. Tanner
- Max Planck Institute for Demographic Research, Rostock
  A. Fabig
- Max-Planck-Institut für Mikrostrukturphysik, Halle/Saale
  Dr. J. Heitmann
- National University of Singapore
  Prof. F. Watt, Dr. T. Osipowicz
- Universität Leipzig, Paul-Flechsig-Institut
  Prof. T. Arendt, M. Morawski, Dr. G. Brückner
- The University of Melbourne, Australia
  Microanalytical Research Centre, Prof. D. Jamison
- TU Wien, Austria
  Prof. K. Schwarz, Prof. P. Blaha
- Universidade de Aveiro, Portugal
  Prof. V.S. Amaral
- Universität Hannover
  Arbeitskreis Prof. P. Behrens
- Universität Hannover
  Arbeitskreis Prof. C. Vogt
- Universität Leipzig
  Prof. R. Hoffmann
- Universität Mainz
  Dr. H. Decker
- Universität Zürich
  Prof. Vašak, Dr. P. Faller, Prof. R. Alberto
- Universitätskliniken Leipzig
  PD Dr. G. Hildebrandt, Prof. Dr. M. Sticherling
- University of Illinois, USA
  Prof. Y. Lu, J. Liu

Industry

- Infineon Technologies Dresden GmbH & Co. OHG
  M. Jerenz
- Dechema
  Dr. E. Zschau, Self-employed expert in materials research

5.20 Publications

Journals

P. Esquinazi, D. Spemann, R. Höhne, A. Setzer, K.-H. Han, T. Butz: *Examples of room-temperature magnetic ordering in carbon-based structures*, Phase Transit. **78**, 155 (2005)

D. Spemann, K. Otte, M. Lorenz, T. Butz: *Elemental depth profiling in Cu(In, Ga)Se_2 solar cells using microPIXE on a bevelled section*, Nucl. Instr. Meth. B **231**, 440 (2005)

D. Spemann, P. Esquinazi, R. Höhne, K.-H. Han, A. Setzer, M. Diaconu, H. Schmidt, T. Butz: *Magnetic carbon: A new application for ion microbeams*, Nucl. Instr. Meth. B **231**, 433 (2005)

F. Menzel, D. Spemann, J. Lenzner, J. Vogt, T. Butz: *Proton beam writing using the high energy ion nanoprobe LIPSION*, Nucl. Instr. Meth. B **231**, 372 (2005)

P. Sidhu, M.L. Garg, P. Morgenstern, J. Vogt, T. Butz, D.K. Dhawan: *Ineffectiveness of Nickel in augmenting the hepatotoxicity in proteindeficient rats*, Nutr. Hosp. **XX**, 378 (2005)

O. Schilling, A. Vogel, B. Kostelecky, H. N. da Luz, D. Spemann, B. Späth, A. Marchfelder, W. Tröger, W. Meyer-Klaucke: *Zinc and iron dependent cytosolic metallo-b-lactamase domain proteins exhibit similar zinc binding affinities, independently of an atypical glutamate at the metal binding site*, Biochem. J. **385**, 145 (2005)

S. Gruhl, C. Vogt, J. Vogt, U. Hotje, M. Binnewies: *Laser Ablation Inductively Coupled Plasma Mass Spectrometry (LA-ICP-MS) of $ZnS_{1-x}Se_x$ Semiconductor Materials*, Microchim. Acta **149**, 43 (2005)

P. Esquinazi, K.-H. Han, R. Höhne, D. Spemann, A. Setzer, T. Butz: *Examples of room-temperature magnetic ordering in carbon-based structures*, Phase Transitions **78**, 155 (2005)

M. Lorenz, E. M. Kaidashev, A. Rahm, T. Nobis, J. Lenzner, G. Wagner, D. Spemann, H. Hochmuth, M. Grundmann: *$Mg_xZn_{1-x}O$ ($0 \leq x < 0.2$) nanowire arrays on sapphire grown by high-pressure pulsed laser deposition*, Appl. Phys. Lett. **86**, 143 113 (2005)

H. Natal da Luz, D. Spemann, W. Meyer-Klaucke, W. Tröger: *Analysis of proteins by Particle Induced X-ray Emission*, Nucl. Instr. Meth. B **231**, 308 (2005)

M. Diaconu, H. Schmidt, H. Hochmuth, M. Lorenz, G. Benndorf, J. Lenzner, D. Spemann, A. Setzer, K.-W. Nielsen, P. Esquinazi, M. Grundmann: *UV optical properties of ferromagnetic Mn-doped ZnO thin films grown by PLD*, Thin Solid Films **486**, 117 (2005)

M. Diaconu, H. Schmidt, A. Pöppl, R. Böttcher, J. Hoentsch, A. Klunker, D. Spemann, H. Hochmuth, M. Lorenz, M. Grundmann: *Electron paramagnetic resonance on $Zn_{1-x}Mn_xO$ thin films and single crystals*, Phys. Rev. B **72**, 085 214 (2005)

T. Butz, D. Spemann, K.-H. Han, R. Höhne, A. Setzer, P. Esquinazi: *The role of nuclear nanoprobes in inducing magnetic ordering in graphite*, Hyperfine Interactions **160**, 27 (2005)

H. von Wenckstern, S. Heitsch, G. Benndorf, D. Spemann, E. M. Kaidashev, M. Lorenz, M. Grundmann: *Incorporation and electrical activity of group V acceptors in ZnO thin films*, Proc. 27th Int. Conf. Phys. Semicond. (ICPS-27), Flagstaff, USA, AIP Conf. Proc. **772**, 183 (2005)

R. Schmidt-Grund, D. Fritsch, M. Schubert, B. Rheinländer, H. Schmidt, H. Hochmuth, M. Lorenz, D. Spemann, C. M. Herzinger, M. Grundmann: *Band-to-band transitions at optical properties of $Mg_xZn_{1-x}O$ (0 < x < 1) films*, Proceedings of the 27th International Conference on the Physics of Semiconductors (ICPS-27), Flagstaff, USA, AIP Conf. Proc. **772**, 201 (2005)

H. Schmidt, M. Diaconu, E. Guzman, H. Hochmuth, M. Lorenz, G. Benndorf, A. Setzer, P. Esquinazi, H. von Wenckstern, D. Spemann, A. Pöppl, R. Böttcher, M. Grundmann: *N-conducting, ferromagnetic Mn-doped ZnO thin films on sapphire substrates*, Proceedings of the 27th International Conference on the Physics of Semiconductors (ICPS-27), Flagstaff, USA, AIP Conf. Proc. **772**, 351 (2005)

P. Sidhu, M. L. Garg, P. Morgenstern, J. Vogt, T. Butz, D. K. Dhawan: *Role of Zinc in Regulating the Levels of Hepatic Elements Following Nickel Toxicity in Rats*, Biol. Trace Element Res. **102**, 161 (2004)

T. Butz, C. Meinecke, F. Menzel, T. Reinert, D. Spemann, J. Vogt, Y. Tong: *Biomedical Imaging with the Leipzig High-Energy Ion-Nanoprobe LIPSION*, Int. J. PIXE **15**, 125 (2005)

G. Wagner, S. Lehmann, S. Schorr, D. Spemann, T. Doering: *The two-phase region in $2(ZnSe)_x(CuInSe_2)_{1-x}$ alloys and structural relation between the tetragonal and cubic phases*, J. Solid State Chem. **178**, 3631 (2005)

T. Butz, C. Meinecke, M. Morawski, T. Reinert, M. Schwertner, D. Spemann: *Morphological and elemental characterisation with the high-energy ion-nanoprobe LIPSION*, Appl. Surf. Sci. **252**, 43 (2005)

K.-H. Han A. Talyzin, A. Dzwilewski, T.L. Makarova, R. Höhne, P. Esquinazi, D. Spemann, L.S. Dubrovinsky: *Magnetic properties of carbon phases synthesized using high-pressure high-temperature treatment*, Phys. Rev. B **72**, 224 424 (2005)

M. Morawski, C. Meinecke, T. Reinert, T. Butz, A.C. Dörffel, T. Arendt: *Determination of trace elements in the human substantia nigra*, Nucl. Instr. Meth. B **231**, 224 (2005)

M. Morawski, T. Reinert, C. Meinecke, T. Arendt, T. Butz: *Antibody meets the microbeam – or how to find neurofibrillary tangles*, Nucl. Instr. Meth. B **231**, 229 (2005)

Books

T. Butz: *Fouriertransformation für Fußgänger*, 4. Ed. (B.G. Teubner, Wiesbaden 2005)

M. Lorenz, H. Hochmuth, D. Spemann, H. von Wenckstern, H. Schmidt, M. Grundmann: *ZnO-Dünnfilme gezüchtet mit Laserplasma-Abscheidung (PLD)-Forschungsstand und Anwendungen*, in *TCO für Dünnschichtsolarzellen und andere Anwendungen*, ed. by K. Ellmer, III. FVS Workshop 2005, 10.-12.04.2005, Freyburg.

in press

S. Schorr, V. Riede, D. Spemann, T. Doering: *Electronic band gap of* $Zn_{2x}(CuIn)_{1-x}X_2$ *solid solution series (X=S,Se,Te)*, J. Alloys Compounds (2005)

M. Diaconu, H. Schmidt, H. Hochmuth, M. Lorenz, G. Benndorf, J. Lenzner, D. Spemann, A. Setzer, P. Esquinazi, A. Pöppl, H. von Wenckstern, K.-W. Nielsen, H. Schmidt, W. Mader, M. Grundmann: *Room-temperature ferromagnetic Mn-doped ZnO films obtained by pulsed laser deposition*, Phys. Rev. B, submitted

P. Esquinazi, D. Spemann, K. Schindler, R. Höhne, M. Ziese, A. Setzer, K.-H. Han, S. Petriconi, M. Diaconu, H. Schmidt, T. Butz, Y.H. Wu: *Proton irradiation effects and magnetic order in carbon structures*, Thin Solid Films

K. Schindler, D. Spemann, M. Ziese, P. Esquinazi, T. Butz: *Magnetism in Carbon: Writing magnetic structures with a proton micro-beam on graphite surfaces*, Acta Physica Polonica A, submitted

P. Reichart, D. Spemann, A. Hauptner, A. Bergmaier, V. Hable, R. Hertenberger, C. Greubel, A. Setzer, T. Butz, G. Dollinger, D.N. Jamieson, P. Esquinazi: *3D-Hydrogen analysis of ferromagnetic microstructures in proton irradiated graphite*, Nucl. Instr. Meth. B

F. Menzel, R. Kaden, D. Spemann, K. Bente, T. Butz: *Ion beam analysis of synthetic cylindrite produced by CVT*, Nucl. Instr. Meth. B, in press

T. Reinert, M. Morawski, D. Spemann, T. Arendt: *Quantitative trace element analysis with sub-micron lateral resolution*, Nucl. Instr. Meth. B

C. Meinecke, M. Morawski, T. Reinert, T. Arendt, T. Butz: *Cellular distribution and localisation of iron in adult rat brain (substantia nigra)*, Nucl. Instr. Meth. B

C. Meinecke, J. Vogt, T. Butz: *RBS studies on coated micro-dimensional glass fibers used as micro-resonators*, Nucl. Instr. Meth. B

F. Menzel, D. Spemann, S. Petriconi, J. Lenzner, T. Butz: *Proton beam writing of microstructures at the ion nanoprobe LIPSION*, Nucl. Instr. Meth. B

D. Spemann, K. Schindler, P. Esquinazi, M. Diaconu, H. Schmidt, R. Höhne, A. Setzer, T. Butz: *Magnetic force microscopy studies on the magnetic ordering in organic materials induced by high energy proton irradiation*, Nucl. Instr. Meth. B

R. Schmidt-Grund, A. Carstens, B. Rheinländer, D. Spemann, H. Hochmuth, M. Lorenz, M. Grundmann, C. M. Herzinger, M. Schubert: *Refractive indices and band-gap properties of rocksalt $Mg_xZn_{1-x}O$ ($0.68 \leq x \leq 1$)*, J. Appl. Phys., submitted

S. Heitsch, G. Benndorf, G. Zimmermann, C. Schulz, D. Spemann, H. Hochmuth, H. Schmidt, T. Nobis, M. Lorenz, M. Grundmann: *Optical and structural properties of MgZnO/ZnO hetero- and double heterostructures grown by pulsed laser deposition*, Appl. Phys. A, submitted

S. Heitsch, G. Zimmermann, H. Hochmuth, D. Spemann, G. Benndorf, H. Schmidt, M. Lorenz, M. Grundmann: *Photoluminescence properties of $Mg_xZn_{1-x}O$ thin films grown by pulsed laser deposition*, J. Appl. Phys., submitted

M. Diaconu, H. Schmidt, H. Hochmuth, M. Lorenz, H. von Wenckstern, G. Biehne, D. Spemann, M. Grundmann: *Deep defects generated in n-conducting ZnO:TM thin films*, Solid State Commun., submitted

Q. Xu, L. Hartmann, H. Schmidt, H. Hochmuth, M. Lorenz, R. Schmidt-Grund, D. Spemann, M. Grundmann: *Magnetoresistance effect in $Zn_{0.90}Co_{0.10}O$ films*, Appl. Phys. Lett., submitted

Q. Xu, L. Hartmann, H. Schmidt, H. Hochmuth, M. Lorenz, R. Schmidt-Grund, C. Sturm, D. Spemann, M. Grundmann: *Metal-insulator transition in Co-doped ZnO*, Phys. Rev. B, submitted

S. Schorr, R. Hoehne, D. Spemann, T. Doering, B.V. Korzun: *Magnetic properties investigations on Mn substituted ABX_2 chalcopyrites*, Phys. Stat. Sol. C, submitted

Talks

T. Butz, C. Meinecke, F. Menzel, T. Reinert, D. Spemann, J. Vogt, Y. Tong: *Biomedical Imaging with the Leipzig High-Energy Ion-Nanoprobe LIPSION*, 5th Int. Symp. BioPIXE, Wellington, New Zealand, 17.–21.01.2005

C. Bundesmann, M. Schubert, D. Spemann, H. von Wenckstern, H. Hochmuth, E.M. Kaidashev, M. Lorenz, M. Grundmann: *Long-wavelength bound and unbound charge excitations in doped ZnO and ZnO based alloy thin films*, 69. Frühjahrstagung der DPG, Berlin, 04.–09.03.2005

H. Schmidt, M. Diaconu, H. Hochmuth, M. Lorenz, G. Benndorf, D. Spemann, A. Setzer, P. Esquinazi, A. Pöppl, H. von Wenckstern, K.-W. Nielsen, R. Gross, H. Schmidt, W. Mader, G. Wagner, M. Grundmann: *Room-temperature ferromagnetism in Mn-alloyed ZnO*, 69. Frühjahrstagung der DPG, Berlin, 04.–09.03.2005

F. Menzel, D. Spemann, J. Lenzner, T. Butz: *Proton beam writing at the nanoprobe LIPSION using MeV ions*, Workshop "Ionenstrahlphysik und -technologie", Leipzig, 11.–12.04.2005

P. Reichart, D. Spemann, A. Hauptner, A. Bergmaier, V. Hable, R. Hertenberger, C. Greubel, A. Setzer, T. Butz, G. Dollinger, D.N. Jamieson, P. Esquinazi: *3D-Hydrogen Analysis of Ferromagnetic Microstructures in Proton Irradiated Graphite*, 17. Int. Conf. Ion Beam Anal., Seville, Spain, 26.06.–01.07.2005

T. Reinert, M. Morawski, D. Spemann, T. Arendt: **Invited:** *Trace element analysis with sub-micron lateral resolution*, 17. Int. Conf. Ion Beam Anal., Seville, Spain, 26.06.–01.07.2005

F. Menzel, D. Spemann, S. Petriconi, J. Lenzner, T. Butz: *Proton beam writing of microstructures at the ion nanoprobe LIPSION*, 13. Int. Conf. Radiat. Effects Insulat., Santa Fe,USA, 28.08.–02.09.2005

D. Spemann, K. Schindler, P. Esquinazi, M. Diaconu, H. Schmidt, R. Höhne, A. Setzer, T. Butz: *Ferromagnetic ordering in organic materials induced by high energy proton irradiation*, 13. Int. Conf. Radiat. Effects Insulat., Santa Fe, USA, 28.08.–02.09.2005

Posters

P. Reichart, D. Spemann, P. Esquinazi, T. Butz, A. Hauptner, G. Dollinger, D.N. Jamieson: *Hydrogen Distribution of Ferromagnetic Microstructures in Carbon created by Proton Microbeam Irradiation*, 16. Biennial Congress 2005, The Australian Institute of Physics, Canberra, Australia, 31.01.–04.02.2005

R. Schmidt-Grund, A. Carstens, M. Schubert, B. Rheinländer, H. Hochmuth, E. M. Kaidashev, M. Lorenz, D. Spemann, A. Rahm, C. M. Herzinger, M. Grundmann: *Refractive indices and optical transitions of* $Mg_xZn_{1-x}O$ $(0 < x < 1)$, 69. Frühjahrstagung der DPG, Berlin, 04.–09.03.2005

C. Bundesmann, M. Schubert, A. Rahm, D. Spemann, H. Hochmuth, E. M. Kaidashev, M. Lorenz, M. Grundmann: *Optical phonons and infrared dielectric functions of hexagonal and cubic MgZnO thin films*, Frühjahrstagung der DPG, Berlin, 04.–09.03.2005

C. Nilsson, T. Reinert, D. Spemann, J. Vogt, T. Butz: *The new irradiation platform at LIPSION*, 14th Annual Ion Beam Centre User Workshop, Guildford, Surrey, UK, 06.04.2005

C. Bundesmann, M. Schubert, D. Spemann, H. v. Wenckstern, M. Lorenz, M. Grundmann: *Phonons in doped ZnO and ZnO based thin films grown by PLD on sapphire*, E-MRS 2005 Spring Meeting, Strasbourg, 31.05.–03.06.2005

C. Meinecke, M. Morawski, T. Reinert, T. Arendt, T. Butz: *Cellular localisation of iron in the substantia nigra of an adult rat brain*, 4. Biotechnologie-Tag der Universität Leipzig 03.06.2005

M. Morawski, C. Meinecke, T. Reinert, A.C. Dröffel, T. Butz, G. Brückner, T. Arendt: *Parkinson's disease - A possible link between accumulation of iron and loss of perineuronal nets in the substantia nigra*, 4. Biotechnologie-Tag der Universität Leipzig, 03.06.2005

C. Meinecke, J. Vogt, T. Butz: *RBS studies on coated micro-dimensional glass fibers used as micro-resonators*, 17th Int. Conf. Ion Beam Anal, Seville, Spain, 26.06.–01.07.2005

C. Meinecke, M. Morawski, T. Reinert, T. Arendt, T. Butz: *Cellular distribution and localisation of iron in adult rat brain (substantia nigra)*, 17th Int. Conf. Ion Beam Anal., Seville, Spain, 26.06.–01.07.2005

F. Menzel, R. Kaden, D. Spemann, K. Bente, T. Butz: *Ion beam analysis of synthetic cylindrite produced by CVT*, 17. Int. Conf. Ion Beam Anal., Seville, Spain, 26.06.–01.07.2005

C. Nilsson, J. Pallon, G. Thungström, N. Arteaga, V. Auzelyte, M. Elfman, P. Kristiansson, C. Nilsson, M. Wegdén: *Evaluation of a pre-cell hit detector for the future single ion hit facility in Lund*, 17. Int. Conf. Ion Beam Anal., Seville, Spain, 26.06.–01.07.2005

5.21 Graduations

Doctorate

- Frank Heinrich
  Der elektrische Feldgradient in Makromolekülen –Experiment und Rechnung
  June 2005

Diploma

- Anja Fiedler
  Bestrahlung lebender Humanzellen mit hochenergetischen Protonen.
  March 2005
- Christian Ostwald
  Thesis Title
  August 2005
- Philipp Eigmüller
  Automatic analysis of photometric data
  November 2005
- Jan Kohnert
  Variabilitäts- und Eigenbewegungssurvey auf digital aufaddierten Schmidtplatten
  November 2005

5.22 Guests

- Prof. Dr. Yongpeng Tong
  Shanghai Institute of Applied Physics – SIAP, Shanghai, China
  January 2005 – December 2005
- Dr. S.K. Das
  Babha Atomic Research Centre, Kolkata, India
  from March 2005

- Dr. C.C. Dey
  Babha Atomic Research Centre, Kolkata, India
  August 2005 – November 2005

6

Physics of Dielectric Solids

6.1 Introduction

The research of the Physics of Dielectric Solids Group is directed to the study of structure and dynamics of dielectric solids, of molecules and molecular systems on solid surfaces and interfaces, of nanostructured materials and of metals and ferroelectrics embedded in micro- and mesoporous materials. The investigations are carried out by using various methods of stationary (continous wave, c.w.) and instationary or pulsed magnetic resonance spectroscopy as nuclear magnetic resonance (NMR), nuclear-nuclear double resonance, electron paramagnetic resonance (EPR), and electron-nuclear double resonance (ENDOR). The modern equipment available for the experimental investigations for NMR studies is characterized by a wide range of d.c. magnetic fields (with magnetic flux densities from 2.5. to 17.6 T) and by special techniques which are suitable for an enhancement of spectral resolution and sensitivity. In this respect the modern techniques are suitable for material analysis and characterization in a broad range of applications. These applications are also offered to other interested research groups. In case of electron paramagnetic resonance methods (EPR) the groups has a long standing experience in the development and application of high-resolution techniques, like c.w. and pulsed ENDOR and ESEEM (Electron spin echo envelope modulation) spectroscopy. The later techniques are especially suitable to study their behavior of paramagnetic probe molecules, of transition metals ions and of defect structures in solids and macromolecular systems. The comprehensive NMR and EPR instrumentation available is supplemented by dielectric methods and by gas adsorption methods. The instrumental and methodological development of magnetic resonance for an advanced application on the field of research is continuously carried out. One of the objectives is the investigation of the microscopic mechanism of phase transitions in ferroelectrics and related materials. Substantial experience is available for the investigation of ferroelectric perowskites. Another topical direction of research is the investigation of the properties of nanostructured materials. These studies include also the electronic structure, the spatial structural arrangement and local dynamics of adsorbed molecules interacting with the internal surfaces of nanostructured porous solids (zeolites, mesoporous silicates). In this context also nanoparticles of crystalline solids and nanoclusters in solid matrices are investigated.

Rolf Böttcher, Dieter Michel, Andreas Pöppl

6.2 Pulsed Field Gradient NMR in Combination with Magic Angle Spinning – New Possibilities for Studying Multi Component Diffusion in Heterogeneous Materials

A. Pampel*

*present address: Max-Planck-Institute for Human Cognitive and Brain Science, Leipzig

The combination of MAS NMR spectroscopy with Pulsed Field Gradient (PFG) NMR opens novel possibilities for investigating diffusion processes and also for NMR microscopy of heterogeneous, non-liquid samples. The advantages are based on the effect of line narrowing and concern (i) a prolongation of the intervals during which the magnetic field gradients may be applied and a corresponding enhancement in the sensitivity towards small molecular displacements as well as higher spatial resolution, and (ii) an enhanced resolution in the chemical shift scale. MAS PFG NMR facilitates investigations of materials that were hardly accessible by conventional PFG NMR-based techniques so far. Recently we have shown that MAS PFG NMR has remarkable advantages in comparison with conventional PFG NMR, if applied to diffusion measurements in beds of nanoporous particles, notably zeolites. Those investigations mainly profit from eliminating the influence of the inhomogeneity of the sample susceptibility [1], which is rather strong in zeolites of the MFI-type. For the first time, investigating the diffusion of organic molecules co-adsorbed in Silicalite-1 became possible [2]. Currently, we are focusing on improving the methodolgical background and on investigations of diffusion long-chained organic molecules in zeolites. This work is being done in cooperation with the group of Jörg Kärger (Institute Experimental Physics I) – see also Sect. 3.6.

[1] J. Roland, D. Michel: Magn. Res. Chem. **38**, 587 (2000)
[2] A. Pampel et al.: Chem. Phys. Lett. **407**, 53 (2005)

6.3 Electron Spin Resonance Studies on Cu(I)-NO Complexes in Cu-ZSM-5 Zeolites Prepared by Solid- and Liquid-State Ion Exchange

V. Umamaheswari, M. Hartmann*, G. Vijayasarthi, A. Pöppl

*Fachbereich Chemie, Universität Kaiserslautern

Cu(I)-NO adsorption complexes were formed over Cu-ZSM-5 zeolites prepared by solid-state ion and liquid-state ion exchange. Electron spin resonance spectroscopy revealed the formation of two different Cu(I)-NO species A and B in both systems, whose spin Hamiltonian parameters are comparable with those already reported for the Cu(I)-NO species formed over 66 % Cu(II) liquid-state ion exchanged Cu-ZSM-5 materials [1, 2, 3]. The population of the species A and B differs for the two systems

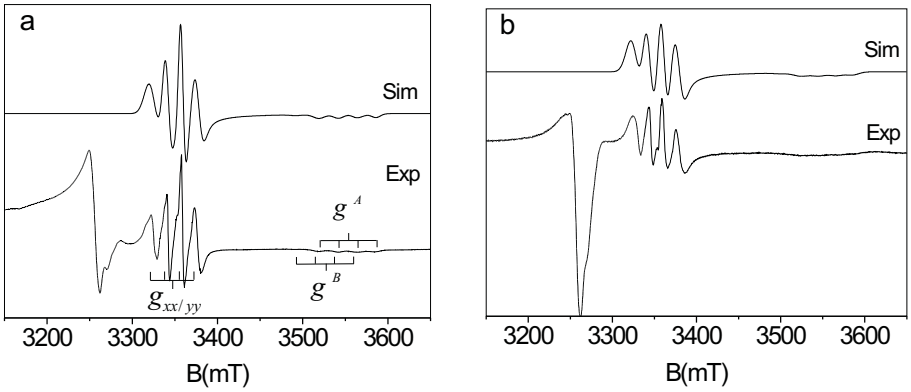

Figure 6.1: Experimental and simulated W-band ESR spectra of Cu(I)-NO complexes formed over Cu-ZSM-5(LE) at (**a**) 6 K and (**b**) 77 K. The stick diagrams indicate the Cu hf splitting of the Cu(I)-NO ESR signal.

studied. Formation of species B is more favored in the solid-state ion exchanged Cu-ZSM-5 when compared to the liquid-state exchanged zeolite. The X-, Q- and W-band electron spin resonance spectra recorded at 6 K and 77 K (Fig. 6.1) reveal the presence of a rigid geometry of the adsorption complexes at 6 K and a dynamic complex structure at higher temperature such as 77 K. This is indicated by the change in the spin Hamiltonian parameters of the formed Cu(I)-NO species in both the liquid- and solid-state ion exchanged Cu-ZSM-5 zeolites from 6 K to 77 K. Possible models for the motional effects found at elevated temperatures are discussed. The temperature dependence of the electron spin phase memory time measured by two pulse electron spin echo experiments indicate likewise the onset of a motional process of the adsorbed NO molecules at temperatures above 10 K. The studies support previous assignments where the NO complexes are formed at two different Cu(I) cationic sites in the ZSM-5 framework and highlight that multifrequency electron spin resonance experiments at low temperatures are essential for reliable determination of the spin Hamiltonian parameters of the formed adsorption complexes for further comparison with Cu(I)-NO complex structures predicted by quantum chemical calculations.

[1] V. Umamaheswari et al.: J. Phys. Chem. B **109**, 19 723 (2005)
[2] V. Umamaheswari et al.: J. Phys. Chem. B **109**, 10 842 (2005)
[3] V. Umamaheswari et al.: Magn. Res. Chem. **43**, 205 (2005)

6.4 Study of the Tetragonal-to-Cubic Phase Transition in $PbTiO_3$ Nanopowders

E. Erdem, R. Böttcher, A. Matthes, H.-J. Gläsel*, E. Hartmann*

*Leibniz-Institut für Oberflöchenmodifizierung, Leipzig

In combination with soft milling, the liquid-precursor based CPPl route (combined polymerisation and pyrolysis of liquid organometalic precursors) yields a target $PbTiO_3$ nanopowder basis for studying temperature and size driven tetragonal-to-cubic phase

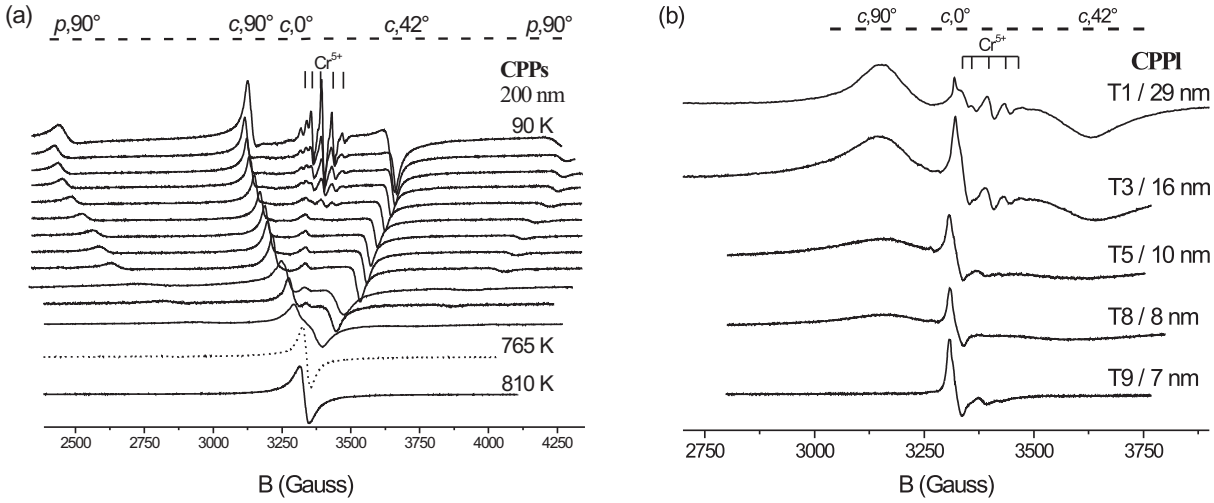

Figure 6.2: Changes in the chromium EPR spectra due to temperature variation (from 90 K up to 810 K in steps by 60 K (**a**) and as a result of size variation at room temperature (**b**)).

transitions in a direct way. Inherent in at least all high-temperature preparation procedures, log-normal particle-size distributions determine nanopowder properties as ensemble averages. The high-qualitative materials basis allowed to extend Müller´s EPR-based approach to perovskitic bulk materials [1] to other such bulk systems and, for the first time to nanosized $BaTiO_3$ and $PbTiO_3$ systems, where the latter $PbTiO_3$ nanopowders form the subject of the present work. The latter two comparative studies brought out for the $BaTiO_3$ and $PbTiO_3$ nanopowders rather different pictures of the temperature and size driven ferroelectric-to-paraelectric phase transitions. Indeed, this difference can be traced back to the rather different binding conditions (strong covalency in $PbTiO_3$ owing to Pb 6*s* participation). In the present observation of temperature and size driven tetragonal-to-cubic phase transitions we were faced with a close cooperation between temperature rise and size reduction to bring about the paraelectric cubic state (Fig. 6.2). In a close correspondence with dielectric measurements, the EPR spectra furnished explicit evidence that tetragonal core and gradient surface region coexist in a particle which is highly reminiscent to the core-shell idea for ferroelectric nanoparticles where the surface boundary conditions play a major role in determining the size effects on ferroelectricity [2]. A consistent and comprehensive block of size and temperature dependent XRD, EPR and dielectric data particularly covers the critical size d_{cr}, and an Ishikawa fit [3] explicitly yields the small critical size of 6 nm which is in qualitative accordance with thin-film derived data. In $PbTiO_3$, probably owing to the participation of the Pb 6*s* orbital in strong covalent binding, tetragonality proves very stable and can only be removed at a rather high temperature, extraordinarily strong reduction of particle size and for a given $PbTiO_3$ particle in an exceptionally thin surface layer. This finding is consistent with comparative estimations of surface relaxations occurring in $BaTiO_3$ and $PbTiO_3$ [4], which in turn readily explain our former finding of a broad surface layer occurring in $BaTiO_3$. In the present study, however, main focus is set on the phenomenology of size effects, which in turn is amenable to physical interpretation by the pertinent solid-state theoreticians.

[1] K.A. Müller, J.C. Fayet: *Topics in Current Physics: Structural Phase Transition II*, Vol. 23, ed by K.A. Müller, H. Thomas (Springer, Berlin 1991)

[2] R. Böttcher et al.: Phys. Rev. B **62**, 2085 (2000)
[3] K. Ishikawa et al.: Phys. Rev. B **37** 5822 (1988)
[4] E. Erdem et al.: Magn. Reson. Chem. **43**, 174 (2005)

6.5 Study of Size and Temperature Driven Tetragonal-to-Cubic Phase Transition in One-Dimensional Ferroelectrics

A. Matthes, E. Erdem, R. Böttcher, H.-J. Gläsel*, E. Hartmann*

*Leibniz-Institut für Oberflöchenmodifizierung, Leipzig

In the this work the CPPs route [1] (combined polymerisation and pyrolysis of solid organometalic precursors) was used to prepare ferroelectric perovskitic nanomaterials with particle size regions, which enable to study the temperature and size driven tetragonal-to-cubic phase transition. Due to the size distribution, the experimental results are ensemble averages. Using AlO_x nanofilters 200-nm-pore Whatman anodisc aluminium oxide membranes) as templates should result in a considerable narrowing of the size distribution. For filling the pores of this nanofilter by precursor, obviously a liquid-precursor based variant (CPPl) is inevitable. The downward shift of the size distribution (below 10 nm) yielded a unique materials basis, allowing for the first time a direct study of temperature and size driven ferroelectric-to paraelectric phase transition by standard methods (FT-Raman, XRD . . .) and, moreover, by EPR [2, 3] and dielectric spectroscopy [4]. After powder research, the advanced CPPl route proved its high potential in a single-step preparation of ferroelectric thin films. In the template

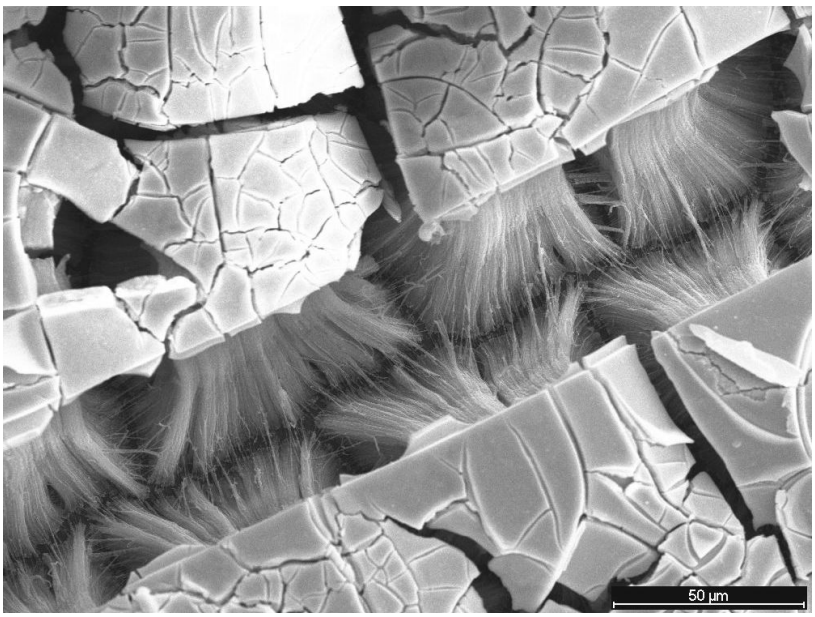

Figure 6.3: REM image of perovskite nanotubes formed during CPPl template synthesis using 200-nm alumina membranes.

preparation ferroelectic nanotubes were obtained of diameter (200 nm) and thickness 3 – 6 nm (Fig. 6.3. Obviously the nanotubes reveal considerable internal strain which, after removal of the template, brings about a nanotube widening by typically a factor of 2. In powder research, EPR spectroscopy proved exceedingly efficient in analysing the internal solid state and one can expect to obtain specific spectral differences between original and released template materials.

[1] E. Erdem et al.: J. Mater. Sci. **38**, 3211 (2003)
[2] E. Erdem et al.: Phys. Stat. Sol. B **239**, R7 (2003)
[3] E. Erdem et al.: Magn. Res. Chem. **43** S174 (2005)
[4] R. Grigalaitis et al.: Proc. III. Int. Mater. Symp., Lisbon (2005), p. 355

6.6 Dehydration of LTA Type Zeolites Studied by Multi Nuclear MAS NMR and DRIFT Spectroscopy

W. Böhlmann, I.A. Betaa*, B. Hunger†

*Department of Physics, Kansas State University, Manhattan, Kansas, USA
†Wilhelm-Ostwald-Institut für Physikalische und Theoretische Chemie

Most applications of zeolites as catalysts and adsorbents require thermal treatment or dehydration of the used zeolites. It has been shown that the presence of water during thermal treatment changes the aluminum coordination [1, 2, 3]. Reversible aluminum coordination was firstly observed by Bourgeat-Lami et al. for protonic zeolite beta [1] and later on zeolite HY [2, 3, 4, 5] too. To our best knowledge, this phenomenon has been not observed by any authors on LTA zeolites exchanged with Ca^{2+} ions. In this study we seek to provide insight into the flexible coordination of lattice aluminum in CaNaA (83 % exchange degree) and pure NaA zeolites using the temperature-programmed DRIFT spectroscopy (TP-DRIFTS) and ^{1}H, ^{27}Al and ^{29}Si MAS NMR. Three main bands at 3608, 3506 and 3565 cm^{-1} of which the first two are due to bridging Si−OH−Al groups located in 6 and 8 rings, respectively, whereas the third corresponds to $Ca(OH)^{+}$ groups dominate the TP-DRIFT spectra of zeolite sample exchanged with Ca^{2+} ions above 573 K. The intensity changes of the individual bands are indicative for two dehydroxylation processes in different temperature ranges [6, 7]. The ^{27}Al MAS NMR spectrum of the untreated CaNaA generally consists of an intense peak at 57.3 ppm assigned to tetrahedrally coordinated aluminum and a weak signal at 78.8 ppm due to calcium alumosilicate groups. With increasing temperature (up to 773 K) a highfield shift of the peak at 57.3 ppm of about 7 ppm is observed while at the same time a weak signal at 12.2 ppm (overlapped with spinning sideband) emerges which is typical for octahedrally coordinated aluminum (Fig. 6.4). Further increase of the temperature causes a downfield shift of the main peak and a disappearance of the peak at 12.2 ppm. It can be estimated from the NMR spectra that about 10 % of the lattice aluminum changes the coordination during the temperature treatment. This finding suggests that the aluminum coordination is flexible in calcium ion-exchanged A zeolite, an observation not yet reported by any earlier investigations. Besides this result, both the ^{29}Si NMR and

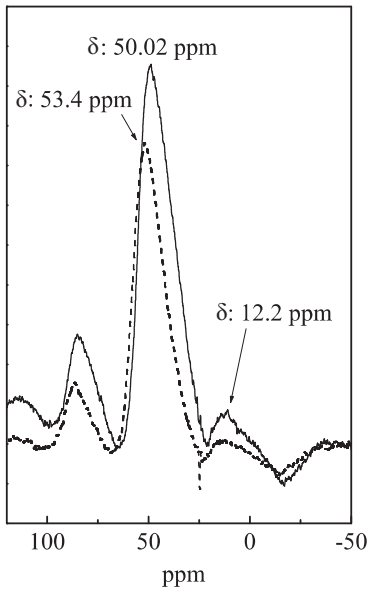

Figure 6.4: ^{27}Al MAS NMR spectra of CaNaA-83 after pre-treatment at 773 K (*solid line*) and at 1023 K (*dashed line*).

the ^{1}H NMR show that significantly structural changes occur during thermal dehydration of CaNaA zeolite, thus suggesting that the reversible aluminum is of a similar nature compared with zeolites HY, H-USY and H-beta [2, 3, 4, 5] where the flexible aluminum species belong to an amorphous silica-alumina phase. Considering the NaA zeolite again structural changes with increasing temperature are observed but flexible aluminum could not be detected. Thus we can assume that the reversible aluminum coordination in the CaNaA zeolite is closely connected with structural hydroxyl groups which are formed due to the dissociative adsorption of water.

[1] E. Bourgeat-Lami et al.: Appl. Catal. **72**, 139 (1991)
[2] B.H. Wouters et al.: J. Phys. Chem. B **105**, 1135 (2001)
[3] J.A. van Bokhoven et al.: Stud. Surf. Sci. Catal. **142**, 1885 (2002)
[4] A. Omegna et al.: J. Phys. Chem. B **107**, 8854 (2003)
[5] B.H. Wouters et al.: J. Am. Chem. Soc. **120**, 11 419 (1998)
[6] I.A. Beta et al.: Micropor. Mesopor. Mat. **79**, 69 (2005)
[7] W. Böhlmann et al.: Stud. Surf. Sci. Catal. **158A**, 781 (2005)

6.7 Molecular Dynamics and Glass Transition of Ethylene Glycol Adsorbed in Zeolites: Influence of Surface–Molecule Interactions, Topology, and Loading Degree

Ö.F. Erdem, D. Michel

Using the ^{1}H-MAS-NMR technique, a good proton chemical shift resolution could be achieved for glass-forming ethylene glycol (EG) molecules adsorbed in NaX zeo-

lites. A clear differentiation was possible between samples which have predominantly molecules in the supercages of NaX and those ones where EG molecules are also located outside the supercages. Hence, the analysis of the proton chemical shifts of the adsorbed EG molecules allows an unambiguous characterisation of the pore filling degree of the samples which is a prerequisite for the study of confinement effects. On this basis we were able to selectively study proton spin relaxation times and to derive correlation times and activation energies for the thermal reorientation for the adsorbed species [1]. Broadband dielectric spectroscopy (BBS) was applied to such systems with adsorbed molecules in zeolites. A Vogel–Fulcher–Tammann (VFT)-type temperature dependence which would indicate a dynamical glass transition, was not detected for the system EG/NaX. This shows that for EG adsorbed in NaX supercages around the calorimetric glass transition temperature no glass-like dynamics is detectable, in particular also for a complete filling of the supercages of NaX zeolites with ca. 10 EG molecules per supercage in a statistical average [2] (Fig. 6.5). The suppression of glass transition in NaX is indicative that besides the EG molecule-molecule interactions in the confined system, further influences should be taken into account. Apparently, interactions of the EG molecules with adsorption sites on the internal surface of the NaX supercages cannot be neglected in the EG/NaX systems. They do strongly compete with molecule-molecule interactions which explains the fact that the "cooperative" motion reflected by the VFT-type behaviour in the other systems is not detectable but instead a restricted "local" motion of EG molecules is seen as reflected in the Arrhenius-type temperature dependence of the dielectric relaxation rates. For this reason by means

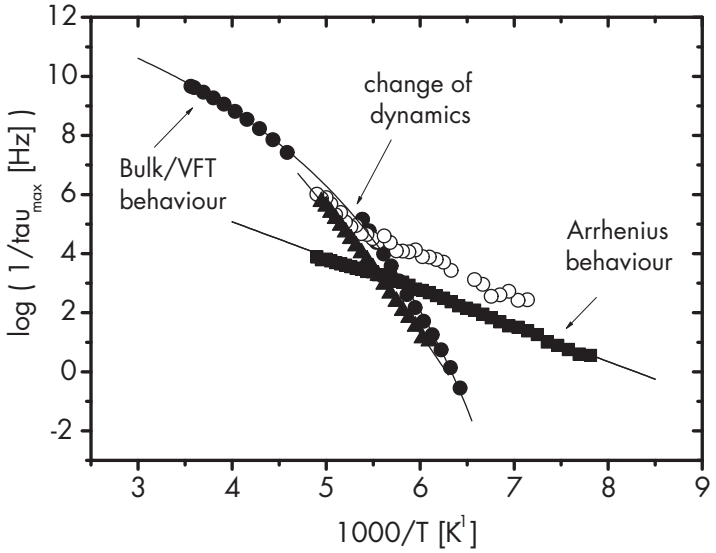

Figure 6.5: Dielectric relaxation rate versus inverse temperature for bulk EG (*filled circles*) and 4 EG molecules adsorbed in zeolite beta with Si/Al ratio of 56 (*filled squares*), 215 (*open circles*) and infinity (*filled triangles*). The 4 EG/beta with Si/Al = ∞ (Al-free) samples follow a similar behavior like bulk EG (VFT function is fitted to the data of both bulk EG and 4 EG/beta with Si/Al = ∞), whereas a change in the dynamics is observed for the sample 4 EG/beta with Si/Al = 215, having completely Arrhenius at low temperatures and more like VFT-type activation at increasing temperatures. 4 EG/beta with Si/Al = 56 follow a complete Arrhenius-type of activation plot in the entire temperature range (Arrhenius function is fitted to the data).

of BBS, EG adsorbed in zeolites was investigated in more detail by varying the loading degree, the type of zeolites, and the Si/Al ratio. We only concentrated to the frequency and temperature range where relaxation processes may be observed which allow conclusions about the glass-transition. The influence is explored by measuring the dielectric relaxation rate for EG adsorbed in zeolite beta, EG/beta, with different Si/Al ratios. For the case of zeolite beta with a very large Si/Al ratio, a glass transition is observed, i.e. a VFT-type of activation is detectable. For the system EG/beta with Si/Al ratio of 56, however, a clear Arrhenius-type activation is observed. Obviously, due to a higher number of adsorption sites, surface-molecule interactions are of greater influence and suppress the glass transition. For EG/beta with a Si/Al ratio between 56 and infinity, there is subtle interplay between "cooperative" and "local" motions, i.e. between VFT- and Arrhenius-type activation behaviour [3]. The main goal of the recent work under progress is to combine broadband dielectric relaxation analysis and 2D ^{2}H exchange NMR [4]. This will be also realised for systems with even higher pore diameter, e. g. SBA-15 with diameters of 3 – 10nm. These materials are highly stable and the surface properties, like acidity, can be controlled and investigated by means of ^{1}H-MAS-NMR [5].

[1] Ö.F. Erdem et al.: J. Phys. Chem. B **109**, 12 054 (2005)
[2] Ö.F. Erdem et al.: Chem. Phys. Lett. **418**, 450 (2006)
[3] Ö.F. Erdem et al.: Micropor. Mesopor. Mat. (2006), submitted
[4] Ö.F. Erdem et al.: in preparation
[5] V. Degirmenci et al.: J. Am. Chem. Soc. (2006), submitted.

6.8 Exceptional Commensurate/Incommensurate Phase Sequences in DMAAS and DMAGaS

J. Banys*, R. Böttcher, D. Michel, G. Völkel†, Z. Czapla‡

*Faculty of Physics, Vilnius University, Lithuania
†private address: Zickra 1A, 07955 Auma
‡Institute of Experimental Physics, University Wroclaw, Poland

Dimethylammonium gallium sulphate hexahydrate [DMAGaS, $(CH_3)_2NH_2Ga(SO_4)_2$ $6H_2O$] belongs to a crystal family with the further members dimethyl-ammonium aluminum sulphate hexahydrate [DMAAS, $(CH_3)_2NH_2Al(SO_4)_2$ $6H_2O$] and dimethylammonium aluminum sulphate selenate hexahydrate [DMAASSe, $(CH_3)_2NH_2Al(S_{1-x}Se_xO_3)_2$ $6H_2O$]. The crystal structure is build up of Ga or Al atoms coordinating six water molecules, regular SO_4 or SeO_4 tetrahedra and DMA $[(CH_3)_2NH_2]^+$ cations, where all these units are interconnected by a three-dimensional framework of hydrogen bonds. In their high-temperature phase, ferroelastic DMAGaS and DMAAS crystals have been found to be isomorphic in structure, showing the monoclinic space group P_{21m}. Both crystals exhibit a structural transition into a ferroelectric phase. The ferroelectric transition is thought to be of the order-disorder type [1, 2]. However, in contrast to most of the representatives of hydrogen-bonded ferroelectrics, the driving

force for the ferroelectric transition seems to be the ordering process of the dimethyl ammonium cations rather than that of the protons in the hydrogen bond system. DMAAS undergoes a ferroelectric transition of the second order at T_c = 152 K, whereas DMAGaS shows two successive first-order transitions: at first into a ferroelectric phase at T_{c1} = 134 K and then into a low-temperature non-polar phase at T_{c2} = 115 K. The reason for the different behaviour of DMAAS and DMAGaS was not yet understood. Both of the ferroelectric transitions are close to a critical behaviour, whereas the transition into the nonpolar phase in DMAGaS is strongly of the first order. At the transition into the ferroelectric phase, the twofold screw axis disappears and the crystal adopts a structure with the space group Pn. A spontaneous polarisation results along the glide direction of the glide mirror plane n. It can be assumed that the ferroelectric transition is associated with the polar dimethyl ammonium cations, which execute hindered rotations around their C−C axis in the ferroelastic phase and then order statistically in the ferroelectric phase along the polar axis. Dielectric investigations of dimethylammonium gallium sulphate [1] have revealed that in the vicinity of T_{c1}, the crystal shows a critical slowing-down of the polarisation fluctuations. In the far paraelectric phase, ferroelectric dispersion of the Debye type is caused by a single relaxational soft mode related to the flipping motion of the dimethyl-ammonium groups in a double well potential with the activation energy 0.09 eV = $7.6kT_{c13}$ in the paraelectric phase. Near T_{c13} and in the ferroelectric phase, the ferroelectric dispersion overlaps with the domain wall dispersion and causes a complex dielectric spectrum. Very similar results have been obtained by Czapla and Tchukvinskyi [3]. Dielectric investigations of ferroelectric $(CH_3)_2NH_2Al(S0_4)_2\ 6H_2O$ crystals have shown a critical slowing-down process of polarisation, with an extremely long relaxation time for the dipole system ($t = 1.6\times10^{-7}$ s at the phase transition temperature). The dielectric response over the frequency range up to 56 GHz in the paraelectric phase has been well described in terms of a monodispersive Debye-type formula. The activation energy of dipoles in the paraelectric phase has been found to be 0.11 eV = $0.85kT_c$. EPR studies have revealed complex structural changes in a chromium-doped DMAGaS crystal (see work cited in [2]). It was demonstrated that the low-temperature phase of DMAGaS below T_{c2} = 115 K shows a sequence of commensurate and incommensurate phases. At T^* = 60 K the crystal becomes antiferroelectric. This unusual phase sequence can be explained [2] by means of a Landau approach using a greater number of sublattice polarizations, and more generally by the semimicroscopic extended DIFFOUR model. According to the theoretical considerations of the phase diagram of DMAGaS, the change in chemical composition should change the phase transition temperatures: T_{c1} should be shifted to higher temperatures and T_{c2} should be shifted to lower temperatures. There should be a similar effect to that of changing the pressure. Recent very interesting and fundamental experiments have been reported dealing with the influence of high hydrostatic pressure on the phase diagram of DMAAS and DMAGaS. It was shown that under high hydrostatic pressure the ferroelectric phase of DMAGaS disappears, whereas in DMAAS new phases of unknown character appear between the paraelectric and ferroelectric phases. The extended DIFFOUR model permits the understanding of all these phenomena in a congruent manner [2].

[1] J. Banys et al.: Phase Trans. **78**, 337 (2005)
[2] G. Völkel et al.: J. Phys. Cond. Matter **17**, 4511 (2005)
[3] Z. Czapla, R. Tchukvinskyi: Acta Physica Polon. A **93**, 527 (1998)

6.9 Preparation and Studies of Ferroelectric Sodium Nitrite Nanoparticles in Confined Geometry

D. Michel, W. Böhlmann, E.V. Charnaya*

*Institute of Physics, St. Petersburg State University, Russia

The ferroelectric materials are embedded in MCM-41 and SBA-type mesoporous materials. The MCM-41 and SBA-15 molecular sieves with pore sizes of 2.0, 2.4, and 3.7 nm for MCM-41 and 5.2 nm for SBA-15 were synthesized and characterized by various physical methods (XRD, adsorption measurements). The mesoporous matrices prepared in Leipzig were filled with sodium nitrite ($NaNO_2$) in the Blagoveschensk State Pedagogical University under the supervision of Prof. Yu.A. Kumzerov from the Physico-Technical Institute A.S. Ioffe of the Russian Academy of Science (RAS), St. Petersburg. After cooling the samples, the pellets were pressed under a pressure of 8000 kg/cm^2. The behavior of $NaNO_2$ in these mesoporous materials was investigated by means of ^{23}Na NMR in Leipzig. Dielectric and acoustic measurements were carried out at the St. Petersburg State University. The results of the NMR and dielectric studies were published in [1, 2]. ^{23}Na spin–lattice relaxation and lineshape as well as the complex impedance were measured in a large temperature range up to 535 K covering the ferroelectric phase transition point for the bulk $NaNO_2$ material. It was shown that confined $NaNO_2$ below the bulk sodium nitrite melting point consists of two parts with relaxation times which differ by two orders in magnitude. A portion of $NaNO_2$ exhibits bulk-like properties with the ferroelectric phase transition in the vicinity of the bulk transition temperature. The bulk-like $NaNO_2$ prevails below and near the ferroelectric phase transition and its amount decreases strongly when the temperature approaches the bulk melting point. Fast nuclear relaxation in another portion of confined $NaNO_2$ revealed very high molecular mobility. This portion increases with increasing temperature and dominates above 510 K. It was suggested that the fast relaxation is related to the melted or pre-melted state of confined $NaNO_2$ caused by confinement. This suggestion is confirmed by the temperature evolution of the ^{23}Na NMR line. The amount of $NaNO_2$ which possesses high molecular mobility depends on pore size and is maximum for the MCM-41 porous matrix with a 2 nm pore size. The correlation time for the electric field gradient fluctuations of this part was found to be similar to that in viscous liquids with an activation energy of about 0.42 eV. The existence of two parts of $NaNO_2$ was found for all experimental data of $NaNO_2$ under the condition of a restricted geometry. Acoustic studies showed that the velocity and attenuation of longitudinal ultrasound are very sensitive to gradual melting of confined sodium nitrite. The results obtained by acoustic techniques are currently prepared for publication. In extension of this work, we have studied the behavior of Rochelle salt embedded into nanoporous matrices. For this reason, MCM-41 mesoporous molecular sieves with pore size 2.0, 2.4, and 3.7 nm were synthesized and characterized at the Leipzig University. The mesoporous matrices were filled with the ferroelectric Rochelle salt in solution. After drying the samples, the pellets were pressed under a pressure of 8000 kg/cm^2. Again the sample preparation was carried out at the Blagoveschensk State Pedagogical University under the supervision of Prof. Yu.A. Kumzerov (A.S. Ioffe Institute of the RAS). Preliminary NMR and dielectric stud-

ies of the samples prepared were carried out in the St. Petersburg State University and in the Leipzig University. The studies showed that both NMR and dielectric measurements are sensitive to the ferroelectric phase transition in confined Rochelle salt as well as to the melting phase transition of the Rochelle salt within nanopores. The ferroelectric properties of confined Rochelle salt were found to be strongly influenced by continuous melting and freezing processes within the nanopores. Preliminary ^{23}Na MAS NMR measurements at room temperature revealed the coexistence of solid and melted state of the Rochelle salt nanoparticles. The studies will be continued in the framework of the DFG project.

[1] C. Tien et al.: Phys. Rev. B **72**, 104 105 (2005)
[2] S.V. Baryshnikov et al.: Solid State Phys. **48**, 593 (2006) [Fizika Tverdogo Tela, in Russian, February 2006]

6.10 Preparation and Studies of Nanoporous Matrices Filled with Metallic Gallium and Mercury

D. Michel, E.V. Charnaya*

*Institute of Physics, St. Petersburg State University, Russia

In extension of our former work, phase transitions and self-diffusion in gallium and mercury were studied which are confined in porous materials. The porous glasses with pore sizes of 2, 12, and 16 nm and synthetic opals (photonic crystals) consisting of silica spheres with diameter of 240 nm, were prepared in the Physico-Technical Institute A.S. Joffe of the Russian Academy of Siences (RAS), St. Petersburg. Vycor glass with a pore size of 8 nm was provided by the Corning Glass company. Pore size and pore size distribution were characterized by mercury porosimetry in the Physico-Technical Institute. Liquid gallium was introduced into the pores under high pressure. The samples with mercury were prepared by means of the mercury intrusion porosimetry. NMR studies were carried out in Leipzig. Acoustic studies were run in the St. Petersburg State University. The results of NMR studies of nuclear spin-lattice relaxation in liquid metallic gallium confined within random pore networks of two porous glasses with 16 and 2 nm pore sizes were presented in [1, 2]. The measurements were run in the temperature range from 330 K to the freezing temperature of confined gallium. The relaxation for both gallium isotopes, ^{71}Ga and ^{69}Ga, was found to accelerate remarkably compared to the bulk melt, the dominant mechanism of relaxation changed from the magnetic to the quadrupole coupling. The correlation time of electric field gradient fluctuations caused by atomic motions was estimated at various temperatures using data for quadrupolar relaxation contribution and was found to increase drastically compared to bulk, which corresponded to a pronounced slowdown of atomic mobility in confined liquid gallium. The influence of confinement was more effective for smaller pore sizes. The temperature dependence of the correlation time for confined gallium was found to be noticeably stronger than in bulk, an additional slowdown of atomic mobility being observed at low temperatures. The temperature dependences of spin-lattice relaxation for gallium embedded into porous opals were also studied and the

results are under preparation for publication. Acoustic studies of porous glasses with 12 and 8 (Vycor) nm pore size filled with mercury were presented in [3, 4]. It was shown for the first time that the pore filling factors influences drastically the temperatures of the melting and freezing phase transitions. The critical size of mercury nanoparticles that corresponds to the zero melting point was estimated and the threshold value of the filling factor was observed below which the ultrasound velocity is no longer sensitive to the mercury melting and freezing transitions.

[1] E.V. Charnaya et al.: Phys. Rev. B **72**, 035 406 (2005)
[2] E.V. Charnaya et al.: Diffusion Fundamentals **2**, 68 (2005)
[3] B.F. Borisov et al.: Acoust. Phys. **52**, 138 (2006)
[4] E.V. Charnaya et al.: World Congress on Ultrasonics - Ultrasonics International Program and Paper Abstracts, September, 2005, Peking, China, p.45.

6.11 ^{13}C NMR Study of the Influence of the Aerosil Surface Charge on the Short-Chain Surfactant Adsorption

M.V. Popov*, Y.S. Tchernyshev*, D. Michel

*Institute of Physics, St. Petersburg State University, Russia

The adsorption of surfactants at solid/liquid interface is widely used in many industrial processes such as mineral flotation, emulsion polymerization, dewatering and many others. The structure of adsorption sites, adsorption kinetics and dynamics were studied in detail by various NMR techniques, infrared spectroscopy, calorimetric measurements, fluorescence and ESR. On the basis of experimental and theoretical investigations it is shown that the adsorption process results from energetically favorable interactions between the solid adsorbate and the solute species. It is often a very complex process because of the influence of all components of the systems (solid, solvent and solute). Previous experimental results (see for example [1]) have demonstrated that the adsorption process depends on surface charge density, pH, surfactant structure and concentration, electrolyte concentration, and the type of the adsorbent surface (hydrophobic or hydrophilic). It is shown that several interactions can contribute to the adsorption process, such as electrostatic attraction, covalent and hydrogen bonding, hydrophobic interaction between the adsorbed molecules and these molecules with adsorbent surface, as well as the lateral interaction between the adsorbed species and their desolvatation. Our recent work [2] has shown that the adsorption of short-chain surfactant (potassium nonanoate) from aqueous solution strongly depends on the Aerosil surface charge. On the basis of ^{13}C chemical shifts we investigated structural changes of the adsorbed layers at various surfactant concentration and/or surface charges. Measurements of the ^{13}C spin-lattice relaxation time T_1 for separate segments of the hydrophobic chain allowed conclusion the molecular dynamics in the adsorbed state. Thus, we confirmed the results already derived from the chemical shifts [2]. In this article we show that the diamagnetic shielding of the carbon atoms is very sensitive to the bonding between the active sites on the Aerosil surface and the adsorbed surfactant

molecule. The changes is especially essential for the first and second carbon atoms of the amphiphilic molecules. In ternary systems with a nearly neutral Aerosil surface we observed a maximum downfield change of the chemical shifts of ca. 1 ppm. For relatively strongly charged Aerosil surface a upfield shift of 3 to 4 ppm was observed for these atoms. We have carried out similar measurements for four different short-chain ionic surfactants with different chain hydrophobic length. The aim of this study was to investigate the influence of the hydrophobic chain length and Aerosil surface charge on the adsorption of the short-chain amphyphilic molecules and to confirm our previous conclusions [3].

[1] R. Atkin et al.: Adv. Coll. Int. Sci. **103**, 219 (2003)
[2] M.V. Popova et al.: Coll. Surf. A **243**, 139 (2004)
[3] M.V. Popova et al.: to be published

6.12 NMR Studies on Crystals with Structurally Incommensurately Modulated Phases

D. Michel, A. Taye, J. Petersson*

*Department of Physics, University of Saarland

Several crystals exhibit a structural phase transition from a high temperature paraelectric (N) phase into a structurally incommensurately (IC) modulated phase, where at least one local physical quantity is modulated in such a way that the characteristic wave vector qi is not a rational multiple of the reciprocal lattice vectors of the N phase. The dynamics of the incommensurate (IC) modulation is investigated for several one-dimensionally incommensurately modulated crystals near the transition to the normal high temperature phase at the temperature T_i (see [3] and papers cited here). Using nuclei with nuclear quadrupole moments as local probe, nuclear magnetic resonance (NMR) line shape and spin-lattice relaxation have shown to be very sensitive to study the order parameter dynamics and slow elementary excitations in crystals with IC phases. All results can be described consistently in terms of a static modulation in the IC phase without any indication for "floating" or large scale fluctuations of the modulation wave. The critical exponents derived from the NMR line shape and the relaxation times $T1$ very nicely fit to the universality class of the 3d-XY model. Recently, the validity of this conclusion was also confirmed for the particular IC system of bis(4-chlorophenyl)sulphone, $(ClC_6H_4)_2SO_2$. For Rb_2ZnBr_4 and Rb_2ZnCl_4 crystals the characteristic frequency of the critical dynamics of the order parameter (OP) slows down to a frequency range which has been estimated to lie between $2-10$ MHz. In this particular case one can derive the characteristic frequency of the critical dynamics of the OP above T_i and of the phason below T_i from the Larmor frequency dependence of ^{87}Rb NMR relaxation times $T1$. The relatively broad temperature range where the critical dynamics was observed may be explained on the basis of renormalization group theory.

[1] D. Michel et al.: Ferroelectrics **314**, 244 (2005)

6.13 NMR Studies on Small $BaTiO_3$ Particles

D. Michel, G. Klotzsche, P. Sedykh

In the ^{137}Ba NMR measurements on $BaTiO_3$ powder samples, only the central line transitions $\left(m = +\frac{1}{2} \leftrightarrow m = -\frac{1}{2}\right)$ could be detected in the various phases. The line shape for the central transition NMR lines is dominated by the quadrupole coupling tensor (proportional to the electric field gradient tensor, EFG) in second-order of perturbation theory. This assumption has been checked at first by comparing the results of line shape measurements on microcrystalline samples with those ones derived from the rotation patterns of satellite-transition NMR lines. The same single crystals were used from which the powder was produced. NMR measurements at two different d.c. magnetic fields (B_0 = 11.7 and 17.6 T) showed the typical proportionality to $1/B_0$. Relatively sharp ^{137}Ba NMR lines (with Gaussian lineshape and widths at half-heights of ca. 200 Hz) were observed for the polycrystalline material in the cubic phase above the Curie temperature T_c where the EFG is zero. The lines are broadened abruptly on cooling below the phase transition into the tetragonal phase. In the tetragonal phase the Ba atoms are at sites of axial symmetry where the EFG tensor has zero asymmetry parameter. The quadrupole perturbed NMR line shape for microcrystalline samples was simulated by means of the Bruker WinNMR program [1]. The central transition NMR line shapes in the various phases are shown in Fig. 6.6. In the powder pattern the distance between the edge singularities of thecentral transition is given by the second-order effect. This treatment allows to derive the quadrupole coupling constant $C_Q = |e^2qQ/h|$ in the tetragonal phase directly from the distance of the egde singularities. The values are in a complete agreement with the results from single crystal measurements [2, 3]. The coupling constant C_Q was found [4] to be proportional to the square of the order parameter (spontaneous ferroelectric polarization). Hence, the ^{137}Ba NMR spectra allow to derive conclusions about the ferroelectric order parameter similarly as shown for the fine structure tensor which was studied by means of EPR spectroscopy [5]. The influence of the grain size on the ^{137}Ba NMR spectra is clearly reflected in the spectra measured in the tetragonal phase at ca. 300 K [5, 6]. In comparison to the NMR measurements on microcrystalline $BaTiO_3$ samples, the powder pattern of the central line for the samples with mean particle sizes of 155, 55, and 25 nm may be explained by a superposition of two tetragonal contributions. For each of which the line shape calculation has been carried out in a similar way as described for the EPR spectra. To simulate the NMR spectra in the tetragonal phase (where the asymmetry parameter can be assumed to be zero), we started from the NMR frequencies for the central transition in second-order of the quadrupole Hamiltonian relative to the Larmor frequency. To simulate the line shape $I(\upsilon)$, the frequencies $\nu^{(2)}(\Theta)$ of the central transitions (relative to the Larmor frequency ν_L) were averaged over the polar angles Θ by taking into account of Gaussian distribution of the quadrupole coupling constant C_Q with mean values $\langle C_{Q,k}\rangle$ and widths $\Delta C_{Q,k}$. One line shape component for the nanoparticles shows the typical line shape for the tetragonal phase ($\langle C_{Q,k}\rangle$ = 2.6 MHz) and a relatively small distribution of the quadrupolar constant ($\Delta C_{Q,2}$ = 0.5 MHz). Recently a program has been developed which enables the calculation of the spectra for nanoparticles for arbitrary asymmetry parameters and anisotropy parameters. The spectra for samples with an average particle size in the range between 25 nm $< d_m <$ 155 nm can be described by a superposition

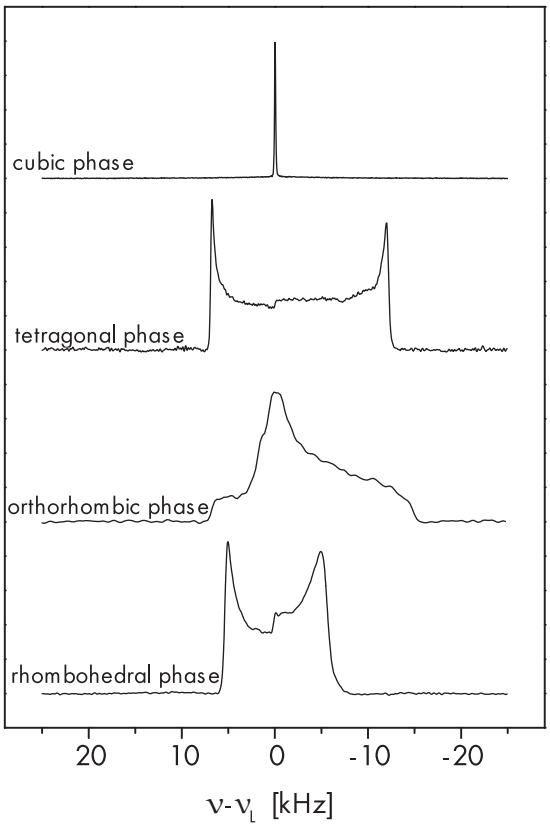

Figure 6.6: ^{137}Ba NMR spectra of microcrystalline $BaTiO_3$ powder, prepared from single crystals, at various temperatures. Resonance frequency: 55.6 MHz (d.c. magnetic field of 11.7 T). Temperatures: rhombohedral phase at 160 K, orthorhombic phase at 260 K, tetragonal phase at 300 K, and cubic phase at 416 K.

of two lines with different values $\langle C_{Q,k} \rangle$ and $\Delta C_{Q,k}$ for the quadrupolar constants and the distribution widths, respectively. One line shape component for the nanoparticles shows the typical line shape for the tetragonal phase ($\langle C_{Q,2} \rangle \gg 2.6$ MHz) and a relatively small distribution of the quadrupolar constant ($\Delta C_{Q,2} \gg 0.5$ MHz). This situation leads to the conclusion that one part of the sample possesses a tetragonal symmetry with small distortions. The other component obviously belongs to regions where the mean quadrupole coupling constant is smaller (2.2 MHz – 1.6 MHz, depending on the particle size) and where a relatively broad distribution occurs. The simulation of the NMR spectra is nicely consistent with the following structural model for fine $BaTiO_3$ particles which was already supported by the previously obtained EPR data: A weakly distorted tetragonal core is surrounded by a highly distorted shell where the local symmetry can be only characterized by a strong distribution of the internal electrical fields (electric field gradients). The fraction of the distorted regions increase when the particle diameters are reduced from 155 nm to 25 nm. But at 25 nm still a tetragonal ordered part occurs (fraction ca. 30 %). For the sample with the smallest diameters (15 nm) the strongly distorted component dominates and it was not possible to find a tetragonal center. We hope that more extensive ^{137}Ba NMR measurements on nanoparticles, which are progress over a wide temperature range in the tetragonal phase, may help to further elucidate this question.

[1] WinNMR version 6.0 and WinSim, © Bruker-Franzen Analytik GmbH
[2] T.J. Bastow: J. Phys. Cond. Matter **1**, 4985 (1989)
[3] A. Taye et al.: J. Phys. Cond. Matter **11**, 871 (1999)
[4] O. Kanert et al.: Solid State Commun. **91**, 465 (1994)
[5] E. Erdem et al.: Adv. Solid State Phys. **45**, 337 (2005)
[6] E. Erdem et al.: Ferroelectrics **316**, 43 (2005)

6.14 Funding

Strukturaufklärung nanokristalliner Ferroelektika mit Perowoskitstruktur durch Hochfeld-EPR-Spektroskopie
Investigation of nanocrystalline ferroelectrics with pervoskite structure by means of high-field-EPR spectroscopy
R. Böttcher
DFG, Bo 1080/6-3 (im Rahmen des Schwerpunktprogrammes 1051)

Synthese und Charakterisierung eindimensionaler Ferroelektrika mit Perowskitstruktur
Synthesis and characterisation of one dimensional ferroelectrics with perovskite structure
R. Böttcher, E. Hartmann
DFG Bo1080/8-1 (im Rahmen der Forschergruppe 522)

Synthese und Strukturaufklärung von Vanadium-Phosphat-Systemen mittels ENDOR- und ESEEM-Spektroskopie
Synthesis and determination of the structure of vanadium-phosphate systems by means of ENDOR and ESEEM spectroscopy
A. Pöppl, K. Köhler
DFG PO 426/3-1.

Experimental proof of the predictions of renormalization theory on the critical exponents in systems with incommensurately structurally modulated phases
D. Michel
DFG Mi 390/21-1.

Phase transitions in metals and ferroelectrics embedded into porous glasses and other porous matrices
D. Michel, E.V. Charnaya
DAAD, Leonhard-Euler programme.

NMR studies of short-chain surfactants in a heavy water solutions
D. Michel, V.I. Chizhik
DAAD, Leonhard-Euler programme.

New materials for the information technology
R. Böttcher, D. Michel, J. Banys
Joint research project supported by Humboldt-Stiftung.

6.15 Organizational Duties

D. Michel

- Vorsitzender des Verwaltungsrates des Studentenwerkes Leipzig
- Vorsitzender der Haushaltkommission de Universität Leipzig
- Mitglied der Sächsischen Akademie der Wissenschaften
- Mitglied des Internationalen Komitees der Groupement Ampere
- Mitglied des Internationalen Komitees der EENC (European Experimental Nuclear Magnetic Resonance Conferences)
- Mitglied des Internationalen Komitees der EMF (European Meeting on Ferroelectricity)
- Mitglied des Internationalen Komitees der IMF (International Meeting on Ferroelectricity)
- Mitglied des Beirates des Mathematisch - Naturwissenschaftlichen Fakultätentages der Bundesrepublik Deutschland
- Vertrauensdozent des Evangelischen Studienwerkes Villigst
- Gutachter der Zeitschriften Physical Review, Physical Review Letters, Journal of Chemical Physics, Journal of Physics: Condensed Matter, Zeitschrift für Naturforschung, physica status solidi

R. Böttcher

- Gutachter der Zeitschriften Physical Review, Journal of Physics: Condensed Matter, Langmuir, Journal of Magnetic Resonance

A. Pöppl

- Gutachter der Zeitschriften Journal of Magnetic Resonance, Journal of American Chemical Society, Physical Chemistry Chemical Physics, Chemical Physics Letters

A. Pampel

- Journal review: Journal of the American Chemical Society, Biophysical Journal

6.16 External Cooperations

Academic

- Institut für Oberflächenmodifizierung (IOM), Leipzig
  Dr. E. Hartmann
- Universität Kaiserslautern, Fachbereich Chemie, Technische Chemie
  Dr. M. Hartmann
- Technische Universität München, Anorganisch-chemisches Institut
  Prof. K. Köhler
- The Weizmann Institute of Science, Department of Physical Chemistry, Rehovot, Israel
  Prof. D. Goldfarb
- University of Vilnius, Radiophysics Department, Lithuania
  Prof. J. Banys

- University of Wroclaw, Institute of Experimental Physics, Poland
  Prof. Z. Czapla
- University of Opole, Institute of Mathematics, Poland
  Prof. V. A. Stephanovich
- Max-Delbrück-Centrum für Molekulare Medizin Berlin-Buch
  Dr. R. Reszka
- Universität des Saarlandes, Saarbrücken
  Prof. J. Petersson
- St. Petersburg State University, Russia
  Prof. E.V. Charnaya, Prof. B.N. Novikov, Prof. V.I. Chizhik
- Ioffe Institute of the RAS, St. Petersburg, Russia
  Prof. J.A. Kumzerov
- Kirensky Institute of Physics of the Sibirian Branch of the Russian Academy of Sciences, Krasnoyarsk, Russia
  Prof. I.P. Aleksandrova, Dr. J. Ivanov
- A. Mickiewicz University of Poznan, Poland
  Prof. S. Jurga
- Universität Leipzig, Fakultät für Biowissenschaften, Pharmazie und Psychologie
  Prof. A. Beck-Sickinger
- Martin-Luther-Universität Halle-Wittenberg, Department of Physics
  Prof. H. Beige, Dr. H. T. Langhammer
- Martin-Luther-Universität Halle-Wittenberg, School of Pharmacy, Institute for Pharmaceutics
  Prof. R.H.H. Neubert, Prof. S. Wartewig
- Technische Universität Darmstadt, Institut für Materialwissenschaften
  Prof. H. Fuess
- Universität Leipzig, Fakultät für Chemie und Mineralogie, Institut für Technische Chemie
  Prof. H. Papp, Dr. O. Klepel
- Universität Leipzig, Fakultät für Chemie und Mineralogie, Institut für Anorganische Chemie
  Prof. R. Kirmse

Industry

- Bruker BioSpin, Rheinstetten, Germany
  F. Engelke, K. Zick, D. Gross

6.17 Publications

Journals

V. Umamaheswari, M. Hartmann, A. Pöppl: *EPR Spectroscopy of Cu(I)-NO Adsorption Complexes Formed over Cu-ZSM-5 and Cu-MCM-22 Zeolites*, J. Phys. Chem. B **109**, 1537 (2005)

A. Vinu, B.M. Devassy, S.B. Halligudi, W. Böhlmann, M. Hartmann: *Highiy active and seiective AISBA-15 catalysis for the vapor phase tert-butylation of phenol*, Appl. Catal. A **281**, 207 (2005)

I.A. Beta, B. Hunger, W. Böhlmann, H. Jobic: *Dissociative adsorption of water in CaNaA zeolites studied by TG, DRIFTS and ^{1}H and ^{27}Al MAS NMR spectroscopy*, Micropor. Mesopor.s Mat. **79**, 69 (2005)

R. Böttcher, E. Erdem, H.T. Langhammer, T. Müller, H.-P. Abicht: *Incorporation of chromium into hexagonal bariumtitanate: an electron paramagnetic resonance study*, J. Phys. Cond. Matter **17**, 2763 (2005)

V. Umamaheswari, M. Hartmann, A. Pöppl: *EPR Spectroscopy of Cu(I)-NO Adsorption Complexes Formed over Cu-ZSM-5 and Cu-MCM-22 Zeolithes*, J. Phys. Chem. B **109**, 1537 (2005)

U. Roland, F. Holzer, A. Pöppl, F.-D. Kopinke: *Combination of non-thermal plasma and heterogeneous catalysis for oxidation of volatile organic compounds Part 3. Electron paramagnetic resonance (EPR) studies of plasma-treated porous alumina*, Appl. Catal. B **58**, 227 (2005)

V. Umamaheswari, M. Hartmann, A. Pöppl: *Pulsed ENDOR Study of Cu(I)-NO Adsorption Complexes in Cu-L Zeolite*, J. Phys. Chem. B **109**, 10 842 (2005).

J. Banys, M. Kinka, J. Macutkevic, G. Völkel, W. Böhlmann, V. Umamaheswari, M. Hartmann, A. Pöppl: *Broadband dielectric spectroscopy of water confined in MCM-41 molecular sieve matreials-low-temperature freezing phenomena*, J. Phys. Cond. Matter **17**, 2843 (2005)

Ö.F. Erdem, D. Michel: *^{1}H MAS NMR Investigations of Ethylene Glycol Adsorbed in NaX*, J. Phys. Chem B **109**, 12 054 (2005)

J. Banys, G. Völkel, R. Böttcher, D. Michel, Z. Czapla: *Dielectric properties of a DMAGaS/DMAAS mixed crystal*, Phase Trans. **78**, 337 (2005)

E. Erdem, R. Böttcher, H.J. Gläsel, E. Hartmann, G. Klotzsche, D. Michel: *Size Effects in $Ba(Pb)TiO_3$ Nanopowders by EPR and NMR*, Adv. Solid State Phys. **45**, 337 (2005)

G. Völkel, R. Böttcher, D. Michel, Z. Czapla, J. Banys: *Dimethylammonium gallium sulfate hexahydrate and dimethylammonium aluminium sulfate hexahydrate-members of crystal family with exceptional commensurate/incommensurate phase sequences*, J. Phys. Cond. Matter **17**, 4511 (2005)

E. Erdem, R. Böttcher, H.-J. Gläsel, E. Hartmann, G. Klotzsche, D. Michel: *Size Effects in $BaTiO_3$ Nanopowders Studied by EPR and NMR*, Ferroelectrics **316**, 43 (2005)

H. Trommer, R. Böttcher, C. Huschka, W. Wohlrab, R.H.H. Neubert: *Further investigations on the role of ascorbic acid in stratum corneum lipid models after UV exposure*, J. Plant Physiol. **57**, 963 (2005)

R. Böttcher, H.T. Langhammer, T. Müller, H.-P. Abicht: *Evaluation of lattice site and valence of manganese in hexagonal $BaTiO_3$ by electron paramagnetic resonance*, J. Phys. Cond. Matter **17**, 4925 (2005)

M. Diaconu, H. Schmidt, A. Pöppl, R. Böttcher, J. Hoentsch, A. Klunker, D. Spemann, H. Hochmuth, M. Lorenz, M. Grundmann: *Electron paramgnetic resonance of $Zn_{1-x}Mn_xO$ thin films and single crystals*, Phys. Rev. B **72**, 852 140 (2005)

W. Böhlmann, I.A. Beta, B. Hunger, H. Jobic: *Dehydration of LTA type zeolites studied by ^1H, ^{27}Al, ^{29}Si MAS NMR, and DRIFT spectroscopy Studies*, Surf. Sci. Catal. **158A**, 781 (2005)

S. Ernst, M. Hartmann, S. Tontisirin, W. Böhlmann: *Characterization and catalytic evaluation of zeolite MCM-71 Studies*, Surf. Sci. Catal. **158B**, 1287 (2005)

E. Erdem, R. Böttcher, H.-J. Gläsel, E. Hartmann: *Size effects in chromium-doped $PbTiO_3$ nanopowders observed by multi-frequency EPR*, Magn. Reson. Chem. **43**, 174 (2005)

V. Umamaheswari, M. Hartmann, A. Pöppl: *Electron spin resonance studies of Cu(I)-NO complexes formed over copper-exchanged three- and unidimensional zeolites*, Magn. Reson. Chem. **43**, 205 (2005)

V. Umamaheswari, M. Hartmann, A. Pöppl: *Critical Assessment of Electron Spin Resonance Studies on Cu(I)-NO Complexes in Cu-ZSM-5 Zeolites Prepared by Solid- and Liquid-State Ion Exchange*, J. Phys. Chem. B **109**, 19 723 (2005)

C. Tien, E.V. Charnaya, M.K. Lee, S.V. Baryshnikov, S.Y. Sun, D. Michel, W. Böhlmann: *Coexistence of melted and ferroelectric states in sodium nitrite within mesoporous sieves*, Phys. Rev. B **72**, 104 105 (2005)

V. Nagarajan, D. Rings, L. Moschkowitz, M. Hartmann, A. Pöppl: *Location of Vanadium (IV) in VAPO-5 as Studied by Hyperfine Sublevel Correlation Spectroscopy*, Chem. Lett. **34**, 1614 (2005)

E.V. Charnaya, C. Tien, W. Wang, M.K. Lee, D. Michel, D. Yaskov, S.Y. Sun, Yu.A. Kumzerov: *Atomic mobility in liquid gallium under nanoconfinement*, Phys. Rev. B **72**, 035 406 (2005)

V. Umamaheswari, W. Böhlmann, A. Pöppl, A. Vinu, M. Hartmann: *Spectroscopic characterization of iron-containing MCM-58*, Micropor. Mesopor. Mat. **89**, 47 (2005)

D. Michel, A. Taye, J. Petersson: *NMR Studies on Crystals with Structurally Inkommensurately Modulated Phases*, Ferroelectrics **314**, 233 (2005)

E.V. Charnaya, C. Tien, D. Michel, M.K. Lee, W. Wang: *Self-Diffusion Slowdown in Liquid Indium and Gallium under Confinement*, Diffusion Fundamentals **2**, 80 (2005)

M. Diaconu, H. Schmidt, A. Pöppl, R. Böttcher, J. Hoentsch, A. Rahm, H. Hochmuth, M. Lorenz, M. Grundmann: *EPR study on magnetic $Zn_{1-x}Mn_xO$*, Superlatt. Microstruct. **38**, 413 (2005)

M. Kinka, J. Banys, W. Böhlmann, E. Bierwirth, M. Hartmann, D. Michel, G. Völkel, A. Pöppl: *Dielectric spectroscopy of $BaTiO_3$ confined in MCM-41 mesoporous molecular sieve materials*, J. Phys. IV France **128**, 81 (2005)

J. Banys, M. Kinka, A. Meskauskas, J. Macutkevic, G. Völkel, W. Böhlmann, V. Umamaheswari, M. Hartmann, A. Pöppl: *Broadband Dielectric Spectroscopy of Water Confined in MCM-41 Molecular Sieve Material*, Ferroelectrics **318**, 201 (2005)

M. Kinka, J. Banys, J. Macutkevic, A. Pöppl, W. Böhlmann, V. Umamaheswari, M. Hartmann, G. Völkel: *Dielectric response of water confined in MCM-41 molecular sieve material*, Phys. Stat. Sol. B **242**, R100 (2005)

T. Bräuniger, T. Müller, A. Pampel, H.-P. Abicht: *Study of Oxygen-Nitrogen Replacement in $BaTiO_3$ by ^{14}N Solid-State Nuclear Magnetic Resonance*, Chem. Mater. **17**, 4114 (2005)

A. Pampel, M. Fernandez, D. Freude, J. Kärger: *New Options for Measuring Molecular Diffusion in Zeolites by MAS PFG NMR*, Chem. Phys. Lett. **407**, 53 (2005)

Books

D. Gross, K. Zick, T. Oerther, V. Lehmann, A. Pampel, J. Goetz: *Hardware, Software and Areas of Application of Non-medical MRI*, in *NMR Imaging in Chemical Engineering*, ed. by S. Stapf, S.-I. Han (Wiley-VCH, Weinheim 2005) p. 47

Talks

A. Pöppl: *Characterization of Active Surface Sites in Zeolites by Paramagnetic Probe Molecules*, Universität Antwerpen, Antwerpen, 2005

A. Pöppl: *ESR, ENDOR, and HYSCORE Studies of Vanadium Complexes in Heteropolyacid Materials*, RAMIS, Poznan, 2005

A. Pöppl: *Characterization of Surface Sites in Zeolites by ESR Spectroscopy*, Darmstadt, 2005

A. Pöppl: *Electron spin resonance studies of Cu(I)-NO complexes formed over copper exchanged zeolites*, GDCH, Mainz, 2005

D. Michel: *Proton ordering and conductivity in quasi one-dimensional hydrogen-bonded crystals studied by EPR and NMR*, ETH Zürich, Januar 2005

D. Michel: *Albert Einstein: Experimente in seinem wissenschaftlichen Umfeld*, Sonntagsvorlesung Januar 2005

D. Michel, R. Böttcher, E. Erdem, E. Hartmann, G. Klotzsche, W. Böhlmann: *Size effects in $BaTiO_3$ and $PbTiO_3$ nanopowders and of $BaTiO_3$ embedded in mesoporous materials*, Berlin, March 2005

Ö.F. Erdem, D. Michel: *NMR Investigation of Adsorbed Molecules in Zeolites*, Berlin, March 2005

D. Michel, R. Böttcher, E. Erdem, G. Klotzsche: *NMR spectroscopy to study size effects in $BaTiO_3$ nanopowders and of $BaTiO_3$ embedded in mesoporous mcm41 materials*, RAMIS Conference,April 2005

D. Michel: *NMR-Untersuchungen zum Studium von Ordnungs- und Unordnungsphänomenen an Festkörpern mit strukturellen Phasenübergängen*, Rostock, Mai 2005

D. Michel, W. Böhlmann, Ö.F. Erdem, A. Pampel: *High-resolution ^1H NMR spectroscopy of adsorbed molecules*, Leipzig, Mai 2005

D. Michel, W. Böhlmann, Ö.F. Erdem, A. Pampel: *NMR study of properties on fine particles and phase transitions in metals and ferroelectrics embedded into porous glasses and other porous matrices*, Leipzig, May 2005

D. Michel, J. Petersson, A. Taye: *NMR studies of crystals with structurally incommensurately modulated phases*, Leipzig, May 2005

Ö.F. Erdem, D. Michel: *Proton MAS NMR and Spin-Lattice Relaxation of Ethylene Glycol Molecules Confined in Zeolites*, Zakopane, June 2005

D. Michel: *NMR-Untersuchungen von Ordnungs- und Unordnungsphänomenen in Festkörpern mit strukturellen Phasenübergängen*, MDR-XV-Treffen in Leipzig

A. Pampel, J. Kärger, D. Michel: *Pulsed Field Gradients and Magic Angle Spinning - Prospects for Observing Diffusive Motion and NMR Microscopy in Complex Materials*, NMRCM 2005, St. Petersburg

D. Michel, R. Böttcher, E. Erdem, G. Klotzsche: *NMR and EPR spectroscopy to study size effects in $BaTiO_3$ nanopowders and of $BaTiO_3$ embedded in mesoporous MCM41 materials*, IMF 11, Iguacu, Brasilien 2005

D. Michel: *Introduction to Magnetic Resonance, to nuclear spin Relaxation, and to MRI*; *NMR spectroscopy to study size effects in $BaTiO_3$ nanoparticles and $BaTiO_3$ materials embedded in mesoporous silicates*; *Fundamentals of NMR*; *Solid-State High-Resolution NMR fundamentals of ^2D-NMR, ^2D-NOESY, ^2D-Exchange Spectroscopy*; *Multiple Quantum NMR spectroscopy and NMR relaxation in adsorption and catalysis*, Vorlesungen, Ankara, Türkei, November 2005

Ö.F. Erdem, D. Michel: *NMR Investigations of Adsorbed Molecules in Zeolites*, Jahrestagung der DPG, Berlin, Germany, March 2005

Ö.F. Erdem, D. Michel: *Molecular Dynamics of Ethylene Glycol Adsorbed in NaX: NMR and Broadband Dielectric Spectroscopy*, METU, Ankara, Turkey, November 2005

Ö.F. Erdem, D. Michel: *Quadrupolar Nuclei NMR for Zeolites and Molecular Sieves - New Techniques*, METU, Ankara, Turkey, November 2005

D. Michel: *NMR in solid state physics, study of order and disorder at structural phase transitions*, Bonn, November 2005

E. Erdem, R. Böttcher, A. Matthes, H.-J. Gläsel, E. Hartmann, J. Banys: *Size effects in chromium doped $PbTiO_3$ nanopowders*, DPG, Berlin, March 2005.

D. Michel, R. Böttcher, E. Erdem, G. Klotzche, W. Böhlmann: *Size effects in $BaTiO_3$ nanopowders and of $BaTiO_3$ embedded in mesoporous materials*, DPG, Berlin, March 2005

Posters

D. Michel, A. Taye, J. Petersson: *NMR studies on crystals with structurally incommensurately modulated phases*, 11. IMF, Iguazu, Brazil September, 2005

R. Grigalaitis, J. Banys, S. Lapinskas, E. Erdem, R. Böttcher, H.-J. Gläsel, E. Hartmann: *Dielectric investigations and theoretical investigations of size effects in lead titanate nanocrystals*, III. Int. Mater. Symp., Lisbon, March 2005

E. Erdem, A. Matthes, R. Böttcher, H.-J. Gläsel, E. Hartmann: *Size effects in chromium doped lead titanate nanopowders by multifrequency EPR spectroscopy*, 3. European EPR Summer School, Wiesbaden, July, 2005

W. Böhlmann, I.A. Beta, B. Hunger: *Dehydration of LTAType Zeolites Studied by Multi Nuclear MAS NMR and DRIFT Spectroscopy*, 17. Dt. Zeolithtagung, Giessen, Germany, March 2005

K. Böhme, O. Klepel, W. Böhlmann, W.-D. Einicke, H.C. Papp: *Simultaneous Synthesis of Mesoporous Silica and Carbons Using the Sol-Gel Method*, 17. Dt. Zeolithtagung, Giessen,Germany, March 2005

A. Garsuch, O. Klepel, W. Böhlmann, H. Papp: *Template Synthesis of Microporous Carbons by Using Y Zeolite*, 17. Dt. Zeolithtagung, Giessen, Germany, March, 2005

A. Garsuch, O. Klepel, W. Böhlmann: *^{129}Xe NMR Studies on Carbon Replicas of Y Zeolite*, 17. Dt Zeolithtagung, Giessen, Germany, March, 2005

H.-J. Gläsel, S. Rummel, E. Hartmann, F. Bauer, R. Mehnert, W. Böhlmann: *Radiation cured protective nanocomposites*, DECHEMA, Frankfurt/M., Germany, March, 2005

L. Giebeler, W. Böhlmann, A. Thissen, P. Kampe, H. Fuess: *Spektroskopische Untersuchungen an V-Mo-W-Mischoxiden*, Jahrestreffen Dt. Katalytiker, Weimar, Germany, March 2005

W. Böhlmann, L.A. Beta, B. Hunger, H. Jobic: *Dehydration of LTA type zeolites studied by ^{1}H, ^{27}Al, ^{29}Si MAS NMR, and DRIFT spectroscopy*, 3rd FEZA Conference, Prague, Czech Republic, August 2005

6.18 Graduations

Diploma

- Julia Köhler
  Strukturuntersuchungen von Peptiden in Membranumgebung mittels Festkörper-NMR und Moleküldynamik-Simulationen
  Dezember 2005
- Pavel Sergeevich Sedykh
  Size effects in liquid gallium and NaNO2 crystals
  January 2005 [Universität St. Petersburg]

6.19 Guests

A large number of guests have visited our group in 2005 about which we cannot report here in detail. This includes short-time visits of numerous guests from abroad, e.g. from Israel, France, Lithunia, Poland, Syria, Vietnam, the Russian Federation (St. Petersburg, Kazan), the United States.

Mrs. Dr. Natalya Grunina (St. Petersburg state University) has received a support from the DAAD to realize 3 month's postdoc-stay in our group.

7

Semiconductor Physics

7.1 Introduction

The Semiconductor Physics Group has worked in 2005 with a focus on complex nanostructures and ZnO and related materials. We have successfully fabricated oxide thin films with electrically active and magnetic dopants (transition metals), ZnO/MgZnO quantum wells and bright luminescence for scintillators. In cooperation with FZ Rossendorf we present a (Europe's first) ZnO *pn*-diode which allowed us the study of deep acceptor levels. Our theoretical calculations allow a direct comparison of the various band-band transitions in MgZnO with the experimentally determined dielectric function. The growth of ZnO and MgZnO nanowhiskers has been perfected. Our in-depth analysis of the optical modes in ZnO nanowhiskers with hexagonal cross-section allows a parameter-free fit to the optical spectra. Other nanostructures under investigation were ZnO nanopillars surrounded by Bragg mirrors, III–V nanowires and GaAs-based nanoscrolls.

The FAHL Academia in Wörlitz on "Nano- and Microdimensional Building Blocks" was well received by the many attendants. It was a pleasure to cooperate with many colleagues throughout the year. We are looking forward to new guests coming in 2006 and our guests of 2005 returning. Please do not hesitate to contact us if you would like further information.

Marius Grundmann

7.2 Growth of ZnO Nanowires by Pulsed Laser Deposition

A. Rahm, M. Lorenz, E.M. Kaidashev, T. Nobis, J. Lenzner, G. Wagner, G. Zimmermann, M. Diaconu, B. Fuhrmann*, F. Syrowatka*, M. Grundmann

*Interdisziplinäres Zentrum für Materialwissenschaften, Martin-Luther-Universität Halle-Wittenberg

A regular lateral alignment of zinc oxide nanostructures that have very promising optical properties is necessary for practical device applications. We have grown free standing nanowire arrays with uniform hexagonal arrangement by high-pressure Pulsed

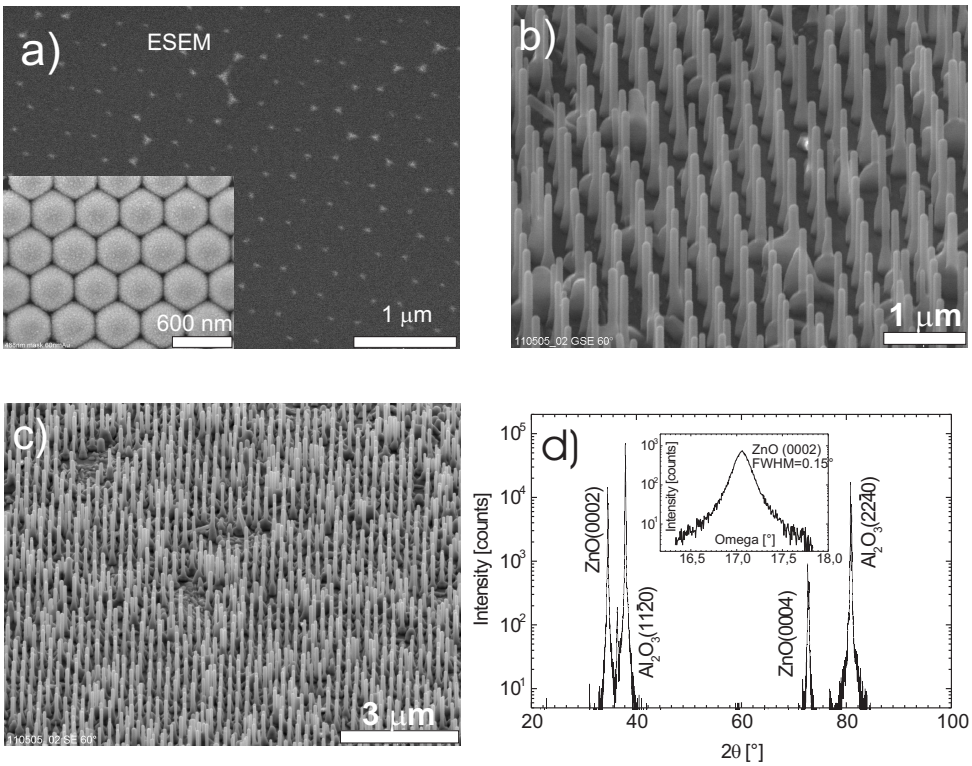

Figure 7.1: (**a**) Gold seeds on sapphire obtained by mask transfer technique; *inset*: stabilized polystyrene sphere mask (488 nm). (**b**,**c**) SEM pictures of as-grown samples. (**d**) X-ray results of an ordered ZnO nanowire array showing only the ZnO(000l) and the substrate reflection.

Laser Deposition [1, 2]. In order to achieve this we prepared an ordered array of catalytic gold particles by nanosphere lithography [3] using monodisperse spherical polystyrol nanoparticles (Fig. 7.1). These templates were investigated by Scanning Electron Microscopy and Atomic Force Microscopy prior to growth. Using XRD we determined the crystallographic relations between the ZnO wires and the a-plane sapphire substrates (Fig. 7.1d).

Furthermore, we report on the high-pressure pulsed laser deposition growth of zinc oxide nanowires containing about 0.2 at % Co and 0.5 at % Mn by NiO and Au catalyst [4]. Scanning electron microscopy and X-ray diffraction measurements revealed arrays of parallel-standing nanowires with hexagonal cross section and uniform in-plane epitaxial relations without rotational domains. Elemental analysis was carried out using particle induced X-ray emission and Q-band electron spin resonance. The valence of the incorporated Mn was determined to be 2+. Atomic and magnetic force microscopy measurements indicate that Mn is incorporated preferentially at the nanowire boundaries.

This work was supported by DFG within the project Gr 1011/11-2 (FOR522).

[1] M. Lorenz et al.: Appl. Phys. Lett. **86**, 143 113 (2005)
[2] A. Rahm et al.: Appl. Phys. A, in press
[3] J.C. Hulteen, R.P. van Duyne: J. Vac. Sci. Technol. A **13**, 1553 (1995)
[4] A. Rahm et al.: Microchim. Acta, in press

7.3 Whispering Gallery Modes in ZnO Nanopillars

T. Nobis, A. Rahm, M. Lorenz, M. Grundmann

Hexagonal ZnO nanostructures are frequently envisioned as a key material for future nanophotonic devices. We analyzed the formation of optical whispering gallery modes (WGMs) within the cross section of such nanopillars both theoretically and experimentally. Therefore, the solutions of a two-dimensional Helmholtz-equation with complex wave number k have been determined for the hexagonal resonator geometry utilizing a boundary element method (BEM) recently presented by Wiersig [1]. Slight modifications of the BEM allowed us for the calculation of lowest order hexagonal WGMs [2] concerning mode energies $\mathrm{Re}(k)$, line widths $2|\mathrm{Im}(k)|$ and mode patterns (Fig. 7.2a). All values have been determined in dependence of the refractive index of the resonator material and for both TM and TE polarization.

Luminescence spectra of individual ZnO nanopillars, recorded using polarization resolved micro-photoluminescence spectroscopy (μ-PL), exhibit series of characteristic resonance lines. On the basis of our numerical results we are able to simulate such luminescence spectra by multiplying the unmodulated emission of bulk material of the same sample with a superposition of normed Lorentzians, one for each resonant mode (Fig. 7.2b). Applying literature values for the spectral dispersion of the refractive index of ZnO bulk material, the line shape and relative intensities of the WGMs are qualitatively and quantitatively reproduced. Theoretical resonator diameters mostly agree with respective experimental values within the experimental error level.

This work was supported by DFG within the project Gr 1011/11-2 (FOR522).

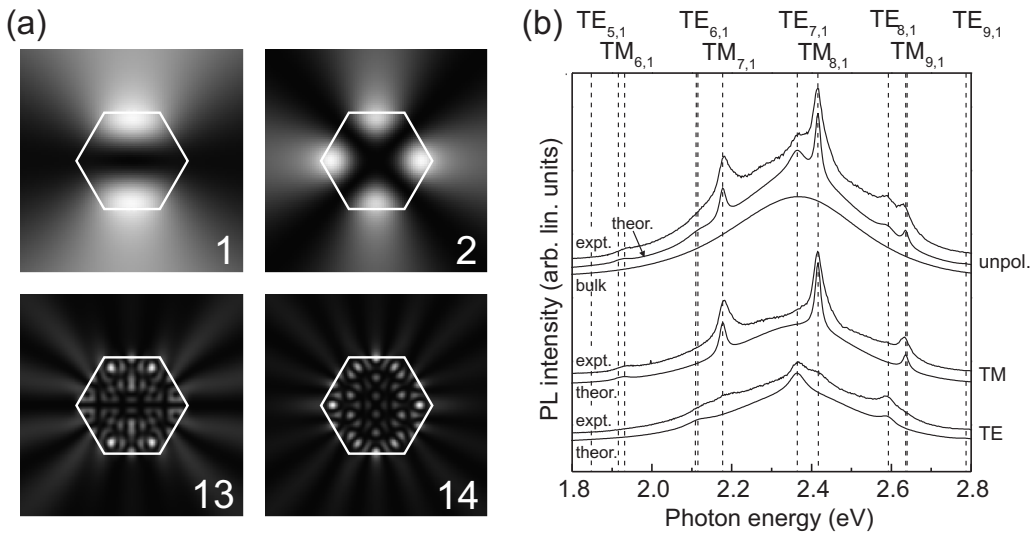

Figure 7.2: Hexagonal WGMs. (**a**) Calculated near-field intensity patterns of selected hexagonal TM-WGMs given in linear grey scales. Respective mode numbers are shown on the lower right of each pattern. (**b**) Polarization resolved μ-PL spectra of a ZnO nanopillar, each shifted vertically for clarity. Kurves labelled "expt." ("theor.") show experimental (theoretical) data, "bulk" spectra give the unmodulated emission of bulk material of the same sample. Spectra are arranged with respect to their polarisation (TM, TE, umpolarized). Dashed lines indicate the spectral position of dominant WGMs – each labelled with their respective mode number.

[1] J. Wiersig: J. Opt. A **5**, 53 (2003)
[2] T. Nobis, M. Grundmann: Phys. Rev. A **72**, 063 806 (2005)

7.4 Optimized $Mg_xZn_{1-x}O$ Thin Films for Pulsed Laser Deposition of $Mg_xZn_{1-x}O$/ZnO Quantum Wells

S. Heitsch, G. Zimmermann, C. Schulz, J. Lenzner, H. Hochmuth, G. Benndorf, T. Nobis, M. Lorenz, M. Grundmann

$Mg_xZn_{1-x}O$/ZnO quantum wells (QW) have attracted much attention recently, due to their potential application in ZnO-based UV-lasers. In such structures, excitonic laser processes could possibly be used at room temperature, which would lead to a lower laser threshold than that of comparable electron-hole plasma lasers. In order to produce such QW, the $Mg_xZn_{1-x}O$ layers have to possess a smooth surface and a laterally homogeneous distribution of the Mg atoms in the layer.

We have grown $Mg_xZn_{1-x}O$ thin films of different thickness by pulsed laser deposition (PLD), either on *a*-plane sapphire substrates directly, or on ZnO/*a*-Al_2O_3 structures. The substrate temperature during deposition was about 675 °C. We investigated their surface roughness by atomic force microscopy (AFM), their lateral homogeneity by scanning cathodoluminescence (CL), and the broadening mechanisms of the $Mg_xZn_{1-x}O$ photoluminescence (PL).

The AFM investigations on 250 nm thick $Mg_xZn_{1-x}O$ thin films on *a*-Al_2O_3 showed, that the smoothest thin films can be grown at a PLD oxygen partial pressure of $p(O_2) = (1-2)\times10^{-3}$ mbar. Deposition of thinner films (100 nm) on a 100-nm ZnO buffer lead to a minimal root mean square (rms) surface roughness of ~ 0.5 nm. This makes the films feasible for subsequent growth of QW's with smooth interfaces.

Fig. 7.3 shows the full width of half maximum (FWHM) of the PL maximum peaks ($FWHM_{PL}$) of different $Mg_xZn_{1-x}O$ thin films as a function of the energy position of the maximum E_{PL} (which can be related approximately linearly to the Mg content of the samples [1]) (open symbols). The dashed line in the figure represents the approximation

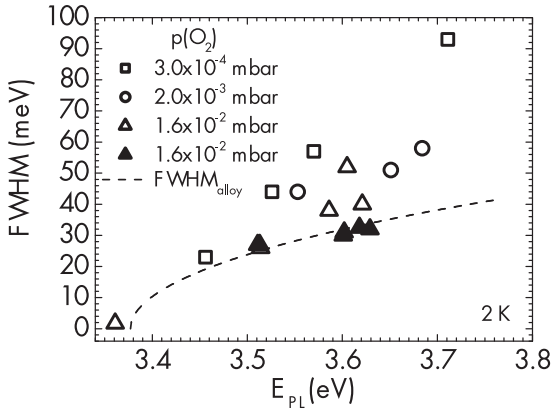

Figure 7.3: FWHM of PL ($FWHM_{PL}$) and approximated alloy broadening ($FWHM_{alloy}$) of $Mg_xZn_{1-x}O$ thin films. The closed symbols refer to samples grown on a ZnO buffer layer, the open symbols to samples without buffer.

of the alloy broadening ($FWHM_{alloy}$) for the $Mg_xZn_{1-x}O$ according to [1, 2, 3], including the change of the dielectric constant with increasing x [4]. It is observed, that for $E_{PL} > 3.51$ eV ($x > 7.3$ %) additional broadening effects play an important role for the PL line broadening, e.g. scattering of the exciton polaritons in the crystal at defects or impurities, or lateral inhomogeneity of the Mg distribution in the thin films. The impact of the latter has been investigated by the performance of CL scans over an area of $10 \times 10\ \mu m^2$. The obtained histograms of the maximum energy position have been fitted by a Gaussian distribution and its FWHM ($FWHM_{lat}$) has been taken as a measure for the homogeneity of the samples. The results showed that for samples grown at $p(O_2) \leq (1-2) \times 10^{-3}$ mbar the lateral inhomogeneity leads to a minor additional broadening which lies below 6 meV. Those samples can be considered laterally homogeneous, and scattering effects determine their line broadening in addition to alloy broadening. However, samples grown at $p(O_2) = (1-2) \times 10^{-2}$ mbar show a lateral inhomogeneity which causes additional line broadening in the order of the difference between $FWHM_{PL}$ and $FWHM_{alloy}$.

CL investigations at $Mg_xZn_{1-x}O$ thin films on 100 nm thick ZnO buffer layers showed, that those films are laterally homogeneous ($FWHM_{lat}$ is in the order of the energy resolution of the measurement), independent on the oxygen partial pressure during their deposition. This could also be confirmed by PL measurements: all samples grown at $p(O_2) = 1.6 \times 10^{-2}$ mbar possessed a $FWHM_{PL}$ near the theoretically approximated value of the alloy broadening (Fig. 7.3, closed symbols).

In conclusion, we could optimize the PLD grown $Mg_xZn_{1-x}O$ thin films by depositing them on a ZnO buffer layer. The $Mg_xZn_{1-x}O$ layers are laterally homogeneous and 100 nm thick films posses a minimal rms roughness of ~ 0.5 nm. Therefore, they are suitable for subsequent growth of $Mg_xZn_{1-x}O$/ZnO quantum wells.

This work was supported by DFG within the project Gr 1011/14-2 (FOR404).

[1] S. Heitsch et al.: submitted
[2] E.F. Schubert et al.: Phys. Rev. B **30**, 813 (1984)
[3] R. Zimmermann: J. Cryst. Growth **101**, 346 (1990)
[4] C. Bundesmann et al.: Appl. Phys. Lett. **85**, 905 (2004)

7.5 MgZnO/ZnO Quantum Wells Grown on ZnO/Sapphire Substrates by Pulsed Laser Deposition

S. Heitsch, G. Zimmermann, J. Lenzner, H. Hochmuth, G. Benndorf, M. Lorenz, M. Grundmann

The production of ZnO-based UV-lasers requires ZnO-based quantum wells (QW), in order to define the emission wavelength of the lasers. One example of such QW's is the $Mg_xZn_{1-x}O$/ZnO/$Mg_xZn_{1-x}O$ double heterostructure (DHS). Generally, the growth of QW's is a challenge, because laterally homogeneous mixed crystals and smooth interfaces are required to achieve the desired result of defined structure properties.

We have grown $Mg_{0.12}Zn_{0.88}O$/ZnO/$Mg_{0.12}Zn_{0.88}O$ DHS by pulsed laser deposition (PLD) on *a*-plane sapphire substrates covered by a 100 nm thick ZnO buffer layer. The ZnO well layer thickness L_z is nominally 25, 12, 6, or 3 nm. All samples were grown

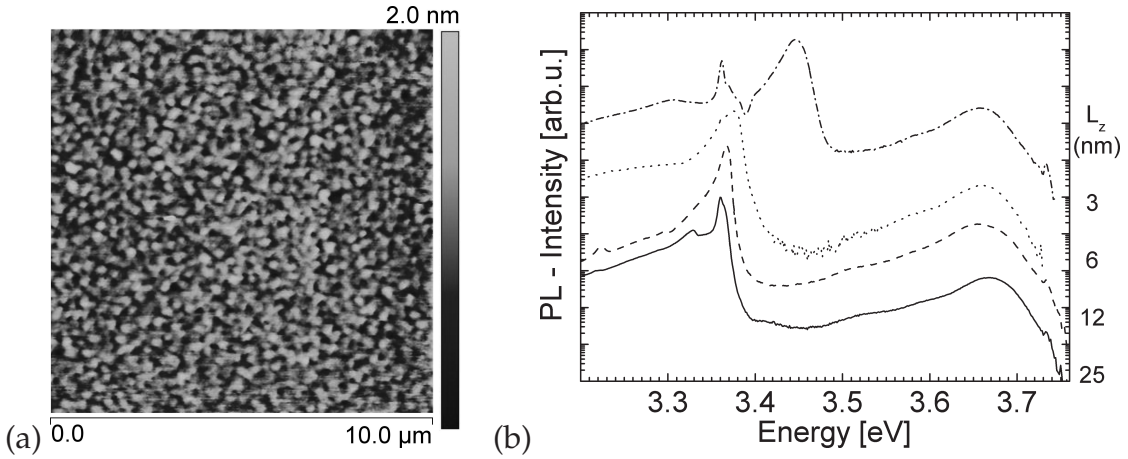

Figure 7.4: (**a**) AFM image of a ZnO/$Mg_{0.12}Zn_{0.88}O$ heterostructure with nominally $L_z = 3$ nm ZnO. (**b**) PL spectra of $Mg_{0.12}Zn_{0.88}O$/ZnO/$Mg_{0.12}Zn_{0.88}O$ DHS with well widths $L_z = 25$, 12, 6, and 3 nm (from *bottom* to *top*). The baselines are shifted for clarity.

at a substrate temperature of approximately 675 °C and an oxygen partial pressure of 2×10^{-3} mbar. Additionally, for atomic force microscopy (AFM) investigations, the corresponding ZnO/$Mg_{0.12}Zn_{0.88}O$ heterostructures (HS) were grown on the same type of substrates.

The AFM investigations at the HS showed smooth ZnO surfaces with a root mean square roughness of less than 0.5 nm. This means that the DHS contain smooth interfaces as they are required in QW's. Fig. 7.4a shows the AFM image of the HS with nominally $L_z = 3$ nm ZnO. Unlike in previous investigations at HS [1, 2], a smooth surface without spot-like elevations is observed. This indicates, that the ZnO layers form continuous films on the MgZnO and true QW's are formed in the corresponding DHS.

The lateral homogeneity of the mixed crystal layers has been confirmed by investigations at $Mg_xZn_{1-x}O$ thin films grown on ZnO/*a*-Al_2O_3 substrates under the same conditions as the $Mg_{0.12}Zn_{0.88}O$ layers for the QW samples (see Sect. 7.4). The cathodoluminescence (CL) maximum energy distribution of the thin films has been determined by scanning CL. The obtained histograms only show statistical fluctuations (the full width of half maximum is in the order of the energy resolution of the measurement), which means that the $Mg_xZn_{1-x}O$ thin films used for subsequent growth of QW's are laterally homogeneous.

The photoluminescence (PL) of the DHS is depicted in Fig. 7.4b. The $Mg_{0.12}Zn_{0.88}O$ PL is observed at ~ 3.658 eV. At 3.361 eV ZnO luminescence can be observed, which stems from the ZnO buffer layer and, in case of the thickest DHS, from the ZnO well layer itself. With decreasing well width the ZnO luminescence from the well shifts to higher energies. This can be due to onsetting quantum confinement effects or to Mg diffusion into the ZnO, which cannot be excluded. However, in the 3 nm QW, the well luminescence is shifted with respect to the ZnO free exciton luminescence by 69 meV and, despite the small amount of ZnO, it is still one order of magnitude more intense than the $Mg_{0.12}Zn_{0.88}O$ PL. This result can clearly be ascribed to quantum confinement.

We have shown that PLD is suitable for the growth of $Mg_xZn_{1-x}O$/ZnO QW's with excellent properties. Our DHS contain laterally homogeneous barrier layers with smooth interfaces and we proved the occurence of quantum confinement effects.

This work was supported by DFG within the project Gr 1011/14-2 (FOR404).

[1] S. Heitsch et al.: Appl. Phys. A in press
[2] S. Heitsch et al.: in *The Physics Institutes of Universität Leipzig, Report 2004*, ed. by M. Grundmann (Universität Leipzig 2005) p 152

7.6 Investigation of Deep Acceptor States in ZnO Single Crystals

H. von Wenckstern, R. Pickenhain, H. Schmidt, G. Biehne, M. Lorenz, M. Grundmann, G. Brauer*

*Institut für Ionenstrahlphysik und Materialforschung, Forschungszentrum Rossendorf

We report the investigation of deep acceptor states in ZnO single crystals grown by pressurized melt growth by means of deep level transient spectroscopy (DLTS). The observation is facilitated by using a *pn*-junction allowing the injection of both electrons and holes. The *pn*-junction was realized by implanting a virgin ZnO single crystals by N^+ ions using an acceleration voltage of 150 keV and a fluence of 10^{14} cm^{-2}. The crystal was annealed for 30 min at 500 °C to reduce the concentration of defects created during implantation. For metallization Au was sputtered on the non-implanted side of the crystal yielding ohmic contacts and Pd was thermally evaporated through a shadow mask onto the implanted surface. Current–voltage (*IV*) measurements obtained using two of the Pd contacts (f-f) revealed ohmic behavior. *IV* measurements using a Pd and the ohmic Au back contact (f-b) are highly rectifying (see Fig. 7.5a). Thus a thin *p*-type layer was formed on the surface during the implantation/annealing process. The *pn*-diode was investigated by DLTS for temperatures ranging from 20 to 325 K (Fig. 7.5b). If the filling pulses used result in a forward biased *pn* diode holes are injected in the *n*-type part of the junction and two acceptor states labelled A2 and A3, respectively, as

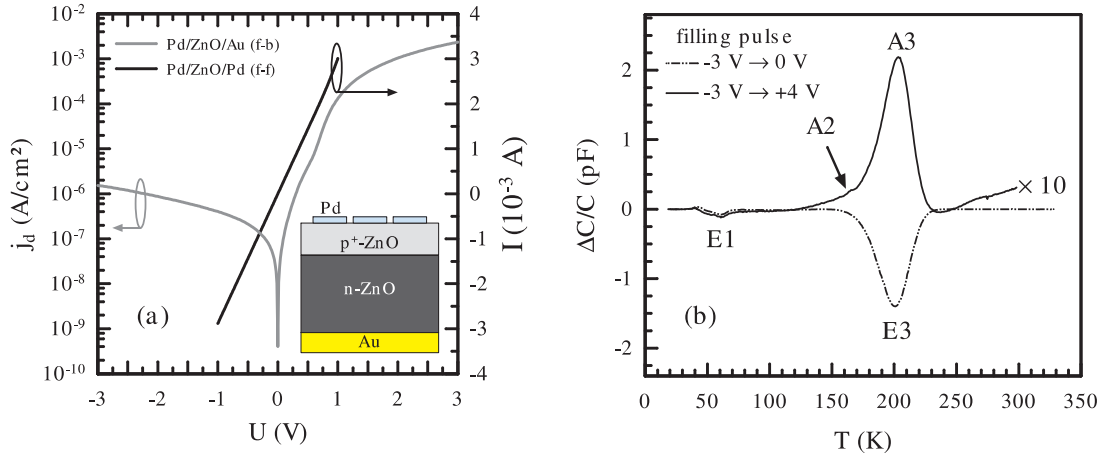

Figure 7.5: (**a**) Rectifying *IV* characteristics of *pn*-diode (f-b) and linear behavior for Pd/*p*-ZnO/Pd (f-f) contact configuration. The *inset* is a schematic of the structure investigated. (**b**) DLTS signals recorded with or without an excess of holes.

well as a broad acceptor band were observed in ZnO by DLTS (Fig. 7.5b) for the first time. The thermal activation energy of the states labelled A2 (attributed to an intrinsic defect) and A3 (tentatively attributed to Li_{Zn}) was determined to be about 150 meV and 280 meV, respectively. If the filling pulses used do not result in a forward biased *pn*-junction (excess of electrons within depletion region), electron traps (E1, E3) commonly observed in ZnO are dominating the DLTS spectrum.

This work was supported by DFG within the project Gr 1011/10-2 (FSPP1136).

7.7 FTIR-Photocurrent Spectroscopy of Deep Donor Levels in Thin ZnO Films

H. Frenzel, H. von Wenckstern, A. Weber, G. Biehne, H. Hochmuth, M. Lorenz, M. Grundmann

Pd-ZnO-Schottky diodes were investigated both by the purely electrical method of deep level transient spectroscopy (DLTS) and by the optical method of Fourier transform infrared photocurrent (FTIR-PC) spectroscopy in the mid-infrared wavelength range. FTIR-PC spectra show several well-resolved peaks between 100 meV and 400 meV due to transitions from deep donor-like states to the conduction band. They include the commonly observed defects E1 at ~ 120 meV and E3 at ~ 290 meV, which have been detected via DLTS before [1]. E3 was assigned to intrinsic defects like zinc interstitials or oxygen vacancies [2].

Figure 7.6a depicts a typical correlation between FTIR-PC and DLTS, where only donor-like defects with a sufficiently large electron capture cross-section are observable. Besides E1 and E3, several other peaks can be observed by the optical absorption which do not appear in electrical measurements. Peaks that behave similar after different treatments or in different samples are assorted in groups labeled A, B, C and D. Figure 7.6b

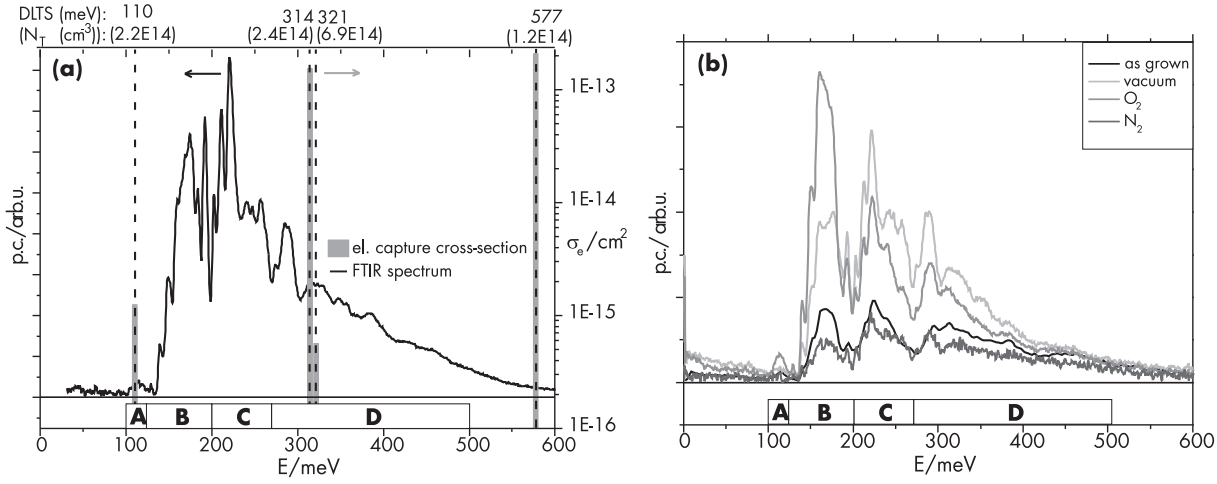

Figure 7.6: FTIR-PC spectrum of thin ZnO films. (**a**) Correlation between FTIR-PC and DLTS. Dashed lines are the spectral position of deep levels measured by DLTS. The light grey columns correspond to the electronic capture cross-section σ_e. N_T designates the concentration of the specific trap. (**b**) Series of measurements after different annealing conditions. A, B, C, D label groups of peaks which behave similar after different treatments.

shows a series of measurements, where samples of one ZnO film were annealed at a temperature of 700 ℃ for 2 hours in vacuum (10^{-6} mbar), oxygen and nitrogen atmosphere (800 mbar), respectively. The A- and B-group increase overproportionally after oxygen annealing while the C-group is dominant after annealing in vacuum. In the D-group, DLTS observed two adjacent peaks at ~ 280 meV and ~ 315 meV in the nitrogen and vacuum annealed samples. This was confirmed by FTIR-PC.

[1] H. von Wenckstern et al.: Adv. Solid State Phys. **45**, 263 (2005)
[2] F.D. Auret et al.: Appl. Phys. Lett. **80**, 1340 (2002)

7.8 Properties of ZnO:P

H. von Wenckstern, J. Sann*, A. Krtschil†, M. Brandt, H. Schmidt, M. Lorenz, M. Grundmann,

*1. Physikalisches Institut, Justus Liebig Universität Gießen
†Institut für Experimentelle Physik, Otto von Guericke Universität Magdeburg

We report on electrical and optical properties of epitaxial phosphorous-doped ZnO thin films. The samples were grown by pulsed-laser deposition on a-plane sapphire at temperatures ranging from about 400 ℃ to 800 ℃ in oxygen background gas. The

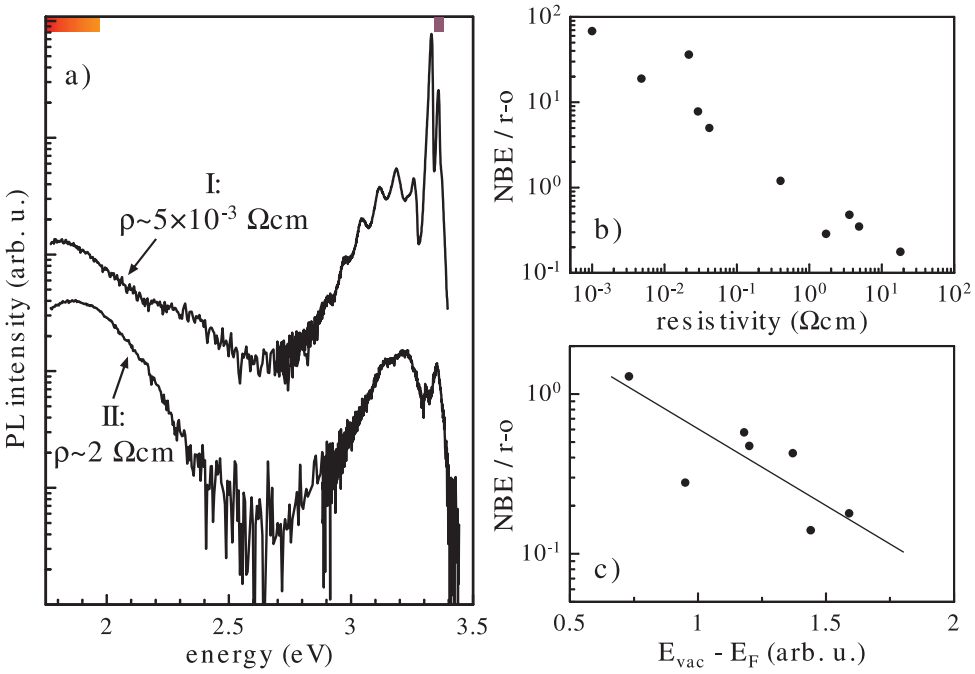

Figure 7.7: a) Recombination spectra at 2 K of ZnO thin films containing (I) 0.1 and (II) 10^{-3} wt. % P_2O_5 grown at about 800 ℃ at (I) p_{O_2} = 0.1 mbar and (II) p_{O_2} = 0.03 mbar on a MgO buffer layer, respectively. (**b**) Peak intensity ratio of the near band edge emission (NBE, indicated by *violet rectangle*) and the red-orange emission (r-o, indicated by *red-orange rectangle*) for ZnO:P thin films in dependence on the sheet resistivity (note: log–log scale). (**c**) Peak intensity ratio of NBE and r-o luminescence in dependence on surface Fermi level (note: semi-logarithmic scale).

oxygen partial pressures p_{O_2} range from 10^{-4} to 1 mbar. An about 50 nm thick MgO buffer layer is used to suppress the indiffusion of Al from the substrates. The samples are post-growth annealed at 800 °C for about 5 min in streaming nitrogen. Typical recombination spectra recorded at 2 K are depicted in Fig. 7.7a for an *n*-conducting and a semi-insulating ZnO:P thin film. All of our ZnO:P thin films exhibit a broad luminescence band centered around 1.9 eV. This band dominates the recombination spectra for semi-insulating samples. Nominally undoped ZnO thin films show this band only, if they are grown under extremely large p_{O_2} ($\geq$ 10 mbar) suggesting that oxygen interstitials O_i create the final state (close to mid-gap) involved. Indeed it is very likely that O_i is formed by the decomposition of P_2O_5 during the thermal annealing. The ratio of the peak intensities of the near band edge emission and the red-orange emission show a strong correlation with the sample resistivity (Fig. 7.7), note the log–log scale). This peak intensity ratio is depicted again versus the surface Fermi level E_F which was determined for selected samples by means of scanning surface potential microscopy in Fig. 7.7c. Note, that the trend depicted in Fig. 7.7b is found again in Fig. 7.7c if a linear *x*-axis is used.

This work was supported by DFG within the project Gr 1011/10-2 (SPP1136).

7.9 Cathodoluminescence of ZnO Scintillator Films Measured in Reflection and Transmission

M. Lorenz, R. Johne, H. Hochmuth, J. Lenzner, H. von Wenckstern, G. Zimmermann, H. Schmidt, R. Schmidt-Grund, M. Grundmann

Epitaxial ZnO thin films on sapphire substrates can be used as fast and laterally homogeneous scintillators to convert electrons into photons, e.g. for imaging purpose in an electron microscope. An increase of the cathodoluminescence (CL) intensity of epitaxial pulsed laser deposited ZnO thin films on a-plane sapphire substrates with diameter up to 33 mm by a factor of more than two in relation to the earlier results [1] was achieved by weak CdO doping of the ZnO target and process optimization [2]. High CL intensities were obtained for both small grain films with 300 nm grain size and for films with much bigger hexagonal crystallites of about 20 µm diameter . The lateral homogeneity of the integral CL intensity was inspected by a modified RHEED setup. 92 % of the sample area show a normalized CL intensity within ±10 % around the average intensity. CL spectra were excited at the ZnO side of the samples and detected both in reflection and in transmission geometry, as shown in Fig. 7.8a. The redshift of the excitonic CL peak in transmission relative to reflection and the peak shift with the excitation depth (both shown in Fig. 7.8b) can be quantitatively explained by a model based on self absorption of the generated luminescence inside the ZnO film [2].

[1] M. Lorenz et al.: Thin Solid Films **486**, 205 (2005)
[2] R. Johne et al.: Appl. Phys. A in press (2006)

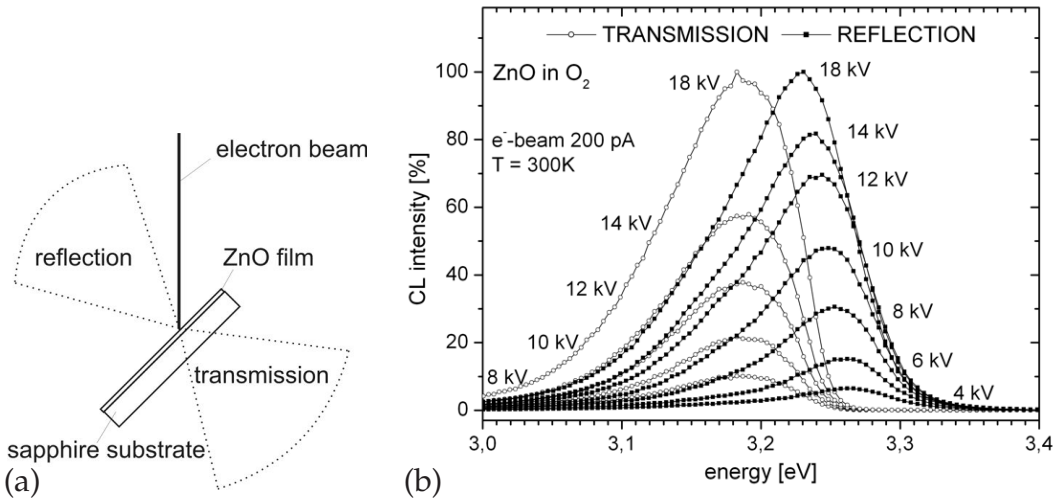

Figure 7.8: (**a**) Scheme of the cathodoluminescence spectrometry in reflection and transmission geometry. (**b**) CL spectra measured in transmission and reflection with different excitation energies on a ZnO thin film. The maximum intensities of transmission and reflection are each set to 100 % for 18 kV.

7.10 Exchange Polarization Coupling in PLD-grown ZnO–$BaTiO_3$-type Heterostructures

M. Lorenz, M. Schubert*, N. Ashkenov, H. Hochmuth, R. Voora, H. von Wenckstern, M. Grundmann

*present address: Department of Electrical Engineering, University of Nebraska-Lincoln, Lincoln, USA

ZnO (wurtzite structure) and $BaTiO_3$ (perovskite structure) are promising materials for next generation UV-opto- and microelectronic devices. The spontaneous electric polarizations in both materials have received little attention so far, especially if combined in heterostructures. Whereas the spontaneous wurtzite-type polarization is inherently connected to one distinct lattice direction and orientation, the spontaneous perovskite-type polarization can be reversed and switched by external electric fields. Coupling between the fixed ionic wurtzite interface charges and the switchable ferroelectric interface charges should give rise to ferroelectric polarization exchange coupling phenomena.

Various ZnO–$BaTiO_3$- and ZnO–$BaTiO_3$–ZnO-type heterostructures have been grown by pulsed laser deposition (PLD) on silicon and sapphire. Pt electrodes are used as bottom and top contacts, with ohmic properties on ZnO, and Schottky characteristics on $BaTiO_3$. Temperature-dependent electric polarisation, current-voltage (I–V), and capacitance–voltage (C–V) studies result in distinct polarization hysteresis behaviour strongly depending on the type of device structure. Figure 7.9 shows the I–V and C–V response of a ZnO–$BaTiO_3$ and a ZnO–$BaTiO_3$–ZnO structure, respectively, with hysteresis effects and clear evidence of exchange coupling of switchable ferroelectric and fixed wurtzite polarization charges. Temperature dependent Raman scattering confirms a broad ferroelectric phase transition in the heterostructures. The observed polarization

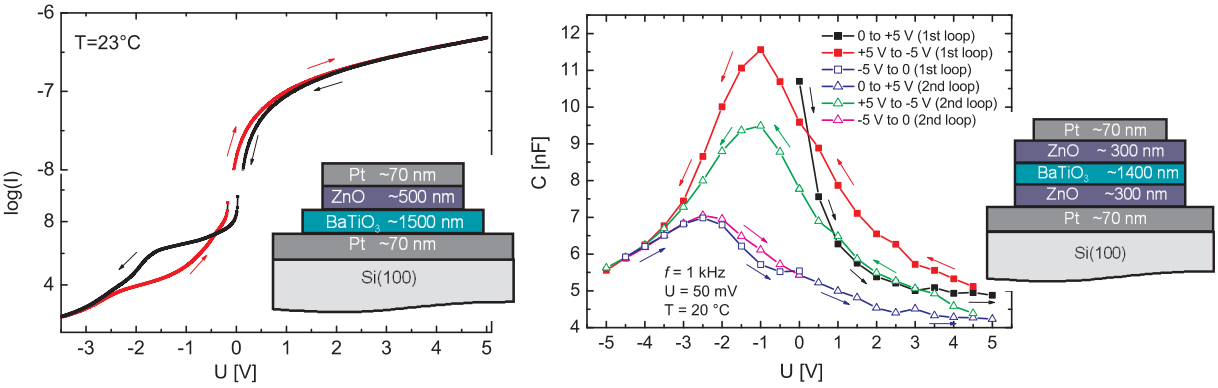

Figure 7.9: *Left: I–V* measurement of a ZnO–$BaTiO_3$ heterostructure with rectifying behavior and asymmetric ferroelectric hysteresis (resistive switching) for forward bias ($U < 0$). The hysteresis loop is shifted by the ZnO ionic surface charges. *Right:* Asymmetric *C–V* loop of a ZnO–$BaTiO_3$–ZnO structure with bistable capacitance maxima at negative bias-voltages: Depending on the bias-voltage sweep direction, the capacitance of the structure switches by more than e.g., 30 % at 23 °C and 100 % at 120 °C.

exchange coupling phenomena may find use in future transparent nano-optoelectronic device structures.

This work was supported by DFG within the project Schu 1338/4-1 (FOR404).

7.11 Magnetic Zn(Mn,P)O and Zn(Mn,Sn)O Thin Films

M. Diaconu, H. Schmidt, M. Fecioru-Morariu*, G. Güntherodt*, H. Hochmuth, M. Lorenz, M. Grundmann

*II. Physikalisches Institut, RWTH Aachen

Theory predicts that transition metal ions substituted in ZnO could produce ferromagnetism above 300 K [1]. Experimental results indicated weak ferromagnetic behavior in ZnMnO films grown at low temperatures [2]. In an attempt to increase the magnetic moment in ZnMnO films, we used P or Sn as co-dopants [3].

Wurtzite Zn(Mn,P)O and Zn(Mn,Sn)O films, with a Mn content around 5 at % and 1 µm thickness, have been grown on *a*-plane sapphire substrates by pulsed laser deposition (PLD). Magnetic properties were investigated using a SQUID magnetometer, the substrates have been investigated separately after etching off the films by HCl dip and the substrate contribution was substracted from the magnetization curves.

Temperature dependent magnetization curves were measured as field cooled (FC) and zero field cooled (ZFC) curves. Non-coincidence between the FC and ZFC curves indicates the presence of magnetic order in the system. The superparamagnetic and spin-glass behaviors can be excluded from the shape of the temperature dependent magnetization curves for the investigated films, no peak being present on the ZFC curve. In Fig. 7.10a we present the FC and ZFC curves measured at 250 Oe for a Zn(Mn,P)O film which shows ferromagnetic behavior above 300 K. The film, with 5 % Mn and 0.1 % P, has been grown at 627 °C and 0.3 mbar. The field dependent magnetization curves at 5 K and 300 K for the same film are shown in Fig. 7.10b.

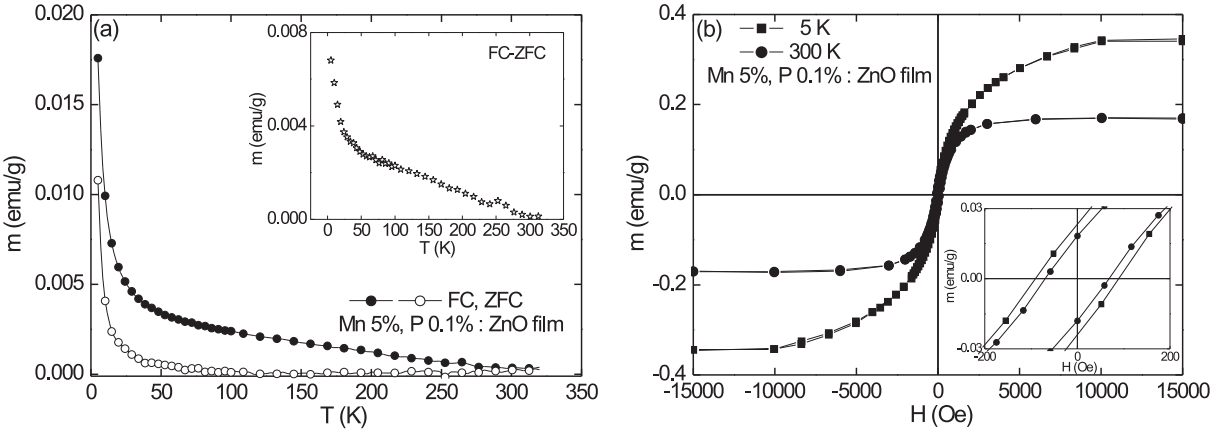

Figure 7.10: (**a**) Temperature dependent magnetization curves for a Zn(Mn,P)O film with 5 % Mn and 0.1 % P. (**b**) Field dependent magnetization curves for a Zn(Mn,P)O film with 5 % Mn and 0.1 % P.

This work is financially supported by BMBF (FKZ03N8708).

[1] T. Dietl et al.: Science **287**, 1019 (2000)
[2] M. Diaconu et al.: Thin Solid Films **486**, 117 (2005)
[3] M. Diaconu et al.: Phys. Lett. A **351**, 323 (2006)

7.12 Magnetoresistance of Al-codoped ZnTMO Thin Films

Q. Xu, L. Hartmann, H. Schmidt, H. Hochmuth, M. Lorenz, R. Schmidt-Grund, C. Sturm, D. Spemann, M. Grundmann

The magnetotransport properties of ZnTMO films alloyed with different 3d transition metals (TM=Co,Mn) and prepared by pulsed laser deposition were studied in dependence on magnetic field strength (0 – 6 T) and temperature (5 – 290 K). The substrate temperature, film thickness and oxygen pressure were adjusted to modify the electron concentration n in the ZnTMO films. For Al-codoped $Zn_{0.9}Co_{0.1}O$ films, the metal insulator transition (MIT) was observed at a critical electron concentration n_c of about 4.0×10^{19} cm^{-3} (Fig. 7.11a). This is consistent with the theoretical calculation of n_c amounting to 4.9×10^{19} cm^{-3} [1]. At 5 K positive magnetoresistance (MR) was observed in the insulating range ($n < n_c$), and negative MR was observed in the metallic range ($n > n_c$). Furthermore, in the vicinity of the MIT ($n \approx n_c$) negative MR at low magnetic field and positive MR at high field was observed. Anomalous Hall effect was only observed in ZnCoO with $n < n_c$. Similar behavior was also observed in Al-codoped $Zn_{91.2}Mn_{8.8}O$ thin films. At 5 K the critical electron concentration n_c amounts to 10^{19} cm^{-3} (Fig. 7.11b). However, at 5 K positive MR can still be observed in ZnMnO films with $n > n_c$. No anomalous Hall effect was observed in ZnMnO films. We consider the critical electron concentration n_c as an important material parameter for ZnO alloyed with 3*d* TM because n_c does not depend on film thickness, substrate temperature, oxygen

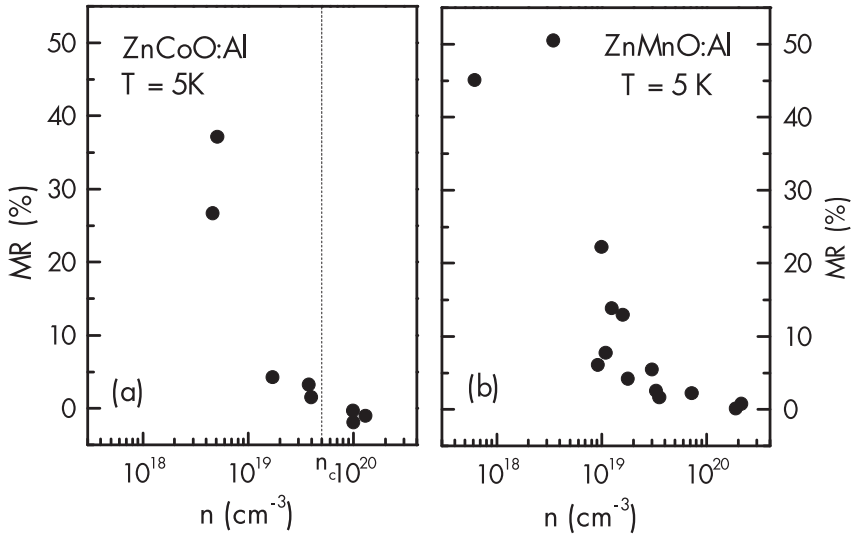

Figure 7.11: (**a**) Positive magnetoresistance at a magnetic field of 6 T in ZnCoO films in dependence on electron concentration n at 5 K. The estimated critical electron concentration n_c is also indicated. (**b**) Maximum positive magnetoresistance in ZnMnO films in dependence on electron concentration n at 5 K.

pressure, and the TM content. The observation of critical electron concentration n_c may help to realize ZnTMO thin films being ferromagnetic above room temperature.

This work is financially supported by BMBF (FKZ03N8708).

[1] T. Dietl: *Semimagnetic Semiconductors and Diluted Magnetic Semiconductors*, ed. by M. Averous, M. Balkanski (Plenum Press, New York 1991) p 83

7.13 Deep Defects in *n*-Conducting ZnO:TM Thin Films

H. Schmidt, M. Diaconu, H. Hochmuth, M. Lorenz, H. von Wenckstern, G. Biehne, D. Spemann, M. Grundmann

The ferromagnetism in highly transparent and intrinsically *n*-type conducting zinc oxide doped with 3d transition metals (TM), is predicted to be carrier- and defect-mediated. Co generates a hole level in ZnO, Mn an isolated impurity level, and Ti an electron level [1]. Different growth conditions and low reproducibility in the reported saturation magnetization and Curie temperature of 3*d* TM doped ZnO may result from the employment of measurement techniques that are incapable of distinguishing carrier-mediated from extrinsic ferromagnetism. We investigated the generation of deep defects in *n*-conducting 1 µm thick ZnO:TM films (TM = Co, Mn, Ti) with a nominal TM content of 0.02, 0.20 and 2.00 at % grown by pulsed laser deposition on *a*-plane sapphire substrates using deep level transient spectroscopy [2]. We found that a defect level is generated, independent of the TM content, located 0.31 eV and 0.27 eV below the conduction band minimum of ZnO:Mn and ZnO:Ti, respectively. Different defect levels are generated in dependence on the Co content in ZnO:Co (Tab. 7.1). This work shows that an optimization of defect-related ferromagnetism in *n*-conducting ZnO:TM

Table 7.1: Parameters of deep electron traps generated in ZnO:Co in dependence on the nominal Co content. The thermal activation energy E_T, capture cross section σ_n, and trap concentration N_T are given in units of eV, 10^{-16} cm^2, and 10^{16} cm^{-3}, respectively.

Co content [at%]	Trap	E_T [eV]	σ_n [10^{-16} cm^2]	N_T [10^{16} cm^{-3}]
	Ea1	0.29 ± 0.02	1.7 ± 0.5	0.1 – 2.0
0.02	Ea2	0.37 ± 0.01	1.8 ± 0.5	0.1 – 1.0
	Ea3	0.45 ± 0.03	2.5 ± 1.0	0.1 – 0.5
	Eb1	0.34 ± 0.01	6.0 ± 2.0	0.1 – 0.5
0.20	Eb2	0.39 ± 0.01	1.8 ± 0.5	0.5 – 2.0
	Eb3	0.59 ± 0.02	80 ± 20	0.1 – 0.3
	Ec1	0.17 ± 0.02	9.0 ± 3.0	1 – 2
2.00	Ec2	0.30 ± 0.01	1.7 ± 0.5	3 – 5
	Ec3	0.33 ± 0.01	16 ± 0.3	5 – 10

thin films will only be possible if the preparation sensitive formation of deep defects is controlled in the same time.

This work is financially supported by BMBF (FKZ03N8708).

[1] Y. Imai, A. Watanabe: J. Mat. Sci. Mater. Electron. **15**, 743 (2004)
[2] M. Diaconu et al.: Solid State Comm. **137**, 417 (2006)

7.14 Thermally-Assisted Tunnelling Processes in InGaAs Quantum Dots

M. Gonschorek, H. Schmidt, M. Grundmann

An ensemble of self-assembled InGaAs quantum dots (QD) has been grown in *n*-conducting GaAs with a low dislocation density by molecular beam epitaxy. The dots exhibit a high photoluminescence efficiency in the technologically important 1.3 µm spectral range. We studied thermal escape by means of deep level transient, photocurrent and conductance measurements (Fig. 7.12) and observed thermally-assisted tunnelling processes out of the quantum dot electron ground state 190 meV below the GaAs conduction band minimum. Even at room temperature the intersubband relaxation of photogenerated electrons from the first excited state E_2 into the electron ground state E_1 is faster than thermally-assisted tunnelling out of the first excited state E_2, thus electrons always leave the dot from the ground state E_1.

Assuming that the depletion layer edge is situated spatially at the QD layer and oscillates with an angular frequency $\omega = 2\pi f$ and an AC amplitude δV, then the QD levels are alternately charged and discharged. The time-dependent charging/discharging causes a time-dependent current δI. The conductance is defined as the real part of $\delta I/\delta V$. In first order perturbation the time-dependent occupation yields the following conductance [1]:

$$G(\omega, T) = \alpha \frac{f_{eq}(1 - f_{eq})}{k_B T} \left(\frac{\omega^2 \tau}{1 + \omega^2 \tau^2} \right), \tag{7.1}$$

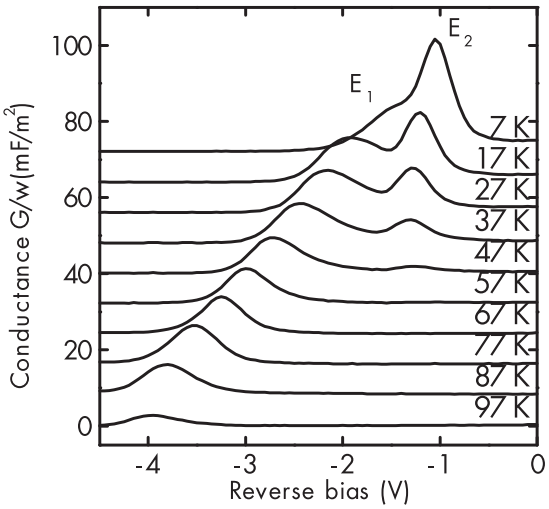

Figure 7.12: Conductance resonance peaks of an InGaAs QD sample measured in a temperature range from 97 K to 7 K at a frequency of f=1 kHz. The curves are shifted for clearity by 8 μF/m^2.

with $f_{eq} = n^0_{QD}/N_{QD}$ being the occupation fraction that is equal to the ratio between the number of electrons per dot in equilibrium n^0_{QD}, and the number of available states per dot N_{QD}. ω denotes the angular frequency and $\tau = (1 - f_{eq})/e_n$ the time constant, with emission rate e_n. α is a scaling constant. The expression $f_{eq}(1 - f_{eq})$ reaches a maximum for $f_{eq} = 1/2$, which is equal to the condition $E_n = E_F$, i.e., the conductance reaches a maximum at a reverse bias where the QD state E_n crosses the Fermi level.

From (7.1) follows that the amplitude of the conductance increases with decreasing temperature, with the number of electrons per dot and state in equilibrium, and for constant τ with increasing angular frequency.

In Fig. 7.12 the conductance resonance peaks of an InGaAs QD sample are shown in a temperature range between 7 K and 97 K. If a double conductance peak is visible, the conductance peak at larger reverse biases can be related with the discharging of the ground state E_1. Taking into account that the ground state is always occupied with two electrons in the whole temperature range from 4 K up to 300 K, then the increasing peak amplitude with decreasing temperature can be explained with the $G \sim 1/T$ dependence (e.g. the temperature range from 97 K to 7 K in Fig. 7.12). Therefore, for a temperature above 100 K, no conduction resonance peak can be observed. For temperatures below $T = 57$ K a second resonance peak becomes visible (the peak at smaller reverse bias, if a double conductance peak is visible) due to the increasing probability of the occupation of the first excited state in equilibrium at lower temperatures. At 7 K the Fermi level lies only ≈ 3 meV below the GaAs conduction band and the conductance peak at the small reverse bias has twice the height of the E_1 conductance amplitude. According to (7.1) the amplitude should be proportional to the number of electrons per state. Therefore, we conclude that four electrons occupy the excited states at 7 K.

The experiments have been performed by N. Geller and A. Marent (TU Berlin) and are supported by NoE SANDiE. We are grateful to the Ioffe Institute, St. Petersburg, for providing the samples.

[1] W.-H. Chang et al.: Phys. Rev. B. **64**, 125315 (2001)

7.15 Quantitative Scanning Capacitance Microscopy

S. Jaensch, H. Schmidt, M. Grundmann

Scanning capacitance microscopy (SCM) is an analytical technique able to provide direct carrier distribution information on the nanoscale using HF amplitude detection and lock-in techniques. For the reliability analysis of semiconductor devices also defect characterisation is necessary on the nanoscale. On the μm-scale the important parameters of deep defects in semiconductors (emission barrier energy, capture cross section, defect distribution) are determined by deep level transient spectroscopy (DLTS) where capacitance transients are measured within time windows ranging between μs and several s as a function of temperature. We designed an HF coaxial resonator in combination with a IQ-demodulator system with a bandwidth of 200 kHz and a resolution of 1.4×10^{-17} F for temperature dependent quantitative static and dynamic capacitance measurements on the nanoscale around the resonance frequency of the sample-resonator unit [1, 2].

We performed *C–V* measurements with a SCM tip at room temperature on *p*-type and *n*-type conducting GaAs substrates with back side alloyed ohmic contacts and native oxide surface layers which have been fixed on the coaxial resonator. Results from isothermal spectroscopy measurements on a *n*-type conducting GaAs sample ($n = 10^{18}$ cm^{-3}) with native oxide are shown in Fig. 7.13 and reveal a "textbook" *CV* plot shifted on the voltage axis by −1 V due to mobile ions. During the *C–V* measurements where the sample bias has been varied between −4 V and +1 V and between −1 V and +4 V (Fig. 7.13), the circuit has been operated at 2.138 GHz. After a second VCO tuning we repeated the *C–V* measurements by varying the sample bias between −4 V and +4 V with a slightly different resonance frequency of 2.139 GHz (Fig. 7.13). Since all *CV* sweeps begin with the MOS structure in inversion, errors due to sweeping rate and inversion capacitance determination while sweeping are eliminated. As for standard Schottky contact formation the choice of the conductor material which will form the Schottky barrier is of importance for the feasibility of scanning capacitance measurements.

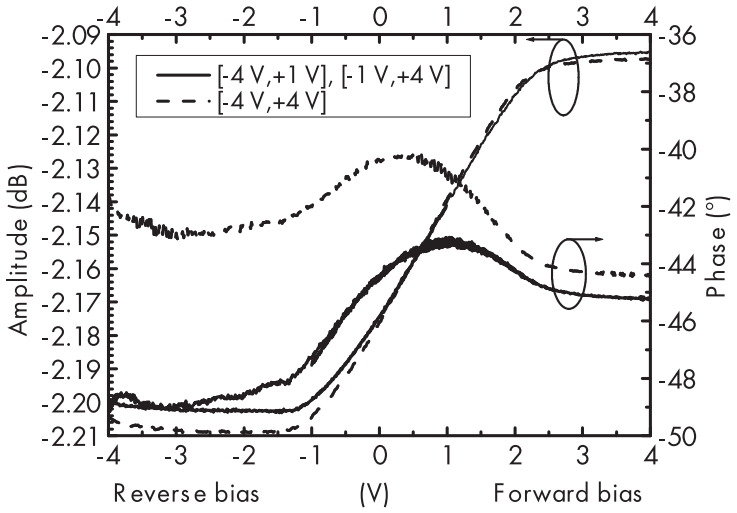

Figure 7.13: Isothermal *CV* spectroscopy measurements on *n*-GaAs with native oxide using a NSG20 tip with the circuit operated at 2.138 GHz (*solid lines*) and at 2.139 GHz (*dashed lines*).

We acknowledge the reviving of interest in the measurement of capacitance transients under cryogenic conditions on the nanoscale by R. Pickenhain and W. Grill (Uni Leipzig) and O. Breitenstein (MPI Halle). This work is financially supported by BMBF (FKZ03N8708).

[1] S. Jaensch, H. Schmidt: *Verfahren und Vorrichtung zur elektrischen Charakterisierung von Halbleiterbauelementen auf der Nanometerskala* (AKZ: P 10 2005 006 928.2)
[2] S. Jaensch et al.: Physica B (2006), in press

7.16 Bragg Reflectors for ZnO-Based Resonator Structures

R. Schmidt-Grund, H. Hochmuth, J. Lenzner, B. Rheinländer, M. Lorenz, M. Grundmann

For future ZnO-based resonant light emitters in the UV (excitonic luminescence at $\approx 3.37\,\mathrm{eV}$) and visible (the so called green luminescence, $\approx 2-3\,\mathrm{eV}$) spectral range, Bragg reflectors (BR) are essential. In order to reach high reflectivity (R) values of the BR with already a low number N of layer-pairs, a large difference between the refractive indices of the used materials is necessary. The materials a-Si and SiO_x fulfill this requirement [1], but due to the absorption of a-Si in the spectral range of the ZnO luminescence, BR based on these materials are not appropriate (Fig. 7.14a). High-gap materials, as e.g. MgO and ZrO_2, match the transparency condition and could be used for these BR, but with the disadvantage of higher values of N, as can be seen in Fig. 7.14b, where spectra of R of BR based on several materials are shown [2].

Using pulsed laser deposition we have grown resonator-structures which consist of a ZnO cavity (layer thickness $\approx 0.5\lambda_{\mathrm{medium}}$) placed between ZrO_2/MgO (layer thicknesses $\approx 0.25\lambda_{\mathrm{medium}}$) front- and backside BR with $N = 5.5$. We have measured cathodoluminecence (CL) in order to investigate the emission characteristics of the resonator-structures. Note, that the luminescence is detected with an angle of $\approx 40^\circ$ with respect to the sample surface and with a finite angle spread. The layer thicknesses and the spectra of R and T (transmitivity) of the structures were obtained from layer-model

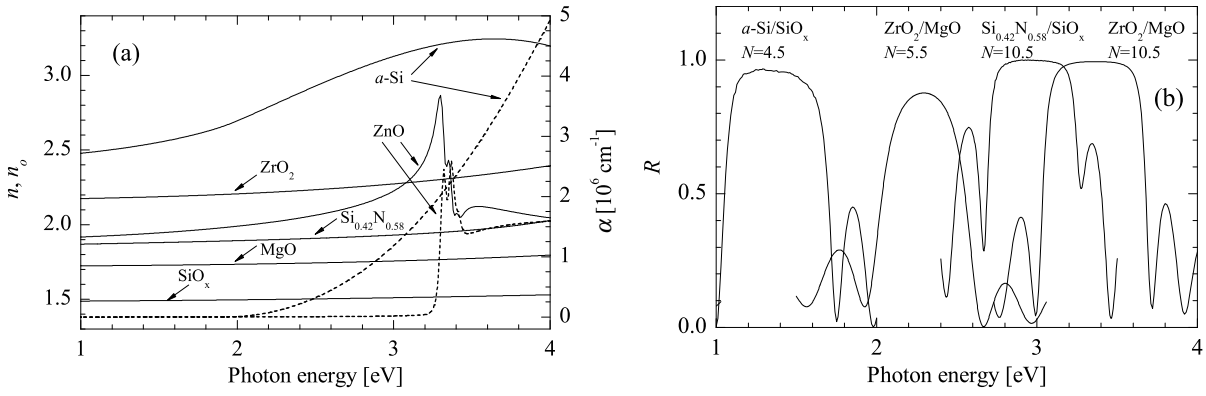

Figure 7.14: (**a**): Refractive index dispersion of materials which are useful for BR (**solid lines**). The dashed lines represents the absorption coefficient α for a-Si and ZnO. (**b**): R of BR based on several materials determined using spectroscopic ellipsometry.

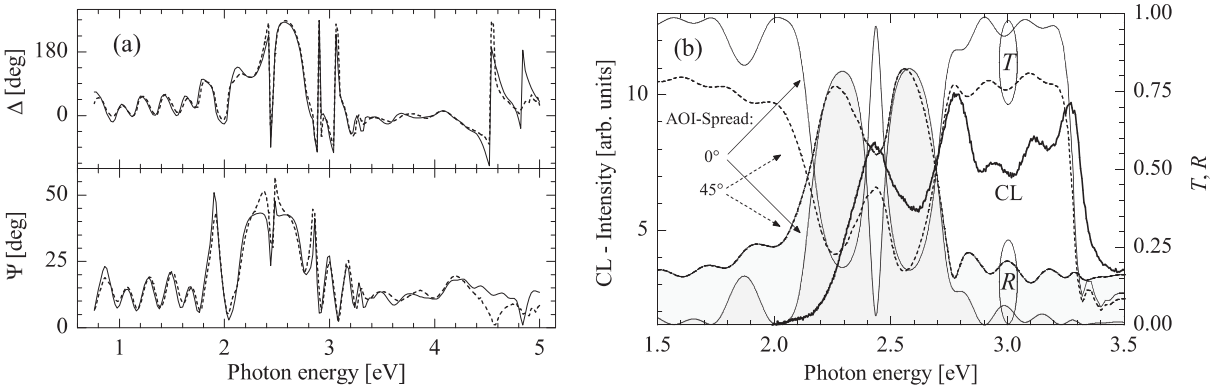

Figure 7.15: Resonator structure with a ZnO-cavity placed between front- and backside ZrO_2/MgO BR ($N = 5.5$). (**a**): Experimental (*dashed lines*) and model-calculated (*solid lines*) spectra of Ψ and Δ for an AOI of 70°. (**b**): Spectra of R and T calculated from the layer-model analysis for an AOI of 67° along with spectra of the CL-intensity (*bold line*). The R spectra are filled in gray for clarity.

analysis of Ψ and Δ spectra, which were measured by means of spectroscopic ellipsometry. The experimental and the model-generated Ψ and Δ spectra of such a resonator structure are shown in Fig. 7.15a. In Fig. 7.15b, the calculated spectra of R and T for an angle-of-incidence (AOI) of 67° and AOI-spreads of 0° and 45° (in order to match the condition of the CL-experiment) are shown along with the CL-intensity. Within the spectral range of the stop band (2.1 – 2.7 eV), the cavity mode (at 2.42 eV) is shown as a dip in R and a peak in T respective the CL-intensity. The peaks in the CL-intensity at higher photon energies are originated in the green and excitonic luminescence, which passes through the BR due to small values of R besides the stop band (note the excellent spectral match between the CL- and T-maxima). The sharpness of the cavity mode of the shown resonator-structure is not satisfying and should be further improved by using BR with larger values of N.

This work was supported by the DFG within the project No. Gr 1001/14-2 (FOR 404).

[1] V. Gottschalch et al.: Thin Solid Films **416**, 224 (2002), doi: 10.1016/S0040-6090(02)00704-6

[2] R. Schmidt-Grund et al.: Proc. SPIE **6038**, 489 (2006), doi: 10.1117/12.638585; R. Schmidt-Grund et al.: Appl. Phys. Lett. **82**, 2260 (2003), doi: 10.1063/1.1565185; R. Schmidt-Grund et al.: J. Appl. Phys., submitted (2005)

7.17 Ellipsometry on Cylinders with Circularly Basal Planes

R. Schmidt-Grund, B. Rheinländer, V. Gottschalch*, M. Grundmann

*Fakultät für Chemie und Mineralogie, Universität Leipzig

Lateral confinement in cylindrical micro resonator light emitters improves the ratio of the number of the axial resonant modes to the number of the spontaneous emitting

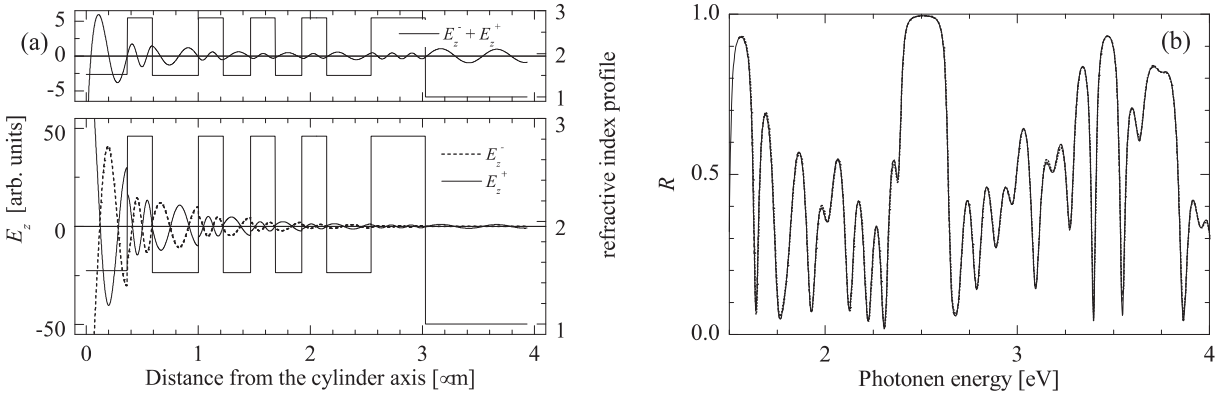

Figure 7.16: (**a**) Distribution of the TM-mode (E_z) within a glass cylinder coated with a BR in the plane perpendicular to the cylinder axis (outwards propagating mode: E_z^+, inwards propagating mode: E_z^-, sum of both: $E_z^- + E_z^+$). The step-lines indicate the refractive index profile. (**b**) Spectra of R for the structure in (**a**) (TM-mode: *dotted line*, TE-mode: *dashed line*) and for a accordant planar structure (*solid line*).

lateral modes. We have investigated cylinders with circularly shaped basal planes which were coated with single layers or Bragg reflectors (BR).

In order to calculate the electromagnetic-field distribution within such structures and to properly describe the properties of optical investigation techniques, such as spatially resolved confocal spectroscopic ellipsometry (CFμE) and reflection measurements, we have used cylindrical waves as solutions of the Helmholtz-equation. The light propagation was calculated in the plane perpendicular to the cylinder axis using a transfer-matrix algorithm [1]. In Fig. 7.16a, the radial distribution of the TM-mode (E_z: electric field parallel to the cylinder axis) with the azimuthal quantum number $m = 0$ along with the refractive index profile of a cylindrical layer structure consisting of a glass cavity coated with a *a*-Si/SiO_x BR and the symmetry axis at 0 μm. With larger distance from the symmetry axis, a decrease of the field amplitude is observable. It is, in comparison with a uncoated cylinder, stronger due to the confinement by the BR. The corresponding spectra of the reflectivity R for the TM- and TE-mode is shown in Fig. 7.16b. It was found, that for structures with diameters $> 10\lambda_{\text{medium}}$ the calculations can be performed with common planar algorithms. This can be seen in Fig. 7.16b from the comparison of R calculated with cylindrical and planar approaches.

Due to the focusing in the CFμE technique (spot size 200 μm), the beam profile matches only nearly the cylinder symmetry of the glass cylinder (Fig. 7.17a), and the reflected light is partially depolarized [2]. Therefore, spectra of the Mueller matrix elements have to be measured. In the case of structures for which the planar approach applies, this effect can be well described with an angle-of-incidence spread $\Delta\Phi$ assumed adequately in the model analysis.

We have applied CFμE to a glass cylinder with 65 μm diameter coated using plasma-enhanced chemical vapour deposition with an *a*-Si/SiO_x BR with 4.5 layer pairs [2]. Since the diameter is larger than $10\lambda_{\text{medium}}$, we have used a model consisting of planar layers in order to analyse the experimental data. The experimental and calculated Mueller-matrix spectra are shown in Fig. 7.17b. As can be seen, the model matches well to the experimental spectra.

This work was supported by the DFG within the project No. Go 629/5, Rh 28/4-2 (FOR 522).

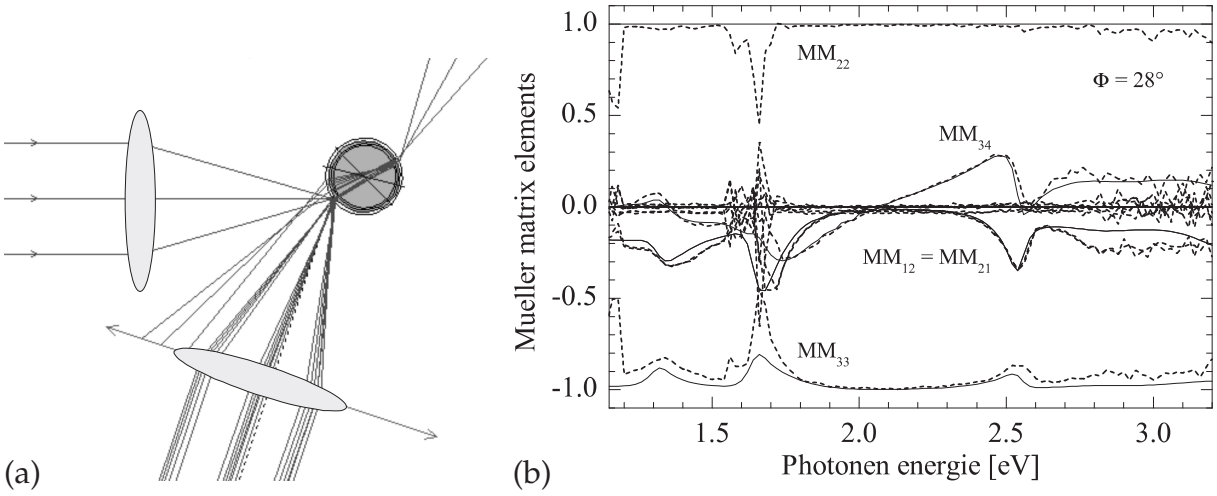

Figure 7.17: (**a**): Beam profile for CFμE applied to an cylinder coated with an BR. The gray circles stands for the cylindrical layers, the gray ellipses for the focussing units. (**b**): Experimental (*dashed lines*) and layer model calculated (*solid lines*) spectra of the Mueller matrix elements $M_{12} = M_{21}$ (equality holds for optically isotropic materials), M_{22}, M_{33} und M_{34} obtained using CFμE of a glass cylinder ($\oslash \approx 65$ μm coated with an *a*-Si/SiO_x BR with 4.5 layer pairs.)

[1] M.A. Kaliteevski et al.: J. Mod. Optic. **46**, 875 (1999), doi: 10.1080/095003499149593; M.A. Kaliteevski et al.: J. Mod. Optic. **47**, 677 (2000), doi: 10.1080/095003400147980; W.M.J. Green et al.: Appl. Phys. Lett. **85**, 3669 (2004), doi: 10.1063/1.1807970; J. Scheuer et al.: J. Opt. Soc. Am. B **20**, 2285 (2003)

[2] R. Schmidt-Grund et al.: Thin Solid Films **483**, 257 (2005), doi: 10.1016/j.tsf.2004.12.048; R. Schmidt-Grund et al.: Proc. SPIE **6038**, 489 (2006), doi: 10.1117/12.638585

7.18 ZnO Wires With Concentric Bragg Reflectors

R. Schmidt-Grund, T. Gühne*, H. Hochmuth, B. Rheinländer, A. Rahm, V. Gottschalch*, J. Lenzner, M. Grundmann

*Fakultät für Chemie und Mineralogie, Universität Leipzig

In order to develop microresonators on the basis of ZnO wires, the coating of the lateral surface of the wires with Bragg reflectors (BR) was studied in order to obtain confinement of the lateral optical modes.

We have deposited *a*-Si/SiO_x BR using plasma-enhanced chemical vapour deposition and ZrO_2/MgO BR using pulsed laser deposition at the lateral surface of free-standing ZnO wires with diameters in the range between 0.8 μm and 10 μm [1]. The optical properties of the Bragg reflectors were investigated using confocal microreflectometry (μR) and spatially resolved cathodoluminescence (CL) measurements.

The μR measurements were performed perpendicular to the axis of the hexagonally shaped ZnO wires. Therefore, a stack of plane parallel layers consisting of the front-side BR (at one of the lateral surfaces), the ZnO cavity, and the respective back-side BR (at the opposite lateral surface) contribute to the reflectivity spectra. As an example, in

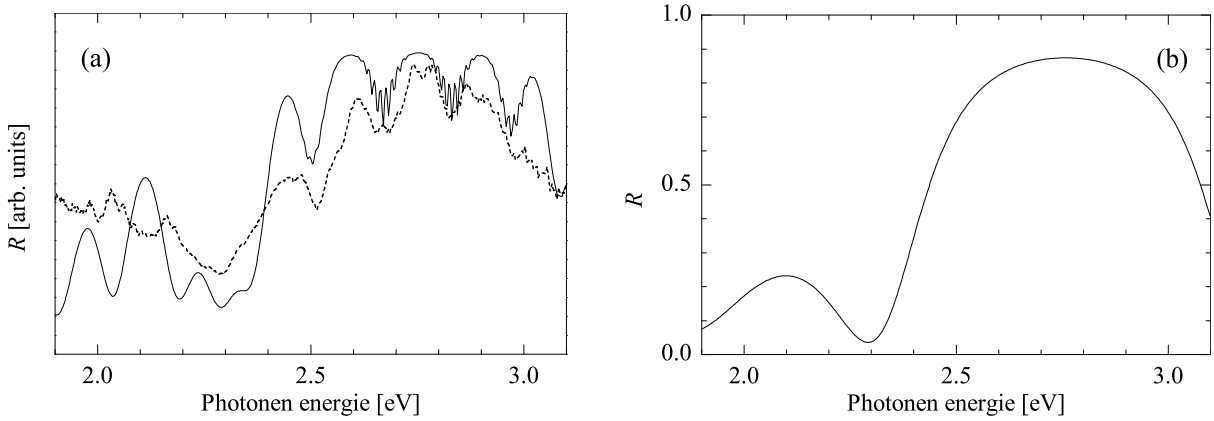

Figure 7.18: (**a**): Experimental (*dashed lines*) and model calculated (*solid lines*) spectra of the reflectivity of a ZnO wire coated with a ZrO_2/MgO BR. (**b**): Reflectivity of the BR to the wire internal (at one of the six boundaries) calculated from the model analysis.

Fig. 7.18a, experimental μR and calculated R spectra of the light collected from a lateral surface of a ZnO wire (inner diameter 1 μm) coated with a ZrO_2/MgO BR (5.5 pairs) are shown. The modulation of R with varying photon energy between 2.4 eV and 3.1 eV within the stop band (SB) is due to multiple-reflection induced interferences within the ZnO cavity. This indicates the resonator behaviour of the coated ZnO wires. As it can be seen at the four minima within the SB, four resonator modes are present. Fig. 7.18b shows the reflectivity of the BR seen from inside the wire (at one of the six boundaries) calculated from the model analysis. The reflectivity reaches values larger 0.8. CL studies confirm the resonator behaviour of the BR coated wires.

This work was supported by the DFG within the project No. Go 629/5, Rh 28/4-2 (FOR 522).

[1] R. Schmidt-Grund et al.: Proc. SPIE **6038**, 489 (2006), doi: 10.1117/12.638585

7.19 Optical Properties of Cylindrite

C. Sturm, R. Schmidt-Grund, R. Kaden*, B. Rheinländer, K. Bente*, H. von Wenckstern, M. Grundmann

*Institut für Mineralogie, Kristallographie und Materialwissenschaft, Universität Leipzig

Cylindrite, $FeSn_4Pb_3Sn_2S_{14}$, is a sulfosalt that naturally occurs as lamellae and cylinders. Its lattice structure consists of two alternating layers: a pseudo-tetragonal slab and a pseudo-hexagonal slab. Therefore, optical anisotropy could be expected.

Cylindrite crystals were synthesized as lamellae and as cylinders by chemical vapour transport (CVT) with iodine as transport agent. The size of the lamella-type samples was 2 mm × 3 mm. The cylinder-type samples had diameters between 4 μm and 12 μm. The sample surface was found to be inhomogeneous.

By microreflection technique lamella- and cylinder-type samples were measured in a spectral range from 1.8 eV to 3.2 eV. From these reflectivity spectra it can be concluded that the chemical composition of the cylinder-type and lamella-type samples is different. The lamella-type samples were studied by ellipsometry in a spectral range

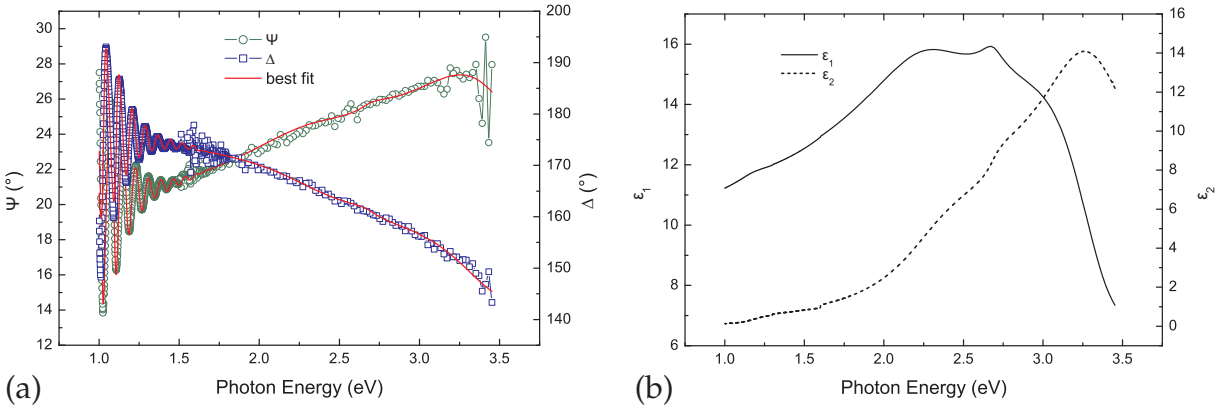

Figure 7.19: (**a**): Experimental and model-calculated Ψ and Δ spectra of cylindrite for an angle of incidence of 60°. (**b**): The dielectric function of Cylindrit.

from 1.0 eV to 3.5 eV. Since the optical anisotropy was found to be negligibly small, standard ellipsometry has been used. The spectra in the ellipsometric parameters Ψ and Δ show multiple-reflection interferences up to 1.5 eV (Fig. 7.19a). The experimental ellipsometry data were analysed by a layer structure model using a model-dielectric functions approach. The dielectric function of cylindrite was obtained (Fig. 7.19b). This dielectric function was found to be typical for semiconductors. A soft absorption edge was found around 1.1 eV. The model-dielectric function parameter E_0 representing the band gap energy of a semiconductor was found to be 1.5 eV. From Hall-effect measurements, carrier density and electron mobility values were determined and found to lie in the data ranges of semiconductors. Therefore, we conclude that cylindrite behaves as a semiconductor.

This work was funded by the DFG within the project FOR 522 (Rh 28/4-2).

7.20 Polarization Dependent Optical Transitions at the Band Gap and Higher Critical Points of Wurtzite ZnO

D. Fritsch, R. Schmidt-Grund, H. Schmidt, C.M. Herzinger*, M. Grundmann

*J.A.Woollam Co., Lincoln, Nebraska, USA

We have performed band structure calculations of wurtzite ZnO by means of the Empirical Pseudopotential Method (EPM) including spin-orbit interactions and taking into account the temperature dependence by means of the Brooks-Yu theory [1]. The model potential parameters of our empty core model potential were fitted to experimentally well-known low-temperature transition energies of wurtzite ZnO [2] utilizing a Levenberg-Marquardt fitting procedure.

The incorporation of the temperature dependence into band structure calculations is done by weighting the pseudopotential structure factors with Debye-Waller factors which are directly related to the mean square of temperature dependent relative displacements. In our work we used the value $\langle u^2 \rangle$ (293 K) = 0.002 46 Å^2 [3]. The resulting

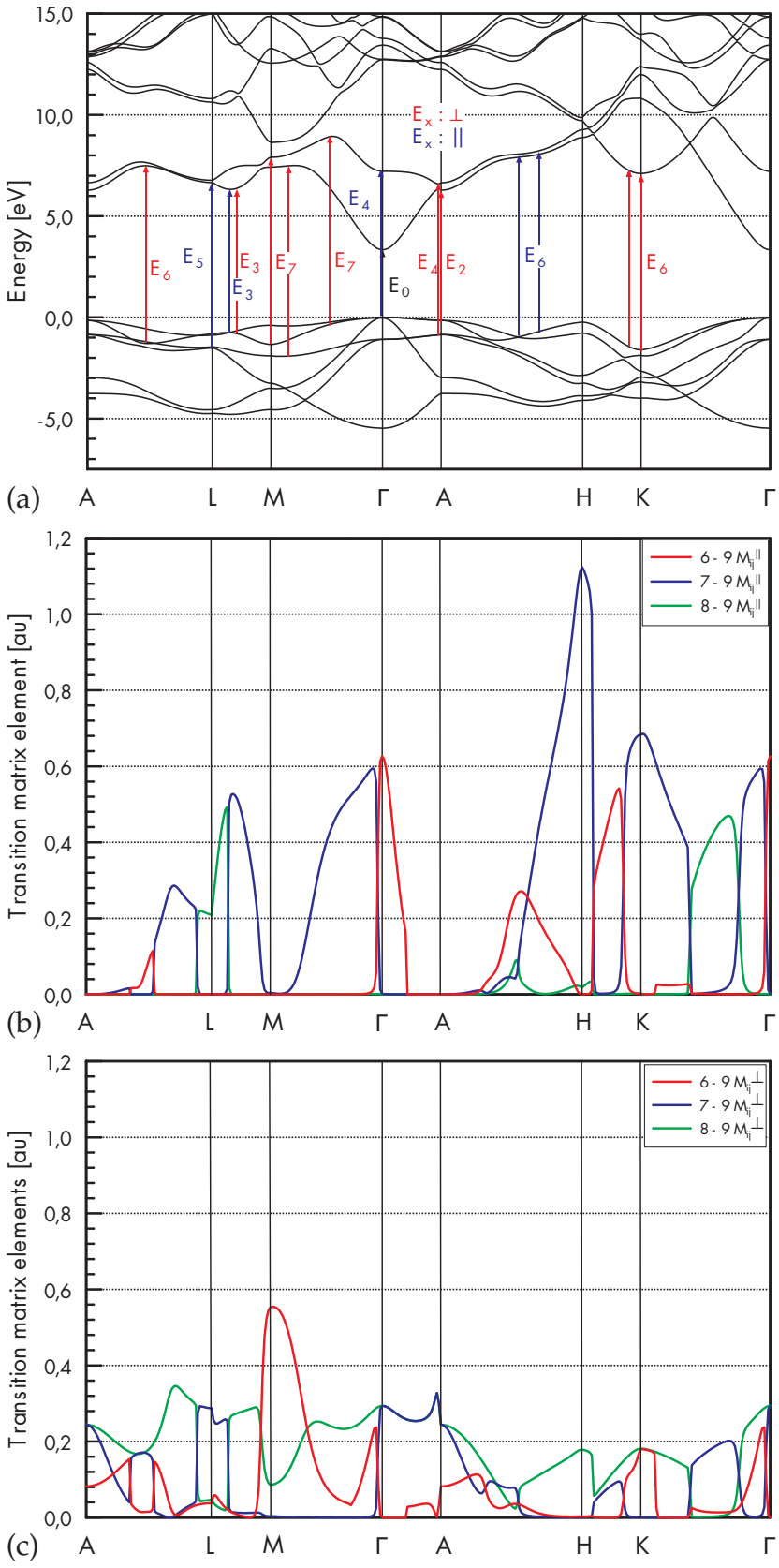

Figure 7.20: Room-temperature band structure of wurtzite ZnO along high symmetry lines in the Brillouin zone (**a**) together with the transition matrix elements for polarization parallel (**b**) and perpendicular (**c**) to the optical axis.

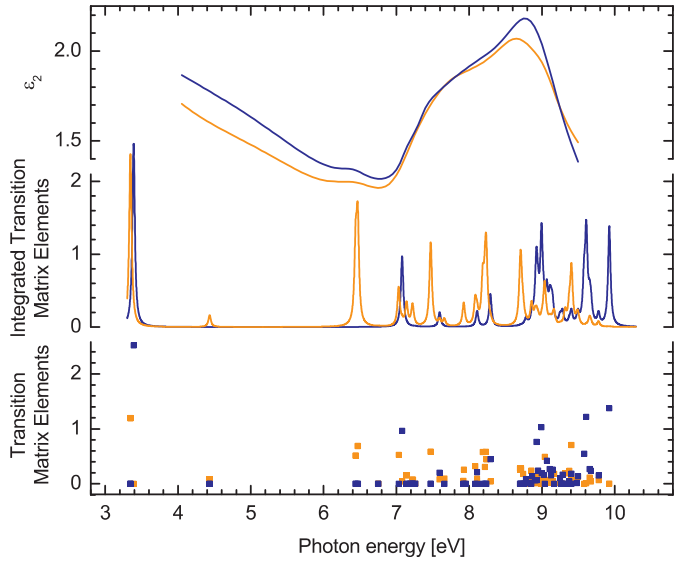

Figure 7.21: Experimentally determined dielectric function of wurtzite ZnO; sum of Lorentz-broadened transition matrix elements; scaled transition matrix elements for allowed direct transitions in the Brillouin zone.

room-temperature band structure of wurtzite ZnO is shown in Fig. 7.20a. The room-temperature band gap energy amounts to 3.34 eV which is in favourable agreement with experimental values obtained by spectroscopic ellipsometry. Using the expansion coefficients c_i and c_j from plane wave band structure calculations we were able to calculate the transition matrix elements for polarizations parallel and perpendicular to the optical axis. These results are shown in Fig. 7.20b,c for transitions from the three highest valence bands to the lowest condution band throughout the Brillouin zone. To compare our theoretical results with experimental data obtained by spectroscopic ellipsometry we analyzed the band dispersion data with respect to k points where direct transitions are allowed to occur. As one results we identified the location of several band-to-band transitions in the Brillouin zone which are known to contribute to the dielectric function. These direct transitions at critical point energies (E_1 to E_7) are also shown in the band structure diagram for polarizations parallel (blue) and perpendicular (orange) to the optical axis. The other results of this investigation are shown in Fig. 7.21. In the lower part the transition matrix elements are arranged with increasing transition energy followed by the sum of the Lorentz-broadened transition matrix elements. For comparison we also show the experimentally determined dielectric function of wurtzite ZnO in the upper part of Fig. 7.21. On the basis of these results we will implement a routine to perform Brillouin zone integrations by means of the linear tetrahedron method to directly compute the imaginary part of the dielectric function from band structure data.

This work was financially supported by the Network of Excellence SANDiE (NMP4-CT-2004-500101).

[1] Y.W. Tsang, M.L. Cohen: Phys. Rev. B **3**, 1254 (1971)
[2] D. Fritsch et al.: Proc. NUSOD '05, 69 (2005)
[3] T.I. Nedoseikina et al.: J. Phys. Cond. Mat. **12**, 2877 (2000)

7.21 Band Structure of Rocksalt MgO, ZnO, and $Mg_{1-x}Zn_xO$

D. Fritsch, H. Schmidt, M. Grundmann

MgO is the prototype of an ionic semiconductor which has recently attracted much attention because it can be alloyed with ZnO to tune the band gap of ZnO from 3.4 up to 7.8 eV depending on the alloy concentration x of Mg content in $Zn_{1-x}Mg_xO$. With the achievement of reliable p-type doping of ZnO band-gap engineered electro-optical devices based on this material will have a wide variety of applications. While MgO crystallizes under normal conditions in the rocksalt crystal structure, ZnO only transforms to the rocksalt crystal structure by the application of high pressure. The relaxed lattice constant of rocksalt ZnO is reported to be 4.28 Å [1].

We use the Empirical Pseudopotential Method (EPM) to calculate the electronic band structure of the rocksalt phase of MgO and ZnO and in combination with the Virtual Crystal Approximation (VCA) we describe the electronic properties of the rocksalt alloy $Mg_{1-x}Zn_xO$ for $x < 0.5$. Utilizing the transferability of pseudopotential form factors we were able to calculate the band structure of the metastable rocksalt ZnO with the same model potential parameters of our empty core model potential which were used before to correctly describe the electronic properties of wurtzite ZnO. Those model potential parameters were fitted to experimentally well-known low-temperature transition energies of wurtzite ZnO and rocksalt MgO with the emphasis placed on obtaining *one* single set of model potential parameters of the O anion. The resulting band structure of rocksalt ZnO is shown in Fig. 7.22a.

While we are using a local model potential we are not sensitive to p–d hybridization. This p–d repulsion would shift the p valence bands of rocksalt ZnO upwards along the directions Γ–K and Γ–L resulting in an indirect semiconductor. Nevertheless, at the center of the Brillouin zone, the mixing between p and d states is symmetry forbidden, so we can investigate the properties of the alloy at the Γ point within our local approach using VCA taking into account the disorder effects [2]. The results are shown in Fig. 7.22b.

This work was financially supported by the Network of Excellence SANDiE (NMP4-CT-2004-500101).

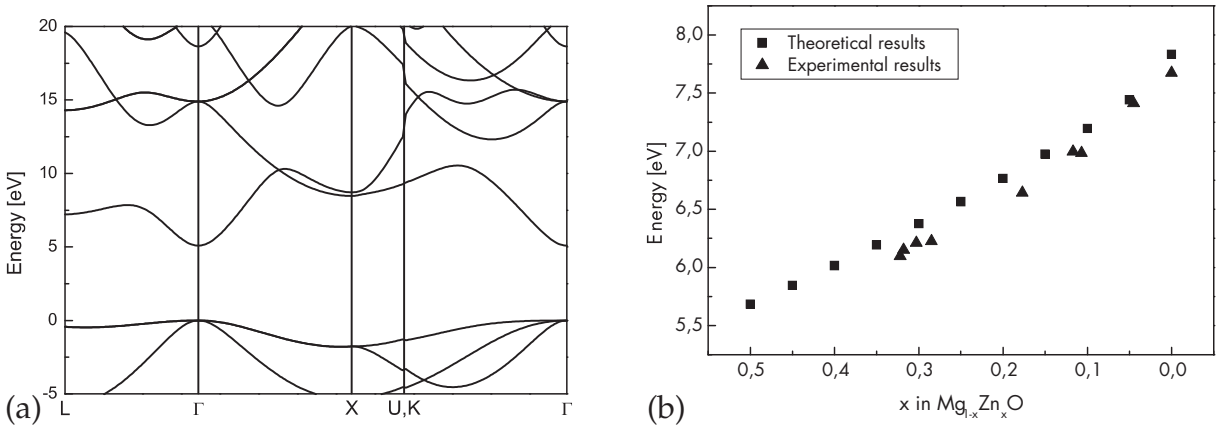

Figure 7.22: (**a**) Band structure of rocksalt ZnO along high symmetry lines in the Brillouin zone. (**b**) Band gap variation of $Mg_{1-x}Zn_xO$ alloys at low temperature for $0.0 < x < 0.5$.

[1] C.H. Bates et al.: Science **137**, 993 (2002)
[2] D. Fritsch et al.: Appl. Phys. Lett. **88**, 134 104 (2006)

7.22 Optical Phonons and Dielectric Constants in $Mg_xZn_{1-x}O$

C. Bundesmann*, U. Teschner†, M. Lorenz, M. Grundmann, M. Schubert‡,

*present address: Leibniz-Institut für Oberflächenmodifizierung, Leipzig
†Solid State Optics and Acoustics group
‡present address: Department of Electrical Engineering, University Nebraska-Lincoln, Lincoln, USA

Long-wavelength optical phonons and dielectric constants of PLD-grown $Mg_xZn_{1-x}O$ films were studied by combination of infrared spectroscopic ellipsometry (IRSE) and Raman scattering spectroscopy [1, 2]. The ternary alloy $Mg_xZn_{1-x}O$ exhibits a phase transition with change of coordination number from four-fold coordinated, hexagonal wurtzite structure (ZnO) to six-fold coordinated, cubic rocksalt structure (MgO).

It was found that both phonon mode frequencies (Fig. 7.23) and dielectric constants (Fig. 7.24) change abruptly upon phase transition, which is assigned to the change of coordination number.

The change of dielectric constants must be related to the change of electronic properties, for instance, the exciton binding energy. In a simple approach, the exciton binding energy is proportional to the ratio of the reduced exciton mass and the square of the static dielectric constant. Because the exciton binding energy was found to change only slightly upon phase transition, the reduced exciton mass must increase up to a factor of

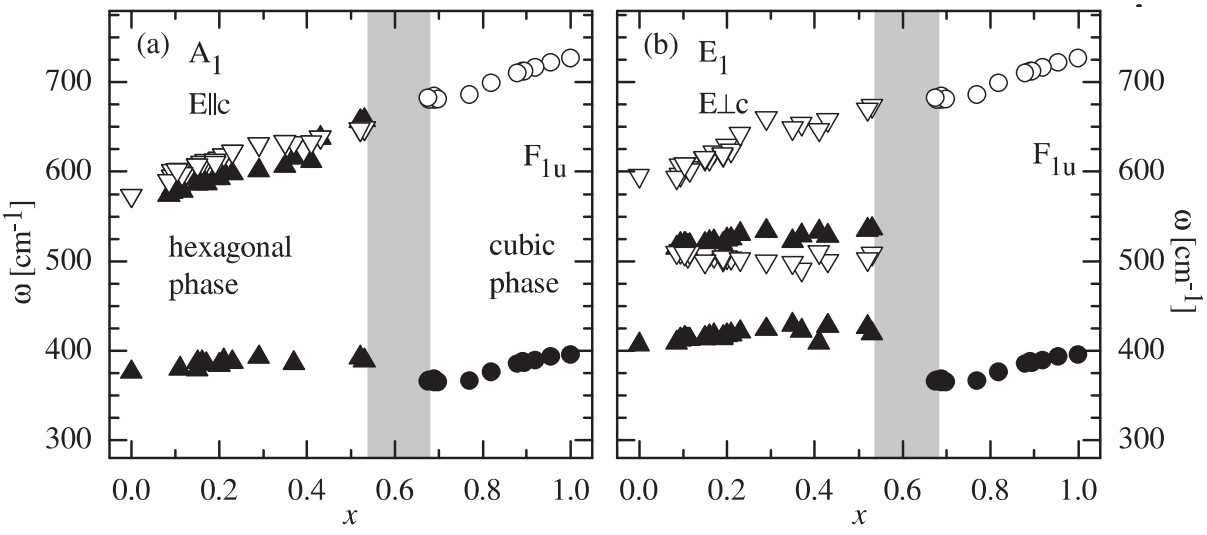

Figure 7.23: Phonon mode frequencies of hexagonal $Mg_xZn_{1-x}O$ films with A_1- (**a**) and E_1- (**b**) symmetry (*triangles*), and of cubic $Mg_xZn_{1-x}O$ films (*circles*) versus Mg mole fraction x. *Open* and *solid symbols* represent TO- and LO-modes, respectively. The shaded area marks the composition range of the phase transition.

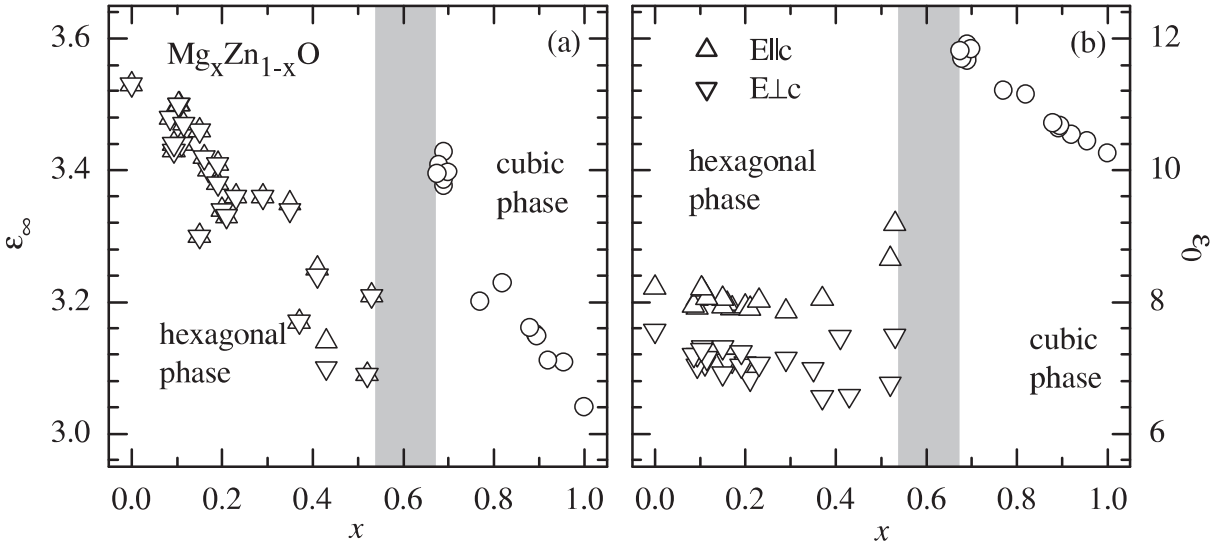

Figure 7.24: High-frequency dielectric constants (**a**) and static dielectric constants (**b**) of hexagonal ($E\|c$: *upright triangles*, $E\perp c$: *downright triangles*) and cubic (*circles*) $Mg_xZn_{1-x}O$ films. High-frequency dielectric constants were obtained by IRSE analysis, static dielectric constants are calculated using the Lydanne-Sachs-Teller relation.

two upon change from wurtzite to rocksalt structure. In consequence of that, the effective mass parameters should change too. For quantitative conclusions concerning the effective mass parameters further experiments are necessary, because no experimental value of the electron or hole effective mass of $Mg_xZn_{1-x}O$ have been reported yet.

[1] C. Bundesmann: PhD Thesis, Universität Leipzig, 2005 (Shaker, Aachen 2006)
[2] C. Bundesmann et al.: J. Appl. Phys (2006), in press

7.23 Clustering of Peptides on Semiconductor Surfaces

K. Goede, M. Grundmann

Peptide adhesion to semiconductors is both substrate and sequence specific [1]. The surface coverage by peptide clusters can differ by a factor of 25 under the same standard conditions, depending on the interplay between polar amino-acid side chains of the respective peptide and the substrate atoms with their respective electronegativity. Now we go further [2] by looking on properties of the cluster ensemble as they turn out to be system specific as well. The larger, higher and softer clusters appear on the surfaces with lower peptide adhesion. A qualitative explanation of this phenomenon is given by arguing that for peptide molecules direct adhesion to the surface competes with forming molecular aggregates which offer an overall reduced surface contact.

The pronounced cluster softness (as indicated by the phase lag of the probing AFM tip) in the low-adhesion systems could either be due to the large cluster size (be it diameter or height) in such systems or indeed be a consequence of the low affinity of the peptide to the substrate. A peptide's affinity to stick to a given surface might impact density and packaging of the molecules within the resulting peptide clusters. This

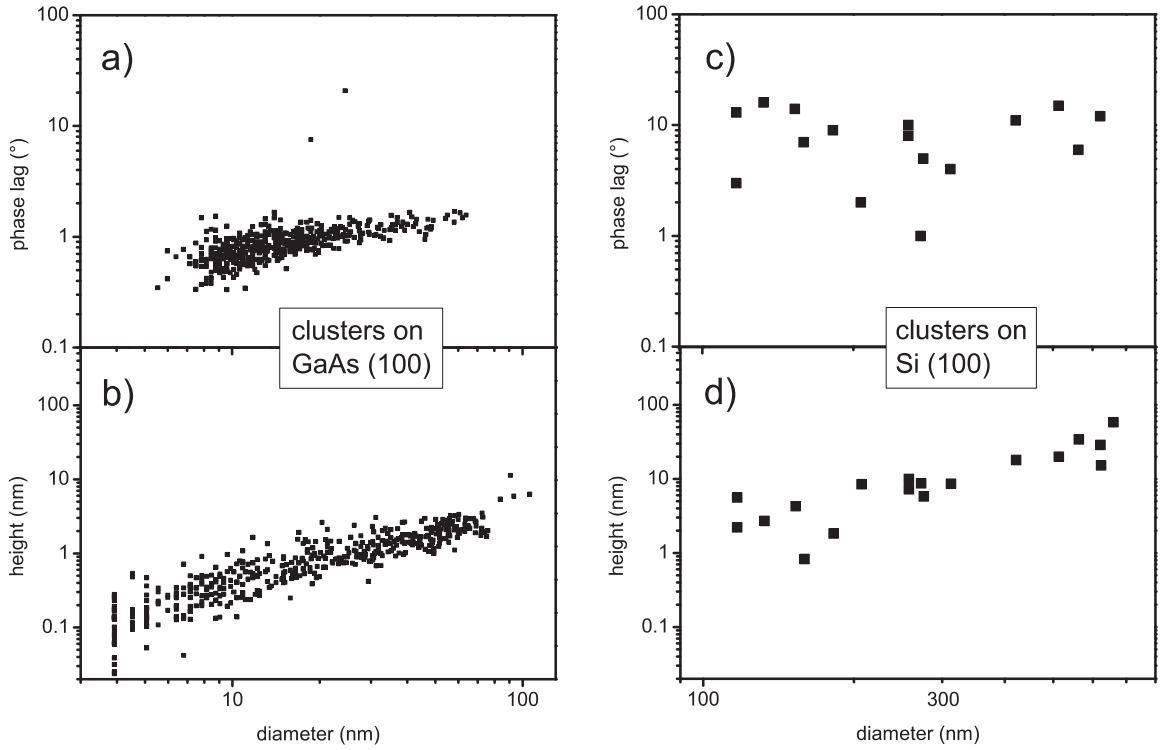

Figure 7.25: Two exemplary cluster ensembles of the peptide AQNPSDNNTHTH as measured by AFM on 1 μm^2 GaAs (100) (**a**,**c**) and (10 μm)^2 Si (100) (**b**,**d**). The phase lag of the clusters, which indicates the cluster softness, as a function of the respective cluster size is shown in (**a**,**c**) and the height–size dependence is portrayed in (**b**,**d**). There are 455 clusters on GaAs and $\sim$ 17 on Si.

softness issue shall now be discussed by comparing two exemplary cluster ensembles of the peptide AQNPSDNNTHTH on GaAs (100) and Si (100), respectively (Fig. 7.25). If Hooke's law is assumed to hold for the case of pressing the rather soft peptide cluster balls by the AFM tip on hard surfaces, one can assume the phase lag to be independent of the cluster size as long as the "spring constant" (i.e., the cluster softness) is size-independent and the cluster is not so flat that it can be completely compressed by the tip when even an additional force could not make a deeper impact. The validity of this model is considered in the following. The cluster height increases for both substrates roughly linearly with the cluster diameter (Figs. 7.25b,d), while for Si the phase lag of a cluster seems to be independent of its size (Fig. 7.25c). For GaAs, however, the picture is different (Fig. 7.25a): A strong phase-lag increase with size for small clusters weakens for bigger ones. We have empirically found this behaviour to be very typical for GaAs (the high-adhesion surface for this peptide) and its missing typical for low-adhesion surfaces of this peptide such as Si. Large clusters (diameter > 40 nm) may thus approximately be described by Hooke's law. Such weak or nonexistent size–phase lag dependencies within the same ensemble (Figs. 7.25a,c) allow for the conclusion that the much more pronounced adhesion dependence of the phase lag (look on the different total phase lags for clusters on GaAs and Si, respectively) is largely not due to an adhesion–cluster size dependency but due to the changing substrate-specific material density within the clusters.

[1] K. Goede, P. Busch, M.Grundmann: Nano Lett. **4**, 2115 (2004)
[2] K. Goede, M.Grundmann, A. Beck-Sickinger:submitted

7.24 Diode Non-Radiative Recombination Current

M. Grundmann

The non-radiative recombination current in pn-diodes is treated within Shockley-Read-Hall kinetics in the spirit of Sah, Noyce and Shockley [1]. Often simply a constant rate is integrated over the depletion layer. In [1] a linear electric field was assumed for the depletion layer. We use the actual local electric field E_{mr} at the maximum recombination rate. This way the involved integral can be solved analytically, and we obtain for the current ($\beta = e/kT$):

$$j_{\mathrm{nr}} = \frac{2\sigma v_{\mathrm{th}} N_{\mathrm{t}} n_{\mathrm{i}} kT}{E_{\mathrm{mr}}} \arctan\left[\left(\frac{\exp(\beta V/2)-1}{\exp(\beta V/2)+1}\right)^{1/2}\right]\left[\exp\left(\frac{eV}{kT}\right)-1\right]^{1/2} . \tag{7.2}$$

This formula for the non-radiative recombination current j_{nr} is very close (Fig. 7.26a) to the numerical solution [2]. The ideality factor is thus typically close to but smaller than 2 (Fig. 7.26).

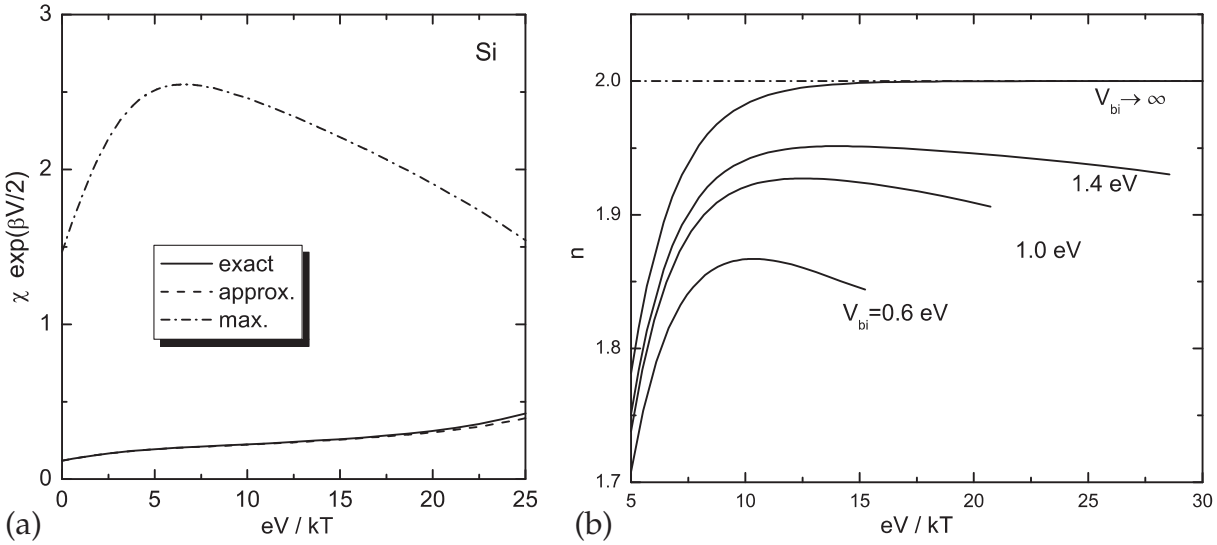

Figure 7.26: (**a**) Forward bias dependence of a quantity proportional to j_{nr}, multiplied by $\exp(\beta V/2)$ in order to extract the differences on a linear scale. *Solid line*: Exact numerical calculation, *dash-dotted line*: standard approximation with constant maximum rate, *dashed line*: this work (approximation with constant field). As material parameters we have used room temperature and $n_{\mathrm{i}} = 10^{10}\,\mathrm{cm}^{-3}$ (Si), $n_{\mathrm{n_0}} = 10^{18}\,\mathrm{cm}^{-3}$ and $p_{\mathrm{p_0}} = 10^{17}\,\mathrm{cm}^{-3}$. (**b**) Logarithmic slope of band-impurity recombination current in the forward bias regime for various values of the built-in voltage $V_{\mathrm{bi}} = 0.6$, 1.0, and 1.4 eV and in the limit $V_{\mathrm{bi}} \to \infty$.

[1] C.-T. Sah et al.: Proc. IRE **45**, 1228 (1957)
[2] M. Grundmann: Solid State Electron. **49**, 1446 (2005)

7.25 Metalorganic Vapor Phase Growth and Characterization of $B_xGa_{1-x}P$ and $B_xGa_{1-x-y}In_yP$ Epitaxial Layers

V. Gottschalch*, G. Leibiger†, J. Bauer*, H. Paetzelt*, G. Benndorf, G. Wagner‡, D. Hirsch§

*AK Halbleiterchemie, Institut für Anorganische Chemie, Universität Leipzig
†Freiberger Compound Materials GmbH, Freiberg
‡Institut für Mineralogie und Kristallographie, Universität Leipzig
§Leibniz-Institut für Oberflächenmodifizierung, Leipzig

Ternary $B_xGa_{1-x}P$- and related quaternary alloys are novel materials for light emitters or detectors in the visible spectral range.

We have studied the metalorganic vapor phase epitaxial growth of tensile strained $B_xGa_{1-x}P$-layers and highly compressively strained $B_xGa_{1-x-y}In_yP$ quantum wells deposited on (001)-GaP substrates. In this novel material systems layers with various mole fractions of boron in a range of 0 to 0.05 and mirrorlike surfaces could be deposited at growth temperatures T_g in the range of 500 to 780 ℃ (Fig. 7.27). The standard precursors trimethylgallium, trimethylindium, triethylboron and phosphine were used as source materials.

The mole fractions of boron were determined with high-resolution X-ray diffraction, transmission electron microscopy and secondary ion-mass spectroscopy. In particular, this measurements by (BGa)P/GaP superlattices have shown the excellent interface characteristic and that a boron carry-over is not important under these growth conditions (Fig. 7.28, 7.29). In addition, we have grown highly compressively strained

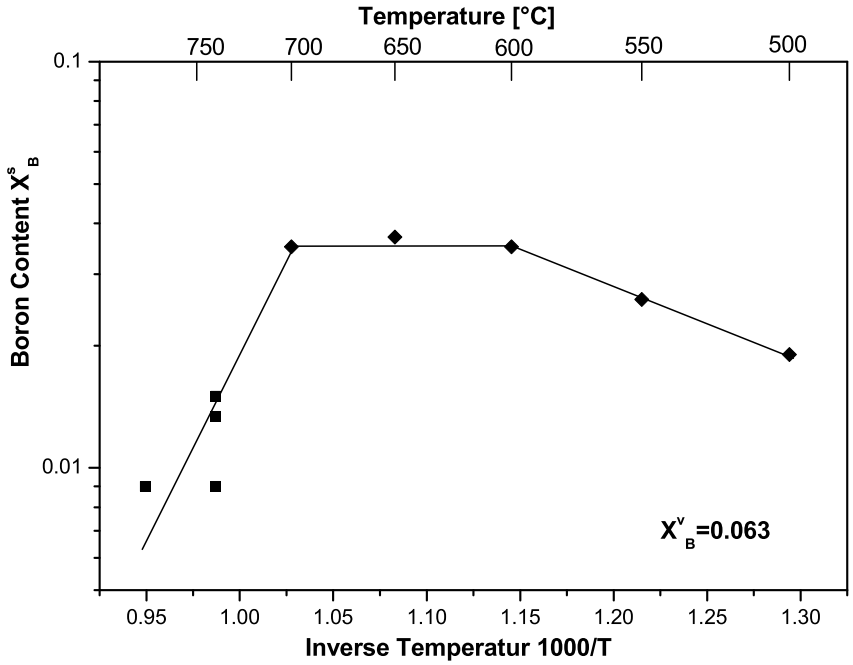

Figure 7.27: Temperature dependence of the boron incorporation (X^x_{boron} = 0.063).

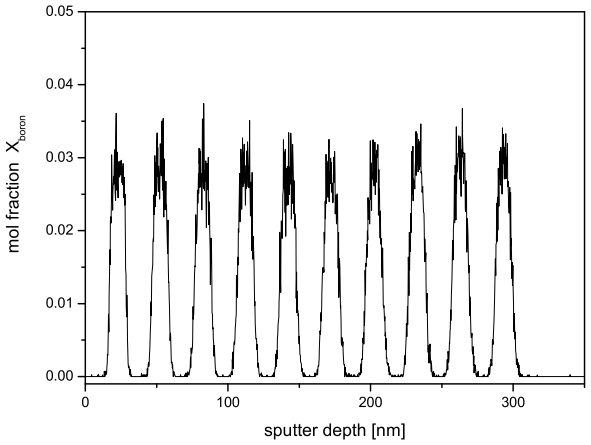

Figure 7.28: Secondary ion mass spectroscopy investigations of the B-incorporation in (BGa)P superlattice ($X^V_B = 0.063$).

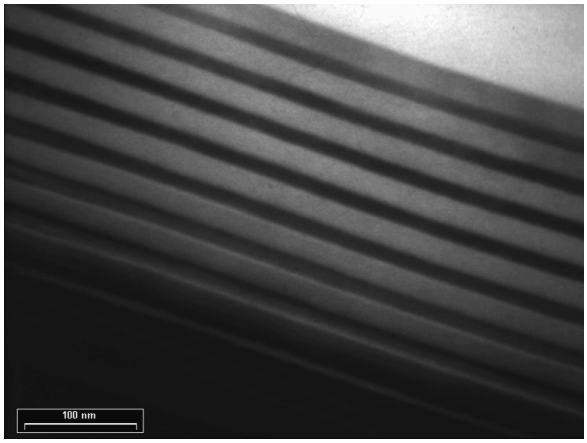

Figure 7.29: (BGa)P superlattice ($X^V_B = 0.063$) cross section TEM image.

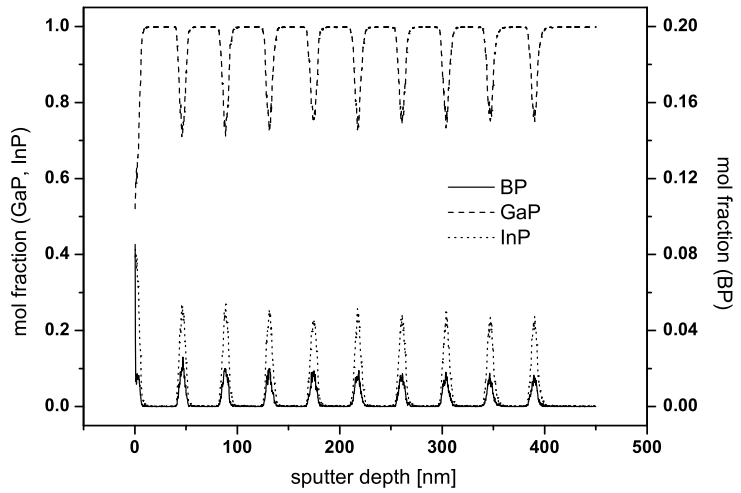

Figure 7.30: Secondary ion mass spectroscopy investigations of the B-incorporation in (BGaIn)P superlattice ($X^V_B = 0.048$).

$B_xGa_{1-x-y}In_yP$/GaP superlattices on (001)-oriented GaP substrates. SIMS and X-ray investigations of these structures (compared with the vapor dates) indicate a small interaction between the boron and the indium incorporation (Fig. 7.30).

Raman investigations at room temperature show BP-like optical phonons which develop from the localized vibration modes due to B_{Ga} isoelectronic substitution. The direct interband critical-point transitions E_0^{direct} and E_1 of $B_xGa_{1-x}P$-alloys were determined using spectroscopic ellipsometry. In addition to the SE-investigations we performed PL-measurements at $T = 2$ K. We assigned the dominant peaks to donator-acceptor-pair transitions. In contrast to the giant redshift of the GaN_yP_{1-y} band-gap energy with y the PL peak energy do not significantly shift with boron incorporation. The experimental observation can be explained as a result of bond ionicity, B−P bond is almost purely homopolar (Phillips/Van Vechten ionicity of a bond: $f_i = 0.006$), whereas the Ga-N bond has a large ionic contribution ($f_i = 0.5$).

7.26 MOVPE-Growth of GaN-Nanowires

V. Gottschalch*, G. Wagner†, J. Bauer*, H. Paetzelt*, M. Shirnow*, J. Lenzner, G. Benndorf

*AK Halbleiterchemie, Institut für Anorganische Chemie, Universität Leipzig
†Institut für Mineralogie und Kristallographie, Universität Leipzig

Because of its wide direct bandgap (E_g = 3.4 eV) GaN is an ideal candidate for many optoelectronic devices (LED´s, laser diodes, UV photodetectors etc). Nanoscale structures (nanowires) have great potential for realizing new optoelectronic devices.

We compare the growth of GaN layers and freestanding GaN wires using the two nitrogen precursors 1.1-dimethylhydrazine (DMHy/$(CH_3)_2N_2H_2$) and ammonia (NH_3).

The precursor combination DMHy/TMGa was used for the growth of GaN at low substrate temperature. We have studied the MOVPE GaN growth on GaAs $(111)_{As}$-, $(111)_{Ga}$- and (100)-substrates and the formation of wurtzite or the cubic GaN structure. The variation of the growth temperature in the range of 550 °C to 750 °C and partial pressure revealed a small range of "catalyst free" formation of wires (T_{growth} = 550 – 650 °C, V/III = 27) (Fig. 7.31). Between the substrate and the wires a complete intermediate GaN layer exists (thickness 30 – 50 nm). The cross-section TEM investigations show the transition from the wurtzite structure to the cubic GaN in growth direction.

TEM investigations of GaN wires show, that the core of the wire consists of cubic GaN and its shell is formed by GaN with wurtzite-type structure, stacking faults and twins. The CL spectra consist of one broad emission feature (Fig. 7.32). The peaks resulted from defects or surface states.

We fabricated GaN wires on (0001)-, $(10\bar{1}2)$-Al_2O_3 and (111)-Si surfaces using the precursors TEGa and NH_3. The carrier gas was N_2. We used Ni, Bi and Au as initiators for vapor-liquid-solid (VLS) wire growth. Fig. 7.33 shows a GaN nanowire grown on (111) Si-substrate at 950 °C and a V/III ratio of 180. A typical CL spectra of GaN wires with a low defect concentration is shown in Fig. 7.34. The Band-edge luminescence is dominate at structures with low defect densities.

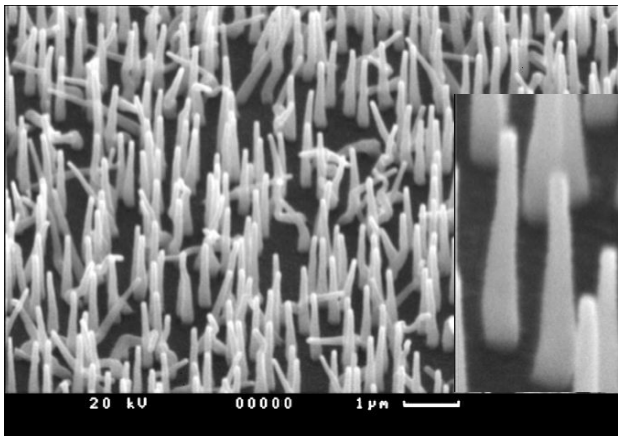

Figure 7.31: SEM images of the GaN wires (T_{growth} = 600 °C, V/III = 27).

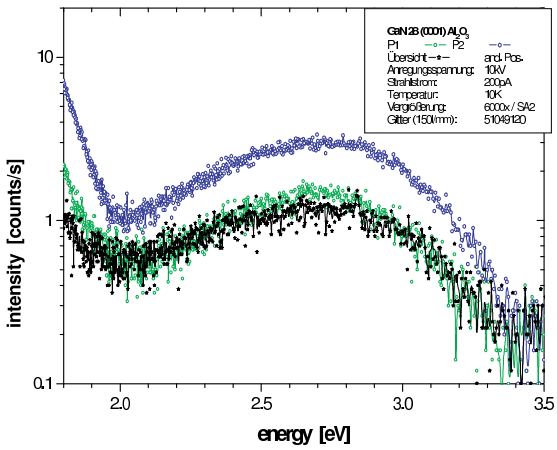

Figure 7.32: Cathodoluminescence (CL) spectra of GaN wires grown of (0001) Al_2O_3-substrates at 650 °C.

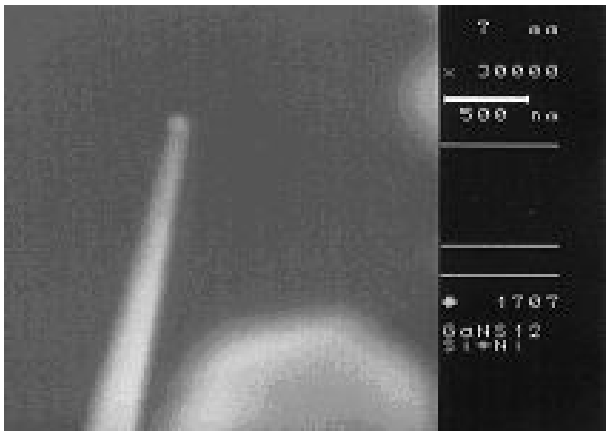

Figure 7.33: GaN nanowire grown on (111)-Si surface (Ni as initiator).

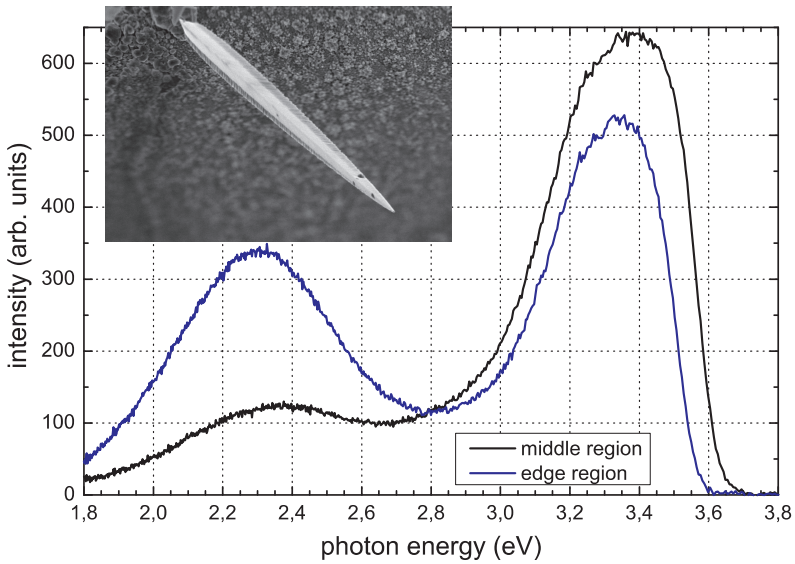

Figure 7.34: CL spectrum of GaN wires grown on (111)-Si substrates at 950 °C.

7.27 Structural Investigations of AIII-BV Nano- and Microtubes

H. Paetzelt*, V. Gottschalch*, J. Bauer*, H. Herrnberger*, G. Wagner†, J. Lenzner

*Institut für Anorganische Chemie, Universität Leipzig
†Institut für Mineralogie und Kristallographie, Universität Leipzig

The structural properties of nanotubes built from BGaAs/InGaAs bilayer-systems with an AlAs sacrificial layer on (001) oriented GaAs-substrate had been studied in detail [1] (Fig. 7.35). Cross-sectional transmission electron microscopy (TEM) images on the rolled structures showed, that the tubes-wall consist of alternating crystalline and non-crystalline layers with constant space. Investigations on the influence of a layer-thickness variation due to multiatomic steps on the structural properties of BGaAs/InGaAs-tubes grown on (110) oriented GaAs-substrate and on a new material-

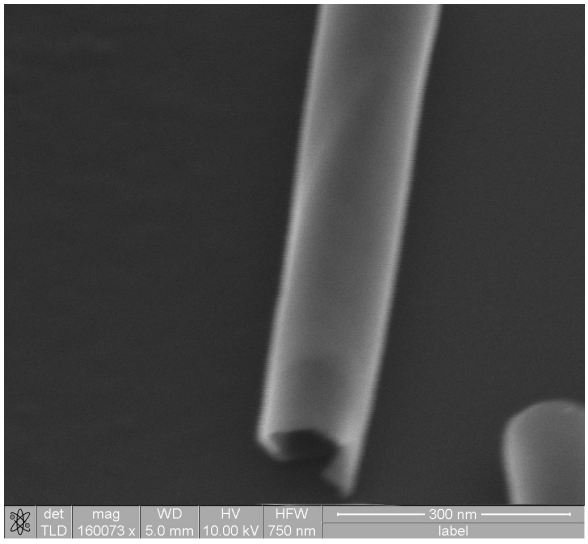

Figure 7.35: SEM image of a two-layer tube with a outer diameter of 146 nm. Layer-system: BGaAs 1.7 nm/ InGaAs 2.3 nm

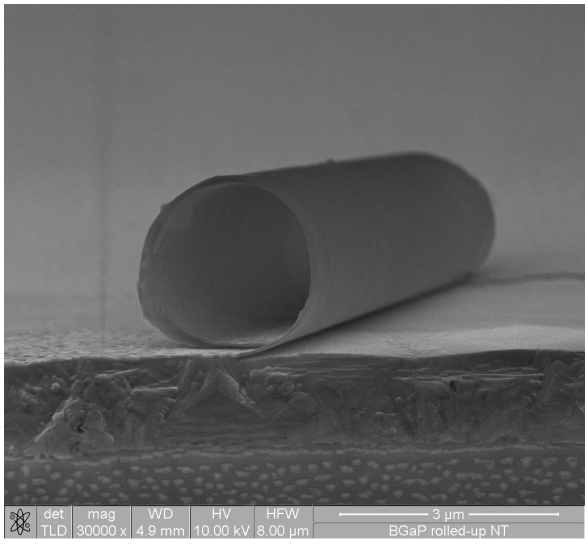

Figure 7.36: SEM image of a two-layer tube built from the layer-system BGaP/InGaP.

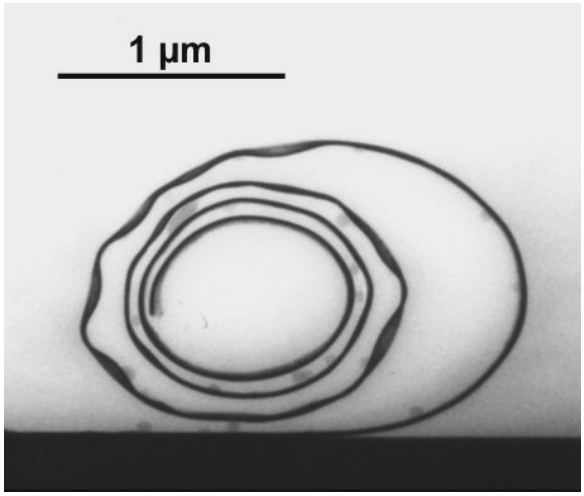

Figure 7.37: Cross-sectional TEM image of a two-layer tube built from the layer system BGaAs/InGaAs on (110)-oriented GaAs-substrate.

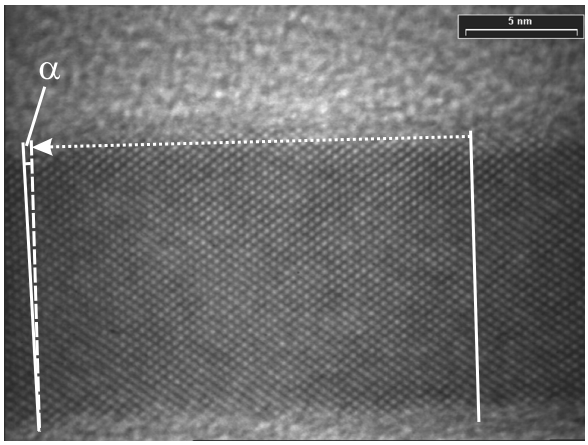

Figure 7.38: HRTEM image of a part of the two-layer tube shown in Fig. 7.37.

system for fabrication of rolled-up nanotubes (RUNTs): BGaP/InGaP with an AlGaP sacrificial layer on (110) oriented GaP-substrate (Fig. 7.36) were made.

All layers were grown using low-pressure (p_{tot} = 50 mbar) metal-organic vapor-phase epitaxy in an Aixtron AIX200 reactor at temperatures between 550 to 700 °C. Triethylboron, trimethylgallium and trimethylindium were used as group-III and arsine and phosphine as group-V sources. The layer-system BGaAs/InGaAs (bilayer thickness: 11 – 13 nm) was grown on an AlAs sacrificial layer (10 nm) on (110) oriented GaAs-substrate. The layer-system (4 nm) BGaP/(3 nm) InGaP with AlGaP sacrificial-layer (110 nm) was grown on (110) oriented GaP-substrate. With material selective etching of the sacrificial layer with solutions of HF:H_2O the layers rolled-up and formed tubes

powered by strain relaxation of the system. Figure Fig. 7.36 shows a scanning electron microscopy (SEM)-image of a RUNT rolled in $[\bar{1}10]$ direction with a diameter of around 2.5 μm built from the layer-system BGaP/InGaP. To study the influence of thickness variations in the nanotubes wall, BGaAs/InGaAs bilayer systems were grown on (110) oriented GaAs-substrates with multiatomic steps at the surface.

These steps cause a thickness variation in the tubes wall after releasing the layer system from the substrate and therefore there is a different effect on the strain relaxation in this section of the tube. The effect of thickness variations on the diameter can be calculated via continuum relaxation theory by define the strain-tensor components ϵ_{ij} after the release in the tube. Cross-sectional TEM-image of a BGaAs/InGaAs two-layer tube rolled in ⟨110⟩ direction (Fig. 7.37) showed a spirally rolled tube wall with different curvature along the tube layer in good agreement to the calculations. High-resolution TEM-images (Fig. 7.38) showed, that the formation of the tube is a result of minimization of the total strain energy of the layer system by strain relaxation due to bending of the lattice plane in the rolling direction.

[1] H. Paetzelt et al.: Phys. Stat. Sol. A **203**, 817 (2006)

7.28 Fabrication and Properties of (Al,Ga,In)As Nanowire Structures

J. Bauer [*], V. Gottschalch [*], H. Paetzelt [*], G. Wagner[†], B. Fuhrmann[‡], G. Benndorf

[*]Institut für Anorganische Chemie, Universität Leipzig
[†]Institut für Mineralogie und Kristallographie, Universität Leipzig
[‡]Interdisziplinäres Zentrum für Materialwissenschaften, Universität Halle

III-V one-dimensional, nanoscale single-crystals (nanowires - NWs) were grown using low-pressure metal-organic vapor phase epitaxy. Applying the vapor-liquid-solid growth mechanism with gold based alloy droplets GaAs, AlAs and InAs nanowires were fabricated on GaAs, Si and Ge substrates with different orientations. Figure 7.39 shows a GaAs-NW directed in the preferred $\langle\bar{1}\bar{1}\bar{1}\rangle_{As}$ growth direction. Our previous investigations concerning the effect of the growth parameters temperature, precursor partial pressures and growth time with respect to the NW diameter allow a reproducible NW growth with a defined geometry independent on the droplet size. The substrate preparation with gold dots patterns allows the fabrication ordered NW-arrays. We used nanosphere lithography to deposit nano-scale honeycomb-like gold patterns in micro-scale domains on GaAs-substrates. The gold dots were fixed by a *a*-SiO_x- or *a*-SiN_x-layer (plasma-enhanced chemical vapor deposition) to avoid moving of the gold droplets alloying with the substrate during temperature increases to the NW growth temperature. In Figure 7.40 arrays of ordered GaAs-NWs are shown.

To combine materials with different physical properties nanoheterostructures were investigated. NWs allow two forms of heterostructures: axial and lateral junctions. In Figure 7.41 a graded GaAs/AlAs-axial junctions is shown. The growth of $Al_xGa_{1-x}As$-alloy NWs until $x = 0.8$ was achieved (EDX-measurements in the inset of Fig. 7.41). At higher x-values oxidation in the TEM-preparation procedure occurs. We used

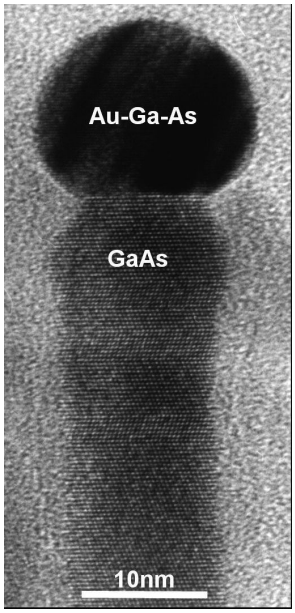

Figure 7.39: HRTEM image of a GaAs-NW grown on GaAs$\left(\bar{1}\bar{1}\bar{1}\right)_{\mathrm{As}}$-substrate.

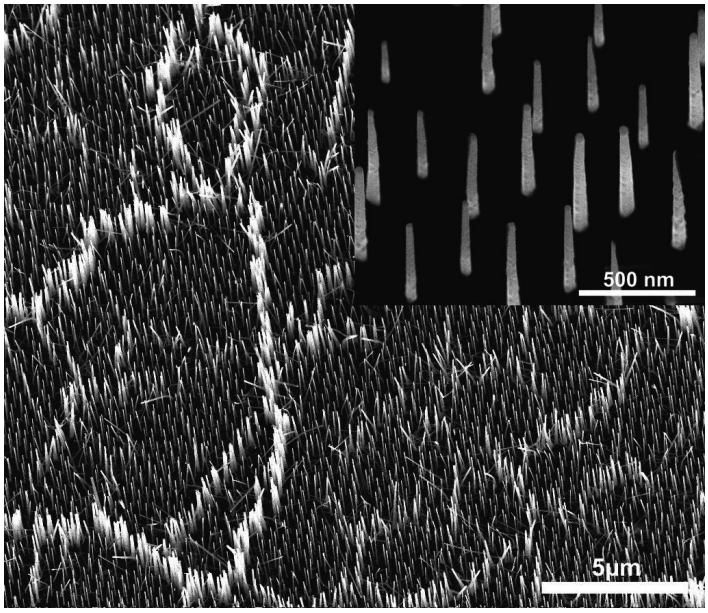

Figure 7.40: GaAs-NW arrays fabricated with honeycomb-like gold dot patterns produced by nanosphere lithography.

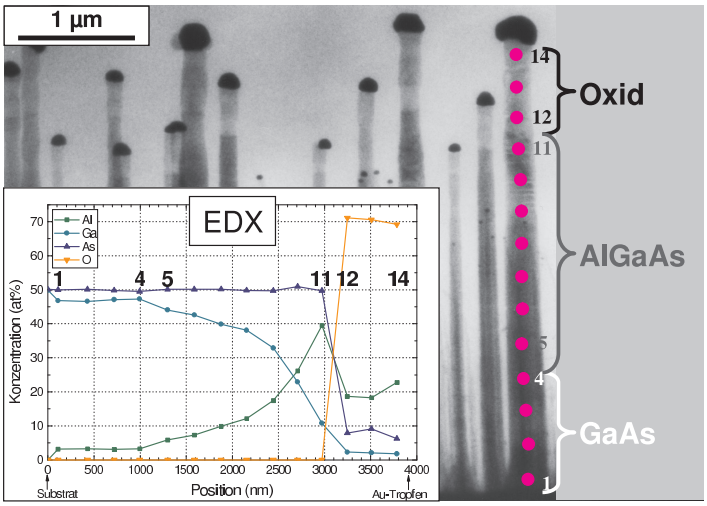

Figure 7.41: Bright field TEM-image of a graded axial GaAs/AlAs-nanoheterojunction. *Inset*: EDX-investigation of the material composition along the NW.

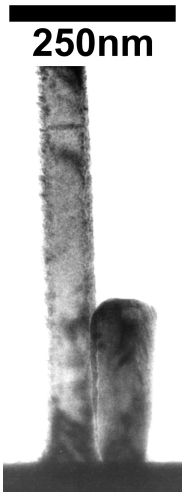

Figure 7.42: Bright field TEM-image of a lateral GaAs/GaN-nanoheterojunction.

GaAs/(AlGa)As- and GaAs/GaN-lateral junctions ("core-shell"-structures) for passivation and carrier confinement in the NW (Fig. 7.42). Thus, in columnar shaped GaAs-NWs the photoluminescence yield could be significantly increased. Furthermore, because of the lattice misfit between NW and the cover material, the NW is strained. (AlGa)As causes a tensile and GaN a compressive strain of the GaAs-NWs (Fig. 7.43 and 7.44). Using k×p-pertubation theory the effect of strain on the electronic structure of the NW (in bulk material approximation) reflects the measured PL band shifts well.

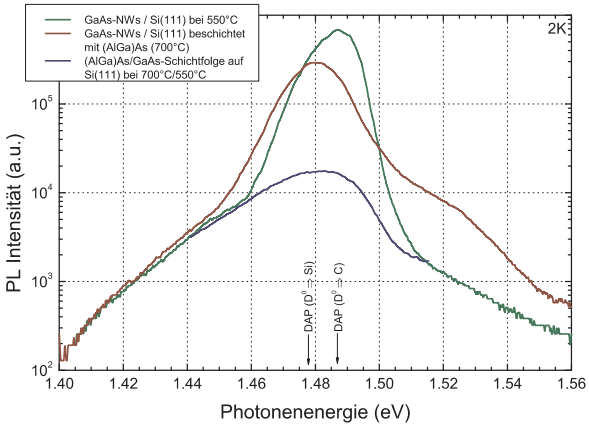

Figure 7.43: Low-temperature photoluminescence spectrum of GaAs/(AlGa)As-"core-shell"-NWs. The (AlGa)As-cover layer causes a tensile strain in the GaAs-NW leading to a red-shift of the luminescence band.

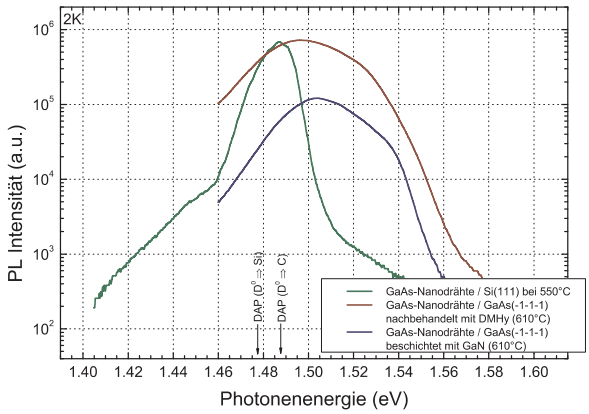

Figure 7.44: Low-temperature photoluminescence spectrum of GaAs/GaN-"core-shell"-NWs. The GaN-cover layer causes a compressive strain in the GaAs-NW leading to a blue-shift of the luminescence band.

7.29 Anisotropy of the Γ-Point Effective Mass and Mobility in Hexagonal InN

T. Hofmann*, T. Chavdarov, V. Darakchieva†, H. Lu‡, W.J. Schaff‡, M. Schubert*

*present address: Department of Electrical Engineering, University of Nebraska-Lincoln, Lincoln, USA

†Department of Physics and Measurement Technology, Linköping University, Sweden

‡Department of Electrical and Computer Engineering, Cornell University, USA

We study the Γ-point electron effective mass and mobility parameters including anisotropy in wurtzite InN by infrared magnetooptic generalized ellipsometry (IRMOGE),

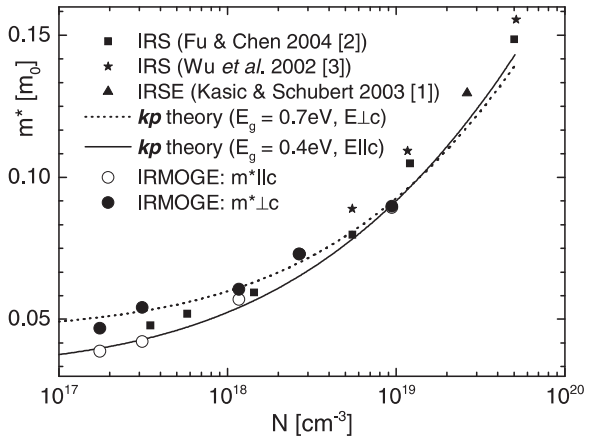

Figure 7.45: Wurtzite InN effective mass parameters obtained in this work (IRMOGE), in comparison with previous reports from combined infrared spectroscopy and Hall-effect measurements and **kp** calculations.

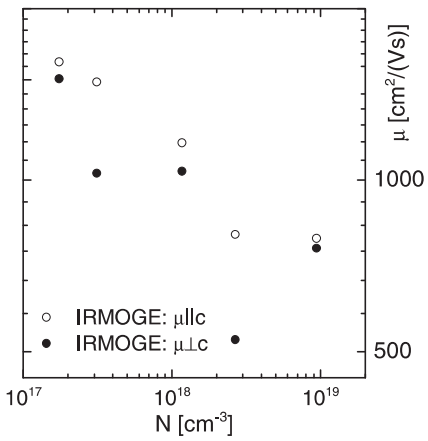

Figure 7.46: Anisotropic optical electron mobility parameters obtained in this work.

extending previous work where we used a combined infrared spectroscopic ellipsometry (IRSE) and electrical Hall effect measurement approach for the InN effective mass determination [1]. Specifically, we apply IRMOGE for the first time to a situation, where both mobility and effective mass parameters differ for polarizations parallel or perpendicular to a certain direction, here the InN lattice *c*-axis. The anisotropic electron effective mass and mobility parameters in wurtzite InN thin films with free electron concentration N from $1.8\times10^{17}\,\mathrm{cm}^{-3}$ to $9.5\times10^{18}\,\mathrm{cm}^{-3}$ were determined at room temperature (Figs. 7.45, 7.46). For the Γ-point we obtain $m^\star_\perp = 0.047m_0$ and $m^\star_\parallel = 0.039m_0$ for polarization perpendicular and parallel to the *c*-axis, respectively. We observe a decrease of mobility for polarization parallel to the *c*-axis from $1600\,\mathrm{cm}^2/(\mathrm{Vs})$ to $800\,\mathrm{cm}^2/(\mathrm{Vs})$ with increase in N, which we tentatively assign to scattering by impurities or ionized donors. The perpendicular mobility is further decreased, likely caused by additional grain boundary scattering [2].

[1] A. Kasic et al.: Phys. Stat. Sol. (C) **0**, 1750 (2003)
[2] T. Hofmann et al.: Phys. Stat. Sol. (C) (2006), in press

7.30 Chirality in Sculptured Nanostructure Thin Films

M. Schubert*, E. Schubert†

*present address: Department of Electrical Engineering, University of Nebraska-Lincoln, Lincoln, USA

†Leibniz-Institut für Oberflächenmodifizierung, Leipzig

Sculptured thin films (STF) with complex chiral or non-chiral geometries are promising candidates for a large variety of applications in the field of photonics, optics, sensors, and engineering mechanics, for example. Thermal expansion, mechanical, electronic, and optical properties may vary at great length from their bulk crystal analogues due to the highly-rotational convoluted lattice planes of structures with nanodimensions. STF samples from silicon with different structures are deposited by ion beam assisted deposition under conditions with very oblique particle flux angle of incidence. Generalized ellipsometry Mueller matrix measurements reveal an intriguing fingerprint of STF samples, and suggest immediate chirality assessment [1, 2, 3].

Figs. 7.47a–k, and 7.48a–k present gray-scale plots of Mueller matrix elements M_{ij}, normalized to the element M_{11}, versus sample rotation and angle of incidence for a STF with *chevron* structure, and a left-handed 3-fold *tire-bouchon* structure, respectively. The elements M_{ij} reflect the highly optically anisotropic behavior of the STF samples, and serve as fingerprints to reveal the intrinsic birefringence of the inclined columns through elaborate model calculations [4]. The plots of elements M_{12} and M_{21} can be transformed into each other by a mirror reflection at the line where $\Phi_a \approx 135^\circ$, equivalent with the plane of inclination in the chevron structure STF sample! The same holds for elements M_{13} and M_{31}, and M_{32} and M_{23}, which is intrinsic to arbitrary non-chiral anisotropic mediums. No such mirror transformation exists in the case of the left-handed structure (Fig. 7.48), due to the handedness now being added to this sample. Note that the individual building blocks, i.e., the inclined columns, are primarily similar to the ones used for the chevron structure, and possess similar intrinsic birefringence.

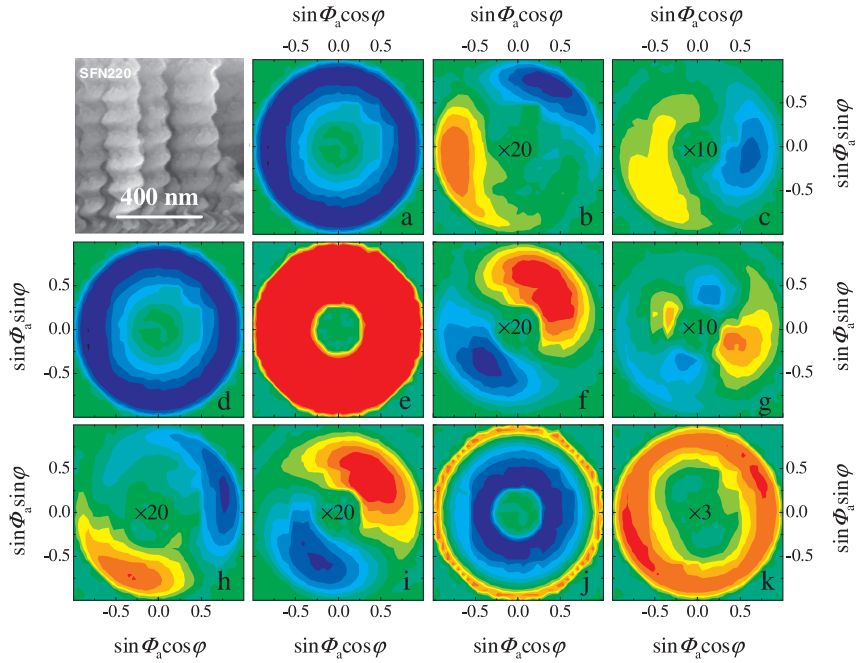

Figure 7.47: Three-dimensional (x, y, z) gray-scale plots at $\lambda = 1550$ nm of Mueller matrix elements ($z - axis$) M_{12} (**a**), M_{13} (**b**), M_{14} (**c**), M_{21} (**d**), M_{22} (**e**), M_{23} (**f**), M_{24} (**g**), M_{31} (**h**), M_{22} (**i**), M_{33} (**j**), and M_{34} (**k**) from a STF sample with *chevron* structure shown in the upper left panel (SEM image). Data are shown versus in-plane azimuth angle φ and angle of incidence Φ_a in polar coordinates ($-1 \leq x = sin\Phi_a cos\varphi \leq 1$, $-1 \leq y = sin\Phi_a sin\varphi \leq 1$). The z-coordinates of the measured data points are plotted from the upper (lower) hemisphere at their respective positions x, y according to Φ_a, φ in *red* = 1 to *yellow* = 0.5 to *green* = 0 (*blue* = −1 to *light blue* = −0.5 to *green* = 0) scale. Intensities in plots (**b**), (**f**), (**g**), (**h**), (**j**) and (**k**) are multiplied as indicated.

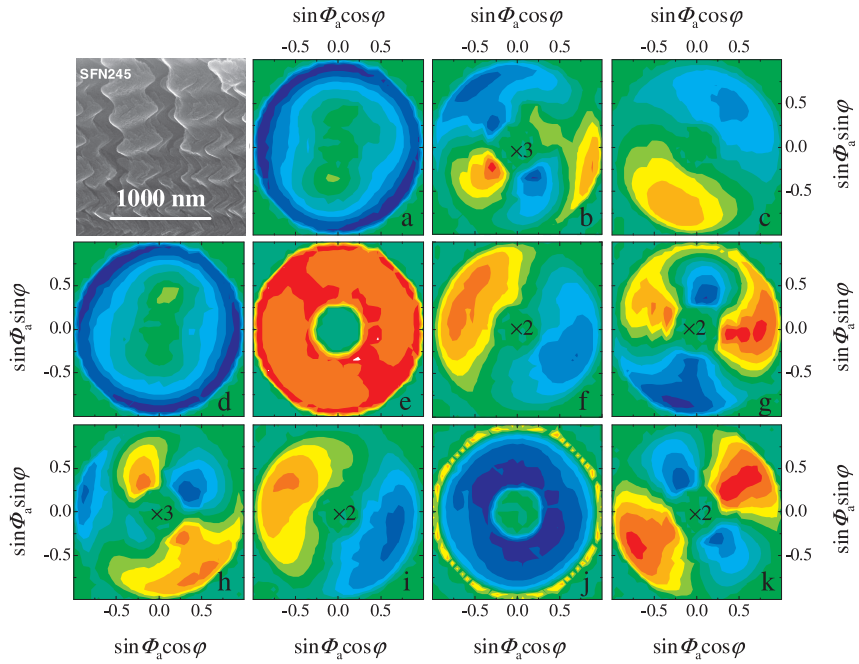

Figure 7.48: Same as Fig. 7.47 for a STF sample with left-handed 3-fold *tire-bouchon* structure.

For the chiral structures investigated by us so far we observe this following symmetry property: The pair M_{12} - M_{21} requires rotation around the z-axis by π, whereas the pairs $M_{13} - M_{31}$, and $M_{23} - M_{32}$ are congruent only after rotation around the z-axis by π and subsequent inversion at the $x-y$-plane.

[1] E. Schubert et al.: Nucl. Instr. Meth. B **244**, 40 (2006)
[2] E. Schubert et al.: J. Appl. Phys. (2006), in press
[3] E. Schubert et al.: Adv. Phys. (2006), in press
[4] M. Schubert: Ann. Phys. (2006), in press

7.31 The Optical Hall Effect in Quantum Regimes: Landau Level Transitions

M. Schubert*, T. Hofmann*, P. Esquinazi†, U. Schade‡

*present address: Department of Electrical Engineering, University of Nebraska-Lincoln, Lincoln, USA
†Superconductivity and Magnetism group
‡BESSY, Berlin

The electronic states of two-dimensionally confined charge carrier systems split into Landau levels if subjected to external magnetic fields with direction parallel to the confinement direction. Provided the temperature of the free-charge-carrier system is smaller than the equivalent of their cyclotron resonance energy $\hbar\omega_c$, transitions between individual Landau levels can be revealed optically by ellipsometry measurements at low temperatures and very long wavelengths. This is shown here – exemplarily as well as for the first time – for an often investigated two-dimensional charge system: Highly oriented pyrolytic graphite (HOPG) [1]. Specifically, a synchrotron source with high-brilliant terahertz radiation was used as the light source in addition to a thermal radiation source for this generalized ellipsometry experiment [2, 3]. Graphite remains a challenging material with many physical properties to be explored and explained. Yet as one of the best studied materials concerning its electronic and optical properties, many questions remain open for this semimetal or semiconductor with zero band gap, which is thought to be endowed with unique massless linear dispersion relation for the conduction band [4]. Recently, observation of plateaus in Hall resistance data for a HOPG sample in the quasi-quantum limit suggested Quantum-Hall effect characteristics of the two-dimensional electron system [5], which forms with high electron mobility at low temperatures. Ferromagnetism-like signals and defect-related magnetism in graphite was recently reported [6]. Reentrant magnetic-field driven metal-insulator transitions were also reported [7]. Landau transitions occur for circular polarizations and propagation directions parallel $\vec{c}$, and only in presence of $\vec{H}_{\mathrm{slow}} \| \vec{c}$. Fig. 7.49a presents generalized ellipsometry spectra taken from a natural cleavage of a HOPG sample under 45° angle of incidence and various external magnetic field strengths. The Muller matrix element M_{23} evolves with the magnetic field due to the induced anisotropy. The broad resonance near $\omega \approx 150\,\mathrm{cm}^{-1}$, which evolves with increasing field, can be

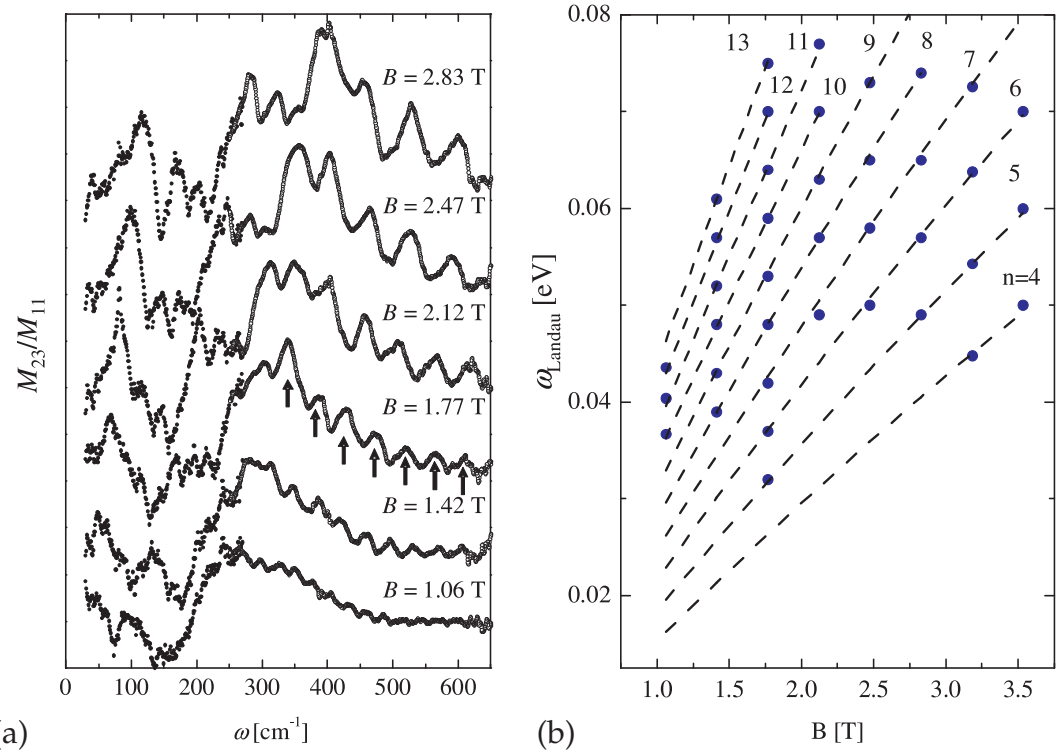

Figure 7.49: (**a**) Terahertz (*black symbols*) and far-infrared range (*gray symbols*) magnetic-field induced non-reciprocal anisotropy in HOPG rendered by the Muller matrix element M_{23} normalized to M_{11}. The component of the magnetic field B vertical to the graphite c axis is indicated. Landau quantization of the two-dimensional electron density within the graphene layers at 4.5 K causes intraband transitions between Landau electron levels (*vertical arrows*), separated by multiple amounts of the cyclotron frequency ω_c. (**b**) A fan of transition energies between individual Landau levels versus applied magnetic field.

explained by coupling of the Landau level transitions with an isotropic electronic interband transition. The fine-structure oscillations, which are superimposed onto all spectra, increase in amplitude and period with increasing field, and correspond to the circularly polarized Landau Level transitions with almost perfectly equal polarizabilities for both field orientations, as will be discussed elsewhere in more detail. The periods within the far-infrared region follow

$$\hbar\omega_{\mathrm{Landau},\nu} = \hbar\omega_c(\nu + \nu_0),\ \omega_c \approx \frac{e\mu_0 H}{m(1+\beta\mu_0 H)}, \qquad \nu = 1, 2, \ldots\ , \tag{7.3}$$

where $\omega_c = (3.27 \pm 0.02)$ meV at $\mu_0 H = 1$ T, $\nu_0 = 0.849 \pm 0.006$. The effective mass parameter is field dependent $m = m_{H=0}(1 + \beta\mu_0 H)$, with $m_{H=0} = 0.0354 \pm 0.0002$ and $\beta = (0.034 \pm 0.002)\,\mathrm{T}^{-1}$. H is the component of $\vec{H}_{\mathrm{slow}}$ along the $\vec{c}$ axis in this experiment. While both ν_0 and β are indicative for coupling between intra- and interband transitions, the band dispersion at zero field appears parabolic, with linearly increasing m by ≈ 10 % for fields up to 3 T, and no indication seems to exist for massless carrier dispersion in graphite in the quantum regime.

[1] M.S. Dresselhaus, G. Dresselhaus: Adv. Phys. **51**, 1 (2002)
[2] T. Hofmann et al.: Rev. Sci. Instr. (2006), in press

[3] M. Schubert: Ann. Phys. (2006), in press
[4] T. Matsui et al.: Phys. Rev. Lett. **94**, 226 403 (2005)
[5] Y. Kopelevich et al.: Phys. Rev. Lett. **90**, 156 402 (2003)
[6] P. Esquinazi et al.: Phys. Rev. B **66**, 024 429 (2002)
[7] H. Kempa et al.: Phys. Rev. B **65**, 241 101(R) (2002)

7.32 Funding

One-dimensional heterostructures and nanowire arrays
Prof. Dr. M. Grundmann, Dr. M. Lorenz
DFG Gr 1011/11-1 within DFG Forschergruppe FOR 522 *Architecture of nano- and microdimensional building blocks*

Lateral optical confinement of microresonators
Prof. Dr. B. Rheinländer, Dr. V. Gottschalch
DFG Rh 28/4-1 within DFG Forschergruppe FOR 522 *Architecture of nano- and microdimensional building blocks*

Transferability of the codoping concept to ternary ZnO:(Cd,Mg)
Prof. Dr. M. Grundmann, Dr. H. Schmidt
DFG Gr 1011/10-2 im DFG-Schwerpunktprogramm 1136 *Substitutionseffekte in ionischen Festkörpern*

Self-assembled Semiconductor Nanostructures for New Devices in Photonics and Electronics (SANDiE)
Coordinator: Universität Leipzig, Prof. Dr. M. Grundmann
Sixth Framework Programme, European Network of Excellence, Contract NMP4-CT-2004-500101

III-V-Semiconductor Nano-Heterostructures for Advanced Opto-Electronic Devices
Prof. Dr. B. Rheinländer
BMBF: Bilaterale Zusammenarbeit BRD-Slowakei: SVK 01/001

New gallium phosphide grown by vertical gradient freeze method for light emitting diodes
Prof. Dr. B. Rheinländer
(VGF GaP - LED's) No. IST - 2001-32793, EU-FP5-Projekt und BMBF: Bilaterale Zusammenarbeit BRD-Slowakei: SVK 01/001

Intraband and interband carrier transitions in type I and type II nanostructures with quantum dots, quantum dot molecules and impurities
Prof. Dr. Marius Grundmann
INTAS 01-0615

Interface-related properties of oxide quantum wells
Prof. Dr. M. Grundmann, Dr. V. Gottschalch
DFG Gr 1011/14-1 within DFG Forschergruppe FOR 404 *Oxidic interfaces*

Interface-induced electro-optical properties of oxide semiconductor-ferroelectric thin film heterostructures
Dr. M. Schubert, Dr. M. Lorenz
DFG Schu 1338/4-1 within DFG Forschergruppe FOR 404 *Oxidic interfaces*

Semiconductor oxides for UV optoelectronics, surface acoustics and spintronics
Prof. Dr. M. Grundmann, Dr. M. Lorenz
SOXESS European Network on ZnO (Thematic Network), Fifth Framework Programme, Competitive and sustainable growth, Contract G5RT-CT-2002-05075

Nanophotonic and nanoelectronic Devices fom Oxide Semiconductors (NANDOS)
Prof. Dr. M. Grundmann
EU STReP Contract No. 016424

BMBF-Nachwuchsgruppe "Nano-Spinelektronik"
Dr. H. Schmidt
BMBF FKZ 03N8708

Deutsch-Chinesische Kooperation zur Entwicklung von transparenten und halbleitenden GMR und TMR Prototyp-Bauelementen
Dr. H. Schmidt
BMBF CH05/010

7.33 Organizational Duties

Marius Grundmann

- Vertrauensdozent der Studienstiftung des deutschen Volkes
- Direktor des Institut für Experimentelle Physik II
- Coordinator of the European Network of Excellence on 'Self-Assembled semiconductor Nanostructures for new Devices in photonics and Electronics' (SANDiE, www.sandie.org)
- Sprecher der DFG Forschergruppe 'Architektur von nano- und mikrodimensionalen Strukturelementen' (FOR 522, http://www.uni-leipzig.de/~for522)
- Sprecher der Fächerübergreifenden Arbeitsgemeinschaft Halbleiterforschung Leipzig (FAHL, http://www.uni-leipzig.de/~fahl)
- Mitglied des Beirat Ionenstrahlzentrum, FZR, Rossendorf
- Berufungskommission: Nachfolge Michel, Vorsitzender; Nachfolge Lösche, Vorsitzender
- Project Reviewer: Deutsche Forschungsgemeinschaft (DFG), Alexander-von-Humboldt Stiftung (AvH), Schweizerischer Nationalfonds zur Förderung der wissenschaftlichen Forschung (FNSNF), Fonds zur Förderung der Wissenschaften (FWF)
- Referee: Appl. Phys. Lett., Phys. Rev. B., Phys. Rev. Lett., Nature, Electr. Lett., Physica E, Phys. Stat. Sol., J. Appl. Phys.

M. Lorenz

- Project Reviewer: United States - Israel Binational Science Foundation (BSF)

- Referee: Appl. Phys. Lett., IEEE Transact. Appl. Supercond., J. Am. Chem. Soc., J. Phys. D Appl. Phys., Thin Solid Films, J. Cryst. Growth, Mater. Lett., Appl. Surf. Sci., Appl. Phys. A, J. Phys. Chem., Mat. Sci. Eng. B, Semicond. Sci. Technol.

H. Schmidt
- Referee: J. Appl. Phys., J. Magn. Magn. Mat., Solid State Comm., J. Phys. Cond. Matter

7.34 External Cooperations

Academic

- Leibniz-Institut für Oberflächenmodifizierung e.V., Leipzig
  Prof. Dr. B. Rauschenbach, Dr. E. Schubert
- Universität Leipzig, Fakultät für Biowissenschaften, Pharmazie und Psychologie
  Prof. Dr. A. Beck-Sickinger
- Universität Leipzig, Fakultät für Chemie und Mineralogie
  Dr. V. Gottschalch, Prof. Dr. K. Bente
- Universität Halle-Wittenberg
  Prof. Dr. I. Mertig
- Max-Planck-Institut für Mikrostrukturphysik, Halle/Saale
  Dr. O. Breitenstein, Dr. A. Ernst, Dr. P. Werner
- Oak Ridge National Laboratory, Condensed Matter Science Division, TN, USA
  Dr. H.M. Christen
- Technische Universität Berlin
  Prof. Dr. D. Bimberg, Dr. A. Hoffmann
- Universidade de Aveiro, Portugal
  Prof. Dr. N. Sobolev
- Kinki University, Dept. of Electronics Systems and Information Engeneering, Japan
  Dr. M. Kusunoki
- Paul Scherer Institut, Villingen
  Prof. Dr. H. Sigg
- Université Paris-Sud, France
  Prof. Dr. F. Julien
- Chinese Academy of Sciences, Institute of Physics, Beijing, P.R. China
  Prof. Dr. Yusheng He
- Universität Gießen
  Prof. Dr. B. Meyer, Dr. D. Hofmann, Prof. Dr. J. Janek
- Universität Magdeburg
  Prof. Dr. A. Krost, Dr. A. Dadgar, Prof. Dr. J. Christen
- Universität Bonn
  Prof. Dr. W. Mader

- Universität Hannover
  Prof. Dr. M. Binnewies
- Göteborg University, Sweden
  Prof. Dr. M. Willander
- NCSR "Demokritos", Institute of Materials Science, Greece
  Prof. Dr. A. Travlos
- Univerité Joseph Fourier - Grenoble, France
  Prof. Dr. L.S. Dang

Industry

- Solarion GmbH, Leipzig
  Dr. Alexander Braun
- El-Mul Technologies, Yavne, Israel
  Dr. Armin Schön
- PhysTech GmbH, Moosburg, Germany
  Dr. L. Cohausz
- OSRAM Opto-Semiconductors GmbH, Regensburg, Germany
  Dr. V. Härle

7.35 Publications

Journals

N. Ashkenov, M. Schubert, E. Twerdowski, B.N. Mbenkum, H. Hochmut, M. Lorenz, H. von Wenckstern, W. Grill, M. Grundmann: *Asymmetric ferroelectric polarization loops and offsets in Pt-$BaTiO_3$-ZnO-Pt thin film capacitor structures*, Thin Solid Films **486**, 153 (2005)

C. Bundesmann, M. Schubert, N. Ashkenov, M. Grundmann, G. Lippold, J. Piltz: *Combined Raman scattering, X-ray fluorescence and ellipsometry in-situ growth monitoring of $CuInSe_2$-based photoabsorber layers on polyimide substrates*, Proc. Int. Conf. Phys. Semicond. (ICPS-27), Flagstaff 2004, AIP Conf. Proc. **772**, 165 (2005)

M. Diaconu, H. Schmidt, A. Pöppl, R. Böttcher, J. Hoentsch, A. Klunker, D. Spemann, H. Hochmuth, M. Lorenz, M. Grundmann: *Electron paramagnetic resonance of $Zn_{1-x}Mn_xO$ thin films and single crystals*, Phys. Rev. B **72**, 085 214 (2005)

M. Diaconu, H. Schmidt, A. Pöppl, R. Böttcher, J. Hoentsch, A. Rahm, H. Hochmuth, M. Lorenz, M. Grundmann: *EPR study on magnetic $Zn_{1-x}Mn_xO$*, Superlatt. Microstruct. **38**, 413 (2005)

M. Diaconu, H. Schmidt, H. Hochmuth, M. Lorenz, G. Benndorf, J. Lenzner, D. Spemann, A. Setzer, K.-W. Nielsen, P. Esquinazi, M. Grundmann: *UV optical properties of ferromagnetic Mn-doped ZnO thin films grown by PLD*, Thin Solid Films **486**, 117 (2005)

D. Fritsch, R. Schmidt-Grund, H. Schmidt, C.M. Herzinger, M. Grundmann: *Polarization-dependent optical transitions at the fundamental band gap and higher critical points of wurtzite ZnO*, IEEE Proc. 5th Int. Conf. Num. Simul. Optoelectron. Dev., 69 (2005)

D. Fritsch, H. Schmidt, M. Grundmann: *Pseudopotential band structures of rocksalt Mg, Zno and $Mg_{1-x}Zn_xO$*, Appl. Phys. Lett. **88**, 134 104 (2006)

K. Goede, M. Grundmann, K. Holland-Nell, A. Beck-Sickinger, M. Bachmann, W. Janke: *Peptide auf neuen Wegen*, Bioforum **10**, 53 (2005)

M. Grundmann: *The bias dependence of the non-radiative recombination current in p-n diodes*, Solid-State Electron. **49**, 1446 (2005)

M. Grundmann, H. von Wenckstern, R. Pickenhain, T. Nobis, A. Rahm, M. Lorenz: *Electrical Properties of ZnO Thin Films and Optical Properties of ZnO-based Nanostructures*, Superlatt. Microstruct. **38**, 317 (2005)

M. Grundmann, H. von Wenckstern: *Electrical Properties of ZnO Thin Films*, Proc. FVS-Workshop "TCOs für Dünnschichtsolarzellen und andere Anwendungen" Freyburg 2005, p 86

S. Heitsch, C. Bundesmann, G. Wagner, G. Zimmermann, A. Rahm, H. Hochmuth, G. Benndorf, H. Schmidt, M. Schubert, M. Lorenz, M. Grundmann: *Low-Temperature Photoluminescence and infrared dielectric functions of pulsed laser deposited ZnO thin films on silicon*, Thin Solid Films **496**, 234 (2006)

T. Hofmann, M. Schubert, C. von Middendorff, G. Leibiger, V. Gottschalch, C.M. Herzinger, A. Lindsay, E. O'Reilly: *The inertial-mass scale for free-charge-carriers in semiconductor heterostructures*, Proc. Int. Conf. Phys. Semicond. (ICPS-27), Flagstaff 2004, AIP Conf. Proc. **772**, 455 (2005)

A. Jenichen, C. Engler, G. Leibiger, V. Gottschalch: *Growth and annealing of GaInAsN: density-functional calculations on the reactions of surface and bulk structures*, Surf. Sci. **574**, 144 (2005)

A. Jenichen, C. Engler, G. Leibiger, V. Gottschalch: *Nitrogen substitutions in GaAs(001) surfaces: Density-functional supercell calculations of the surface stability*, Phys. Stat. Sol. (B) **242**, 2820 (2005)

M. Lorenz, H. Hochmuth, J. Lenzner, M. Brandt, H. von Wenckstern, G. Benndorf, M. Grundmann: *ZnO thin films grown by pulsed laser deposition on 6H-SiC single crystals*, Wiss.-Techn. Berichte FZ Rossendorf **433**, 57 (August 2005)

M. Lorenz, H. Hochmuth, A. Jammoul, G. Ferro, C. Förster, J. Pezoldt, J. Zúñiga Pérez, G. Benndorf, J. Lenzner, R. Schmidt-Grund, M. Grundmann: *Luminescence of ZnO thin films grown by pulsed laser deposition on 3C-SiC buffered Si*, Wiss.-Techn. Berichte FZ Rossendorf **433**, 74 (August 2005)

M. Lorenz, E.M. Kaidashev, A. Rahm, T. Nobis, J. Lenzner, G. Wagner, D. Spemann, H. Hochmuth, M. Grundmann: *$Mg_xZn_{1-x}O$ ($0 \le x < 0.2$) nanowire arrays on sapphire grown by high-pressure pulsed-laser deposition*, Appl. Phys. Lett. **86**, 143 113 (2005)

M. Lorenz, H. Hochmuth, J. Lenzner, T. Nobis, G. Zimmermann, M. Diaconu, H. Schmidt, H. von Wenckstern, M. Grundmann: *Room-temperature cathodoluminescence of n-type ZnO thin films grown by pulsed laser deposition in N_2, N_2O, and O_2 background gas*, Thin Solid Films **486**, 205 (2005)

M. Lorenz, H. Hochmuth, D. Spemann, H. von Wenckstern, H. Schmidt, M. Grundmann: *ZnO-Dünnfilme gezüchtet mit Laserplasma-Abscheidung (PLD) - Forschungsstand und Anwendungen*, Proc. FVS-Workshop "TCOs für Dünnschichtsolarzellen und andere Anwendungen" Freyburg 2005, p 19

B.N. Mbenkum, N. Ashkenov, M. Schubert, M. Lorenz, H. Hochmuth, D. Michel, M. Grundmann, G. Wagner: *Temperature-dependent dielectric and electro-optic properties of a ZnO-$BaTiO_3$-ZnO heterostructure grown by pulsed-laser deposition*, Appl. Phys. Lett. **86**, 091 904 (2005)

B.N. Mbenkum, N. Ashkenov, M. Schubert, M. Lorenz: *Electro-optic Raman observation of low temperature phase transitions in ZnO-BaTiO3-ZnO heterostructures*, Proc. Int. Conf. Phys. Semicond. (ICPS-27), Flagstaff 2004, AIP Conf. Proc. **772**, 401 (2005)

T. Nobis, M. Grundmann: *Low order whispering gallery modes in hexagonal nanocavities*, Phys. Rev. A **72**, 063 806 (2006)

T. Nobis, E.M. Kaidashev, A. Rahm, M. Lorenz, J. Lenzner, M. Grundmann: *Optical Resonances Of Single Zinc Oxide Microcrystals*, Proc. Int. Conf. Phys. Semicond. (ICPS-27), Flagstaff 2004, AIP Conf. Proc. **772**, 849 (2005)

A. Rahm, G.W. Yang, M. Lorenz, T. Nobis, J. Lenzner, G. Wagner, M. Grundmann: *Two-dimensional ZnO:Al nanosheets and nanowalls obtained by Al_2O_3-assisted thermal evaporation*, Thin Solid Films **486**, 191 (2005)

A. Rahm, T. Nobis, E.M. Kaidashev, M. Lorenz, G. Wagner, J. Lenzner, M. Grundmann: *High-pressure Pulsed Laser Deposition and Structural Characterization of Zinc Oxide Nanowires*, Proc. Int. Conf. Phys. Semicond. (ICPS-27), Flagstaff 2004, AIP Conf. Proc. **772**, 875 (2005)

K. Schindler, M. Ziese, P. Esquinazi, H. Hochmuth, M. Lorenz, K. Zimmer, E.H. Brandt: *A novel method for the determination of the flux-creep exponent from higher harmonic ac-susceptibility measurements*, Physica C **417**, 141 (2005)

H. Schmidt, M. Diaconu, H. Hochmuth, M. Lorenz, A. Setzer, P. Esquinazi, A. Pöppl, D. Spemann, K.W. Nielsen, R. Gross, G. Wagner, M. Grundmann: *Weak ferromagnetism in textured Zn1-xTMxO thin films*, Superlatt. Microstruct. **39**, 334 (2006)

H. Schmidt, M. Diaconu, E. Guzman, H. Hochmuth, M. Lorenz , G. Benndorf, A. Setzer, P. Esquinazi, H. von Wenckstern, D. Spemann, A. Pöppl, R. Böttcher, M. Grundmann: *N-conducting, ferromagnetic Mn-doped ZnO thin films on sapphire substrates*, Proc. Int. Conf. Phys. Semicond. (ICPS-27), Flagstaff 2004, AIP Conf. Proc. **772**, 351 (2005)

R. Schmidt-Grund, T. Nobis, V. Gottschalch, B. Rheinländer, H. Herrnberger, M. Grundmann: *a-Si/SiOx Bragg-reflectors on micro-structured InP*, Thin Solid Films **483**, 257 (2005)

R. Schmidt-Grund, D. Fritsch, M. Schubert, B. Rheinländer, H. Schmidt, H. Hochmut, M. Lorenz, C.M. Herzinger, M. Grundmann: *Band-to-band transitions and optical properties of $Mg_xZn_{1-x}O$ ($0 \leq x \leq 1$) films*, Proc. Int. Conf. Phys. Semicond. (ICPS-27), Flagstaff 2004, AIP Conf. Proc. **772**, 201 (2005)

H. von Wenckstern, S. Heitsch, G. Benndorf, D. Spemann, E.M. Kaidashev, M. Lorenz, M. Grundmann: *Incorporation and electrical activity of group V acceptors in ZnO thin films*, Proc. Int. Conf. Phys. Semicond. (ICPS-27), Flagstaff 2004, AIP Conf. Proc. **772**, 183 (2005)

H. von Wenckstern, R. Pickenhain, S. Weinhold, M. Ziese, P. Esquinazi, M. Grundmann: *Electrical properties of Ni/GaAs and Au/GaAs Schottky contacts in high magnetic fields*, Proc. Int. Conf. Phys. Semicond. (ICPS-27), Flagstaff 2004, AIP Conf. Proc. **772**, 1333 (2005)

H. von Wenckstern, S. Weinhold, G. Biehne, R. Pickenhain, E.M. Kaidashev, M. Lorenz, M. Grundmann: *Static and transient capacitance spectroscopy on ZnO*, Proc. Int. Conf. Phys. Semicond. (ICPS-27), Flagstaff 2004, AIP Conf. Proc. **772**, 197 (2005)

J. Zúñiga Pérez, V. Munoz-Sanjose, M. Lorenz, G. Benndorf, S. Heitsch, D. Spemann, M. Grundmann: *Structural characterization of a-plane $Zn_{1-x}Cd_xO$ ($0 < x < 0.085$) thin films grown by MOCVD*, J. Appl. Phys. **99**, 023 514 (2006)

Books

M. Grundmann: *The Physics of Semiconductors* (Springer, Heidelberg 2006)

M. Grundmann: *Quantum devices of reduced dimensionality*, in *Encyclopedia of Condensed Matter Physics*, ed. by F. Bassani, J. Liedl, P. Wyder (Elsevier, Kidlington 2005)

M. Grundmann, H. von Wenckstern, R. Pickenhain, S. Weinhold, B. Chengnui, O. Breitenstein: *Electrical properties of ZnO thin films and single crystals*, in *Zinc Oxide - a Material for Micro- and Optoelectronic Applications*, ed. by N.H. Nickel, E. Terukov (Springer, Berlin 2005) p 47

T. Nobis, E.M. Kaidashev, A. Rahm, M. Lorenz, M. Grundmann: *Whispering gallery modes in hexagonal zinc oxide micro- and nanocrystals*, in *Zinc Oxide - a Material for Micro- and Optoelectronic Applications*, ed. by N.H. Nickel, E. Terukov (Springer, Berlin 2005) p 83

H. von Wenckstern, S. Weinhold, G. Biehne, R. Pickenhain, H. Schmidt, H. Hochmuth, M. Grundmann: *Donor levels in ZnO*, in: *Advances in Solid State Physics*, Vol. 45, ed. by B. Kramer (Springer, Berlin 2005) p 263

in press

G. Brauer, W. Anwand, W. Skorupa, H. Schmidt, M. Diaconu, M. Lorenz, M. Grundmann: *Structure and ferromagnetism of Mn ion implanted ZnO thin films on sapphire*, Superlatt. Microstruct. (2005), in press

M. Diaconu, H. Schmidt, H. Hochmuth, M. Lorenz, H. von Wenckstern, G. Biehne, M. Grundmann: *Deep defects generated in n-conducting ZnO:TM thin films*, Solid State Commun. (2005), in press

M. Diaconu, H. Schmidt, M. Fecioru-Morariu, G. Guentherodt, H. Hochmuth, M. Lorenz, M. Grundmann: *Ferromagnetic behavior in Zn(Mn,P)O thin films*, Phys. Lett. A (2005), submitted

M. Diaconu, H. Schmidt, H. Hochmuth, M. Lorenz, G. Benndorf, J. Lenzner, D. Spemann, A. Setzer, P. Esquinazi, A. Pöppl, H. von Wenckstern, K.-W. Nielsen, R. Gross, H. Schmid, W. Mader, G. Wagner, M. Grundmann: *Room-temperature ferromagnetic Mn-alloyed ZnO films obtained by pulsed laser deposition*, J. Magn. Magn. Mater. (2005), submitted

M. Diaconu, H. Schmidt, H. Hochmuth, M. Lorenz, H. von Wenckstern, G. Biehne, M. Grundmann: *Deep defects generated in n-conducting ZnO:TM thin films*, Appl. Phys. Lett. (2005), submitted

S. Heitsch, G. Benndorf, G. Zimmermann, C. Schulz, D. Spemann, H. Hochmuth, H. Schmidt, T. Nobis, M. Lorenz, M. Grundmann: *Optical and structural properties of MgZnO/ZnO hetero- and double heterostructures grown by pulsed laser deposition*, Appl. Phys. A, in press

S. Heitsch, G. Zimmermann, C. Schulz, H. Hochmuth, D. Spemann, G. Benndorf, H. Schmidt, T. Nobis, M. Lorenz, M. Grundmann: *Photoluminescence properties of $Mg_xZn_{1-x}O$ thin films grown by pulsed laser deposition*, J. Appl. Phys., submitted

R. Johne, M. Lorenz, H. Hochmuth, J. Lenzner, H. von Wenckstern, G. Zimmermann, H. Schmidt, R. Schmidt-Grund, M. Grundmann: *Cathodoluminescence of large-area PLD grown ZnO thin films measured in transmission and reflection*, Appl. Phys. A, in press

A. Rahm, E.M. Kaidashev, H. Schmidt, M. Diaconu, A. Pöppl, R. Böttcher, C. Meinecke, T. Butz, M. Lorenz, M. Grundmann: *Growth and characterization of Mn- and Co-doped ZnO nanowires* Microchim. Acta (2005), in press

A. Rahm, M. Lorenz, Th. Nobis, G. Zimmermann, M. Grundmann, B. Fuhrmann, F. Syrowatka: *Pulsed Laser Deposition and characterization of ZnO nanowires with regular lateral arrangement*, Appl. Phys. A, in press

H. Schmidt, M. Diaconu, H. Hochmuth, G. Benndorf, H. von Wenckstern, G. Biehne, M. Lorenz, M. Grundmann: *Electrical and optical spectroscopy on ZnO:Co thin films*, Appl. Phys. A, in press

R. Schmidt-Grund, A. Carstens, B. Rheinländer, D. Spemann, H. Hochmuth, M. Lorenz, M. Grundmann, C.M. Herziger, M. Schubert: *Refractive indices and band-gap properties of rocksalt $Mg_xZn_{1-x}O$ ($0.68 < x < 1$)*, J. Appl. Phys. (2005), in press

H. von Wenckstern, G. Biehne, R.A. Rahman, H. Hochmuth, M. Lorenz, M. Grundmann: *Mean barrier height of Pd Schottky contacts on ZnO films*, Appl. Phys. Lett. (2005), in press

H. von Wenckstern, M. Brandt, H. Schmidt, G. Biehne, R. Pickenhain, H. Hochmuth, M. Lorenz, M. Grundmann: *Donor like defects in ZnO substrate materials and ZnO thin films*, Appl. Phys. A, in press

H. von Wenckstern, G. Benndorf, S. Heitsch, J. Sann, M. Brandt, H. Schmidt, J. Lenzner, M. Lorenz, A.Y. Kuznetsov, B.K. Meyer, M. Grundmann: *Properties of P-doped ZnO*, Appl. Phys. A, in press

Q. Xu, L. Hartmann, H. Schmidt, H. Hochmuth, M. Lorenz, R. Schmidt-Grund, D. Spemann, A. Rahm, M. Grundmann: *Magnetoresistance in pulsed laser deposited 3d transition metal doped ZnO films*, Thin Solid Films (2005), submitted

Talks

C. Bundesmann, M. Schubert, H. von Wenckstern, M. Lorenz, M. Grundmann: *Optische Bestimmung der Eigenschaften freier Ladungsträger in ZnO-Dünnfilmen mittels spektroskopischer Infrarotellipsometrie*, Proc. FVS-Workshop "TCOs für Dünnschichtsolarzellen und andere Anwendungen", Freyburg, 10.–12. April 2005, p 34

D. Fritsch, H. Schmidt, R. Schmidt-Grund, M. Grundmann: *Empirical Pseudopotential Calculation of* $Mg_xZn_{1-x}O$ *(*$0 < x < 1$*)*, 69. Frühjahrstagung der DPG, Berlin, March 2005

M. Grundmann: *ZnO thin films and photonic nanostructures*, 69. Frühjahrstagung der DPG, Symposium "ZnO rediscovered", Berlin, March 2005, invited

M. Grundmann, H. von Wenckstern: *Electrical Properties of ZnO Thin Films*, Proc. FVS-Workshop "TCOs für Dünnschichtsolarzellen und andere Anwendungen", Freyburg, 10.–12. April 2005, p 86, invited

M. Grundmann: *ZnO thin films and nanostructures*, EMRS Meeting, Strasbourg, France, June 2005, invited

M. Grundmann: *Selbstorganisation von Halbleiter-Nanostrukturen: Kontrolle und komplexe Strukturen*, VDI-TZ "Technische Anwendung der Selbstorganisation", Düsseldorf, June 2005, invited

S. Heitsch, G. Zimmermann, C. Schulz, H. Hochmuth, G. Benndorf, H. Schmidt, T. Nobis, M. Lorenz, M. Grundmann: *Optische und strukturelle Eigenschaften von MgZnO/ZnO-Hetero- und Doppelheterostrukturen*, 69. Jahrestagung der DPG, Berlin, March 2005

M. Lorenz, H. Hochmuth, D. Spemann, H. von Wenckstern, H. Schmidt, M. Grundmann: *ZnO-Dünnfilme gezüchtet mit Laserplasma-Abscheidung (PLD) - Forschungsstand und Anwendungen*, Proc. FVS-Workshop "TCOs für Dünnschichtsolarzellen und andere Anwendungen", Freyburg, 10.–12. April 2005, p 19

M. Lorenz, H. Hochmuth, H. von Wenckstern, H. Schmidt, S. Heitsch, D. Spemann, G. Benndorf, M. Diaconu, R. Schmidt-Grund, J. Lenzner, M. Grundmann: *ZnO based thin films and heterostructures - device related properties and applications*, THIOX

III Topical Meeting Workshop on oxides-at-the-nanoscale, Zaragoza, Spain, November 2005

M. Lorenz: *ZnO thin film heterostructures by PLD - state of the art and applications*, HET-SiC-05 Workshop, Krippen, 29. April 2005

M. Lorenz: *Epitaxy of ZnO and related compounds - state of the art and applications*, SOXESS Epitaxy Workgroup Meeting, Paris, 12. May 2005

M. Lorenz, H. Hochmuth, J. Lenzner, H. Schmidt, H. von Wenckstern, D. Spemann, G. Benndorf, S. Heitsch, R. Schmidt-Grund, G. Zimmermann, A. Rahm, T. Nobis, G. Brauer, M. Grundmann: *Pulsed laser deposition of ZnO based thin films and nanostructures – state of the art and applications*, 3rd SOXESS Workshop 2005, Gallipoli, Italy, 28. September – 01. October 2005

M. Lorenz: *Halbleitende ZnO-Dünnfilme mittels gepulster Laserdeposition – Forschungsstand und Anwendungspotenzial*, Colloquium Analytische Atomspektroskopie (canas05), Freiberg, 06.–10. March 2005

M. Lorenz: *PLD-Züchtung von ZnO-basierten Dünnfilmen und Nanostrukturen – Forschungsstand und Anwendungspotenzial*, Kolloqiumsvortrag Solarenergie-Forschung, Hahn-Meitner-Institut Berlin, 15. June 2005

R. Schmidt-Grund, N. Ashkenov, D. Fritsch, W. Czakai, M. Schubert, H. Hochmuth, M. Lorenz, M. Grundmann: *Temperature-dependency of the fundamental band-gap properties of (0001)ZnO thin films*, 69. Frühjahrstagung der DPG, Berlin, March 2005

R. Schmidt-Grund, B. Rheinländer, T. Gühne, H. Hochmuth, A. Rahm, J. Lenzner, M. Grundmann: *Cylindric Resonators With Coaxial Bragg-Reflectors*, 14th Int. Workshop Heterostruc. Technol. (HETECH), Smolenice, Slovakia, October 2005

H. von Wenckstern, M. Brand, R. Pickenhain, H. Schmidt, G. Biehne, M. Lorenz, H. Hochmuth, M. Grundmann: *Electrical characterization of ZnO*, 3rd SOXESS Workshop 2005, Gallipoli, Italy, 28. September – 01. October 2005

H. von Wenckstern, G. Benndorf, M. Brand, H. Schmidt, M. Lorenz, M. Grundmann: *Optical and electrical properties of Phosphorous-doped ZnO thin films*, 3rd SOXESS Workshop 2005, Gallipoli, Italy, 28. September – 01. October 2005

H. von Wenckstern: *Electrical and Optical Characterization of ZnO*, SOXESS workshop, Gießen, 20. May 05

H. von Wenckstern, S. Weinhold, R. Pickenhain, G. Biehne, H. Hochmuth, M. Lorenz, M. Grundmann: *Electrical characterization of ZnO using Schottky contacts*, 69. Frühjahrstagung der DPG, Berlin, March 2005

Posters

W. Anwand, G. Brauer, W. Skorupa, H. Schmidt, M. Diaconu, M. Lorenz, M. Grundmann: *Structure and ferromagnetism of Mn^+ ion implanted ZnO thin films on sapphire*, E-MRS Meeting, Strassbourg 2005

N. Ashkenov, H. von Wenckstern, G. Wagner, H. Hochmuth, M. Lorenz, M. Grundmann, M. Schubert: *Exchange polarization coupling in wurtzite-perovskite oxide interfaces: New concepts for electronic device heterostructures?*, THIOX III Topical Meeting Workshop on oxides-at-the-nanoscale, Zaragoza, Spain, November 2005

S. Heitsch, G. Benndorf, G. Zimmermann, C. Schulz, H. Hochmuth, H. Schmidt, T. Nobis, M. Lorenz, M. Grundmann: *Optical and structural properties of MgZnO/ZnO hetero- and double heterostructures*, 2nd Int. Workshop "Oxidic Interfaces", Wittenberg, 24.–26. February 2005

M. Brandt, H. von Wenckstern, G. Zimmermann, S. Heitsch, G. Benndorf, H. Hochmuth, M. Lorenz, M. Grundmann: *Hall effect measurements on ZnO thin films*, 69. Frühjahrstagung der DPG, Berlin, March 2005

G. Braunstein, H. Saxena, G. Benndorf, H. von Wenckstern, M. Lorenz, G. Brauer: *Acceptor Formation by Ion Implantation if Nitrogen into ZnO*, 12th Int. Workshop Oxide Electron. (WOE-12), Cape Cod, Massachusetts, USA, October 2005

D. Fritsch, R. Schmidt-Grund, H. Schmidt, C.M. Herzinger, M. Grundmann: *Polarization-dependent optical transitions at the fundamental band gap and higher critical points of wurtzite ZnO*, IEEE Proc. 5th Int. Conf. Num. Simulat. Optoelectron. Dev. (2005) p 69

K. Goede, M. Bachmann, W. Janke, M. Grundmann: *Binding specificity of peptides on semiconductor surfaces*, in *4th Biotechnology Symposium 2005 - Abstracts*, ed. by A.A. Robitzki, A.G. Beck-Sickinger, S. Brakmann, S. Eichler (Universität Leipzig 2005) p 192

T. Gühne, V. Gottschalch, G. Leibiger, H. Herrnberger, J. Kovac, J. Kovac jr., R. Schmidt-Grund, B. Rheinländer, D. Pudis: *(InGa)As-Diodenlaser ($\lambda \sim 1,2\,\mu m$) mit vergüteten Resonatoren*, 69. Frühjahrstagung der DPG, Berlin, March 2005

S. Heitsch, G. Zimmermann, C. Schulz, H. Hochmuth, G. Benndorf, H. Schmidt, T. Nobis, M. Lorenz, M. Grundmann: *Optical and structural properties of MgZnO/ZnO hetero- and double heterostructures grown by pulsed laser deposition*, 3rd SOXESS Workshop 2005, Gallipoli, Italy, 28. September – 01. October 2005

R. Kaden, G. Wagner, K. Bente, D. Döring, S. Schorr, D. Oppermann, C. Sturm, R. Schmidt-Grund, B. Reinländer, V. Riede, J. Lenzner, F. Menzel, R. Höhne, P.D. Esquinazi, K. Nielsch: *Architecture, micro structure and physical properties of cylindrite* $Fe_{1\pm x}Sn_{4\pm y}Pb_{3\pm z}Sb_{2\pm v}S_{14}$, 55. BHT, Freiberg, June 2005

M. Lorenz, H. Hochmuth, A. Jamoul, G. Ferro, C. Förster, J. Petzold, G. Wagner, G. Benndorf, H. von Wenckstern, T. Nobis, R. Schmidt-Grund, J. Lenzner, M. Grundmann: *ZnO thin films grown by PLD on 3C-SiC buffered Si and on 6H-SiC single crystals*, 12th Int. Workshop Oxide Electron. (WOE-12), Cape Cod, Massachusetts, USA, October 2005

M. Lorenz, H. Hochmuth, H. von Wenckstern, H. Schmidt, S. Heitsch, D. Spemann, G. Benndorf, M. Diaconu, R. Schmidt-Grund, J. Lenzner, M. Grundmann: *ZnO based thin films and heterostructures - device related properties and applications*, THIOX III Topical Meeting Workshop on oxides-at-the-nanoscale, Zaragoza, Spain, November 2005

M. Lorenz, A. Rahm, E.M. Kaidashev, G. Benndorf, T. Nobis, H. Hochmuth, G. Zimmermann, J. Lenzner, M. Grundmann: *ZnO based nanostructures by pulsed laser deposition: flexibility and luminescence*, THIOX III Topical Meeting Workshop on oxides-at-the-nanoscale, Zaragoza, Spain, November 2005

M. Lorenz, H. Hochmuth, T. Nobis, J. Lenzner, G. Zimmermann, M. Diaconu, H. Schmidt, H. von Wenckstern, A. Schön, D. Schenk, M. Grundmann: *Room-temperature cathodoluminescence of ZnO thin films grown by PLD in N_2, N_2O, and O_2 background gas*, 69. Frühjahrstagung der DPG, Berlin, March 2005

A. Rahm, M. Lorenz, T. Nobis, G. Zimmermann, M. Grundmann, B. Fuhrmann, F. Syrowatka: *Pulsed laser deposition and characterization of ZnO nanowires with regular lateral arrangement*, 3rd SOXESS Workshop 2005, Gallipoli, Italy, 28. September – 01. October 2005

T. Nobis, A. Rahm, M. Lorenz, M. Grundmann: *Analysis of optical modes in zinc oxide nanoresonators*, 12th Int. Workshop Oxide Electron. (WOE-12), Cape Cod, Massachusetts, USA, October 2005

H. Schmidt, M. Diaconu, H. Hochmuth, G. Benndorf, H. von Wenckstern, G. Biehne, M. Lorenz, M. Grundmann: *Electrical and optical spectroscopy on ZnO:Co thin films*, 3rd SOXESS Workshop 2005, Gallipoli, Italy, 28. September – 01. October 2005

M. Schmidt, H. von Wenckstern, R. Pickenhain, M. Ziese, P. Esquinazi, M. Grundmann: *Investigation of Schottky diodes in high magnetic fields*, 69. Frühjahrstagung der DPG, Berlin, March 2005

R. Schmidt-Grund, T. Gühne, B. Rheinländer, V. Gottschalch, H. Herrnberger, T. Nobis, M. Grundmann: *Concentric a-Si/SiO_x Bragg-Reflectors*, 69. Frühjahrstagung der DPG, Berlin, March 2005

R. Schmidt-Grund, A. Carstens, M. Schubert, B. Rheinländer, H. Hochmuth, E.M. Kaidashev, M. Lorenz, D. Spemann, A. Rahm, C.M. Herzinger, M. Grundmann: *Refractive indices and optical transitions of $Mg_xZn_{1-x}O$ ($0 < x < 1$)*, 69. Frühjahrstagung der DPG, Berlin, March 2005

R. Schmidt-Grund, T. Gühne, H. Hochmuth, A. Rahm, J. Lenzner, V. Gottschalch, B. Rheinländer, M. Grundmann: *Cylindric Resonators With Coaxial Bragg-Reflectors*, 9th Opt. Excit. Conf. Syst. (OECS 9), Southampton, UK, September 2005

R. Schmidt-Grund, T. Gühne, H. Hochmuth, A. Rahm, J. Lenzner, V. Gottschalch, B. Rheinländer, M. Grundmann: *Cylindric Resonators With Coaxial Bragg-Reflectors*, SPIE Int. Symp. Microelec. MEMS Nanotechnol., Brisbane, Australia, December 2005

M. Schubert, N. Ashkenov, E. Twerdowski, H. von Wenckstern, H. Hochmuth, M. Lorenz, M. Grundmann: *Exchange polarization coupling in wurzite-perovskite interfaces: Electrical and optical properties of Pt/ZnO/$BaTiO_3$/Pt/Si and Pt/ZnO/$BaTiO_3$/ZnO/Pt/Si heterostructures*, 2nd Int. Workshop "Oxidic Interfaces", Wittenberg, 24.–26. February 2005

H. von Wenckstern, G. Benndorf, S. Heitsch, J. Lenzner, M. Lorenz, M. Grundmann: *Influence of the incorporation of group V elements on the electrical properties of ZnO*, 69. Frühjahrstagung der DPG, Berlin, March 2005

J. Zúñiga-Pérez, V. Muñoz-Sanjosé, M. Lorenz, H. Hochmuth, G. Benndorf, S. Heitsch, D. Spemann, M. Grundmann: *Growth of ZnCdO thin films by MOCVD and PLD*, 3rd SOXESS Workshop 2005, Gallipoli, Italy, 28. September – 01. October 2005

7.36 Graduations

Diploma

- Swen Weinhold
  Untersuchungen von tiefen Niveaus in ZnO mittels DLTS
  01/2005
- Tobias Gühne
  Metallorganische Gasphasenepitaxie von AIII-BV-Laserstrukturen ($\lambda = 1,2\,\mu m$)
  04/2005
- Marcus Gonschorek
  Capacitance spectroscopy on self-assembled InAs quantum dots
  06/2005

7.37 Guests

- Dr. Evgeny M. Kaydashev
  Rostov-on-Don State University, Russia
  30.07.2005 – 29.10.2005
- Jesús Zúñiga Pérez
  Universitat de València, Spain
  01.04.2005 – 30.06.2005

8

Solid State Optics and Acoustics

8.1 Development of a Miniaturized Advanced Diagnostic Technology Demonstrator 'DIAMOND' - Technology Study Phase 2

W. Grill, R. Wannemacher

A miniaturized universal scanning microscope ('space microscope') is being developed for potential operation on board of the International Space Station ISS, which allows diagnostics of samples by means of optical scanning microscopy, partly combined with spectral resolution, as well as by means of acoustic microscopy with vector contrast. Foreseen microscopic techniques are confocal optical microscopy in reflection, scanning microscopy in transmission, as well as spectrally resolved fluorescence and Raman microscopy. Acoustic microscopy permits spatially resolved determination of micromechanical sample properties.

This work is supported by European Space Organization ESA/ESTEC

8.2 Ultrasound Diagnostics of Directional Solidification

W. Grill, E. Twerdowski, M. von Buttlar, R. Wannemacher, S. Knauth, O. Lenkeit

An ultrasonic measuring device based on guided waves has been developed in order to determine the growth rate of alloys, in particular of opaque metallic alloys. Experimental tests show that a high resolution is achievable in the determination of the position of the solid-liquid interface, down to 0.01 mm. The ultrasonic technique is therefore an appropriate tool for the measurement of the solidification velocity for stable as well as unstable solidification processes. The aim consists in the investigation of the impact of process parameters on the resulting material properties. Controlled non-stationary growth presently appears to become a main research object for the next future, in particular in the context of industrial applications. The measurement of the solidification velocity by ultrasound is a diagnostic tool for directional solidification experiments. It was developed in the framework of the Technological Research Programme of the European Space Organization. An ultrasound pulse launched from the cold end of the

sample and being reflected from the phase boundary of solidification allows to determine the position of the solid-liquid interface. Given the speed of sound in the sample the position of the phase boundary can be determined as a function of time and, hence, the solidification velocity via precise measurement of the propagation time by means of an autocorrelation technique.

Funded by European Space Organization ESA/ESTEC

8.3 Development and Verification of the Applicability of Ultrasonic Methods

W. Grill, Z. Kojro

Possible applications associated with the company Schott GLAS of the ultrasound techniques developed and published by our group are investigated. Techniques, sensors, and measurement devices are being developed. The work is conducted in cooperation with Schott GLAS. New techniques were developed and tested.

Funded by Schott GLAS Mainz

8.4 Development and Verification of the Applicability of Ultrasonic Methods

W. Grill, Z. Kojro

Based on techniques developed and published by us dedicated ultrasonic techniques, sensors, and devices are being developed for use at the company PFW Technologies GmbH. The work is conducted in cooperation with PFW Technologies GmbH. The developed techniques are a spin-off of the projects of our group financed by the European Space Organization (ESA).

Funded by PFW Technologies GmbH

8.5 Support in the Development of Ultrasound Based Sensors

W. Grill, Z. Kojro

Based on techniques developed and published by us dedicated ultrasonic sensors and devices are being developed for use at the company Ashland, Drew Marine Division. The work is conducted in cooperation with Ashland, Drew Marine Division. The developed techniques are a spin-off of the projects of our group financed by the European Space Organization (ESA).

Funded by Ashland, Drew Marine Division

8.6 Combinatory Phase-sensitive Scanning Acoustic Microscopy (PSAM) and Confocal Laser Scanning Microscopy (CLSM)

A. Kamanyi, W. Ngwa*, T. Betz, R. Wannemacher, W. Grill

*Department of Physics, University of Central Florida, Orlando, Florida, USA

Combinatory phase-sensitive acoustic microscopy (PSAM) at 1.2 GHz and confocal laser scanning microscopy (CLSM) in reflection and fluorescence has been implemented and applied to polymer blend films and fluorescently labeled fibroblasts and neuronal cells in order to explore the prospects and the various contrast mechanisms of this powerful technique. Topographic contrast is available for appropriate samples from CLSM in reflection and, with significantly higher precision, from the acoustic phase images. Material contrast can be gained from acoustic amplitude $V(z)$ graphs. In the case of the biological cells investigated, the optical and acoustic images are very different and exhibit different features of the samples (Fig. 8.1).

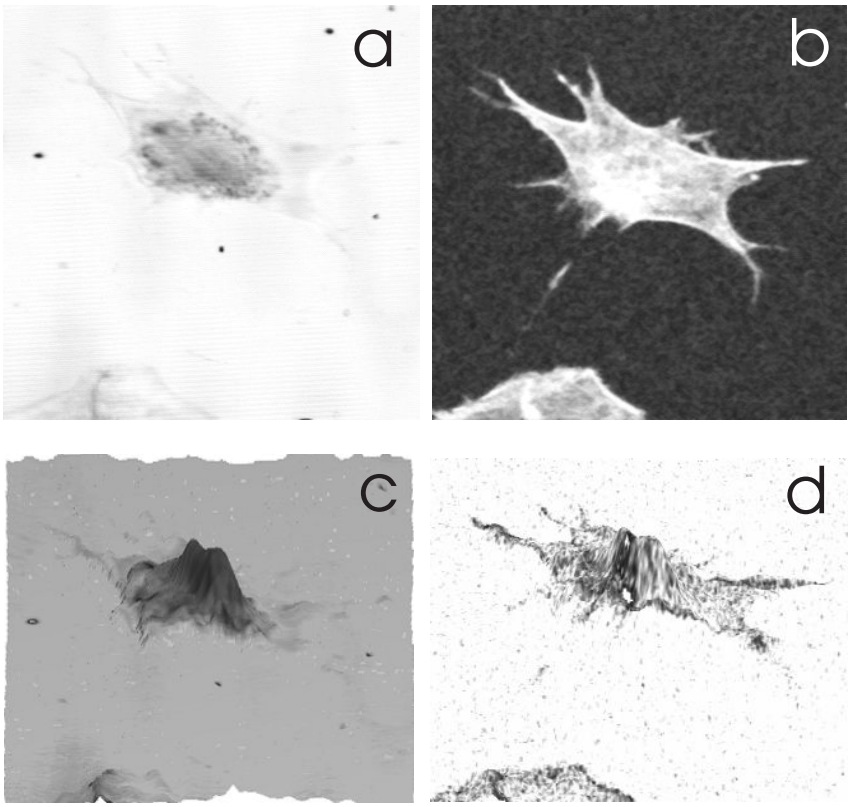

Figure 8.1: Fibroblast cell. (**a**) PSAM amplitude image. Image shows strong contrast and detail, with different cell parts easily recognisable (Image size: $100 \times 100\,\mu m^2$). (**b**) CLSM fluorescence image. Strong fluorescence indicates presence of actin. (Image size: $100 \times 100\,\mu m^2$). (**c**) 3-dimensional image from PSAM phase and amplitude. (**d**) 3-dimensional image from PSAM phase and CLSM fluorescence.

[1] A. Kamanyi et al.: Ultrasonics, in press

8.7 Characterization of Malaria Infected Red Blood Cells by Scanning Confocal Laser and Acoustic Vector Contrast Microscopy

E.T.A. Mohamed, S. Schubert*, T.W. Gilberger†, A. Kamanyi, R. Wannemacher, W. Grill

*Department of Infectious Diseases and Tropical Medicine, Faculty of Medicine
†Research Group Malaria II, Bernhard Nocht Institute for Tropical Medicine, Hamburg

Acoustic and optical multiple contrast microscopy has been employed in order to explore characterizable parameters of red blood cells, including cells infected by the parasite Plasmodium falciparum, in order to investigate cellular modifications caused by the infection and to identify possible detection schemes for disease monitoring (Fig. 8.2). Imaging schemes were based on fluorescence, optical transmission, optical reflection, and amplitude and phase of ultrasound reflected from the cells. Contrast variations observed in acoustic microscopy, but not in optical microscopy, were tentatively ascribed to changes caused by the infection.

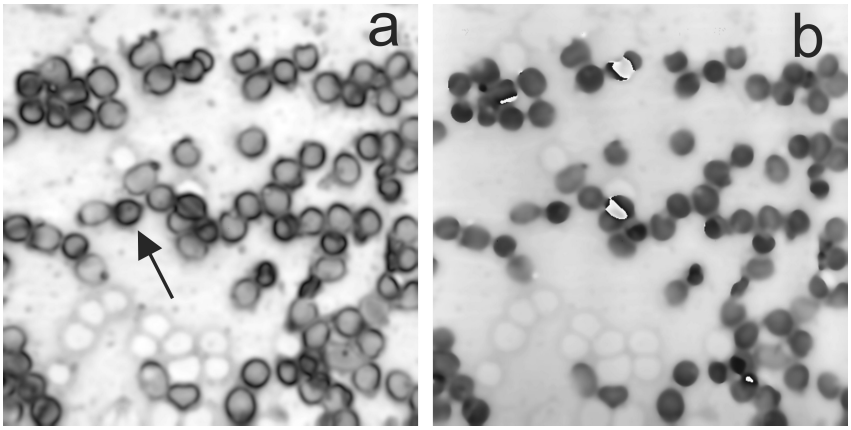

Figure 8.2: Ultrasound amplitude (**a**) and phase (**b**) images of P. falciparum infected RBCs. The size of the images is ($150 \times 150\ \mu m^2$).

[1] E.T.A. Mohamed et al.: Ultrasonics, in press

8.8 Combined Surface-Focused Acoustic Microscopy in Transmission and Scanning Ultrasonic Holography

E. Twerdowski, M. von Buttlar, N. Razek*, R. Wannemacher, A. Schindler*, W. Grill

*Leibniz Institute for Surface Modification (IOM), Leipzig

Employment of ultrasound techniques in nondestructive testing may require identification of the acoustic modes contributing to imaging. Such identification can be achieved,

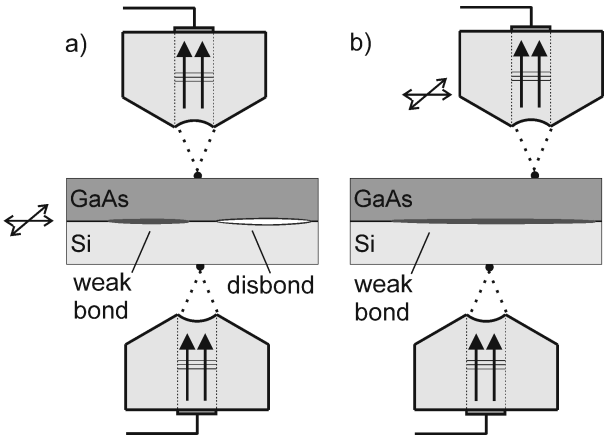

Figure 8.3: Application of scanning transmission microscopy (**a**) and scanning holography (**b**) to weak bond and disbond defect imaging in directly bonded wafers.

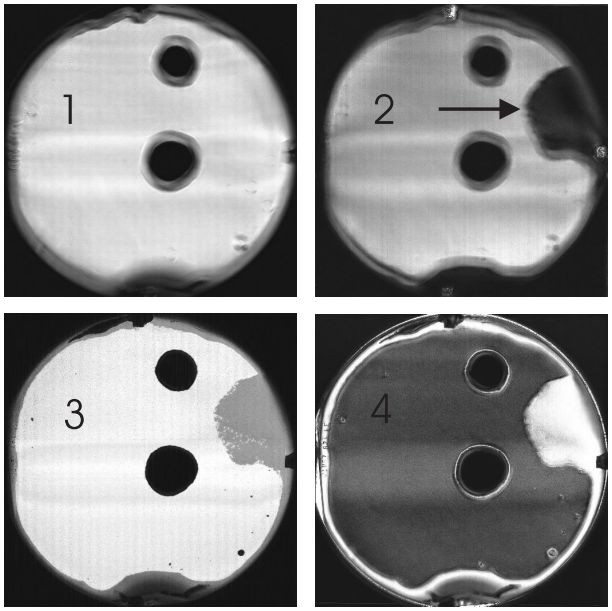

Figure 8.4: GaAs-Si bonded wafer scanned with non-confocal PSAM at 86 MHz. Normalized amplitude images are result of time gating of recorded signal at increasing times. Image range 50×50 mm^2. The *arrow* in the *second image* indicates weak bond area.

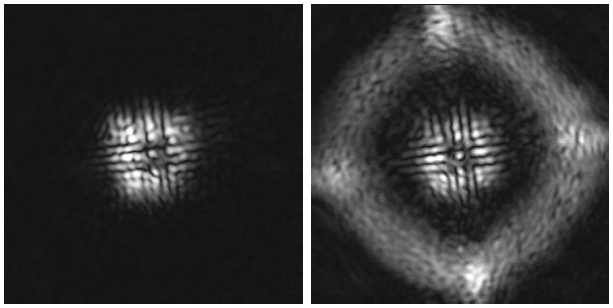

Figure 8.5: Holographic patterns obtained at same delay on a well bonded area (*left image*) and weakly bonded area (*right image*).

with some restrictions, by time-of-flight analysis. Another approach is acoustic holography that reveals the propagation properties of any selected mode. In anisotropic media, the propagation features are distinct and allow for a reliable classification of the selected mode. Both techniques were applied for classification of bonded, disbonded, and weakly bonded areas in directly bonded semiconductor wafers (Figs. 8.3–8.5).

[1] E. Twerdowski et al.: Ultrasonics, in press

8.9 Scanning Acoustic Defocused Transmission Microscopy with Vector Contrast Combined with Holography for Weak Bond Imaging

E. Twerdowski, M. von Buttlar, W. Grill

Surface focused acoustic transmission microscopy is employed for projection (tomographic) imaging of bonded materials including wafers. Short pulse excitation with apodized focusing transducers operated in transmission and two channel quadrature transient detection are employed for multiple contrast imaging. The achievable contrast schemes are based on mode selection for longitudinal, transverse, mode converted, and scattered modes. The identification of the involved modes including conversion schemes is experimentally accessible by time-gating of the recorded signal and by observation of spatially selected holograms. Perfect bonding, disbonding, and weak bonding can be studied and characterized by the developed mode selective imaging scheme. The characteristic features of weak bonding phenomena are demonstrated and characterized (Fig. 8.6).

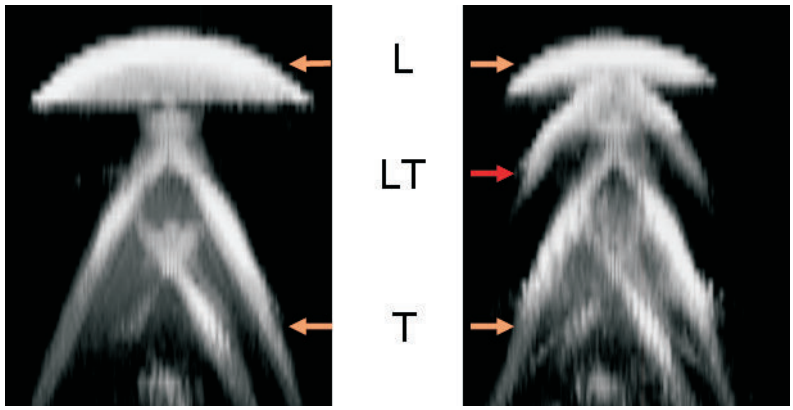

Figure 8.6: Ultrasound holography of good (*left*) and weak bonds (*right*). Only the magnitude is shown here. *L*, *T*, and *LT* stand for longitudinal, transverse, and mode-converted from longitudinal to transverse Waves, respectively.

[1] E. Twerdowski et al.: Proc. SPIE, in press

8.10 Acoustic Holography of Piezoelectric Materials by Coulomb Excitation

A. Habib, E. Twerdowski, M. von Buttlar, M. Pluta*, M. Schmachtl, R. Wannemacher, W. Grill

*Institute of Physics, Wroclaw University of Technology, Poland

Electric surface excitation of ultrasound in the Coulomb field of scanned electrically conductive spherical local probes and similar detection has been employed for imaging of the transport properties of acoustic waves in piezoelectric materials including singlecrystalline wafers. The employed Coulomb scheme leads to a fully predictable and almost ideal point excitation and detection. In combination with two-channel quadrature transient detection it allows high precision spatially and temporally resolved holographic imaging. Via modeling of the excitation and propagation properties, the effective elastic tensor and the piezoelectric properties of the observed materials can be determined with high resolution from a single measurement. The generation and detection scheme as well as the theoretical background are demonstrated and applications are exemplified (Figs. 8.7 and 8.8).

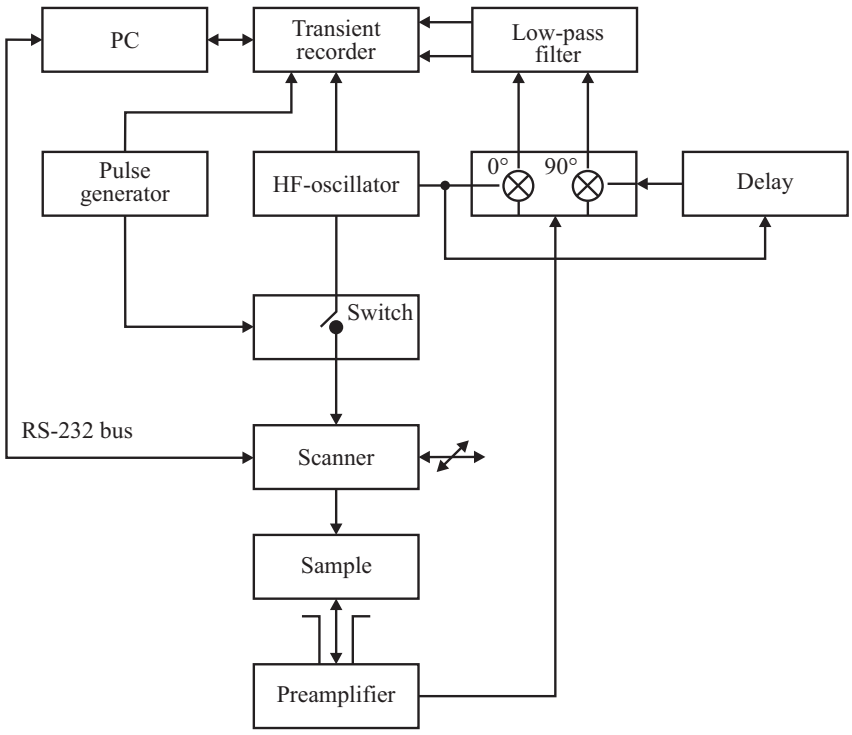

Figure 8.7: Schematic diagram of the signal generation, detection and processing.

[1] A. Habib, E. Twerdowski, M. von Buttlar, M. Pluta, M. Schmachtl, R. Wannemacher, and W. Grill,Acoustic holography of piezoelectric materials by Coulomb excitation, Proc. SPIE, in press

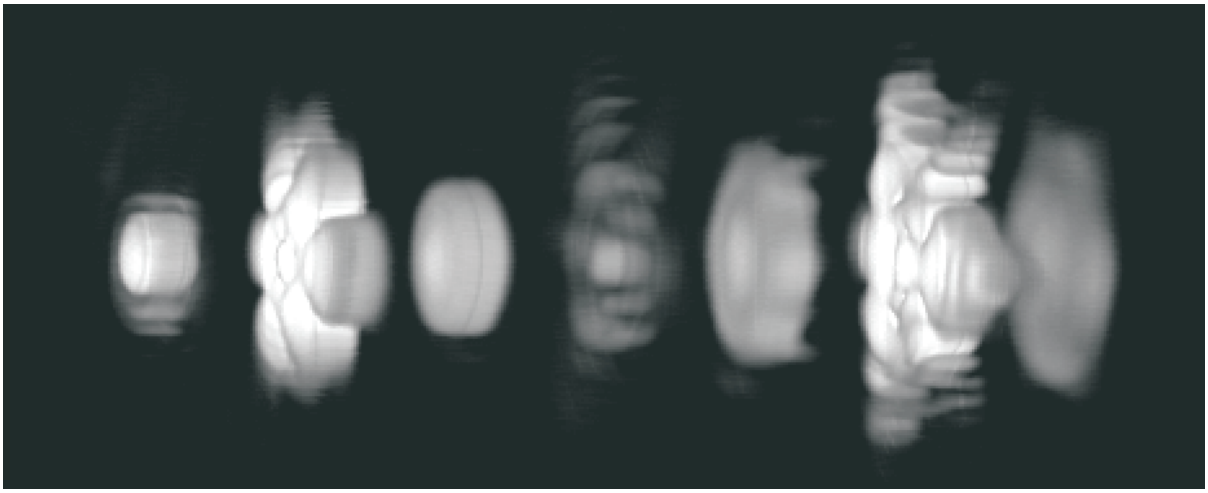

Figure 8.8: Pseudo 3-dimensional representation of the magnitude of the ultrasonic wave packages detected at the surface of a lithium niobate single-crystal (5.02 mm thick z-cut disc) opposing the area of excitation from a localized electric field generated with a scanned metallic sphere (diameter about 0.3 mm). *Horizontal*: time of arrival, full range about 5.5 μs. The other two dimensions give the position of the excitation area with a full range of about 15 mm in both directions. The brightness is proportional to the detected magnitude.

8.11 Funding

Mesoscale Acoustics on Soft Matter Systems
W. Grill
GR 566/11-2

Einsatz und Entwicklung akustischer Mikroskopieverfahren zur Untersuchung der Funktionsmorphologie von Planktonorganismen
W. Grill, R. Tollrian
GR566/10-1

Development of a Miniaturized Advanced Diagnostic Technology Demonstrator 'DIAMOND' - Technology Study Phase 2
W. Grill, R. Wannemacher
European Space Organization ESA/ESTEC

Ultrasound Diagnostics of Directional Solidification
European Space Organization ESA/ESTEC

Development and verification of the applicability of ultrasonic methods
Schott GLAS Mainz

Development and verification of the applicability of ultrasonic methods
PFW Technologies GmbH

Support in the Development of Ultrasound Based Sensors
Ashland, Drew Marine Division

8.12 Organizational Duties

W. Grill

- Adjunct Professor and Member of the Graduate School, The University of Georgia, Athens, GA, USA
- Project Reviewer: Deutsche Forschungsgemeinschaft, Alexander von Humboldt Foundation

R. Wannemacher

- Referee: Appl. Opt., Eur. Phys. J. B, J. Opt. Soc. Am., Mater. Res. Bull., Nat. Mater., Opt. Expr., Opt. Lett.

8.13 External Cooperations

Academic

- University of the Witwatersrand, Johannesburg, South Africa
  Prof. Dr. A. Every
- Wroclaw Institute of Technology, Wroclaw, Poland
  Dr. M. Pluta
- University of Arizona, Tucson, Arizona, USA
  Prof. Dr. T. Kundu
- University of Central Florida, Orlando, Forida, USA
  Prof. Dr. W. Luo, Dr. W. Ngwa
- Johann Wolfgang Goethe-Universität Frankfurt
  Prof. Dr. J. Bereiter-Hahn
- Universität Dortmund
  Prof. Dr. U. Woggon

International Organizations

- European Space Organization ESA/ESTEC

Industry

- Schott GLAS Mainz
- PFW Technologies GmbH
- Ashland, Drew Marine Division
- Kayser-Threde GmbH

8.14 Publications

Journals

W. Ngwa, W. Luo, A. Kamanyi, K.W. Fomba, W. Grill: *Characterization of polymer thin films by phase-sensitive acoustic microscopy and atomic force microscopy: A comparative review*, J. Microscopy **218**, 208 (2005)

W. Ngwa, W. Luo, T. Kundu, W. Grill: *Acoustic phase micrographs in mesoscale materials characterization*, Proc. SPIE **5768**, 27 (2005)

E. Twerdowski, R. Wannemacher, A. Schindler, N. Ratzek, W. Grill: *NDT of wafer direct bonding by nonconfocal transmission phase-sensitive acoustic microscopy*, Proc. SPIE *5768*, 204 (2005)

N. Ashkenov, M. Schubert, E. Twerdowski, H. v. Wenckstern, B.N. Mbenkum, H. Hochmuth, M. Lorenz, W. Grill, M. Grundmann: *Rectifying semiconductor-ferroelectric polarization loops and offsets in Pt-$BaTiO_3$-ZnO-Pt thin film capacitor structures*, Thin Solid Films **486**, 153 (2005)

in press

A. Kamanyi, W. Ngwa, T. Betz, R. Wannemacher, W. Grill: *Combinatory Phase-sensitive Scanning Acoustic Microscopy (PSAM) and Confocal Laser Scanning Microscopy (CLSM)*, Ultrasonics

E. Twerdowski, M. von Buttlar, N. Razek, R. Wannemacher, A. Schindler, W. Grill: *Combined surface-focused acoustic microscopy in transmission and scanning ultrasonic holography*, Ultrasonics

E. Twerdowski, R. Wannemacher, A. Schindler, N. Razek, W. Grill: *Application of spatially and temporally apodized nonconfocal acoustic transmission microscopy to imaging of directly bonded wafers*, Ultrasonics

9

Superconductivity and Magnetism

9.1 Introduction

Research into the basic properties of ferromagnetic and superconducting materials has a long-standing tradition. The present focus of the Division of Superconductivity and Magnetism is on two branches of contemporary magnetism: (1) magnetic and transport phenomena in carbon-based materials and (2) oxide spin-electronics.

After the discovery of ferromagnetism in proton-irradiated graphite in the year 2003 (see P. Esquinazi *et al.*, Phys. Rev. Lett. **91**, 227201 (2003)) through an intensive cooperation between our group and the Division of Nuclear Solid State Physics, we have continued studying the effects on the magnetism of amorphous carbon and fullerene films produced by irradiation. This research is extended to other carbon-based structures.

In the field of oxide spin-electronics research is focused on the study of magneto-transport processes at interfaces. Future aims of this project are the study of magnetic oxide nanocontacts and the fabrication of spin-transistors.

Pablo Esquinazi

9.2 Magnetic Properties of Carbon Phases Synthesized Using High-Pressure High-Temperature Treatment

K.-H. Han*, A. Talyzin*, A. Dzwilewski*, T.L. Makarova*, R. Höhne, P. Esquinazi, D. Spemann, L.S. Dubrovinsky†

*Department of Physics, Umea University, Sweden

†Bayerisches Geoinstitut, Universität Bayreuth

Two sets of samples were synthesized at 3.5 GPa near the point of C_{60} cage collapse at different annealing times. A clear structural transformation from mixture of C_{60} polymeric phases to graphite-like hard carbon phase was confirmed by X-ray diffraction and Raman spectroscopy. Magnetic force microscopy and a superconducting quantum interference device were used to characterize the magnetic properties of the synthesized samples. We found that the sample preparation conditions used in this study are not suitable to produce bulk magnetic carbon.

9.3 Higher Harmonics of AC Voltage Response in Narrow Strips of $YBa_2Cu_3O_7$ Thin Films: Evidence for Strong Thermal Fluctuations

J.G. Ossandon*, S. Sergeenkov*, P. Esquinazi, H. Kempa

*Department of Engineering Sciences, Universidad de Talca, Curicó, Chile

We have investigated the higher harmonics of the ac voltage response in strips of $YBa_2Cu_3O_7$ thin films as a function of temperature, frequency and ac current amplitude. The third (fifth) harmonic of the local voltage is found to exhibit a negative (positive) peak at the superconducting transition temperature and their amplitudes are closely related to the slope (derivative) of the first (ohmic) harmonic. The peaks practically do not depend on frequency and no even (second or fourth) harmonics are detected. The observed data can be interpreted in terms of ac current induced thermal modulation of the sample temperature added to strong thermally activated fluctuations in the transition region.

9.4 Magnetoresistance and Electrical Hysteresis in Stable Half-Metallic $La_{0.7}Sr_{0.3}MnO_3$ and Fe_3O_4 Nanoconstrictions

O. Céspedes*, S.M. Watts*, J.M.D. Coey*, K. Dörr†, M. Ziese

*Physics Department, CRANN, Trinity College, Dublin, Ireland
†Leibniz Institute for Solid State and Materials Research, Dresden

We have studied the transport properties of mechanically stable Fe_3O_4 and $La_{0.7}Sr_{0.3}MnO_3$ nanoconstrictions patterned by focused ion-beam milling. The magnetoresistance decreases with the square of the applied voltage and scales with the resistance of the constriction, with values up to 8000 % for magnetite and 100 % for $La_{0.7}Sr_{0.3}MnO_3$. These results are interpreted within a model for domain-wall magnetoresistance. Some samples exhibit electrical hysteresis with discrete changes of resistance that disappear in the presence of a magnetic field, indicating domain-wall displacement driven by a spin-polarized current.

9.5 Grain-Boundary Magnetoconductance and Inelastic Tunnelling

M. Ziese, A. Bollero, I. Panagiotopoulos*, N. Moutis†

*Department of Materials Science and Engineering, University of Ioannina, Greece
†Institute of Materials Science, National Center of Scientific Research "Demokritos", Athens, Greece

Measurements of the magnetoconductance of $La_{0.7}Sr_{0.3}MnO_3$ pressed powder samples in both the low and high field regime are reported. The magnetoconductance was calculated in a model based on inelastic tunneling via Mn sites situated in the tunneling barrier. This model satisfactorily accounts for the strong decrease of the low field magnetoconductance as a function of temperature due to spin depolarization in the inelastic tunneling processes. The susceptibility of the tunneling barrier was derived by two different methods showing the consistency of the model.

9.6 Size and Shape Dependence of the Exchange-Bias Field in Exchange-Coupled Ferrimagnetic Bilayers

M. Ziese, R. Höhne, A. Bollero, H.-C. Semmelhack, P. Esquinazi, K. Zimmer*

*Institute for Surface Modification, Leipzig

Exchange biasing was studied in an exchange-spring system consisting of two ferrimagnetic films with different coercivity. Magnetite and Co-Fe ferrite were chosen as the soft and hard magnetic bilayer components, respectively. The samples were epitaxially grown on MgO single crystal substrates by pulsed laser deposition. The exchange-bias field was investigated as a function of system size and shape, magnetic field direction and magnetization reversal in the hard layer. A clear dependence of the exchange-bias field on the sample size and shape was found. This was attributed to an interplay between exchange and dipolar energies. Micromagnetic simulations agree with the experimental results.

9.7 Schottky-Barrier and Spin-Polarization at the Fe_3O_4-Nb:$SrTiO_3$ Interface

M. Ziese, U. Köhler, A. Bollero, R. Höhne, P. Esquinazi

The interface between magnetite (Fe_3O_4) and Nb-doped $SrTiO_3$ shows typical characteristics of a Schottky barrier. The magnetoresistance was found to depend on the bias current through the junction. This can be understood within a model for a Schottky contact with a ferromagnetic component. The spin polarization of the magnetite layer was determined to be about 60 %.

9.8 Funding

Room Temperature Ferromagnetism in Graphite and Fullerenes (FERROCARBON)
Prof. P. Esquinazi
EU

The origin of carbon-based magnetism and the role of hydrogen
Prof. P. Esquinazi
DFG ES 86/11-1

Magnetotransport in Oxide Thin Film Systems
Prof. P. Esquinazi and Dr. M. Ziese
DFG Es 86/7-4

Mercator Visiting Professorship
Prof. P. Esquinazi and Prof. Y. Kopelevich
DFG

Oxidische Heterostrukturen für die Spin-Elektronik
Dr. M. Ziese
DAAD D/03/43168

9.9 Organizational Duties

P. Esquinazi

- Project Reviewer: Deutsche Forschungsgemeinschaft (DFG), National Science Foundation (USA), German-Israeli Foundation
- Referee: Phys. Rev. Lett, Phys. Rev. B., Physica C, Phys. Lett. A, phys. stat. sol., J. Low Temp. Phys., Carbon, J. Chem. Phys., Eur. J. Phys. B, J. Magn. Magn. Mater.

R. Höhne

- Referee: phys. stat. sol., Thin Solid Films

M. Ziese

- Referee: Phys. Rev. Lett., Phys. Rev. B., J. Phys.: Condens. Matter, J. Phys. D: Appl. Phys., phys. stat. sol., J. Magn. Magn. Mater., Eur. J. Phys. B, Thin Solid Films

9.10 External Cooperations

Academic

- State University of Campinas, Campinas, Brazil
  Prof. Dr. Yakov Kopelevich
- Umea University, Sweden
  Dr. Tatiana Makarova
- Universidad Autónoma de Madrid, Spain
  Prof. Dr. Miguel Angel Ramos
- Universidad Autónoma de Madrid, Spain
  Prof. Dr. Sebastian Vieira
- Institute for Metal Physics of National Academy of Sciences of Ukraine, Kiev, Ukraine
  Prof. Dr. V. M. Pan
- Universität Leipzig, Fakultät für Chemie und Mineralogie
  Prof. R. Szargan
- Max-Planck-Institut für Metallforschung
  Dr. E. H. Brandt

- University of Ioannina, Greece, Ioannina, Greece
  Prof. I. Panagiotopoulos,
- Institute for Materials Science, National Center of Scientific Research "Demokritos", Athens, Greece
  Dr. Nikos Moutis
- Trinity College Dublin, Ireland
  Prof. J. M. D. Coey
- IFW Dresden
  Dr. Kathrin Dörr
- University of Sheffield, UK
  Prof. G. Gehring
- University of the Negev, Beer Sheva, Israel
  Dr. Evgeny Rozenberg
- Institut für Oberflächenmodifizierung e. V., Leipzig
  Dr. Klaus Zimmer

9.11 Publications

Journals

P. Esquinazi, K.-H. Han, R. Höhne, D. Spemann, A. Setzer, T. Butz: *Examples of room-temperature magnetic ordering in carbon-based structures*, Phase Trans. **78**, 155 (2005), doi: 10.1080/01411590412331316627

P. Esquinazi, R. Höhne: *Magnetism in carbon structures*, J. Magn. Magn. Mater. **290-291**, 20 (2005), doi: 10.1016/j.jmmm.2004.11.154

K.-H. Han, A. Talyzin, A. Dzwilewski, T.L. Makarova, R. Höhne, P. Esquinazi, D. Spemann, L.S. Dubrovinsky: *Magnetic properties of carbon phases synthesized using high-pressure high-temperature treatment*, Phys. Rev. B **72**, 224 424 (2005), doi: 10.1103/PhysRevB.72.224424

J.G. Ossandon, S. Sergeenkov, P. Esquinazi, H. Kempa: *Higher harmonics of ac voltage response in narrow strips of $YBa_2Cu_3O_7$ thin films: evidence for strong thermal fluctuations*, Supercond. Sci. Technol. **18**, 325 (2005), doi: 10.1088/0953-2048/18/3/020

S. Schorr, R. Höhne, G. Wagner, V. Riede, W. Kockelmann: *Investigation of the solid solution series 2(MnX)-$CuInX_2$ (X = S, Se)*, J. Phys. Chem. Solids **66**, 1966 (2005), doi: 10.1016/j.jpcs.2005.09.066

D. Spemann, P. Esquinazi, R. Höhne, A. Setzer, M. Diaconu, H. Schmidt, T. Butz: *Magnetic carbon: A new application for ion microbeams*, Nucl. Instr. Meth. B **231**, 433 (2005), doi: 10.1016/j.nimb.2005.01.096

M. Diaconu, H. Schmidt, H. Hochmuth, M. Lorenz, G. Benndorf, J. Lenzner, D. Spemann, A. Setzer, K.W. Nielsen, P. Esquinazi, M. Grundmann: *UV optical properties*

of ferromagnetic Mn-doped ZnO thin films grown by PLD, Thin Solid Films **486**, 117 (2005), doi: 10.1016/j.tsf.2004.11.211

O. Céspedes, S.M. Watts, J.M.D. Coey, K. Dörr, M. Ziese: *Magnetoresistance and electrical hysteresis in stable half-metallic $La_{0.7}Sr_{0.3}MnO_3$ and Fe_3O_4 nanoconstrictions*, Appl. Phys. Lett. **87**, 083 102 (2005), doi: 10.1063/1.2011770

M. Ziese, A. Bollero, I. Panagiotopoulos, N. Moutis: *Grain-boundary magnetoconductance and inelastic tunnelling*, Phys. Rev. B. **72**, 024 453 (2005), doi: 10.1103/PhysRevB.72.024453

M. Ziese, U. Köhler, A. Bollero, R. Höhne, P. Esquinazi: *Schottky-barrier and spin-polarization at the Fe_3O_4-Nb:$SrTiO_3$ interface*, Phys. Rev. B. **71**, 180 406(R) (2005), doi: 10.1103/PhysRevB.71.180406

M. Ziese, U. Köhler, R. Höhne, A. Bollero, P. Esquinazi: *Schottky barrier formation at the Fe_3O_4/Nb:$SrTiO_3$ interface*, J. Magn. Magn. Mater. **290-291**, 1116 (2005), doi: 10.1016/j.jmmm.2004.11.470

A. Bollero, M. Ziese, P. Esquinazi, K. Dörr, I. Mönch: *Magnetoresistance in bicrystal Fe_3O_4 thin films*, J. Magn. Magn. Mater. **290-291**, 1134 (2005), doi: 10.1016/j.jmmm.2004.11.475

M. Ziese, R. Höhne, A. Bollero, H.-C. Semmelhack, P. Esquinazi, K. Zimmer: *Size and shape dependence of the exchange-bias field in exchange-coupled ferrimagnetic bilayers*, Eur. Phys. J. B **45**, 223 (2005), doi: 10.1140/epjb/e2005-00177-4

K. Schindler, M. Ziese, P. Esquinazi, H. Hochmuth, M. Lorenz, K. Zimmer, E.H. Brandt: *A novel method for the determination of the flux-creep exponent from higher harmonic ac-susceptibility measurements*, Physica C **417**, 141 (2005), doi: 10.1016/j.physc.2004.10.013

A. Bollero, M. Ziese, R. Höhne, H.-C. Semmelhack, U. Köhler, A. Setzer, P. Esquinazi: *Influence of thickness on microstructural and magnetic properties in Fe_3O_4 thin films produced by PLD*, J. Magn. Magn. Mater. **285**, 279 (2005), doi: 10.1016/j.jmmm.2004.08.004

M. Ziese: *Magnetocrystalline anisotropy transition in $La_{0.7}Sr_{0.3}MnO_3$ films*, Phys. Stat. Sol. B **242**, R116 (2005), doi: 10.1002/pssb.200541266

in press

M. Ziese: *Study of the micromagnetic structure of a $La_{0.7}Sr_{0.3}MnO_3$ film*, Phys. Stat. Sol. B

I. Panagiotopoulos, N. Moutis, M. Ziese, A. Bollero: *Magnetoconductunce and hysteresis in milled $La_{0.67}Sr_{0.33}MnO_3$ powder compacts*, J. Magn. Magn. Mater. **299**, 94 (2006)

Talks

P. Esquinazi: *Some remarks on the thermal transport in anisotropic HTSC*, 5*th* Heinrich-Hertz Minerva Workshop on High Temperature Superconductivity, Kfar Hamaccabiah (Israel), 08.05.–10.05.2005

P. Esquinazi: *Magnetism in Carbon: Past, Present and Future research*, Tel Aviv University, 09.05.2005

P. Esquinazi: *Magnetism in Carbon: Past, Present and Future research*, Ben Gurion University, 12.05.2005

P. Esquinazi: *Magnetism in Carbon: Past, Present and Future research*, XL Zakopane School of Physics: Breaking Frontiers, Submicron in Physics and Biology, Poland, 20.05.–25.05.2005

P. Esquinazi: *Proton irradiation effects and magnetic order in carbon structures*, International Conference on Materials for Advanced Technologies, ICMAT2005, Singapore July 2005

P. Esquinazi: *Magnetischer Kohlenstoff*, Ostwald Society, Großbothen, 01.10.2005

9.12 Graduations

9.13 Guests

- Prof. José Luis Giorgano
  University of Talca, Chile
  13.01.2005 – 29.01.2005
- Dr. Dhanvir Singh Rana
  Tata Institute of Fundamental Research, Mumbai, India
  31.07.2005 – 04.09.2005
- Prof. Jorge Ossandon
  University of Talca, Chile
  19.09.2005 – 03.10.2005
- Prof. Dr. Yakov Kopelevich, Mercator Visiting Professorship
  State University of Campinas, Campinas, Brazil
  30.09.2005 – 28.02.2006
- Olena Zubaryeva
  University of Odessa, Ukraine
  06.07.2005 – 03.09.2005
- Ampatcha Satornsantikul
  University of Bangkok, Thailand
  17.10.2005 – 30.11.2005

- Prof. Ioannis Panagiotopoulos
  University of Ioannina, Greece
  11.12.2005 – 17.12.2005
- Dr. Nikos Moutis
  National Center of Scientific Research “Demokritos”, Greece
  11.12.2005 – 17.12.2005
- E. Manios
  National Center of Scientific Research “Demokritos”, Greece
  11.12.2005 – 17.12.2005

III

Institute for Theoretical Physics

10

Computational Quantum Field Theory

10.1 Introduction

The Computational Physics Group performs basic research into classical and quantum statistical physics with special emphasis on phase transitions and critical phenomena. In the centre of interest are currently the physics of spin glasses, diluted magnets and other materials with quenched, random disorder, soft condensed matter physics (e.g., membranes and interfaces) and biologically motivated problems (e.g., protein folding and semiflexible polymers). Investigations of a geometrical approach to the statistical physics of topological defects with applications to superconductors and superfluids and research into fluctuating geometries with applications to quantum gravity (e.g., dynamical triangulations) are conducted within the EC-RTN Network "ENRAGE": *Random Geometry and Random Matrices: From Quantum Gravity to Econophysics*. Supported by a Development Host grant of the European Commission, also research into the physics of anisotropic quantum magnets and quantum phase transitions has been established.

The methodology is a combination of analytical and numerical techniques. The numerical tools are currently mainly Monte Carlo computer simulations and high-temperature series expansions. The computational approach to theoretical physics is expected to gain more and more importance with the future advances of computer technology, and will probably become the third basis of physics besides experiment and analytical theory. Already now it can help to bridge the gap between experiments and the often necessarily approximate calculations of analytical work. To achieve the desired high efficiency of the numerical studies we develop new algorithms, and to guarantee the flexibility required by basic research all computer codes are implemented by ourselves. The technical tools are Fortran, C, and C++ programs running under Unix or Linux operating systems and computer algebra using Maple or Mathematica. The software is developed and tested at the Institute on a cluster of PCs and workstations, where also most of the numerical analyses are performed. Large-scale simulations requiring vast amounts of computer time are carried out at the Institute on a recently installed Beowulf cluster with 40 Athlon MP1800+ CPUs and a new Opteron cluster with 18 processors of 64-bit architecture, at the parallel computers of the University computing center, and upon grant application at the national supercomputing centres

in Jülich and München on IBM and Hitachi parallel supercomputers. This combination of various platforms gives good training opportunities for the students and offers promising job perspectives in many different fields for their future career.

The research is embedded in a wide net of national and international collaborations funded by network grants of the European Commission and the European Science Foundation (ESF), and by a binational research grant with scientists in Sweden. Close contacts and collaborations are also established with research groups in Armenia, Austria, China, France, Great Britain, Israel, Italy, Poland, Russia, Spain, Taiwan, Turkey, Ukraine, and the United States.

Wolfhard Janke

10.2 Monte Carlo Studies of Spin Glasses

B.A. Berg*, A. Billoire†, E. Bittner, W. Janke, A. Nußbaumer, D.B. Saakian‡

*Department of Physics, Florida State University, Tallahassee, USA
†CEA/Saclay, Gif-sur-Yvette, France
‡Yerevan Physics Institute, Yerevan, Armenia

Spin glasses are examples for the important class of materials with random, competing interactions [1]. This introduces so-called "frustration", since no unique spin configuration is favoured by all interactions, and consequently leads to a rugged free energy landscape with many minima separated by barriers. To cope with the problems of standard Monte Carlo simulations to overcome those barriers, we developed a multi-overlap Monte Carlo algorithm [2] which can be optimally tailored for the sampling of rare-events [3]. Employing this technique we first studied for the three-dimensional (3D) short-range Edwards-Anderson Ising (EAI) $\pm J$ model the scaling behaviour of the barrier heights [4] and the tails of the overlap-parameter distribution [5]. Recently we improved our methodology by combining it with parallel tempering and N-fold way ideas [6]. First tests with the new algorithm indicate [7] that it will enable us to push the studies of the spin-glass phase further towards the physically more interesting low-temperature regime. Since very large computing times of the order of many years are required for studies of spin glasses, we have adapted our computer codes to the special architecture of the recently installed supercomputer JUMP at NIC/ZAM Jülich.

We also extended our investigations to the Sherrington-Kirkpatrick (SK) mean-field and random orthogonal models where particular focus is placed on studies of inherent structures and inhomogeneities in dynamical response functions. As a first step in this direction we investigated the finite-size scaling behaviour of the free-energy barriers in the SK model which are visible in the probability density of the Parisi overlap parameter. Assuming that the mean barrier height diverges with the number of spins N as N^{α}, our data showed good agreement with the theoretically expected value $\alpha = 1/3$ [8]. This is an important result since by applying precisely the same method of analysis to our data for the short-range EAI model, we obtained a significantly different exponent. As the second main result of our SK model study we found clear evidence that the tails of the barrier-height distribution can be described by the Fréchet extremal-value distibution [8].

[1] K.H. Fischer, J.A. Hertz: *Spin Glasses* (Cambridge University Press, Cambridge 1991)
[2] B.A. Berg, W. Janke: Phys. Rev. Lett. **80**, 4771 (1998)
[3] W. Janke: in *Computer Simulations of Surfaces and Interfaces*, NATO Science Series, II. Mathematics, Physics and Chemistry – Vol. **114**, ed. by B. Dünweg et al. (Kluwer, Dordrecht, 2003), p 137
[4] B.A. Berg et al.: Phys. Rev. B **61**, 12 143 (2000); Physica A **321**, 49 (2003)
[5] B.A. Berg et al.: Phys. Rev. E **65**, 045 102(R) (2002); *ibid.* **66**, 046 122 (2002)
[6] A. Nußbaumer et al.: to be published
[7] A. Nußbaumer: Diploma Thesis, University of Leipzig (2003)
[8] E. Bittner, W. Janke: Europhys. Lett. **74**, 195 (2006)

10.3 Monte Carlo Studies of Diluted Magnets

B. Berche*, P.-E. Berche†, C. Chatelain*, W. Janke

*Laboratoire de Physique des Matériaux, Université Henri Poincaré, Nancy, France
†Groupe de Physique des Matériaux, Université de Rouen, France

The influence of quenched, random disorder on phase transitions has been the subject of exciting experimental, analytical and numerical studies over many years. Generically one expects that under certain conditions quenched disorder modifies the critical behaviour at a second-order transition (Harris criterion) and can soften a first-order transition to become second order (Imry–Wortis effect) [1]. In two dimensions these effects are fairly well understood [2]. In three dimensions (3D), numerical studies have mainly focused on the site-diluted Ising model [3], where good agreement with field theoretical predictions was obtained. For the case of a first-order transition in the pure model, large-scale simulations have only been performed for the 3-state Potts model with site-dilution [4].

In this project we have performed intensive Monte Carlo studies of the 3D Ising and 4-state Potts models with *bond*-dilution. The phase diagrams of the diluted models, starting from the pure model limit down to the neighbourhood of the percolation threshold, were found in very good agreement with the single-bond effective-medium approximation and our parallel high-temperature series expansions for the same models. For the estimation of critical exponents in the Ising case [5, 6], we first performed finite-size scaling analyses at three different dilutions to check the stability of the disorder fixed point. We observe strong cross-over effects between the pure, disorder and percolation fixed points, leading to effective critical exponents apparently dependent on the dilution. In addition also the temperature behaviour of physical quantities was studied in order to characterize the disorder fixed point more accurately. This allowed us to determine critical amplitude ratios which are usually more sensitive to the universality class than critical exponents. Moreover, non-self-averaging properties at the disorder fixed point were found in good agreement with approximate analytical predictions. Overall our numerical results provide strong evidence for universality of bond and site dilution in the 3D Ising model. Similar simulations of the 3D bond-diluted

4-state Potts model [7] yield clear evidence for disorder induced softening to a second-order transition above a (tricritical) disorder strength. Here also the role of rare-event contributions was studied in great detail.

[1] A.B. Harris: J. Phys. C **7**, 1671 (1974); Y. Imry, M. Wortis: Phys. Rev. B **19**, 3580 (1979)
[2] B. Berche, C. Chatelain: in *Order, Disorder, and Criticality*, ed. by Y. Holovatch (World Scientific, Singapore 2004), p 147, arXiv:cond-mat/0207421
[3] S. Wiseman, E. Domany: Phys. Rev. Lett. **81**, 22 (1998); Phys. Rev. E **58**, 2938 (1998); H.G. Ballesteros et al.: Phys. Rev. B **58**, 2740 (1998)
[4] H.G. Ballesteros et al.: Phys. Rev. B **61**, 3215 (2000)
[5] P.-E. Berche et al.: Eur. Phys. J. B **38**, 463 (2004)
[6] B. Berche et al.: Cond. Matter Phys. **8**, 47 (2005)
[7] C. Chatelain et al.: Nucl. Phys. B **719**, 275 (2005)

10.4 High-Temperature Series Expansions for Spin Glasses and Disordered Magnets

M. Hellmund*, W. Janke

*Fakultät für Mathematik und Informatik

Systematic series expansions for statistical models defined on a lattice are a well-known alternative to large-scale numerical simulations for the study of phase transitions and critical phenomena [1]. For quenched disordered systems the extension of this method [2] requires especially adapted graph theoretical and algebraic algorithms. In this project we developed a computer package based on the "star-graph" method [3] which allows the generation of high-temperature series expansions for the free energy and susceptibility. We consider the class of disordered q-state Potts models on d-dimensional hypercubic lattices $\mathbb{Z}^d$ with bimodal probability distributions of quenched couplings parametrized by $P(J_{ij}) = p\delta(J_{ij} - J_0) + (1-p)\delta(J_{ij} - RJ_0)$, which includes spin glasses, diluted ferromagnets, random-bond models and transitions between them. The limiting case $p = 1$ describes the pure ferromagnetic ($J_0 > 0$) models. Even though the method is highly optimized for the problem at hand, it is extremely demanding since the number of contributing graphs grows exponentially with the order of the series (see Fig. 10.1) and all intermediate calculations have to be performed by means of symbolic computer algebra, which we implemented ourselves in C++ since the available standard software products such as MATHEMATICA or MAPLE are too slow and require too much memory.

In the analysis we focused up to now mainly on the bond-diluted Ising model ($q = 2$) for which we used our computer package to generate high-temperature series up to order 21 in $d = 3$ dimensions [4, 5] and up to order 19 in $d = 4, 5$ [5]. Applying various analysis tools we determined the phase diagrams in the temperature-dilution plane and estimated the critical exponent γ, parametrizing the singularity of the susceptibility at criticality, $\chi \sim (T - T_c)^{-\gamma}$. Depending on the dimension, our results can be compared with field-theoretic predictions and estimates from our Monte Carlo simulations performed in another project [6]. For the 4-state Potts model in $d = 3$ dimensions [7], which in the

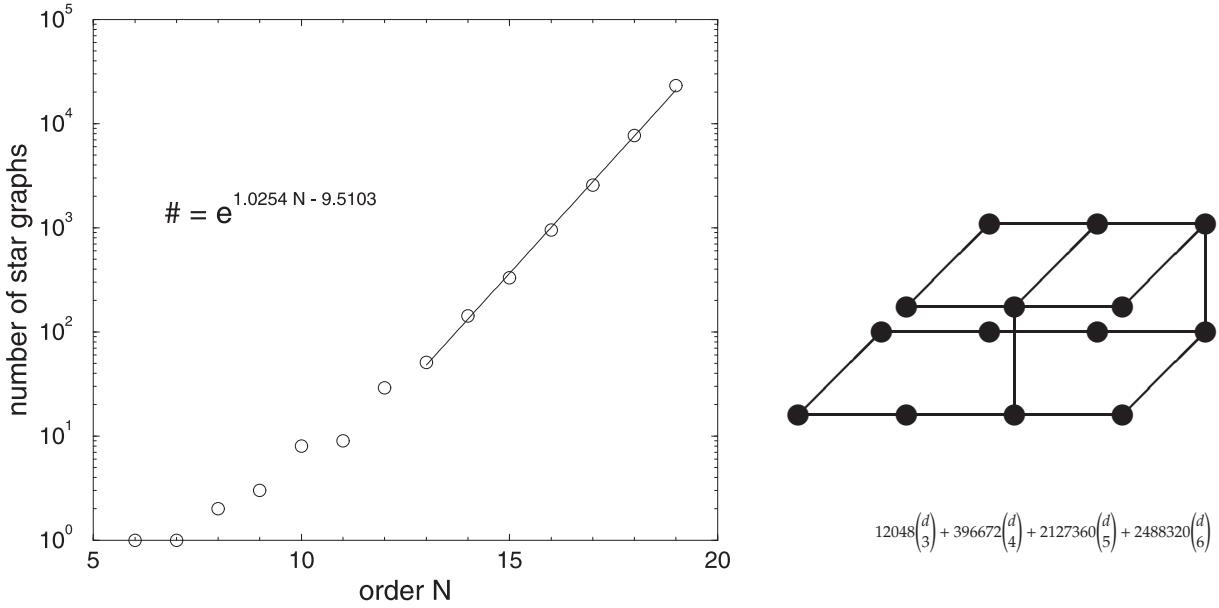

Figure 10.1: *Left*: Growth behaviour of the number of star graphs of order N that can be embedded in hypercubic lattices $\mathbb{Z}^d$. *Right*: A star graph of order 17 and its (weak) embedding number, carrying the dependence on the dimension (up to $d = 6$).

pure case exhibits a first-order phase transition, we observed the expected softening by quenched disorder and estimated the critical exponent of the induced second-order transition.

Further new results were also obtained for the bond-percolation problem in various dimensions d, which is contained in the general formulation as the $q \to 1$ limit [8].

[1] C. Domb, M.S. Green (Eds.): *Phase Transitions and Critical Phenomena*, Vol. 3 (Academic Press, New York 1974)
[2] R.R.P. Singh, S. Chakravarty: Phys. Rev. B **36**, 546 (1987)
[3] M. Hellmund, W. Janke: Cond. Matter Phys. **8**, 59 (2005)
[4] M. Hellmund, W. Janke: Comp. Phys. Comm. **147**, 435 (2002)
[5] M. Hellmund, W. Janke: Leipzig preprint (2005), to be published
[6] W. Janke et al.: invited plenary talk, PoS LAT2005, 018 (2005)
[7] M. Hellmund, W. Janke: Nucl Phys. B (Proc. Suppl.) **106/107**, 923 (2002); Phys. Rev. E **67**, 026 118 (2003)
[8] M. Hellmund, W. Janke: Leipzig preprint (2005), to be published

10.5 Droplet/Strip and Evaporation/Condensation Transitions

E. Bittner, W. Janke, T. Neuhaus* A. Nußbaumer

*John von Neumann-Institut für Computing (NIC), Forschungszentrum Jülich

The free energy of the three-dimensional Edwards-Anderson Ising spin-glass model exhibits in the low-temperature phase a rugged multi-valley structure. Consequently

standard canonical Monte Carlo simulations are severely hampered by an exponential slowing down with increasing system size. This led to the application of multicanonical simulations, e.g. for the overlap parameter, which are designed by means of auxiliary weight factors to smooth out the energy landscape and thus to lead to uniform probability distributions. Given such a flat distribution, a much faster random walk behaviour in the corresponding observable is naively expected. In the actual simulations, however, one still observes jumps in the time series which can be attributed to so-called "hidden barriers".

In recent numerical work, Neuhaus and Hager [1] were able to identify such barriers in the magnetisation M of the much simpler two-dimensional Ising model. They first observed a geometrically induced first-order phase transition from a droplet to a strip domain and showed that even a perfect multimagnetic simulation operating with the optimal weights still needs an exponential time to overcome the associated free energy barrier, which turned out to be in agreement with earlier analytical considerations of Leung and Zia [2]. To obtain more qualitative insights, we determined directly the anisotropy of a configuration during the transition by measuring its structure function. Simulating different system sizes with Kawasaki dynamics (M = const.), the scaling of the anisotropy leads to a value for the barrier height in good agreement with the theoretical prediction. By generalising these considerations to the case of the three-dimensional Ising model, new transitions could be identified analytically and verified numerically. Also the various crystal shapes emerging during the transition could be visualised.

Another first-order like transition can be identified when the first large droplet forms out of the fluctuations around the equilibrium magnetization. Invoking the equivalent lattice-gas picture, Biskup et al. [3] recently studied the behaviour of d-dimensional finite-volume liquid-vapour systems at a fixed excess δN of particles above the ambient gas density. Identifiying a dimensionless parameter $\Delta(\delta N)$ and a universal constant $\Delta_c(d)$, they were able to show that for $\Delta < \Delta_c$ a droplet of the dense phase occurs, while for $\Delta > \Delta_c$ the excess is absorbed in the background (see Fig. 10.2). The fraction λ_Δ of excess particles forming the droplet is given explicitly.

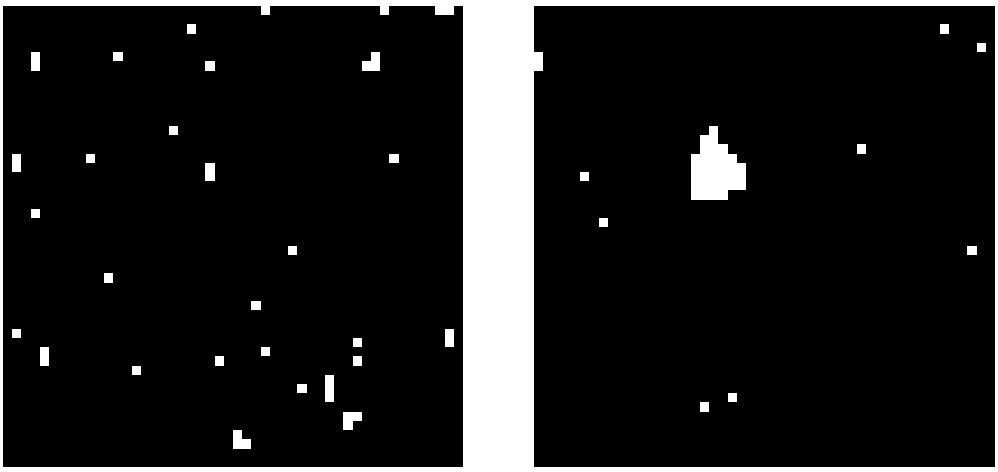

Figure 10.2: Two snapshots of a $L = 50$ Ising system at the same value of the magnetisation. *Left*: Evaporated system, a large number of very small bubbles exists (1 to 3 spins). *Right*: Condensed system, a single large droplet that has absorbed nearly all small bubbles.

To verify these results, we have simulated the spin-1/2 Ising model on a square lattice at constant magnetisation equivalent to a fixed particle excess. We measured the largest minority droplet, corresponding to the liquid phase, at various system sizes ($L = 40, \ldots, 640$). Using analytic values for the spontaneous magnetisation m_0, the susceptibility χ and interfacial free energy τ_W for the infinite system, we were able to determine λ_Δ in very good agreement with the theoretical prediction [4, 5]. In order to test the universal aspects of this evaporation/condensation transition, the measurements were repeated for next-nearest neighbour interactions and on a triangular lattice, giving similarly good results.

[1] T. Neuhaus, J. Hager: Stat. Phys. **113**, 47 (2003)
[2] K. Leung, R. Zia: J. Phys. A **23**, 4593 (1990)
[3] M. Biskup et al.: Europhys. Lett. **60**, 21 (2002)
[4] A. Nußbaumer et al.: PoS LAT2005, 252 (2005)
[5] A. Nußbaumer et al.: Leipzig preprint (2006), to be published

10.6 Harris-Luck Criterion and Potts Models on Random Graphs

W. Janke, G. Kähler*, M. Weigel†

*Department of Physics, University of North Dakota, Fargo, USA
†Department of Physics, University of Waterloo, Canada

The Harris criterion judges the relevance of uncorrelated, quenched disorder for altering the universal properties of physical systems close to a continuous phase transition [1]. For this situation, as e.g., in the paradigmatic case of a quenched random-bond or bond diluted model, a change of universal properties is expected for models with a positive specific heat exponent α, i.e., the relevance threshold is given by $\alpha_c = 0$. For the physically more realistic case of spatially correlated disorder degrees of freedom, Harris' scaling argument can be generalised, yielding a shifted relevance threshold $-\infty < \alpha_c \leq 1$ known as Luck criterion [2]. The value of α_c depends on the quality and strength of the spatial disorder correlations as expressed in a so-called geometrical fluctuation or *wandering exponent*.

We consider the effect of a different, topologically defined type of disorder, namely the result of *connectivity disorder* produced by placing spin models on *random graphs*. As it turns out, the Harris-Luck argument can be generalised to this situation, leading to a criterion again involving a suitably defined wandering exponent of the underlying random graph ensemble. Using a carefully tailored series of finite-size scaling analyses, we precisely determined the wandering exponents of the two-dimensional ensembles of Poissonian Voronoï-Delaunay random lattices as well as the quantum gravity graphs of the dynamical triangulations model, thus arriving at explicit predictions for the relevance threshold α_c for these lattices [3]. As a result, for Poissonian Voronoï-Delaunay random graphs the Harris criterion $\alpha_c = 0$ should stay in effect, whereas for the dynamical triangulations the threshold is shifted to a negative value, $\alpha_c \approx -2$. The latter result is in perfect agreement with Monte Carlo simulations of the q-states Potts model [4] as

well as an available exact solution of the percolation limit $q \to 1$ [5]. For the Voronoï-Delaunay triangulations, the Ising case $q = 2$ with $\alpha = 0$ is marginal and a change of universal properties cannot normally be expected. The $q = 3$ Potts model with $\alpha = 1/3$, on the other hand, should be shifted to a new universality class. Following up on a first exploratory study for small graphs [6], we performed high-precision cluster-update Monte Carlo simulations for rather large lattices of up to 80 000 triangles to investigate this model. Astonishingly, however, the (exactly known) critical exponents of the square-lattice $q = 3$ Potts model are reproduced to high precision [7]. To clarify this situation, we recently studied a generalised model introducing a distance dependence of the interactions [8].

[1] A.B. Harris: J. Phys. C **7**, 1671 (1974)
[2] A. Weinrib, B. I. Halperin: Phys. Rev. B **27**, 413 (1983); J.M. Luck: Europhys. Lett. **24**, 359 (1993)
[3] W. Janke, M. Weigel: Phys. Rev. B **69**, 144 208 (2004), arXiv:cond-mat/0310269
[4] W. Janke, D.A. Johnston: Nucl. Phys. B **578**, 681 (2000)
[5] V.A. Kazakov: Mod. Phys. Lett. A **4**, 1691 (1989)
[6] F.W.S. Lima et al.: Eur. Phys. J. B **17**, 111 (2000)
[7] W. Janke, M. Weigel: Acta Phys. Polon. B **34**, 4891 (2003)
[8] G. Kähler: Diploma Thesis, University of Leipzig (2004)

10.7 The F Model on Quantum Gravity Graphs

W. Janke, M. Weigel*

*Department of Physics, University of Waterloo, Canada

As an alternative to various other approaches towards a theory of quantum gravity, the *dynamical triangulations* method has proved to be a successful discrete Euclidean formulation in two dimensions (2D). There, the integration over all metric tensors as the dynamic variables is performed by a summation over all possible gluings of equilateral triangles to form a closed surface of a given (usually planar) topology. The powerful methods of matrix integrals and generating functions allow for an exact solution of the pure 2D gravity model. Furthermore, matrix models can be formulated for spin models coupled to random graphs and some of them could be solved analytically. More generally, the "dressing" of the weights of $c < 1$ conformal matter coupled to 2D quantum gravity is predicted by the KPZ/DDK formula [1], in agreement with all known exact solutions.

One of the most general models in statistical mechanics is Baxter's 8-vertex model [2]. Thus its behaviour on coupling it to dynamical *quadrangulations*, i.e., surfaces built from simplicial squares, is of general interest. Although a solution of special slices of this model could recently be achieved [3], the general model could not yet be solved. Heading for computer simulations, one first has to ensure the correct handling of the (quite unorthodox) geometry of four-valent graphs or quadrangulations in the dual language. While simulations of three-valent graphs have already been extensively done, the code for ϕ^4 graphs had to be newly developed and tested [4]. Due to the fractal

structure of the graphs being described as a self-similar tree of "baby universes", this local dynamics suffers from critical slowing down. To alleviate the situation, we adapted a non-local update algorithm known as "minBU surgery" [5].

Combining the developed techniques, we simulated the F model, a symmetric case of the 8-vertex model, coupled to planar random ϕ^4 graphs. On regular [6] as well as random lattices [7, 8], this model is expected to exhibit a Kosterlitz-Thouless transition to an anti-ferroelectrically ordered state [2, 3]. The numerical analysis of this model turned out to be exceptionally difficult due to the combined effect of the highly fractal structure of the graphs and the presence of strong logarithmic corrections. Still, a scaling analysis of the staggered polarizability yields results [7] in agreement with the predictions of [3] as far as the order of the transition and the location of the transition point are concerned.

[1] V. Knizhnik et al.: Mod. Phys. Lett. A **3**, 819 (1988); F. David: Mod. Phys. Lett. A **3**, 1651 (1988); J. Distler, H. Kawai: Nucl. Phys. B **321**, 509 (1989)
[2] R. Baxter: *Exactly Solved Models in Statistical Mechanics* (Academic Press, London 1982)
[3] V.A. Kazakov, P. Zinn-Justin: Nucl. Phys. B **546**, 647 (1999); I. Kostov: Nucl. Phys. B **575**, 513 (2000); P. Zinn-Justin: Europhys. Lett. **50**, 15 (2000)
[4] M. Weigel, W. Janke: Nucl. Phys. B (Proc. Suppl.) **106–107**, 986 (2002); M. Weigel: Ph.D. Thesis, University of Leipzig (2002)
[5] J. Ambjorn et al.: Phys. Lett. B **325**, 337 (1994)
[6] M. Weigel, W. Janke: J. Phys. A **38**, 7067 (2005), arXiv:cond-mat/0501222
[7] M. Weigel, W. Janke: Nucl. Phys. B **719**, 312 (2005), arXiv:hep-lat/0409028
[8] W. Janke, M. Weigel: PoS LAT2005, 251 (2005)

10.8 Folding Kinetics and Thermodynamics of Coarse-Grained Protein Models

M. Bachmann, W. Janke, C. Junghans, A. Kallias, J. Schluttig, S. Schnabel, T. Vogel

Functional proteins in a biological organism are typically characterized by a unique three-dimensional molecular structure, which makes the protein selective for individual functions, e.g., in catalytic, enzymatic, and transport processes. In most cases, the free-energy landscape is believed to exhibit a rough shape with a large number of local minima and, for functional proteins, a deep, funnel-like global minimum. This assumed complexity is the reason, why it is difficult to understand how the random-coil conformation of covalently bonded amino acids – the sequence is generated in the ribosome according to a certain genetic sequence in the DNA – spontaneously folds into a well-defined stable "native" conformation within microseconds to seconds. Furthermore, it is expected that there is only a small number of folding paths from any unfolded conformation to this final fold.

Protein folding is hierarchical, i.e, the generation of the sequence (primary structure) is followed by the formation of secondary structures (α-helices, β-sheets, turns) by hydrogen bonding. Eventually, the folding into the "native" conformation, i.e., the tertiary structure, is accompanied by a global conformational transition, which requires

cooperativity of all amino acids in a tertiary protein domain [1]. Effectively, this process is due to the attraction of polar amino acids by the polar aqueous environment, and the resulting effective attractive interaction between hydrophobic amino acids. Therefore, in many cases, a folded protein domain possesses a compact hydrophobic core screened from the solvent by a shell of polar residues.

Computer simulations of protein folding are extremely exhaustive, if all atomic and molecular interactions are involved in the protein model. Since the hydrophobic interaction is expected to be the main driving force in the tertiary folding process, we have studied kinetic and statistical aspects employing and comparing simplified, coarse-grained models, such as the minimalistic hydrophobic-polar (HP) lattice model, different variants of similar off-lattice models (so-called AB-like models), as well as knowledge-based Gō-like C^{α} models. Sophisticated computational methods were applied, e.g., multicanonical chain-growth methods [2] for the lattice models, energy-landscape paving optimization, multicanonical sampling, parallel tempering, as well as molecular dynamics for the off-lattice models. The focus of the kinetic studies was on contact ordering in folding and unfolding events [3, 4], the thermodynamic aspects included the identification of folding channels and, in particular, free-energy landscapes as a function of a suitable system parameter [5, 6, 7].

[1] M. Bachmann, W. Janke: Comp. Phys. Comm. **169**, 111 (2005)
[2] M. Bachmann, W. Janke: Phys. Rev. Lett. **91**, 208 105 (2003)
[3] A. Kallias: Diploma Thesis, Universität Leipzig, 2005
[4] J. Schluttig: Diploma Thesis, Universität Leipzig, 2005
[5] M. Bachmann et al.: Phys. Rev. E **71**, 031 906 (2005)
[6] S. Schnabel: Diploma Thesis, Universität Leipzig, 2005
[7] S. Schnabel et al.: preprints (2006), to be published

10.9 Conformational Transitions and Pseudo-Phase Diagrams of Nongrafted Flexible Polymers and Peptides in a Cavity

M. Bachmann, W. Janke

In this project, we have investigated the temperature- and solubility dependence of polymer and peptide adsorption to planar solid substrates. The generalization of our multicanonical chain-growth algorithm [1] enabled us to determine qualitatively the *whole* temperature-solubility pseudo-phase diagram for such a hybrid system within a single simulation [2].

First, we studied the conformational transitions that flexible polymers of different, but finite lengths experience in the adsorption process [2, 3]. We found transitions between various (pseudo-)phases, but only a few of them are expected to be present in the thermodynamic limit of infinite chain length, i.e., the transitions between these phases are phase transitions in the thermodynamic sense. The main phases are separated into the adsorption phases of single-layer compact conformations (AC1), multiple-layer compact structures (AC2), globular, unstructured conformations (so-called surface-attached globules, AG), and expanded, random-coil conformations (AE). In the region

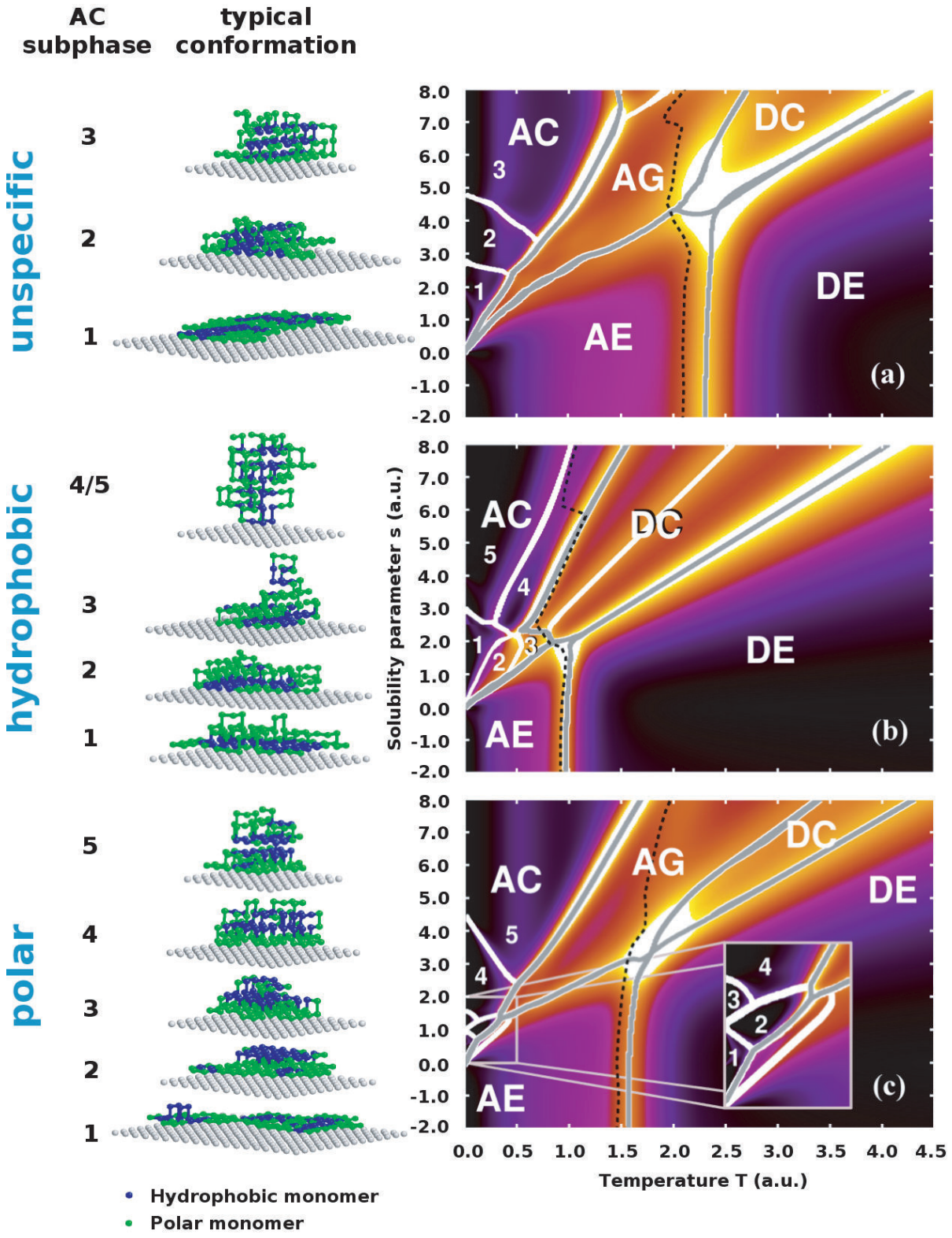

Figure 10.3: Shaded profiles of the specific heats as a function of temperature T and solubility s for a 103-mer in the vicinity of three substrates differing in their affinity to attract hydrophobic and/or polar monomers: (**a**) unspecific, i.e., type-independently attractive, (**b**) hydrophobic, and (**c**) polar. The ridges of this landscape indicate conformational transitions and separate pseudo-phases and subphases (gray and white lines, respectively). Also shown are typical conformations in the respective subphases of the adsorbed-compact (AC) pseudo-phases [4, 5, 6].

of desorbed conformations, we distinguish globular/compact (DC) and random-coil (DE) phases. Furthermore, we find a surprisingly rich structure of subphases, whose properties are highly dependent on the exact number of monomers. Although these subphases are unstable in the thermodynamic limit, they are not less interesting, because with today's high-resolution equipment it should be possible to detect them in experiments. In addition, these subphases might also be of relevance in certain nanotechnological applications.

We also studied the substrate-specificity of the pseudo-phase diagrams for the adsorption of peptides [4, 5, 6]. This project was stimulated by related experiments [7]. We investigated a hydrophobic-polar lattice protein with 103 monomers, whose bulk properties were subject of a recent study [8] in the vicinity of three different substrates. The first was equally attractive to hydrophobic and polar monomers, the second only for hydrophobic, and the third only for polar residues. The specific-heat profile as a function of temperature and solubility is shown in Fig. 10.3. Differences in the locations of the transition lines can be clearly identified as well as the absence of a globular pseudo-phase in the case of the hydrophobic substrate. The most prominent differences appear in the AC phases, where the type-dependence of the concurring forces (surface attraction and intrinsic monomer-monomer interaction) is particularly apparent.

[1] M. Bachmann, W. Janke: Phys. Rev. Lett. **91**, 208 105 (2003)
[2] M. Bachmann, W. Janke: Phys. Rev. Lett. **95**, 058 102 (2005)
[3] M. Bachmann, W. Janke: Phys. Rev. E **73**, 041 802 (2006)
[4] K. Goede et al.: BIOforum 10/2005, p. 53
[5] M. Bachmann, W. Janke: Phys. Rev. E **73**, 020 901(R) (2006)
[6] M. Bachmann, W. Janke: in *Proc. NIC Symp. 2006*, ed. by G. Münster, D. Wolf, M. Kremer, NIC Series, Vol. **32**, (John von Neumann Institute for Computing, Jülich 2006), p 245
[7] K. Goede et al.: Nano Lett. **4**, 2115 (2004)
[8] M. Bachmann, W. Janke: J. Chem. Phys. **120**, 6779 (2004)

10.10 Adsorption Specificity of Semiconductor-Binding Synthetic Peptides

M. Bachmann, W. Janke, K. Goede[*], M. Grundmann[*], A. Beck-Sickinger[†], K. Holland-Nell[†], A. Irbäck[‡], S. Mitternacht[‡], S. Mohanty[§], G. Gökoğlu[¶], T. Çelik[¶]

[*]Institute for Experimental Physics II
[†]Institute of Biochemistry
[‡]Department of Theoretical Physics, Lund University, Sweden
[§]John von Neumann-Institut für Computing (NIC), Forschungszentrum Jülich
[¶]Fizik Mühendisliği Bölümü, Hacettepe Üniversitesi Ankara, Turkey

The interest in understanding the mechanism of specific adsorption of polymers and peptides to solid substrates has enormously grown in the past years as the experimental equipment, biochemical structure analysis, and nanotechnology have reached such

a high level of resolution that the vision of practical biochemical and medical applications of hybrid organic-inorganic systems, such as nanoelectronic circuits, nanosensory devices, and pattern recognition by molecular substances, becomes more and more concrete.

The main inspiration for this joint project of theoretical and experimental physicists and biochemists came from recent adsorption experiments of short synthetic peptides with 12 amino acids to semiconductors [1, 2], where the specificity of binding properties was investigated in detail. In these experiments, it could be shown that the interplay of different specific properties of the solid (crystal orientation of the surface, electronic affinity, polarization), the peptide (amino acid content and, in particular, the sequence), and the surrounding solvent (solubility) strongly influence the adsorption of the peptide at the solid-fluid interface [3]. The binding or docking process, which is possibly accompanied by conformational transitions, is not yet understood. Therefore, the main objective of this interdisciplinary cooperation is the unravelling of the principles of peptide adsorption to solids, in particular semiconductors.

Since we expect that structural properties of the peptide fold and, in particular, conformational transitions in the fluid bulk as well as in the vicinity of the substrate have impact on the binding affinity, we have performed, in an inital step, exhaustive computer simulations investigating bulk properties of the peptides used in the experiment [2]. We found indications for helix-coil transitions employing an all-atom protein model based on the ECEPP/3 force field, extended by an implicit-solvent model [4]. As synthetic peptides are typically less stable than bioproteins selected by evolution, it is not yet clear whether these transitions can also be identified in biochemical analyses. Another reason is that the model used cannot predict precise, realistic transition temperatures. For this reason, these results are to be compared with outputs of other models, e.g., the simplified all-atom model with reduced parameter set developed by the Lund group [5]. A future task is to extend this model by an effective interaction between soft and solid matter to make it applicable for simulations of hybrid systems.

[1] S. R. Whaley et al.: Nature **405**, 665 (2000)
[2] K. Goede et al.: Nano Lett. **4**, 2115 (2004)
[3] K. Goede et al.: BIOforum 10/2005, p. 53
[4] G. Gökoğlu et al.: preprint (2006), to be published
[5] A. Irbäck et al.: Biophys. J. **85**, 1466 (2003)

10.11 Geometrical Approach to Phase Transitions

W. Janke, A.M.J. Schakel

This project aims at a geometrical description for a variety of phase transitions, ranging from thermal transitions in spin models over Bose-Einstein condensation in dilute gases to the deconfinement transition in gauge theories. Since many exact results are known in two dimensions, 2D models form the main focus of the present research. Using Monte Carlo simulations, the fractal structure of the spin configurations of the 2D Ising model was investigated [1], whose thermal critical behaviour can be equivalently described as percolation of suitably defined clusters of spins. The fractal dimension of these so-called Fortuin-Kasteleyn clusters, which encode the entire critical behaviour, and that

of their boundaries have been determined numerically by applying standard finite-size scaling to observables such as the percolation probability and the average cluster size. The obtained results are in excellent agreement with theoretical predictions and partly provide significant improvements in precision over existing numerical estimates [2].

Also the naive "geometrical" spin clusters encode critical behaviour, namely that of the diluted model. Within this project, recently a one-to-one map between the two cluster types could be established. By numerically determining the fractal structure of the geometrical clusters and that of their boundaries, this map was verified to high precision [1]. Based on numerical results on the high-temperature representation of the 2D Ising model [3], a generalization of the famous de Gennes result, that connects the critical behaviour of the O(N) model in the limit $N \to 0$ to the configurational entropy of a polymer chain in a good solvent, to arbitrary $-2 \leq N \leq 2$ was given [4]. The high-temperature representation can be visualized by graphs on the lattice. In the high-temperature phase, where they have a finite line tension, large graphs are exponentially suppressed. Upon approaching the critical temperature, the line tension vanishes and the graphs proliferate. Their fractal structure was shown to encode the entire critical behaviour, so that a purely geometrical description of the phase transition in the O(N) model was obtained.

When including vacancies, it is generally believed that the O(N) model gives in addition to critical behaviour rise to also tricritical behaviour. By gradually increasing the activity of the vacancies, the continuous O(N) phase transition is eventually driven first order at a tricritical point. In the context of polymers ($N \to 0$), the latter obtains by lowering the temperature to the so-called Θ point where the increasingly important van der Waals attraction between monomers causes the polymer chain to collapse. Up to now, relatively little is known about the tricritical behaviour for $N \neq 0$. By arguing that the fractal dimensions of the high-temperature graphs close to the tricritical point are in one-to-one correspondence with those at the critical point, exact, albeit non-rigorous, predictions could be made for the tricritical exponent η and, through scaling relations, for the ratios β/ν and γ/ν [4].

[1] W. Janke, A.M.J. Schakel: Nucl. Phys. B **700**, 385 (2004)
[2] J. Asikainen et al.: Eur. Phys. J. B **34**, 479 (2003); S. Fortunato: Phys. Rev. B **66**, 054 107 (2002)
[3] W. Janke, A.M.J. Schakel: Phys. Rev. E **71**, 036 703 (2005)
[4] W. Janke, A.M.J. Schakel: Phys. Rev. Lett. **95**, 135 702 (2005), arXiv:cond-mat/0502062

10.12 Vortex-Line Percolation in a Three-Dimensional Complex Ginzburg-Landau Model

E. Bittner, W. Janke, A. Krinner*, A.M.J. Schakel, A. Schiller†, S. Wenzel

*Interdisziplinäres Zentrum für Bioinformatik, Universität Leipzig
†Theory of Elementary Particles group

The superfluid phase transition can be described either by a directional XY model or by an O(2) symmetric scalar field theory, whose Hamiltonian is commonly expressed

with a complex field $\psi(\vec{r}) = |\psi(\vec{r})|e^{i\phi(\vec{r})}$ in the Ginzburg-Landau form. Invoking duality arguments, this model can also be represented by the partition function of an equivalent theory in which the spin configurations are replaced by configurations of closed lines. The loops of this equivalent theory can be identified with the vortex lines of the original theory, which thus may play an important role in determining the properties of the λ-transition in liquid helium. A seemingly natural approach to study the vortex degrees of freedom is to associate with every spin configuration generated in a lattice Monte Carlo simulation a number of vortex loops. The hope is then that the transition could be identified with a non-zero probability of finding vortex loops that extend through the whole system [1], a phenomenon which is usually called percolation.

Percolational studies of spin clusters in the Ising model showed that one has to handle this approach carefully. It only works, if one uses a proper stochastic definition of clusters [2, 3, 4, 5]. The Fortuin-Kasteleyn (FK) clusters of spins can be obtained from the geometrical spin clusters, which consist of nearest neighbor sites with their spin variables in the same state, by laying bonds with a certain probability between the nearest neighbors. The resulting FK clusters are in general smaller than the geometrical ones and also more loosely connected. For the different cluster types one obtains in general different percolation thresholds and critical exponents.

In three-dimensional, globally O(2) symmetric theories the percolating objects are vortex lines forming closed networks [6, 7, 8, 9]. One of the main questions we want to address is: Is there a similar clue in the case of vortex networks as for spin clusters, or do they display different features? Therefore we connect the obtained vortex-line elements to closed loops, which are geometrically defined objects. When a branching point, where $n \geq 2$ junctions are encountered, is reached, a decision on how to continue has to be made. This step involves a certain ambiguity. We want to investigate the influence of the probability of treating such a branching point as a knot, see Fig. 10.4.

In discussing the phase transition of the Ginzburg-Landau theory, we study a geometrically defined vortex-loop network as well as the magnetic properties of the system in the vicinity of the critical point. Using high-precision Monte Carlo techniques we consider an alternative formulation of the geometrical excitations in relation to the global O(2) symmetry breaking, and check if both of them exhibit the same critical be-

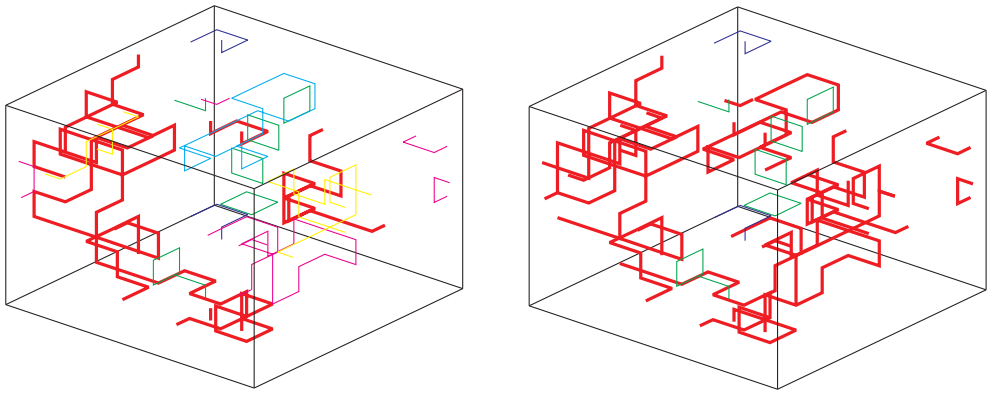

Figure 10.4: *Left*: Vortex-loop network generated at the thermodynamic critical point for lattice size $L = 8$ and probability $c = 0.4$ to treat a branching point as a knot. *Right*: Vortex-loop network generated treating *all* branching points as knots for the same spin configuration as in the left plot.

haviour leading to the same critical exponents and therefore to a consistent description of the phase transition. Different percolation observables are taken into account and compared with each other.

The second part of this project concentrates on an extension of the three-dimensional complex Ginzburg-Landau model by adding a minimal coupling to an external compact U(1) gauge field (Abelian Higgs model) [10, 11], relevant for the universal aspects of superconductors and also for elementary particle physics and cosmology. In the latter case, a first-order phase transition line ending at a critical point was found in the Higgs coupling – "hopping parameter" (λ–κ) plane for small λ at a fixed gauge coupling (β) which, similar to the liquid-gas phase diagram, separates the Higgs and "confinement" phase. Based on our data for the magnetic monopole density and other quantities we present arguments that this phase boundary continues for larger λ as a so-called Kertész line [11], across which no phase transition in a strict thermodynamic sense takes place, but percolation observables do exhibit singular behaviour. This picture is completely analogous to the scenario proposed by Kertész for the liquid-gas phase diagram.

[1] K. Kajantie et al.: Phys. Lett. B **482**, 114 (2000)
[2] P.W. Kasteleyn, C.M. Fortuin: J. Phys. Soc. Jap. **26**, 11 (1969); C.M. Fortuin, P.W. Kasteleyn: Physica **57**, 536 (1972); C.M. Fortuin: Physica **58**, 393 (1972), *ibid.* **59**, 545 (1972)
[3] A. Coniglio, W. Klein: J. Phys. A **13**, 2775 (1980)
[4] S. Fortunato: J. Phys. A **36**, 4269 (2003)
[5] W. Janke, A.M.J. Schakel: Nucl. Phys. B **700**, 385 (2004)
[6] A. Krinner: Diploma Thesis, University of Leipzig (2004)
[7] E. Bittner, W. Janke: Phys. Rev. B **71**, 024 512 (2005)
[8] E. Bittner et al.: Phys. Rev. B **72**, 094 511 (2005)
[9] W. Janke, E. Bittner: in Proc. 8th Int. Conf. *Path Integrals from Quantum Information to Cosmology*, Prague, Czech Republic, 6–10 June 2005, ed. by Č. Burdik et al. (JINR Press, Dubna 2006) [electronically available at: www.jinr.ru/publish/Proceedings/Burdik-2005/index.html]
[10] S. Wenzel: Master Thesis, University of Leipzig (2003)
[11] S. Wenzel et al.: Phys. Rev. Lett. **95**, 051 601 (2005), arXiv:cond-mat/0503599

10.13 Ageing Phenomena in Ferromagnets

W. Janke, D.A. Johnston*, E. Lorenz, R. Megaides†

*School of Mathematical and Computer Sciences, Heriot-Watt University, Edinburgh, UK
†Department of Physics, Brunel University of West London, UK

When a ferromagnet is suddenly quenched from the disordered into the ordered phase at a temperature below the Curie point, its temporal relaxation exhibits ageing phenomena similar to the behaviour of glasses and spin glasses. For ferromagnets this effect could recently be described in quite some detail with the help of dynamical symmetry arguments [1]. While the assumptions underlying these theoretical considerations are very plausible, their validity is not proven and it is hence important to test the predictions by means of alternative methods such as Monte Carlo simulations. Recent studies

of the Ising model in two and three dimensions showed indeed good agreement [2]. Still, to ensure the general applicability of the theoretical framework, typical representative models of other universality classes should be investigated. In this project we therefore performed Monte Carlo studies of the two-dimensional q-state Potts models with $q = 3$ and 8 states per spin which, in equilibrium, exhibit phase transitions of second and first order, respectively. We determined two-time correlators as well as the temporal and spatio-temporal behaviour of the thermoremanent response function. In order to achieve the necessary accuracy, one has to prepare many independent random start configurations and monitors for each copy its stochastic time evolution after the quench into the low-temperature phase. The final results are obtained by averaging over the copies. Also for this model our results [3, 4] show very good agreement with the analytical predictions.

Quite similar phenomena can be observed in the so-called gonihedric lattice spin model which was orginally constructed as a discretized string (or, equivalently, self-avoiding surface) model [5]. Generically it consists of nearest-neighbour, next-nearest neighbour and plaquette interactions with fine-tuned coupling constants. In its original formulation the spins are taken to be of Ising type, i.e., $s = \pm 1$. It was soon recognized that this type of model exhibits a very intricate temporal relaxation behaviour in Monte Carlo simulations reminiscent of ageing phenomena in structural glasses. The analogy is, in fact, closer to (off-lattice) structural than to (lattice) spin glasses since *no* quenched disorder is involved in gonihedric models. The gonihedric model is hence a rare example for lattice models *without* quenched disorder that display ageing phenomena, and from this point of view it has attracted considerable interest also in the statistical physics community. After reproducing the quite intricate relaxation behaviour for the Ising case [6] and refining some of the measurement prescriptions with further input from our experiences with the properties of glasses and spin glasses, we also performed first exploratory computer experiments with suitable generalizations to Potts and O(n) symmetric spin models with $n \geq 2$, in particular the O(2) or XY model [7].

[1] M. Henkel: Nucl. Phys. B **641**, 405 (2002)
[2] M. Henkel, M. Pleimling: Phys. Rev. E **68**, 065 101(R) (2003); M. Henkel et al.: Europhys. Lett. **68**, 191 (2004)
[3] E. Lorenz: Diploma Thesis, University of Leipzig (2005)
[4] E. Lorenz, W. Janke: Leipzig preprint (2006), to be published
[5] G.K. Savvidy, K.G. Savvidy: Phys. Lett. B **337**, 333 (1994)
[6] P. Dimopoulos et al.: Phys. Rev. E **66**, 056 112 (2002)
[7] R. Megaides: Master Thesis, University of Leipzig (2004)

10.14 Critical Amplitude Ratios in the Baxter–Wu Model

W. Janke, L.N. Shchur*

*Landau Institute, Chernogolovka, Russia

At a second-order phase transition not only critical exponents but also certain amplitude ratios are universal, i.e., do not depend on the details of the considered statistical

system. A typical example is provided by the scaling relation for the magnetic susceptibility χ which in the vicinity of the critical temperature T_c behaves according to $\chi \sim \Gamma_{\pm}|T/T_c - 1|^{-\gamma}$, where γ is a critical exponent and Γ_+ and Γ_- denote the critical amplitudes in the high- and low-temperature phase, respectively. The ratio Γ_+/Γ_- is then such a universal amplitude ratio, whose value could recently be predicted analytically for the two-dimensional q-state Potts model with $q = 2$, 3 and 4 states [1, 2]. While for $q = 2$ and 3 this prediction could subsequently be confirmed with numerical techniques (Monte Carlo simulations and high-temperature series expansions) [3], the situation for $q = 4$ remained controversial. The resason for the disagreement lies probably in relatively strong logarithmic corrections of the leading scaling behaviour [4]. In order to test this conjecture, we considered the two-dimensional Baxter-Wu model [5] (a model with three-spin interaction on a triangular lattice) which is known from its exact solution to belong to the $q = 4$ universality class, but does *not* exhibit logarithmic corrections. By employing a special cluster-update algorithm [6] we have performed extensive Monte Carlo simulations of this model which are currently analysed.

[1] G. Delfino, J.L. Cardy: Nucl. Phys. B **519**, 551 (1998)
[2] G. Delfino et al.: Nucl. Phys. B **565**, 521 (2000)
[3] L.N. Shchur et al.: Nucl. Phys. B **620**, 579 (2002)
[4] J. Salas, A.D. Sokal: J. Stat. Phys. **88**, 567 (1997)
[5] R.J. Baxter, F.Y. Wu: Phys. Rev. Lett. **31**, 1294 (1973); Aust. J. Phys. **27**, 357 (1974)
[6] M.A. Novotny, H.G. Evertz: in *Computer Simulation Studies in Condensed Matter Physics*, Vol. VI, ed. by D.P. Landau et al. (Springer, Berlin 1993), p 188

10.15 Quantum Monte Carlo Studies

R. Bischof, L. Bogacz, P.R. Crompton, D. Ihle[*] , W. Janke, I. Juhász Junger[*], Z.X. Xu[†], H.P. Ying[†], B. Zheng[†], S. Wenzel

[*]Condensed Matter Theory group
[†]Zhejiang Institute of Modern Physics, Zhejiang University, Hangzhou, P.R. China

The Valence Bond Solid picture of spin-wave superconductivity developed following Haldane's conjecture [1] gives a precise framework for determining the critical properties of a variety of quasi-one dimensional ferromagnetic spin applications exploiting low-temperature superconductivity phenomena currently being fabricated for use in the computing and recording industries. We investigate valence bond state quantum phase transitions by means of the continuous time Quantum Monte Carlo loop cluster algorithm [2]. The algorithm has allowed for numerical investigation in regimes previously limited by algorithmic development, and also of the analytic conjecture itself (recently generalised for our inhomogeneous-spin cases of interest [3]) with now indications of novel quantum interference effects [4]. The proposal of Haldane was essentially for single-spin chains but the numerical testing of the ideas has subsequently pushed forward the boundaries of potential quantum interference solutions [5, 6]. Making for a closing mapping into experimental systems through the inclusion of higher spin representations and off-diagonal Hamiltonian contributions such as spin-ladder models, treatable via numerical study [7].

Specifically, we are determining the critical exponents that govern the scaling of numerical results to allow both for a closer experimental mapping and to further investigate the range of applicability of the central algorithmic technique [8]. An investigation of the short-time dynamics exponents of this method further establishes the credibility of this approach for the novel states we would intend to investigate [9, 10]. Providing also a means to further develop both improved estimators for the superconducting gap states by means of new cross-correlated statistical measures, and to also gain a deeper understanding of the effect of applying and removing magnetic fields to these systems and magnetic impurities.

Furthermore, the thermodynamic properties (magnetization, isothermal magnetic susceptibility, specific heat) of one- and two-dimensional ferromagnets with arbitrary spin S in a magnetic field are investigated by second-order Green-function theory and compared with quantum Monte Carlo simulations for the $S = 1/2$ chain with $N = 128$ spins and the $S = 1$ ferromagnet on an $N = 64$ chain and an $N = 64 \times 64$ square lattice, employing the so-called stochastic series expansion (SSE) method [11]. Good agreement between the results of both approaches is found [12]. In one dimension and at low magnetic fields, two maxima in the temperature dependence of the specific heat of both the $S = 1/2$ and $S = 1$ ferromagnets are found. For $S > 1$ only one maximum occurs, as in the two-dimensional ferromagnets. This implies that the appearance of two specific-heat maxima is a distinctive effect of quantum fluctuations.

[1] F. D. M. Haldane: Phys. Rev. Lett. **61**, 8 (1988)
[2] B. B. Beard, U.-J. Wiese: Phys. Rev. Lett. **77**, 5130 (1996)
[3] K. Takano: Phys. Rev. B **61**, 13 (2000)
[4] P. Zhang et al.: to appear in Mod. Phys. Lett. A (2005)
[5] Z. Xu et al.: Phys. Rev. B **67**, 214426 (2003)
[6] P. R. Crompton et al.: Nucl. Phys. B (Proc. Suppl.) **140**, 817 (2005)
[7] S. Todo et al.: Phys. Rev. B **64**, 224412 (2001); M. Nakamura, S. Todo: Phys. Rev. Lett. **89**, 077 204 (2002)
[8] R. Bischof et al.: Leipzig preprint (in preparation)
[9] W. Janke, R. Villanova: Phys. Rev. B **66**, 134 208 (2002)
[10] H. P. Ying, K. Harada: Phys. Rev. E **62**, 1 (2000)
[11] L. Bogacz, W. Janke: PoS LAT2005, 241 (2005)
[12] I. Juhász Junger et al.: preprint (2006), to be published

10.16 Analyses of Partition Function Zeroes

W. Janke, D.A. Johnston*, R. Kenna†

*School of Mathematical and Computer Sciences, Heriot-Watt University, Edinburgh, UK
†School of Mathematical and Information Sciences, Coventry University, UK

The distribution of partition function zeroes in the complex magnetic field plane (Lee-Yang zeroes) as well in the complex temperature plane (Fisher zeroes) encode the phase transition properties of statistical physics models. This fact is exploited in this project by developing suitable analyses methods.

Our recently developed technique for the determination of the density of partition function zeroes using data coming from finite-size systems [1] has been extended to deal with cases where the zeroes are not restricted to a curve in the complex plane and/or come in degenerate sets [2]. The efficacy of the approach was demonstrated by application to a number of models for which these features are manifest and the zeroes are readily calculable. Based on this approach properties of higher-order phase transitions could be derived [3].

In another subproject, a Lee-Yang zero approach was used to systematically analyse the exponents of multiplicative logarithmic corrections to scaling which are frequently encountered in the critical behaviour of certain statistical-mechanical systems. As one main result we proposed scaling relations between the exponents of the logarithmic corrections [4]. These proposed relations were then confronted with a variety of results from the literature.

[1] W. Janke, R. Kenna: J. Stat. Phys. **102**, 1211 (2001)
[2] W. Janke et al.: Nucl. Phys. B **682**, 618 (2004); Comp. Phys. Comm. **169**, 457 (2005)
[3] W. Janke et al.: PoS LAT2005, 244 (2005); Nucl. Phys. B **736**, 319 (2006)
[4] R. Kenna et al.: Phys. Rev. Lett. **96**, 115 701 (2006)

10.17 Funding

Random Geometry and Random Matrices: From Quantum Gravity to Econophysics
W. Janke
EU RTN-Network *ENRAGE*, Grant No. MRTN-CT-2004-005616

Hochtemperaturreihen für Random-Bond-Modelle und Spingläser
W. Janke
Deutsche Forschungsgemeinschaft (DFG), Grant No. JA 483/17-3

Dynamik und Statik von Spingläsern
W. Janke
Deutsche Forschungsgemeinschaft (DFG), Grant No. JA 483/22-1

Investigation of Thermodynamic Properties of Lattice and Off-Lattice Models for Proteins and Polymers
M. Bachmann and W. Janke
Deutsche Forschungsgemeinschaft (DFG), Grant No. JA 483/24-1/2

Phasenübergänge in Systemen mit einschränkender Geometrie
W. Janke
Deutsche Forschungsgemeinschaft (DFG), Grant No. JA 483/23-1/2

Two-Dimensional Magnetic Systems with Anisotropy
W. Janke
EU Marie Curie Development Host Fellowship, Grant No. IHP-HPMD-CT-2001-00108

Quantenfeldtheorie: Mathematische Struktur und Anwendungen in der Elementarteilchen- und Festkörperphysik
Dozenten der Theoretischen Physik und Mathematik (Sprecher B. Geyer)
Deutsche Forschungsgemeinschaft (DFG), Graduiertenkolleg, Grant No. 52

Numerical Simulations of Protein Folding
G. Gökoğlu
Fellowship of TÜBITAK (The Scientifc and Technical Research Council of Turkey)

Spin Glass Physics
D. Yang, A. Nußbaumer and W. Janke
DAAD-RISE Internship Programme

Physics of Protein Folding P.E. Green, T. Vogel and W. Janke
DAAD-RISE Internship Programme

Numerical Approaches to Protein Folding
A. Irbäck and W. Janke
DAAD-STINT Collaborative Research Grant with the University of Lund, Sweden, Grant No. D/05/26016

Challenges in Molecular Simulations: Bridging the Length and Time-Scale Gap
W. Janke
ESF Programme *SIMU*

Statistical Physics of Glassy and Non-Equilibrium Systems
W. Janke
ESF Programme *SPHINX*

Disordered Ferromagnets
W. Janke
LRZ Munich (computer time grant for Hitachi), Grant No. h0611

Monte Carlo Simulationen der Statik und Dynamik von Spingläsern
E. Bittner and W. Janke
NIC Jülich (computer time grant for *JUMP*), Grant No. hlz10

Protein and Polymer Models
M. Bachmann and W. Janke
NIC Jülich (computer time grant for *JUMP*), Grant No. hlz11

Quantum Monte Carlo Simulations
W. Janke
NIC Jülich (computer time grant for *JUMP*), Grant No. hlz12

10.18 Organizational Duties

M. Bachmann

- Scientific Secretary of the Workshop *CompPhys05 – 6. NTZ-Workshop on Computational Physics*, ITP, Universität Leipzig, 1–2 December 2005

E. Bittner

- Scientific Secretary of the Workshop *CompPhys05 – 6. NTZ-Workshop on Computational Physics*, ITP, Universität Leipzig, 1–2 December 2005

W. Janke

- Director of the Naturwissenschaftlich-Theoretisches Zentrum (NTZ) at the Zentrum für Höhere Studien (ZHS), Universität Leipzig
- Chairperson of the Programme Committee "Scientific Computing" of Forschungszentrum Jülich and member of the Scientific-Technical-Council of the Supervisory Board ("Aufsichtsrat") of the Forschungszentrum Jülich GmbH
- Organizer of the CECAM Workshop *Rugged Free Energy Landscapes: Common Computational Approaches in Spin Glasses, Structural Glasses and Biological Macromolecules*, Lyon, France, 6–8 June 2005
- Organizer of the Workshop *ProtFold05 – NTZ-Workshop on Protein Folding and Substrate Specificity: Computational and Experimental Approaches for Studying Biological Macromolecules*, ITP, Universität Leipzig, 16 June 2005
- Organizer of the Workshop *CompPhys05 – 6. NTZ-Workshop on Computational Physics*, ITP, Universität Leipzig, 1–2 December 2005
- Permanent Member of International Advisory Board, *Conference of the Middle European Cooperation in Statistical Physics (MECO)*
- Member of Advisory Committee, *VIELAT05 – 15. Workshop on Lattice Field Theory*, Vienna, Austria, 6–8 October 2005
- Member of Advisory Committee, *COVLAT06 – 16. Workshop on Lattice Field Theory*, Coventry, England, 29 Juni – 1 July 2006
- Member of Local Organizing Committee, international Conference *MG11 – 11th Marcel Grossmann Meeting*, FU Berlin, 23–29 July 2006
- Member of International Program Committee, international Conference *Mathematical Modeling and Computational Physics 2006*, High Tatra Mountains, Slovakia, 28 August – 1 September 2006
- Referee: Phys. Rev. Lett., Phys. Rev. B, Phys. Rev. E, Europhys. Lett., Phys. Lett. A, Phys. Lett. B, Eur. Phys. J. B, Physica A, J. Phys. A, Comp. Phys. Commun., J. Stat. Mech. Theor. Exp., New J. Phys.

10.19 External Cooperations

Academic

- EU RTN-Network *ENRAGE – Random Geometry and Random Matrices: From Quantum Gravity to Econophysics* with 13 teams throughout Europe
- Dept. of Physics, Florida State University, Tallahassee, USA
  Prof. Dr. B.A. Berg
- Department of Physics, University of North Dakota, Fargo, USA
  G. Kähler
- Department of Physics, University of Waterloo, Canada
  Dr. M. Weigel

- CEA/Saclay, Service de Physique Théorique, France
  Dr. A. Billoire
- Laboratoire de Physique des Matériaux, Université Henri Poincaré, Nancy, France
  Prof. Dr. B. Berche, Dr. C. Chatelain
- Groupe de Physique des Matériaux, Université de Rouen, France
  Dr. P.-E. Berche
- School of Mathematical and Computer Sciences, Heriot-Watt University, Edinburgh, UK
  Prof. Dr. D.A. Johnston
- School of Mathematical and Information Sciences, Coventry University, UK
  Dr. R. Kenna
- Dept. of Physics, Hacettepe University, Ankara, Turkey
  Prof. Dr. T. Çelik, Dr. H. Arkin, G. Gökoğlu
- Complex Systems Division, Department of Theoretical Physics, Lund University, Lund, Sweden
  Prof. Dr. A. Irbäck, S. Mitternacht
- John von Neumann-Institut für Computing (NIC), Forschungszentrum Jülich
  Prof. Dr. U. Hansmann, Prof. Dr. P. Grassberger, PD Dr. T. Neuhaus, Dr. S. Mohanty
- Institut für Physik, Universität Mainz
  Prof. Dr. K. Binder, Dr. H.-P. Hsu
- Atominstitut, TU Wien, Austria
  Prof. Dr. H. Markum, Dr. R. Pullirsch
- Dept. of Physics, University of Wales Swansea, Swansea, UK
  Dr. S. Hands
- Brunel University of West London, UK
  Dr. G. Akemann, R. Megaides
- Institut für Theoretische Physik, FU Berlin
  Prof. Dr. B. Hamprecht, Prof. Dr. H. Kleinert
- IAC-1, Universität Stuttgart
  PD Dr. R. Hilfer
- Institut für Theoretische Physik, Universität Bielefeld
  Prof. Dr. F. Schmid, PD Dr. Thomas Neuhaus
- Interdisziplinäres Zentrum für Bioinformatik, Universität Leipzig
  A. Krinner
- Institute of Physics, Jagellonian University, Kraków, Poland
  Prof. Dr. Z. Burda
- Landau Institute for Theoretical Physics, Chernogolovka, Russia
  Prof. Dr. L.N. Shchur
- Yerevan Physics Institute, Yerevan, Armenia
  Prof. Dr. D.B. Saakian

- University of Sri Jayewardenepura, Sri Lanka
  Dr. R.P.K.C. Malmini
- Department of Physics, Sri Venkateswara College, University of Delhi, New Delhi, India
  Dr. B. Biswal
- Department of Mechanical Engineering and Intelligent Systems, Tokyo University of Electro-communications, Chofu, Tokyo, Japan
  Prof. Dr. H.-G. Mattutis
- Zhejiang Institute of Modern Physics, Zhejiang University, Hangzhou, P.R. China
  Prof. Dr. H.-P. Ying, Prof. Dr. B. Zheng

10.20 Publications

Journals

G. Akemann, E. Bittner: *Two-Colour Lattice QCD with Dynamical Fermions at Non-Zero Density versus Matrix Models*, PoS LAT2005, 197 (2005)

G. Akemann, E. Bittner, M.-P. Lombardo, H. Markum, R. Pullirsch: *Density Profiles of the Lowest Eigenvalues of the Dirac operator for Two-Color QCD at Non-Zero Chemical Potential Compared to Matrix Models*, Nucl. Phys. B (Proc. Suppl.) **140**, 568 (2005)

M. Bachmann, H. Arkin, W. Janke: *Multicanonical Study of Coarse-Grained Off-Lattice Models for Folding Heteropolymers*, Phys. Rev. E **71**, 031 906 (2005)

M. Bachmann, W. Janke: *Conformational Transitions of Non-Grafted Polymers Near an Adsorbing Substrate*, Phys. Rev. Lett. **95**, 058 102 (2005)

M. Bachmann, W. Janke: *Conformational Transitions of Heteropolymers*, Comp. Phys. Comm. **169**, 111 (2005)

B. Berche, P.-E. Berche, C. Chatelain, W. Janke: *Random Ising Model in Three Dimensions: Theory, Experiment and Simulation – a Difficult Coexistence*, Cond. Matter Phys. **8**, 47 (2005)

E. Bittner, W. Janke: *Nature of Phase Transitions in a Generalized Complex $|\psi|^4$ Model*, Phys. Rev. B **71**, 024 512 (2005)

E. Bittner, A. Krinner, W. Janke: *Vortex-Line Percolation in the Complex $|\psi|^4$ Model* Phys. Rev. B **72**, 094 511 (2005)

E. Bittner, A. Krinner, W. Janke: *Vortex-Line Percolation in the Three-Dimensional Complex Ginzburg-Landau Model*, PoS LAT2005, 247 (2005)

L. Bogacz, Z. Burda, W. Janke, B. Waclaw: *A Program Generating Homogeneous Random Graphs with Given Weights*, Comp. Phys. Comm. **173**, 162 (2005)

L. Bogacz, W. Janke: *QMC Simulations of Heisenberg Ferromagnet*, PoS LAT2005, 241 (2005)

C. Chatelain, B. Berche, W. Janke, P.-E. Berche: *Monte Carlo Study of Phase Transitions in the Bond-Diluted 3D 4-State Potts Model*, Nucl. Phys. B **719**, 275 (2005)

P.R. Crompton, W. Janke, Z.X. Xu, H.P. Ying: *Finite-Size Scaling, Fisher Zeroes and* $N = 4$ *Super Yang-Mills*, Nucl. Phys. **B** (Proc. Suppl.) **140** (2005) 817–819

K. Goede, M. Grundmann, K. Holland-Nell, A.G. Beck-Sickinger, M. Bachmann, W. Janke: *Peptide auf neuen Wegen*, BIOforum **10**, 53 (2005)

H. Hellmund, W. Janke: *High-Temperature Series Expansions for Random Potts Models*, Cond. Matter Phys. **8**, 59 (2005)

R. Hilfer, B. Biswal, H.-G. Mattutis, W. Janke: *Multicanonical Simulations of the Tails of the Order-Parameter Distribution of the 2D Ising Model*, Comp. Phys. Comm. **169**, 230 (2005)

W. Janke, B. Berche, C. Chatelain, P.-E. Berche, M. Hellmund: *Quenched Disordered Ferromagnets*, invited plenary talk, PoS LAT2005, 018 (2005)

W. Janke, D.A. Johnston, R. Kenna: *Critical Exponents from General Distributions of Zeroes*, Comp. Phys. Comm. **169**, 457 (2005)

W. Janke, D.A. Johnston, R. Kenna: *Properties of Phase Transitions of Higher Order*, PoS LAT2005, 244 (2005)

W. Janke, A.M.J. Schakel: *Fractal Structure of Spin Clusters and Domain Walls in the Two-Dimensional Ising Model*, Phys. Rev. E **71**, 036 703 (2005)

W. Janke, A.M.J. Schakel: *Geometrical Phase Transitions*, Comp. Phys. Comm. **169**, 222 (2005)

W. Janke, A.M.J. Schakel: *Fractal Structure of High-Temperature Graphs of O(N) Models in Two Dimensions*, Phys. Rev. Lett. **95**, 135 702 (2005)

W. Janke, M. Weigel: *Simulations of the F Model on Planar* ϕ^4 *Feynman Diagrams*, PoS LAT2005, 251 (2005)

A. Nußbaumer, E. Bittner, W. Janke: *Evaporation/Condensation of Ising Droplets*, PoS LAT2005, 252 (2005)

R. Schiemann, M. Bachmann, W. Janke: *Exact Sequence Analysis for Three-Dimensional Hydrophobic-Polar Lattice Proteins*, J. Chem. Phys. **122**, 114 705 (2005)

R. Schiemann, M. Bachmann, W. Janke: *Exact Enumeration for Three-Dimensional Lattice Proteins*, Comp. Phys. Comm. **166**, 8 (2005)

M. Weigel, W. Janke: *The F Model on Dynamical Quadrangulations*, Nucl. Phys. B **719**, 312 (2005)

M. Weigel, W. Janke: *The Square-Lattice F Model Revisited: A Loop-Cluster Update Scaling Study*, J. Phys. A **38**, 7067 (2005)

S. Wenzel, E. Bittner, W. Janke, A.M.J. Schakel, A. Schiller: *Kertész Line in the Three-Dimensional Compact U(1) Lattice Higgs Model*, Phys. Rev. Lett. **95**, 051 601 (2005)

S. Wenzel, E. Bittner, W. Janke, A.M.J. Schakel, A. Schiller: *Vortex Proliferation and the Dual Superconductor Scenario for Confinement: The 3D Compact U(1) Lattice Higgs Model*, PoS LAT2005, 248 (2005)

Journals January–March 2006

M. Bachmann, W. Janke: *Substrate Specificity of Peptide Adsorption: A Model Study*, Phys. Rev. E **73**, 020 901(R) (2006)

M. Bachmann, W. Janke: *Chain-Growth Simulations of Lattice-Peptide Adsorption to Attractive Substrates*, in *Proc. NIC Symp. 2006*, ed. by G. Münster, D. Wolf, M. Kremer, NIC Series, Vol. **32** (John von Neumann Institute for Computing, Jülich 2006) p 245

M. Bachmann, W. Janke: *Substrate Adhesion of a Nongrafted Polymer in a Cavity*, Phys. Rev. E **73**, 041 802 (2006)

E. Bittner, W. Janke: *Free-Energy Barriers in the Sherrington-Kirkpatrick Model*, Europhys. Lett. **74**, 195 (2006), arXiv:cond-mat/0603526

W. Janke, E. Bittner: *Phase Transitions in a Generalized $|\psi|^4$ Model*, Proc. 8th Int. Conf. *Path Integrals from Quantum Information to Cosmology*, Prague, Czech Republic, 6–10 June 2005, ed. by Č. Burdik, O. Navrátil, S. Pošta (JINR Press, Dubna 2006) (www.jinr.ru/publish/Proceedings/Burdik-2005/index.html)

W. Janke, D.A. Johnston, R. Kenna: *Properties of Higher-Order Phase Transitions*, Nucl. Phys. B **736**, 319 (2006)

R. Kenna, D.A. Johnston, W. Janke: *Scaling Relations for Logarithmic Corrections*, Phys. Rev. Lett. **96**, 115 701 (2006)

In press

W. Janke: *Introduction to Monte Carlo Simulations*, Leipzig preprint (February 2006), Lecture Notes, to appear in: *Ageing and the Glass Transition*, Summer School, University of Luxembourg, September 2005 (in press)

W. Janke, A.M.J. Schakel: *Two-Dimensional Critical Potts and its Tricritical Shadow World*, Leipzig/FU Berlin preprint (October 2005), to appear in Braz. J. Phys. (in press)

Talks

G. Akemann, E. Bittner: *Two-Colour Lattice QCD with Dynamical Fermions at Non-Zero Density versus Matrix Models*, XXIII Int. Symp. Latt. Field Theory, Dublin, July 25–30

M. Bachmann: *Thermodynamic Aspects of Coarse-Grained Heteropolymer Folding*, CECAM Workshop *Rugged Free Energy Landscapes: Common Computational Approaches in Spin Glasses, Structural Glasses and Biological Macromolecules*, Lyon, June 6–8

M. Bachmann: *Minimalistic Models for Substrate Adsorption of Polymers and Peptides*, Workshop ProtFold05, Leipzig, June 16

M. Bachmann: *Polymers Astray: Folding and Binding Near Attractive Substrates*, Theory Seminar of the Computational Biology & Biological Physics Group, Lund University, September 19

M. Bachmann: *Conformational Transitions of Polymers and Peptides near Attractive Substrates*, Workshop CompPhys05, Leipzig, December 1–3

E. Bittner, A. Krinner, W. Janke: *Vortex Line Percolation in the Three-Dimensional Complex Ginzburg-Landau Model*, DPG-Frühjahrstagung, Berlin, March 4–9

E. Bittner, W. Janke: *Free-Energy Barriers in the Sherrington-Kirkpatrick Model*, CECAM Workshop, Lyon, June 6–8

E. Bittner, A. Krinner, W. Janke: *Vortex-Line Percolation in a Three-Dimensional Complex Ginzburg-Landau Model*, XXIII Int. Symp. Latt. Field Theory, Dublin, July 25–30

E. Bittner, A. Krinner, W. Janke: *Phase Transitions in a Generalized Complex Ginzburg-Landau Model*, VIELAT05, 15. Workshop Latt. Field Theory, TU Wien, October 6–8

E. Bittner: *Complex Eigenvalues of the Dirac Operator in Two-Color QCD with Chemical Potential*, Brunel University, London, November 20–23

E. Bittner, W. Janke: *Free-Energy Barriers in a Mean-Field Spin-Glass Model*, Workshop CompPhys05, Leipzig, December 1–3

L. Bogacz, W. Janke: *QMC Simulations of Heisenberg Ferromagnet*, XXIII Int. Symp. Latt. Field Theory, Dublin, July 25–30

L. Bogacz, W. Janke: *Quantum Monte Carlo Simulations of Ferromagnetic Chains*, Workshop CompPhys05, Leipzig, December 1–3

P. Crompton, R. Bischof, W. Janke, S. Wenzel: *Quantum Phase Transitions in Inhomogeneous Spin Chains*, DPG-Frühjahrstagung, Berlin, March 4–9

W. Janke: *Monte Carlo Simulations of the 3D Bond-Diluted Potts Model*, DPG Frühjahrstagung, Berlin, March 4–9

W. Janke: *High-Temperature Series Expansions for Diluted Magnets*, 30th Conf. Middle Eur. Coop. Stat. Phys. (MECO30), Cortona, Italy, April 3–6

W. Janke: *Lecture Series on Monte Carlo Simulations in Statistical Physics*, *Ising Lectures*, Lecture I: *Introduction to Monte Carlo simulations*, Lecture II: *Improved algorithms and generalised ensembles*, Lecture III: *Applications to disordered systems*, Institute for Condensed Matter Physics of the National Academy of Sciences of Ukraine, University of Lviv, Ukraine, May 17–20

W. Janke: *Phase Transitions in a Generalized $|\psi|^4$ Model*, 8th Int. Conf. *Path Integrals: From Quantum Information to Cosmology*, Prague, Czech Republic, June 6–10

W. Janke: *2D Quantum Gravity: Fluctuating Graphs and Quenched Connectivity Disorder*, series of three lectures, Mochima Theoretical Physics Spring School, Joint CEA-IVIV-SFP-Workshop on *Foundations of Statistical and Mesoscopic Physics*, Mochima, Venezuela, June 20–24

W. Janke: *The F Model on Dynamical Quadrangulations*, *Lattice 2005*, Trinity College, Dublin, Ireland, July 25–30

W. Janke: *Quenched Disordered Ferromagnets*, plenary talk, *Lattice 2005*, Trinity College, Dublin, Ireland, July 25–30

W. Janke: *Geometrical Approach to Phase Transitions*, IV Brazilian Meeting on Simulational Physics, Ouro Preto, Brasil, August 10–12

W. Janke: *Introduction to Computer Simulations*, series of lectures, Summer School *Ageing and the Glass Transition*, University of Luxembourg, September 18–24

W. Janke: *Multicanonical Chain Growth Simulations and Exact Enumerations of Lattice Proteins*, VIELAT05 15th Workshop Latt. Field Theory, Vienna University of Technology (VUT), Austria, October 6–8

W. Janke: *Percolating Geometrical Excitations – Critical vs. Tricritical*, VIELAT05 15th Workshop Latt. Field Theory, Vienna University of Technology (VUT), Austria, October 6–8

A. Nußbaumer, E. Bittner, W. Janke: *Evolution of Equilibirum Droplets*, DPG-Frühjahrstagung, Berlin, March 4–9

A. Nußbaumer, E. Bittner, W. Janke: *Evaporation/Condensation of Ising Droplets*, XXIII Int. Symp. Latt. Field Theory, Dublin, July 25–30

A.M.J. Schakel, W. Janke: *Fractal Structure and Critical Properties of Planar Loops*, DPG Frühjahrstagung, Berlin, March 4–9

S. Wenzel, E. Bittner, W. Janke, A.J.M. Schakel, A. Schiller: *Kertész Line in the 3D $U(1)$ Abelian Higgs Model*, XXIII Int. Symp. Latt. Field Theory, Dublin, July 25–30

Poster

M. Bachmann, K. Goede, W. Janke, M. Grundmann: *Bindungsspezifität von Peptiden auf Halbleiteroberflächen*, DPG-Frühjahrstagung Berlin, March 4–9

M. Bachmann, W. Janke: *Conformational Phase Diagram of Nongrafted Polymer near Adsorbing Substrate*, 30th Conf. Middle Eur. Coop. Stat. Phys. (MECO30), Cortona, April 3–6

M. Bachmann, K. Goede, W. Janke, M. Grundmann: *Bindungsspezifität von Peptiden auf Halbleiteroberflächen*, 4th Biotechnol. Symp., Leipzig, June 3

E. Bittner, A. Krinner, W. Janke: *Vortex-Line Percolation in a Three-Dimensional Complex $|\psi|^4$ Model*, 30th Conf. Middle Eur. Coop. Stat. Phys. (MECO30), Cortona, April 3–6

W. Janke, M. Hellmund: *Series Expansions for Disordered Potts Models*, DPG Frühjahrstagung, Berlin, March 4–9

A. Kallias, M. Bachmann, W. Janke: *Crystallization of Two-Dimensional Off-Lattice Lennard-Jones Polymers*, DPG-Frühjahrstagung Berlin, March 4–9

E. Lorenz, W. Janke: *Phase-Ordering and Aging Phenomena in Potts Models*, DPG-Frühjahrstagung Berlin, March 4–9

A. Nußbaumer, W. Janke, T. Neuhaus: *Evaporation/Condensation of Ising Droplets*, 30th Conf. Middle Eur. Coop. Stat. Phys., Cortona, April 3–6

A. Nußbaumer, E. Bittner, W. Janke, T. Neuhaus; *Evaporation/Condensation of Ising Droplets*, Workshop CompPhys05, Leipzig, December 1–3

S. Schnabel, M. Bachmann, W. Janke: *Folding Channels in Coarse-Grained Heteropolymer Models*, DPG-Frühjahrstagung Berlin, March 4–9

T. Vogel, M. Bachmann, W. Janke: *Coarse-Grained Heteropolymer Models: On-Lattice vs. Off-Lattice*, DPG-Frühjahrstagung Berlin, March 4–9

T. Vogel, M. Bachmann, W. Janke: *Coarse-Grained Lattice and Off-Lattice Heteropolymer Models*, 30th Conf. Middle Eur. Coop. Stat. Phys. (MECO30), Cortona, April 3–6

T. Vogel, M. Bachmann, W. Janke: *Coarse-Grained Heteropolymer Models: On-Lattice vs. Off-Lattice*, 4th Biotechnol. Symp., Leipzig, June 3

T. Vogel, M. Bachmann, W. Janke: *HP Proteins on Generalized Lattices*, 3rd Day of Biotechnology, Leipzig, May 19

10.21 Graduations

Diploma

- Eric Lorenz
  Aeging Phenomena in Phase-Ordering Kinetics in Potts Models
  07/2005

- Stefan Schnabel
  Thermodynamische Eigenschaften und Faltungskanäle von Coarse-Grained Heteropolymeren
  07/2005
- Anna Kallias
  Thermodynamics and Folding Kinetics of Coarse-Grained Protein Models
  09/2005
- Jakob Schluttig
  Molecular Mechanics of Coarse-Grained Protein Models
  10/2005

10.22 Guests

- Dipl.-Phys. Sebastian Brandt
  Washington University, St. Louis, USA
  January 06–07, 2005
- Prof. Dr. Yurij Holovatch
  Lviv, Ukraine
  January 17–19, 2005
- Prof. Dr. Hans-Jörg Hofmann
  Institut für Biochemie, Universität Leipzig
  January 20, 2005
- Prof. Dr. Bo Zheng
  Zhejiang University, Hangzhou, P.R. China
  February 03, 2005
- Dr. Christiane P. Koch
  Orsay, France
  March 31 – April 04, 2005
- Thomas Weikl
  MPI Golm
  April 21, 2005
- Prof. Dr. Bernd A. Berg
  Florida State University, Tallahassee, USA
  May – August 2005
- Prof. Dr. Anders Irbäck
  Lund University, Sweden
  June 14–17, 2005
- Dr. Sandipan Mohanty
  Lund University, Sweden
  June 14–17, 2005
- Patrick E. Green
  Ohio University, Athens/Ohio, USA
  June – August 2005

- David Yang
  Simon Fraser University, Canada
  June – August 2005
- Prof. Dr. Hans Gerd Evertz
  TU Graz, Österrreich
  July 06–08, 2005
- Prof. Dr. Tarik Celik
  Ankara, Turkey
  June – July 2005
- Prof. Dr. David P. Landau
  University of Georgia, Athens, GA, USA
  July 20–22, 2005
- Dr. Flavio Nogueira
  FU Berlin
  November 11, 2005
- Prof. Dr. Bernd A. Berg
  Florida State University, Tallahassee, USA
  November 21–25, 2005
- Prof. Dr. Anders Irbäck
  Lund University, Sweden
  November 29 – December 2
- Simon Mitternacht
  Lund University, Sweden
  November 29 – December 2
- Prof. Dr. Desmond A. Johnston
  Heriot-Watt University, Edinburgh, UK
  November 30 – December 4, 2005
- Dr. Ralph Kenna
  Coventry University, UK
  November 30 – December 4, 2005
- Prof. Dr. Kurt Binder
  Universität Mainz
  December 1–2, 2005
- Prof. Dr. Harald Markum
  TU Wien, Österreich
  December 1–4, 2005
- Dr. Martin Weigel
  University of Waterloo, Canada
  December 1–7, 2005

11

Molecular Dynamics/ Computer Simulation

11.1 Introduction

Using methods of statistical physics and computer simulations we investigate classical many-particle systems interacting with interfaces. One aim of the research in our group is to built up a bridge between theoretical and experimental physics. By means of analytical theories of statistical physics and computer simulations (Molecular dynamics, Monte Carlo procedures, percolation theories) using modern workstations and supercomputers we examine subjects for which high interest exists in basic research and industry as well. The examinations involve transport properties (diffusion of guest molecules) in zeolites and the structural and phase behaviour of complex fluids on bulk conditions and in molecular confinements. Especially we are interested to understand

- the diffusion behaviour of guest molecules in zeolites in dependence on thermodynamic parameters, steric conditions, intermolecular potentials and the concentration of the guest molecules,
- structure and phase equilibria of complex (aqueous) fluids in interfacial systems (e.g. pores, thin films, model membranes) in dependence on geometric and thermodynamic conditions,
- and the migration of molecules in (random) porous media by the use of percolation theories

in microscopic detail and to compare the results with experimental data. The use of a network of PC's and workstations (Unix, Linux, Windows), the preparation and application of programs (Fortran, C, C^{++}), and the interesting objects (zeolites, membranes) give excellent possibilities for future careers of undergraduates, graduate students and postdocs. Our research is part of several national and international programs (DFG - Schwerpunktprogramm 1155, an International Research Graduate Training program (IRTG 1056), a joint research project DFG/TRF-Thailand, a joint research project DAAD/TRF-Thailand and joint research projects with UOIT Oshawa and SHARCNET, Canada) and includes a close collaboration with the Institute of Experimental Physics I (Physics of Interfaces and Biomembranes) of Leipzig University and many institutions in Germany and other countries. Details are given in the list of external cooperations.

Horst-Ludger Vörtler and Siegfried Fritzsche

11.2 Investigation of Diffusion Mechanisms of Dumbbell-Shaped Molecules in Cation Free Zeolites

A. Schüring[*†], S.M. Auerbach[‡], S. Fritzsche[*], R. Haberlandt[*]

[*]Institut für Theoretische Physik
[†]Institut für Experimentelle Physik I
[‡]Department of Chemistry, University of Massachusetts, Amherst, Massachusetts, USA

Examining a surprizing temperature dependence of the self diffusion coefficient of ethane in the cation-free LTA zeolite it could be shown that this dependence is caused by an entropic barrier [1]. Investigations of the local free energy, defined as in [2], which is also the potential of mean force, were carried out. It was shown that the temperature dependence of the jump rates is in some cases dominated by entropic barriers [1, 3]. This can lead to the observed decrease of the self-diffusion coefficient as the temperature increases. A random walk treatment was developped that reduces the description of the underlying diffusion process on the essentials and explains the effect in terms of jump rates that can be calculated analytically by use of the transition state theory or evaluated from Molecular Dynamics (MD) computer simulations. These investigations are extended to other dumbbell-shaped molecules.

[1] A. Schüring et al.: J. Chem. Phys. **116**, 10 890 (2002)
[2] D. Chandler: *Introduction to Modern Statistical Mechanics* (Oxford University Press, New York 1987)
[3] A. Schüring: PhD thesis, University of Leipzig, 2003

11.3 Computer Simulations and Analytical Calculations on the Influence of the Crystal Boundaries on the Exchange of Molecules Between Zeolite Nanocrystals and Their Surroundings

A. Schüring[*†], J. Gulín-González[*‡], S. Vasenkov[†§], S. Fritzsche[*]

[*]Institut für Theoretische Physik
[†]Institut für Experimentelle Physik I
[‡]Department of Physics, Instituto Superior Politécnico José Antonio Echeverría, University of Informatics Sciences, La Habana, Cuba
[§]Department of Chemical Engineering, University of Florida, Gainesville, USA

By Molecular Dynamics simulations and analytical calculations the transport of matter trough zeolite crystal boundaries was examined. A new boundary effect arising from the interplay of single file diffusion and normal diffusion close to the crystal boundary could be detected and explained.

The work was done in close cooperation with the group 'Physics of Interfaces' in the Institute of Experimental Physics I and is described in more detail in Sect. 3.13 of this report.

11.4 Quantum Chemical Calculations and Classical MD Simulations of Methane in Silicalite

S. Fritzsche, C. Bussai*, S. Hannongbua*, R. Haberlandt

*Department of Chemistry, Faculty of Sciences, Chulalongkorn University, Bangkok, Thailand

Earlier investigations of the diffusion of water in silicalite-1 by quantum chemical calculations and MD-simulations and - together with Prof. Dr. J. Kärger - NMR PFG experiments have been extended to quantum chemical calculations and MD-simulations of methane in silicalite-1 [1]. The results could be compared with earlier classical simulations of the same system [2] and led to deeper insights.

[1] C. Bussai et al.: Langmuir **21**, 5847 (2005)
[2] S. Fritzsche et al.: Chem. Phys. **289**, 321 (2003)

11.5 How Do Guest Molecules Enter Zeolite Pores? Quantum Chemical Calculations and Classical MD Simulations

S. Fritzsche, R. Haberlandt, S. Hannongbua*, T. Remsungnen†, O. Saengsawang

*Deparment of Chemistry, Faculty of Sciences, Chulalongkorn University, Bangkok, Thailand
†Department of Mathematics, Khon Khaen University, Thailand

This is a common project of the German DFG and the NRTC (Thailand Research Fund). The energetics and dynamics of guest molecules and the surface of zeolites are investigated by quantum chemical calculations and Molecular Dynamics (MD) simulations. The work includes also a cooperation with Prof. Kärger (Institut für Experimentalphysik I, Uni Leipzig). In 2005 the publications [1, 2, 3] appeared.

[1] S. Fritzsche et al.: Chem. Phys. Lett. **411**, 423 (2005)
[2] O. Saengsawang et al.: Stud. Surf. Sci. Catal. **158**, 947 (2005)
[3] O. Saengsawang et al.: J. Phys. Chem B **109**, 5684 (2005)

11.6 Investigation of the Diffusion of Pentane in Silicalite-1

S. Fritzsche, A. Longsinruin*, S. Hannongbua*

*Department of Chemistry, Faculty of Sciences, Chulalongkorn University, Bangkok, Thailand

This is a common project of the German DAAD and the TRF (Thailand Research Fund). Parameters obtained before from quantum chemical calculations (Gaussian, MP2-level) [1] are now used in classical MD simulations to investigate the structural behavior and the diffusion of pentane in silicalite-1. The pentane is used in united atom approximation. The bond and angle elasticity and the torsional elasticity are taken into account. The investigations will lead to deeper insight into mechanisms and interdependencies.

[1] A. Loisruangsin et al.: Chem. Phys. Lett. **390**, 485 (2004)

11.7 Investigation of the Rotation and Diffusion of Pentane in the Zeolite ZK5

S. Fritzsche, O. Saengsawang, A. Schüring, P. Magusin*

*Chemical Engineering and Chemistry Department, TU Eindhoven, The Netherlands

This is a project in the framework of the International Research Training Group (IRTG) "Diffusion in Porous Materials". After construction the lattice of the H-ZK5 bei Molecular Mechanics the rotation and diffusion of pentane within this zeolite is investigated. It turns out that the rotation within the smaller one of the different cavities of the ZK5 (γ-cage) which was examined experimentally in [1] is strongly hindered by lack of space and that therefore the rotation depends critically upon lattice vibrations and upon the choice of the interaction parameters. This is now investigated in detail.

[1] V.E. Zorine et al.: J. Phys. Chem. B **108**, 5600 (2004)

11.8 Diffusion of Water in the Zeolite Chabazite

S. Fritzsche, P. Biswas, A. Schüring, P.A. Bopp*

*Laberatoire de Physico-Chimie Moleculaire, University Bordeaux, France

This is a project in the framework of the International Research Training Group (IRTG) "Diffusion in Porous Materials". Basing on [1] the diffusion of water in the zeolite chabazite is investigated. The diffusion coefficient increases with increasing concentration of guest molecules. This effect is strongly correlated with the presence of extra framwork cations. The diffusion coefficient of water in this system is very small so that

special technics like a multiple-time-step algorithm must be used. Nevertheless, each simulation requires about 3 weeks computer time on modern workstations.

[1] S. Jost: PhD thesis, University of Leipzig, 2004

11.9 Simulation and Molecular Theory of Phase Equilibria and Chemical Potentials of Aqueous Fluids in Bulk Systems and in Thin Films

H.-L. Vörtler, I. Nezbeda *, M. Kettler

*Czech Academy of Sciences, Prague, Czech Republic

In this long-term project we investigate thermodynamic properties and phase equilibria of bulk and confined aqueous fluids on the basis of a hierarchic modelling of intermolecular potentials.

In 2005 we have continued our studies on recent test particle methods for the efficient simulation of chemical potentials in complex fluids. By combining monomer/dimer insertion and gradual particle insertion fluid phase equilibria of strongly associating water models have been estimated [1, 2]. Aqueous phases on both homogeneous and inhomogeneous conditions are under consideration [3]. Some results comparing bulk fluids and planar monolayers are shown in Fig. 11.1.

To reach a more fundamental understanding of structural properties in the critical range cluster distributions are estimated and analyzed by percolation theory. A system-

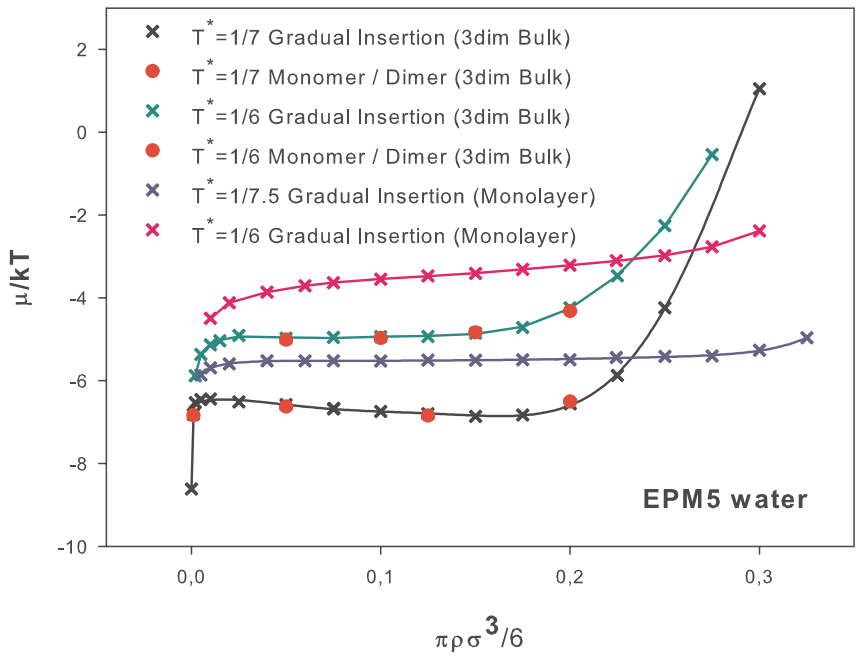

Figure 11.1: Chemical Potential vs. Packing Fraction (Bulk/ Monolayer – critical/subcritical range)

atic study of finite size effects on chemical potential isotherms in the weekly subcritical temperature range is in progress.

The results have to be considered as quasi-experimental reference data for an improvement of hierarchic potential models of aqueous phases and of thermodynamic perturbation theories which contribute to a microscopic understanding of solubility and hydration phenomena of associating fluids in molecular confinements, such as porous media and biomembranes.

The work is part of an international collaboration with the group of Prof. Ivo Nezbeda, Prague. A diploma student from Leipzig and a PhD student from Czech Republic are included in the research.

[1] H.-L. Vörtler, M. Kettler: Mol. Phys. **104**, 233 (2006)
[2] H.-L. Vörtler, M. Kettler: 19th Thermodyn. Conf. Abstr., Sesimbra, Portugal, April 7, 2005, p 54
[3] H.-L. Vörtler: 6th Workshop Comp. Phys. (CompPhys05), Leipzig, Talk, December 02, 2005

11.10 Cavity Distribution Functions and Phase Equilibria in Confined Fluids

H.-L. Vörtler, W.R. Smith *

*Institute of Technology, University of Ontario, Oshawa, Ontario, Canada

Based on our recent studies of the molecular structure of hard-core fluids in simple molecular confinements using cavity- and background correlation functions [1, 2] we have continued in 2005 the estimation of cavity pair distribution functions by means of novel MC Methods which use virtual insertions of particles and cavities. These investigations are crucial for an improvement of integral equations based on a hierarchy of cavity functions (closure relations of BGY-like hierarchies).

In general, the results of these studies provide basic structural information for the understanding of phase equilibria in geometrically restricted fluids on a molecular level. Of particular interest in this context is the estimation of the thermodynamic pressure in coexisting confined phases. We obtained quasi-experimental reference data of local and spreading pressures by a direct calculation of these quantities using our own new developed virtual parameter variation approach, a general method to simulate directly the relevant canonical partition function derivatives.

The long-term goals of our research are contributions to a statistical-mechanical theory of phase equilibria of inhomogeneous fluids with applications to nanoporous materials and biointerfaces.

This research was supported by research fund of University of Ontario Institute of Technology (support of research stay of H.-L. Vörtler in Oshawa) and by the facilities of SHARCNET computer network (Ontario, Canada)

[1] W.R. Smith, H.-L. Vörtler: Mol. Phys **101**, 805 (2003)
[2] S. Fritzsche et al.: in *Molecules in Interaction With Surfaces and Interfaces*, ed. by R. Haberlandt et al. (Springer Verlag, Heidelberg 2004) p 1

11.11 Funding

Analytical Treatment and Computer Simulations of Anomalous Diffusion in the Transition Region Gas/Adsorbent
S. Fritzsche, S. Vasenkov, A. Schüring
SPP1155, DFG-code FR1486/2-1

MD Simulations and Analytical Calculations of Rotation and Longtime Diffusion of Guest Molecules in Zeolites
S. Fritzsche, O. Saengsawang, P. Biswas
DFG: IRTG 1056

How do guest molecules enter zeolite pores? Quantum Chemical calculations and classical MD simulations
S. Fritzsche, R. Haberlandt
DFG-codes FR1486/1-1, FR1486/1-2, FR1486/1-3

11.12 Organizational Duties

H.-L. Vörtler

- Speaker of the MDC group
- Reviewer: Czech Science Foundation
- Referee: J.Chem. Phys, Chem. Phys. Lett, J. Molec. Liq.

S. Fritzsche

- Project leader of one project in the International Research Training Group, IRTG 1056
- Project leader of one project in the SPP1155, DFG-code FR1486/2-1
- Project leader of a German/Thai research project, DFG-codes FR1486/1-1, FR1486/1-2, FR1486/1-3
- Referee: Chem. Phys. Lett., Micropor. Mesopor. Mater., J. Molec. Graph. Model.)

11.13 External Cooperations

Academic

- Chulalongkorn University, Thailand
  Prof. Dr. S. Hannongbua
- Indian Institute of Science, Bangalore, India
  Prof. Dr. S. Yashonath
- Khon Khaen University, Thailand
  Dr. T. Remsungnen
- University Bordeaux, France
  Prof. Dr. P. A. Bopp
- Eindhoven University, The Netherlands
  Prof. Dr. P. Magusin

- University of California, Irvine, USA
  Prof. M. Wolfsberg
- Charles University and Czech Acad. Sci., Prague, Czech Republic
  Prof. I. Nezbeda, Dr. M. Lisal
- University of Ontario Institute of Technology, Oshawa, Canada
  Prof. W.R. Smith
- Universität Regensburg
  Prof. H. Krienke

11.14 Publications

Journals

H.-L. Vörtler, M. Kettler: *Efficient simulation of chemical potentials and phase equilibria in associating fluids: monomer/dimer insertion versus gradual particle insertion in primitive water models*, Mol. Phys. **104**, 233 (2006)

A. Schüring, S. Vasenkov, S. Fritzsche: *Influence of boundaries of nanoporous crystals on the molecular exchange under conditions of single-file diffusion*, J. Phys. Chem B **109**, 16 711 (2005)

C. Bussai, S. Fritzsche, R. Haberlandt, S. Hannongbua: *Concentration Dependence of the Methane Structure in Silicalite-1: A Molecular Dynamics Study Using the Moller-Plesset-Based Potential*, Langmuir **21**, 5847 (2005)

S. Fritzsche, T. Osotchan, A. Schüring, S. Hannongbua, J. Kärger: *Is there a coupling between rotational and translational motion of methane in silicalite-1 and AlPO4-5?*, Chem. Phys. Lett. **411**, 423 (2005)

O. Saengsawang, T. Remsungnen, A. Loisruangsina, S. Fritzsche, R. Haberlandt, S. Hannongbua: *Energy barrier of water and methane molecules due to the silanol groups on the (010) surface of silicalite-1 as studied by quantum chemical calculations*, Stud. Surf. Sci. Catal. **158**, 947 (2005)

O. Saengsawang, T. Remsungnen, S. Fritzsche, R. Haberlandt, S. Hannongbua: *Structure and Energetics of Water-Silanol Binding on the Surface of Silicalite-1: Quantum Chemical Calculations*, J. Phys. Chem B **109**, 5684 (2005)

Talks

H.-L. Vörtler, M. Kettler: *Efficient simulation of chemical potentials of water-like fluid models*, 19th Thermodyn. Conf., Sesimbra, Portugal, April 7, 2005

H.-L. Vörtler: *Simulation of chemical potentials and phase equilibria of bulk and confined fluids by particle insertion methods*, 6th Workshop Comp. Phys. (CompPhys05), Leipzig, December 2, 2005

Posters

O. Saengsawang, P. C.M.M. Magusin, T. Remsungnen, A. Loisruangsin, S. Fritzsche, A. Schüring, S. Hannongbua: *Rotational Motion of Pentane in H-ZK5*, Int. Conf. "Diffusion Fundamentals I", Leipzig 2005

A. Schüring, S.M. Auerbach, S. Fritzsche, R. Haberlandt: *Entropic Barriers for the Diffusion of Molecules under Confinement*, Int. Conf. "Diffusion Fundamentals I", Leipzig 2005

A. Loisruangsin, S. Fritzsche, S. Hannongbua: *Potential Calculations and MD Simulations of n-Pentane in Silicalite-1*, Int. Conf. "Diffusion Fundamentals I", Leipzig 2005

J. Gulin-Gonzalez, S. Vasenkov, A. Schüring, S. Fritzsche, J. Kärger: *Exploring the Extreme Transport Conditions through Membranes by Molecular Dynamics Simulations*, Int. Conf. "Diffusion Fundamentals I", Leipzig 2005

A. Schring, S. Vasenkov, S. Fritzsche: *Investigation of Anomalous Diffusion in the Transition Region Gas/Adsorbent*, Deutsche Zeolithtagung, Gießen, 2–4 March 2005

A. Loisruangsin, A. Schüring, S. Fritzsche, S. Hannongbua: *Entropic Effect on the Distribution of n-Pentane in Silicalite-1*, 2nd Asian Pacific Conf. Theor. Comp. Chem., Bangkok, Thailand, May 2–6, 2005

R. Chanajaree, O. Saengsawang, T. Remsungnen, S. Fritzsche, S. Hannongbua: *Binding Energy of Guest Molecules on the Silanol Covered (010) Silicalite-1 Surface as Studied by Quantum Chemical Calculations*, 2nd Asian Pacific Conf. Theor. Comp. Chem., Bangkok, Thailand, May 2–6, 2005

H.-L. Vörtler, M. Kettler, K. Schäfer: *Simulation of Chemical Potentials and Vapour-Liquid Equilibria in Bulk Fluids and Thin Films Using Particle Insertion Methods*, EMLG/JMLG Annual Meeting 2005, Prague, September 5, 2005

11.15 Guests

- Prof. Dr. S. Hannongbua
  Chulalongkorn University, Thailand
  29.08.-19.09.2006
- S. Yashonath
  Indian Institute of Science, Bangalore
  19.-28.11.2006
- Dr. T. Remsungnen
  Khon Khaen University, Thailand
  03.10.-31.10.2006
- Prof. Ivo Nezbeda
  Czech. Acad. Sci.
  Dec 5 – Dec 10, 2005

12

Quantum Field Theory and Gravity

12.1 Higher Order Correlation Corrections to Color Ferromagnetic Vacuum State at Finite Temperature

M. Bordag, A. Strelchenko, V. Skalozub*, Y. Grebenjuk†

*Physical Faculty, University of Dnepropetrovsk, Russia
†Physical Faculty, University of St. Petersburg, Russia

Topic of the investigation is the stability of the ground state of QCD with temperature and color magnetic magnetic background field by means of the calculation fo the polarization tensor of the gluon field. Special attention was payed to the spontaneous creation of a color magnetic field. A. Strelchenko successfully defended his PhD-thesis *Polarization of neutral gluons in SU(3) gluodynamics in external field at high temperature*.

M. Bordag and V. Skalozub continued the investigation of the polarization tensor for the color charged gluons. Different gauge fixing conditions have been considered and the general structure of the polarization tensor was clarified. The complete polarization tensor was calculated in a magnetic field in covariant gauge. Its non transversality was shown and independently confirmed using the Ward identities. The dependence on the gauge fixing parameter was calculated.

[1] M. Bordag, V. Skalozub: Eur. Phys. J. C **45**, 159 (2006)

12.2 Spectral Zeta Functions and Heat Kernel Technique in Quantum Field Theory with Nonstandard Boundary Condition

M. Bordag, V. Nesterenko*, I. Pirozhenko*

*Joint Institute for Nuclear Research, Dubna, Russia

Spectral zetafunction and heat kernel are the most important instruments for the investigation of the ultraviolet properties of vacuum energy. For a number of boundary

condition, for instance if the leading symbol of the differential operator is not simple or if the ellipticity of the operator is lost, there is so far no general procedure to obtain the coefficients. In this project we try to adopt the method of integral equation for these problems. For the model of thin plasma sheets the spectral function including the heat kernel coefficients were calculated [1, 2].

[1] I.G. Pirozhenko et al.: J. Math. Phys. **46**, 042 305 (2005)
[2] M. Bordag et al.: J. Phys. A **38**, 11 027 (2005)

12.3 Quantization of Electrodynamics with Boundary Conditions

M. Bordag

The quantization of electrodynamics with boundary conditions was reconsidered. It was shown that the conductor boundary conditions do not provide a unique realization. Especially, it was shown that there exists a realization where the normal component of the electric field on the boundary does not obey any condition. Measurable consequences had been found in the Casimir-Polder force which appears reduced by about 13 % in that case [1].

[1] M. Bordag: Int. J. Mod. Phys. A **20**, 2505 (2005)

12.4 Casimir Effect and Real Media

M. Bordag, B. Geyer, G.L. Klimchitskaya*, V.M. Mostepanenko†

*Physics Department, University of St. Petersburg, Russia
†Noncommercial Partnership "Scientific Instruments" of Ministry of Industry, Sciences and Technologies, Moscow, Russia

The vacuum of quantum fields shows a response to changes in external conditions with measurable consequences. The investigation of the electromagnetic vacuum in the presence of real media is of actual interest in view of current experiments as well as nanoscopic electro-mechanical devices [1]. In recent experiments using atomic force microscopy the Casimir effect had been measured with high accuracy. This required a detailed investigation of the influence of real experimental structures on the corresponding force.

It is well known that, beginning in 2000, the behavior of the thermal correction to the Casimir force between real metals has been hotly debated. As was shown by several research groups, the Lifshitz theory, which provides the theoretical foundation for the calculation of both the van der Waals and Casimir forces, leads to different results depending on the model of metal conductivity used. To resolve these controversies, the theoretical considerations based on the principles of thermodynamics and new experimental tests were invoked.

- Previously, using the surface impedance approach the Lifschitz formula for the free energy and the Casimir force between real metals was derived in perfect agreement with thermodynamics; thereby resolving a longstanding controversy [2, 3]. In fact, that approach was shown to be in perfect agreement with both thermodynamics and experimental data.
  Based on these results, the present status of the problem – in particular, the advantages and disadvantages of the approaches based on the surface impedance and on the Drude model of dielectric function – has been analyzed [4] using rigorous analytical calculations of the entropy of a fluctuating field. Also the results of a new precise experiment on the determination of the Casimir pressure between two parallel plates by means of a micromechanical torsional oscillator has been discussed.
- Recently, there have been adduced arguments against the traditional approach to the thermal Casimir force between real metals and in favor of one of the alternative approaches [5]. The latter assumes zero contribution from the transverse electric mode at zero frequency in qualitative disagreement with unity as given by the thermal quantum field theory for ideal metals. The authors of [5] claimed that their approach is consistent with experiments as well as with thermodynamics. In reaction on this, we demonstrated that these conclusions are incorrect [6]. Especially, we showed that their results are contradicted by four recent experiments and also violate the third law of thermodynamics (the Nernst heat theorem).
- Previously, the Casimir interaction between two thick parallel plates, one made of metal and the other of dielectric, was investigated at nonzero temperature [3]. This work has been extended to the Casimir and van der Waals interaction between two dissimilar thick dielectric plates [7] by reconsidering, on the basis of thermal quantum field theory in Matsubara formulation, the old approach of Lifshitz [8]. Based on the main derivations of the Lifshitz formula in the framework of thermal quantum field theory *without* use of the fluctuation-dissipation theorem, a set of special conditions is formulated under which these derivations remain valid in the presence of dissipation. The low-temperature behavior of the Casimir and van der Waals interactions between dissimilar dielectrics is found analytically for both an idealized model of dilute dielectrics and for real dielectrics with finite static dielectric permittivities. The free energy, pressure and entropy of the Casimir and van der Waals interactions at low temperatures demonstrate the same universal dependence on the temperature as was previously discovered for ideal metals. The entropy vanishes when temperature goes to zero proving the validity of the Nernst heat theorem. The obtained asymptotic expressions are compared with numerical computations for both dissimilar and similar real dielectrics and found to be in excellent agreement. It is shown that the inclusion of conductivity in the model of dielectric response leads to the violation of the Nernst heat theorem.

[1] M. Bordag et al.: Phys. Rept. **353**, 1 (2001)
[2] B. Geyer et al.: Phys. Rev. A **67**, 062 102 (2003)
[3] B. Geyer et al.: Phys. Rev. A **70**, 016 102 (2004)
[4] V.M. Mostepanenko et al.: arXiv:quant-ph/0512134
[5] I. Brevik et al.: Phys. Rev. E **71**, 056 101 (2005)
[6] V.B. Bezerra et al.: arXiv:quant-ph/050313
[7] B. Geyer et al.: Phys. Rev. D **72**, 085 009 (2005)
[8] E.M. Lifshitz: Zh. Eksp. Teor. Fiz. **29**, 94 (1956) [Sov. Phys. JETP **2**, 73 (1956)]

12.5 Quantum Field Theory of Light-Cone Dominated Hadronic Processes

B. Geyer, J. Eilers, J. Blümlein*, D. Robaschik†, O. Witzel‡

*Institut für Hochenergiephysik, Zeuthen
†Institute for Theoretical Physics, Brandenburg Technical University
‡Institute for Physics, Humboldt-Universität Berlin

Light-cone dominated, polarized hadronic processes at large momentum transfer factorize into process-dependent hard scattering amplitudes and process-independent non-perturbative generalized distribution amplitudes. Growing experimental accuracy requires the entanglement of various twist as well as (target) mass contributions and radiative corrections. Their quantum field theoretic prescription is based on the nonlocal light-cone expansion [1] and the group theoretical procedure of decomposing *nonlocal, tensor-valued* QCD operators into tensorial harmonic operators with well-defined geometric twist (τ = dimension − spin) developed in our previous work [2, 3].

Continuing these studies the following results were obtained and applied to generic hadronic processes:

- The complete twist-2 part of the Compton amplitude has been studied including all target mass corrections rigorously [4]. Starting from the well-known expression of the Compton operator in coordinate space we performed its Fourier transform and formed the necessary matrix elements afterwards. This procedure allows, besides a clear separation of theoretically different contributions, the consideration of different kinematical decompositions of the matrix element. As a result we derived a closed expressions for the Compton amplitude in terms of iterated generalized parton distribution amplitudes (GPD). Specializing to the forward case the generalized Wandzura-Wilczek relation of Blümlein-Tkabladze and the extended Callan-Gross relation of Georgi-Politzer are rediscovered. In addition, we were able to show that both relations for the imaginary part of the Compton amplitude can be generalized to the non-forward case when introducing suitable new parameters t, being a generalized Nachtmann variable, and ζ into the GPD $\Phi(t, \zeta)$. The non-forward relations between these functions are of the same shape as in the forward case but appear as superposition of amplitudes for different values of ζ. Interestingly, we were able to show that only three independent structure functions, g_1, $\mathcal{W}_1$ and $\mathcal{W}_L$, determine the absorptive part of the complete amplitude at twist-2.
- Generalizing the foregoing studies the power as well as mass corrections for the Compton operator at leading twist are determined at operator level [5]. From the complete off-cone representation of the twist-2 Compton operator integral representations for the trace, antisymmetric and symmetric part of that operator are derived. The operator valued invariant functions are written in terms of iterated operators and may lead to interrelations. For matrix elements they go over into relations for generalized parton distributions. Reducing to the s-channel relevant part one gets operator pre-forms of the Wandzura-Wilczek and the (target mass corrected) Callan-Gross relations whose structure is exactly the same

as known from the case of deep inelastic scattering; taking non-forward matrix elements one reproduces earlier results [4] for the absorptive part of the virtual Compton amplitude. All these relations, obtained without any approximation or using equations of motion, are determined solely by the twist-2 structure of the underlying operator and, therefore, are purely of geometric origin.

- A quantum field theoretic treatment of inclusive deep-inelastic diffractive scattering is considered [6]. The process can be described in the general framework of non-forward scattering processes using the light-cone expansion in the generalized Bjorken region. Target mass and finite-t corrections of the diffractive hadronic tensor are derived at the level of the twist-2 contributions both for the unpolarized and the polarized case. They modify the expressions contributing in the limit $t, M^2 \to 0$ for larger values of β or/and t in the region of low Q^2. The different diffractive structures are expressed through integrals over the relative momentum of non-perturbative t-dependend 2-particle distribution functions. In the limit $t, M^2 \to 0$ these distribution functions are the diffractive parton distribution. Relations between the different diffractive structure functions are derived.

[1] S.A. Anikin, O.I. Zavialov: Ann. Phys. (N.Y.) **116** (1978) 135; D. Müller et al.: Fortschr. Phys. **42**, 101 (1994)
[2] B. Geyer et al.: Nucl. Phys. B **559**, 339 (1999); B **618**, 99 (2001); B. Geyer, M. Lazar: Nucl. Phys. B **581**, 341 (2000), Phys. Rev. D **63**, 094 003 (2001); J. Eilers, B. Geyer: Phys. Lett. B **546**, 78 (2002)
[3] J. Eilers et al.: Phys. Rev. D **69**, 034 015 (2004)
[4] B. Geyer et al.: Nucl. Phys. B **704**, 279 (2005)
[5] B. Geyer, D. Robaschik: Phys. Rev. D **71**, 054 018 (2005)
[6] J. Blümlein et al.: to be published

12.6 Nonperturbative Aspects of 2D Gravity

D. Grumiller, R. Meyer, D.V. Vassilevich

One of the main goals of contemporary theoretical physics is a unification of gravity with quantum theory, i.e., to create a consistent theory of quantum gravity. Due to the complexity and difficulty (both conceptually and technically) of this task there exist many different ways to approach this problem, the most prominent ones being string theory and loop quantum gravity (for a recent survey discussing the status of quantum gravity cf. e.g. [1]). One way to simplify the problem technically (but encountering still essentially the same conceptual problems) is to consider lower dimensional models. For an extensive review on dilaton gravity in two dimensions cf. [2]. The successes of the "Wiener Schule" are intimately related to a first order formulation in terms of Cartan variables and auxiliary fields, a bit in the spirit of Ashtekar's formulation of 4D gravity, but without necessarily invoking a 1+1 split.

In this way, for instance, the phenomenon of virtual black holes arising as intermediate states in S-matrix calculations can be described quantitatively without invoking ad-hoc assumptions and without encountering information loss (for a recent review cf. [3]).

Another example concerns the so-called Witten black hole [4] and its nonperturbative generalization, the exact string black hole (ESBH) [5]. Exploiting first order techniques only recently an action for the ESBH had been constructed which for the first time since the discovery of the ESBH in 1992 allowed a thorough discussion of its mass and entropy, as well as supersymmetric extensions and quantization [6].

Finally, a recent [7] constraint analysis in the presence of boundaries revealed that the presence of a horizon imposes severe constraints on the physical phase space, which leads to a conversion of physical degrees of freedom into gauge degrees of freedom. This result may be of importance for understanding black hole entropy.

[1] S. Carlip: Rept. Prog. Phys. **64**, 885 (2001), arXiv:gr-qc/0108040
[2] D. Grumiller et al.: Phys. Rept. **369**, 327 (2002), arXiv:hep-th/0204253
[3] D. Grumiller: Int. J. Mod. Phys. D **13**, 1973 (2004), arXiv:hep-th/0409231
[4] E. Witten: Phys. Rev. D **44**, 314 (1991)
[5] R. Dijkgraaf et al.: Nucl. Phys. B **371**, 269 (1992)
[6] D. Grumiller: J. High Energy Phys. **0505**, 028 (2005), arXiv:hep-th/0501208
[7] L. Bergamin et al.: to be published, arXiv:hep-th/0512230

12.7 Structure of the Gauge Orbit Space and Study of Gauge Theoretical Models

G. Rudolph, S. Charzynski, C. Fleischhack*, A. Hertsch, J. Huebschmann, P. Jarvis†, J. Kijowski‡, M. Schmidt, I.P. Volobuev§

*Max Planck Institute for Mathematics in the Sciences, Leipzig
†School of Physics, University of Tasmania, Hobart, Australia
‡Faculty of Physics, University of Warsaw, Poland
§Skobeltsyn Institute for Nuclear Physics, Moscow State University, Russia

Based upon our results on the structure of the gauge orbit space [1] and on lattice gauge theories [2, 3, 4], we continued to investigate non-perturbative aspects of quantum gauge theory with special emphasis on the following items:

i) The study of the physical role of nongeneric strata in the gauge orbit space was continued. The topological structure of the reduced configuration space for a lattice of 2 plaquettes space was clarified by means of a cell decomposition [5, 6]. Together with J. Huebschmann from the Department of Mathematics of the University of Lille, who holds a one year DFG Mercator professorship at the Institute for Theoretical Physics of our university the construction of Kähler quantization [7] for lattice gauge models was initiated.

ii) The study of non-perturbative aspects of gauge theories on the lattice in terms of gauge-invariant quantities ('observables') was continued. The structure of the algebra of observables for QCD and the superselection structure of its representations was clarified [8].

iii) The study of the structure of the observable algebra for lattice QCD in purely algebraic (representation independent) terms led to the investigation of nonlinear (super) algebras [9, 10].

iv) Christian Fleischhack continued the study of gauge theories within the Ashtekar approach. The main result obtained is a generalization of the Stone-von Neumann uniqueness theorem to quantum geometry, i.e., diffeomorphism-invariant gauge theories [11].

[1] G. Rudolph et al.: J. Math. Phys. Anal. Geom. **5**, 201 (2002); J. Geom. Phys. **42**, 106 (2002); J. Phys. A: Math. Gen. **35**, R1 (2002)
[2] J. Kijowski et al.: Commun. Math. Phys. **188**, 535 (1997)
[3] J. Kijowski et al.: Annales H. Poincaré **4**, 1137 (2003)
[4] J. Kijowski, G. Rudolph: J. Math. Phys. **43**, 1796 (2002)
[5] S. Charzyński et al.: J. Geom. Phys. **55**, 137 (2005)
[6] S. Charzyński et al.: arXiv:hep-th/0512129
[7] J. Huebschmann, Mem. Amer. Math. Soc. **172**, 814 (2004); Fields Inst. Commun. **43**, 295 (2004); J. Reine Angew. Mathematik **591**, (2006), in press, arXiv:math.sg/0207166
[8] J. Kijowski, G. Rudolph: J. Math. Phys. **46**, 032 303 (2005); Rep. Math. Phys. **55**, 199 (2005)
[9] P. Jarvis, G. Rudolph: J. Phys. A, **36**, 5531 (2003)
[10] P. Jarvis et al.: J. Phys. A **38**, 5359 (2005)
[11] C. Fleischhack: arXiv:math-ph/0407006

12.8 Noncommutative Geometry

G. Rudolph, P. Hajac*, R. Matthes*, W. Szymanski†

*Faculty of Physics, University of Warsaw, Poland
†Faculty of Science and Information Technology, University of Newcastle, UK

The study of quantum principal bundles was continued. The examples of generalized locally trivial Hopf bundles have been further analyzed. One has two nonisomorphic quantum principal bundles living over two different quantum two-spheres. One of these two-spheres is topologically the generic Podleś sphere, the other one results from a gluing of two quantum discs with an extra twist (mirror-type quantum sphere). Meanwhile, several independent proofs of the non-isomorphy of the C^*-algebras of these quantum two-spheres have been found. A publication concerning these matters is under preparation. The total spaces of the bundles coincide and are hybrids of the 3-sphere of the locally trivial bundle and the 3-sphere of Matsumoto [1]. Many of the results known for the locally trivial quantum Hopf bundle (in particular Chern numbers) are true also for these generalizations. The total space can be viewed as a quantum analogue of a Heegaard splitting of the 3-sphere. Its topological properties (in particular K-theory) have been investigated in collaboration with P. Baum [2]. There it is shown that on the C^*-level this quantum 3-sphere is a gluing of two quantum solid

tori (whose C^*-algebras are crossed products of the Toeplitz algebra by an action of the integers), and that its K-groups (being computed by means of the Pimsner-Voiculescu and Mayer-Vietoris sequences) coincide with those of the classical 3-sphere.

As a new project, the investigation of topological invariants (K-theory) of observable algebras has been started. This concerns observable algebras determined by Kijowski and Rudolph [3] for several models of gauge field theory. The hope is to identify superselection sectors of quantum field theory as invariants of K-theory and to relate them to other notions of noncommutative geometry.

[1] K. Matsumoto: Japan J. Math. **17**, 333 (1991)
[2] P. Baum et al.: arXiv:math.kt/0409537, to appear in K-Theory
[3] J. Kijowski, G. Rudolph: J. Math. Phys. **46**, 032 303 (2005); Rep. Math. Phys. **55**, 199 (2005)

12.9 Contributions to Quantum Informatics

A. Uhlmann, P. Alberti, B. Crell, J. Dittmann

The following problems were studied: representation and properties of the fidelity of density operators and related quantities [1, 2], differential geometry of monotonous metrics on the space of states, in particular, of Bures' metric, properties of purifying lifts, transport of states, and geometrical phases [3], refinements of Bures' metric (partial fidelities, decomposition of pairs of states), operators and mappings related to Einstein-Podolski-Rosen channels and quantum teleportation [4]. Furthermore, characteristic parameters (entropy, channel capacity) for quantum channels of length two were calculated [5]. The use of anti-linearity in quantum information and possible connections with k-positivity were discussed. One aim is the algebraic formulation of some basic concepts of quantum information theory.

[1] P. Alberti, A. Uhlmann: Acta Appl. Math. **60**, 1 (2000)
[2] A. Uhlmann: arXiv:quant-ph/9909060; arXiv:quant-ph/9912114
[3] J. Dittmann, A. Uhlmann: J. Math. Phys. **40**, 3246 (1999)
[4] A. Uhlmann: in *Fin De Siecle*, Lecture Notes in Physics 539 (Springer, 2000), p 93; in *Trends in Quantum Mechanics* (World Scientific, 2000) p 128
[5] A. Uhlmann: Open Sys. Inf. Dyn. **12**, 93 (2005)

12.10 Local Approach to Vacuum Polarization

D.V. Vassilevich, P. van Nieuwenhuizen*

*Department of Physics and Astronomy, State University of New York, Stony Brook, USA

The heat kernel approach provides the opportunity to investigate locally properties of models in quantum field theory which are due to global properties of the underlying

manifold. We have investigated the heat kernel expansion on Moyal planes for generalized Laplace operators which contain both left and right star multiplications [1]. It was found that the heat kernel expansion is not local even in the star sense. Anomalies were also evaluated. We were also able to calculate the conformal anomaly on curved two-dimensional noncommutative manifolds [2]. It is known that in supergravities on manifolds with boundaries the ultra-violet divergences do not cancelled even at one loop. Being motivated by this problem we have reconsidered the problem of constructing supersymmetric boundary conditons [3]. We have demonstrated that the usual Gibbons-Hawking set of the boundary conditions cannot be extended toa locally supersymetric one. We also found a set of supersymmetric boundary conditions which require vanishing extrinsic curvature of the boundary. An extension of the classical and quantum integrability results of two-dimansional gravities to euclidean manifolds was obtained in [4]. A review paper on the heat kernel methods of quantum field theory for mathematicians was published [5].

[1] D.V. Vassilevich: J. High Energy Phys. **0508**, 085 (2005)
[2] D.V. Vassilevich: Nucl. Phys. B **715**, 695 (2005)
[3] P. van Nieuwenhuizen, D.V. Vassilevich: Class. Quant. Grav. **22**, 5029 (2005)
[4] L. Bergamin et al.: Class. Quant. Grav. **22**, 1361 (2005)
[5] D.V. Vassilevich: Contemp. Math. **366**, 3 (2005)

12.11 Quantum Field Theoretic and Relativistic Aspects of Quantum Information Theory, Quantum Energy Inequalities, Generally Covariant Quantum Field Theory

R. Verch, P. Marecki, C.J. Fewster*, P. Mazur†, M. Paschke‡, T. Roman§, R. Werner¶

*Department of Mathematics,University of York, UK
†Department of Physics and Astronomy, University of Southern Carolina, USA
‡Max Planck Institute for Mathematics in the Sciences, Leipzig
§Department of Mathematics, University of Connecticut, USA
¶Institute for Mathematical Physics, Technical University of Braunschweig

Relativistic aspects are up to now not prominently considered in quantum information theory, there is however a growing interest in using concepts of quantum information theory also in more fundamental contexts such as black hole entropy. This makes it necessary to extend concepts of quantum information theory to the setting of relativistic quantum field theory. We have begun such a study in [2].

An important question in quantum field theory on curved spacetimes is the question of stability of solutions to the semiclassical Einstein equations of gravity coupled to quantized matter. Of central importance are here the positivity properties of energy densities of quantized matter fields. These properties can be formulated as so-called quantum-energy-inequalities. Therefore, quantum-energy-inequalities have been and

will be continued to be carefully analyzed in quantum field theory and in quantum mechanics [1].

[1] S.P. Eveson et al.: Ann. Henri Poincaré **6**, 1 (2005)
[2] R. Verch, R.F. Werner: Rev. Math. Phys. **17**, 545 (2005)

12.12 One-Particle Properties of Quasiparticles in the Half-Filled Landau Level

W. Weller

Using field theoretical methods, two-dimensional electron systems in strong magnetic fields were studied. The investigations were concentrated on the half-filled lowest Landau level.

The theory for the half-filled lowest Landau level of Halperin et al. [1] transforms from the electrons to Chern–Simons Fermions by eliminating the external magnetic field. The theory leads to an infrared divergent energy. It was shown [2] that this is due to missing diagrams and to the fact that in [1] the ordering of the operators in the path integral was changed. The correct formulation yields a three-particle interaction. For this interaction, a path integral representation was developed [2] with correct ordering of the operators. The energy was computed by evaluating the path integral in various approximations. The calculated energies are convergent and agree well with numerical simulations. The idea of the Singwi-Sjölander approach to the 3d Coulomb problem was extended to the Chern-Simons theory [3] with even better results for the energies. An approximation scheme was developed conserving the particle number and the constraints.

For the numerical evaluation of the analytical field theory we use the Luttinger–Ward variational principle for the thermodynamic potential. Because this is the first numerical application of that principle, the method was tested on the simpler two-dimensional Coulomb system.

From the analytical theory the effective mass of the Composite Fermions was calculated in good agreement with the experimental results.

The development of a field theory of quantum Hall systems for Laughlin filling $\nu = 1/(2m + 1)$ ($m = 1, 2, \ldots$) was started.

[1] B.I. Halperin et al.: Phys. Rev. B **47**, 7312 (1993)
[2] W. Weller et al.: in Proc. 6th Int. Conf. Path Integrals, ed. by R. Casalbuoni et al. (World Scientific, Singapore 1999) p 466
[3] J. Dietel, W. Weller: Phys. Rev. B **64**, 195 307 (2001)

12.13 Funding

Lokale Methoden zur Berechnung der Vakuumpolarisation
PD Dr. M. Bordag
DFG Bo 1112/12-1

Structure of the gluon polarization tensor in a color magnetic field background at finite temperature
PD Dr. M. Bordag, Dr. D. Vassilevich
DFG 436 UKR 17/24/05 and GK QFT

Spectral zeta functions and heat kernel technique in quantum field theory with non-standard boundary condition
PD Dr. M. Bordag, Dr. D. Vassilevich
Heisenberg-Landau programme

Improved study of the Casimir force between real metals and its application to constraints for testing extra-dimensional physics
Prof. Dr. B. Geyer
DFG 436 RUS 113/789/0-1

Nonperturbative aspects of 2D dilaton gravity
Dr. D. Grumiller
Erwin-Schrödinger Stipendium granted by the Austrian Science Foundation (FWF), project J2330-N08

Quantum Gravity, Cosmology and Categorification
Dr. D. Grumiller, Prof. Dr. S. Moskaliuk
Project on scientific cooperation between the Austrian Academy of Sciences and the National Academy of Sciences of Ukraine No. 01/04

Dilaton Supergravity
Dr. D. Grumiller, Dr. L. Bergamin
Travel grants for visits from project P-16030-N08 of FWF

Quantum Theory of Lattice Gauge models
A. Hertsch
Grant of International Max Planck Research School

Mercator professorship September 1, 2005 – August 31, 2006
Prof. Dr. J. Huebschmann
DFG Le 758/22-1

Kosciuszko Foundation Fellowship for a visit to the University of South Carolina
P. Marecki

Untersuchungen zur physikalischen Bedeutung der Stratifizierung des Eichorbitraumes
Prof. Dr. G. Rudolph
DFG RU 692/3-2

Oberwolfach Meeting on Noncommutative Geometry and Quantum Field Theory
R. Verch, S. Doplicher (Rome), M. Paschke (MPI-MIS Leipzig), E. Zeidler (MPI-MIS Leipzig)
Oberwolfach Meeting 0543a, funded by Mathematisches Forschungsinstitut Oberwolfach (MFO), 23-29 October 2005

One-particle properties of quasiparticles in the half-filled Landau level
W. Weller
DFG-Schwerpunktprogramm Quanten-Hall-Systeme, WE 480/3-3

12.14 Organizational Duties

M. Bordag
- Referee: J. Phys. A, Phys. Rev. D, J. Math. Phys.
- Head of International Organizing Committee for the 'Workshop on Quantum Field Theory under the influence of external conditions', September 2005 in Barcelona

C. Fleischhack
- Member of the Search and Selection Committee of Die Junge Akademie (The Young Academy)
- Spokesman Arbeitsgruppe Wissenschaftspolitik (Science Policy) der Jungen Akademie, since October 2003
- Member of the Selection Committee of the Studienstiftung des Deutschen Volkes (German National Merit Foundation)
- Co-organizer of the UK-German "Frontiers of Science" Meeting (Royal Society, March/April 2006)
- Corrector and Coordinator of the Mathematics Olympiad
- Referee: Commun. Math. Phys., J. Math. Phys., Class. Quant. Grav., J. Phys. A

B. Geyer
- Member of electing board Latin America-South of DAAD
- Vertrauensdozent of Gesellschaft Dt. Naturforscher und Ärzte
- Referee: DFG, DAAD, Humboldt Foundation

D. Grumiller
- Co-editor: December 2005 Special Issue of Int. J. Mod. Phys. D
- Referee: Class. Quant. Grav., Int. J. Mod. Phys. D, Mod. Phys. Lett. A
- Member of Editorial Board of FAKT-webpage www.teilchen.at (FAKT="Fachausschuß Kern- und Teilchenphysik" of the Austrian Physical Society)

J. Huebschmann
- Coeditor: J. Pure and Applied Algebra; Homology, Homotopy, and its Applications; Proc. A. Razmadze Mathi. Inst. (Tiflis/Georgien); JHRS (Journal of Homotopy and Related Structures); Travaux Mathématiques (Luxembourg)
- Referee: Acta Math. Hungarica, Annali dell'Universita' di Ferrara, sez. VII, Scienze Matematiche, J. Symbolic Computation, Diff. Geometry and its Applications

G. Rudolph
- Referee: Class. Quant. Grav., J. Math. Phys., J. Geom. Phys., J. Phys. A, Rep. Math. Phys.
- Director of the Institute for Theoretical Physics

M. Schmidt
- Referee: J. Phys. A

A. Uhlmann
- Board member: Rep. Math. Phys., Open Systems and Information Dynamics

D.V. Vassilevich
- Referee: Class. Quant. Grav., J. Phys. A, Nucl. Phys. B, Mod. Phys. Lett. A, J. High Energy Phys., Nuovo Cimento B, London Math. Soc.
- Coordinator, Program on Gravity in Two Dimensions, ESI (Wien)
- Program Committee, Fock School on Advances in Physics (St.Petersburg)

R. Verch
- Vice chairman of the board for the Theoretical and Mathematical Physics Section, Deutsche Physikalische Gesellschaft (DPG)
- Referee for the 'Fonds zur Förderung der wissenschaftlichen Forschung in Österreich' (FWF)
- Referee: Commun. Math. Phys., J. High Energy Phys., J. Math. Phys., Rev. Math. Phys.
- Reviewer for Mathematical Reviews

12.15 External Cooperations

Academic

- Max-Planck Institute for Mathematics in the Sciences (MPI-MIS), Leipzig
  Dr. C. Fleischhack, Dr. M. Paschke
- DESY-Institute of High Energy Physics, Zeuthen
  Dr. J. Blümlein
- Institute of Theoretical Physics, Brandenburg Technical University, Cottbus
  Prof. Dr. D. Robaschik
- Physikalisch-Technische Bundesanstalt
  PD Dr. habil. W. Apel, Dipl.-Phys. M.P. Agnihotri
- Inst. f. Mathematical Physics, TU Braunschweig
  Prof. Dr. R.F. Werner
- Institute for Theoretical Physics, Universität Regensburg
  Prof. Dr. J. Siewert
- Institute of Theoretical Physics, TU Wien, Austria
  Dr. H. Balasin, Dr. L. Bergamin, Dr. C. Böhmer, Prof. W. Kummer
- Institute for Theoretical Physics, University of Wien, Austria
  Prof. Dr. H. Narnhofer
- Spinoza Institute, Department for Physics and Astronomy, Utrecht University, The Netherlands
  Dr. H. Sahlmann
- Université des Sciences et Technologies de Lille, France
  Prof. Dr. J. Huebschmann

- Department of Mathematics, University of York, England, UK
  Dr. C.J. Fewster
- Dipartimento di Matematica, Universita di Trento, Trento, Italy
  Prof. Dr. V. Moretti
- ESA
  Dr. Luzi Bergamin
- Instytut Fizyki Teoretycznej, University of Warsaw, Poland
  Prof. J. Lewandowski
- Polish Academy of Sciences, Center for Theoretical Physics, Warsaw, Poland
  Prof. Dr. J. Kijowski
- Polish Academy of Sciences, Mathematics Institute and University of Warsaw, Poland
  Prof. Dr. P. Hajac, Dr. R. Matthes
- Charles University Prague, Czech Republic
  Dr. A. Iorio
- Skobeltsyn Institute of Nuclear Physics, Lomonosov Moscow State University, Russia
  Dr. I.P. Volobuev
- National University, Dnepropetrovsk, Ukraine
  Prof. V. Skalozub
- St. Petersburg University, Russia
  Prof. Y.V. Novozhilov, Y. Grebenjuk
- Dept. of Physics, North-West Polytechnical University St. Petersburg, Russia
  Prof. Dr. G.L. Klimchitskaya
- Noncommercial Partnership "Scientific Instruments" of Ministry of Industry, Sciences and Technologies, Moscow, Russia
  Prof. Dr. V.M. Mostepanenko
- Department of Mathematics, University of Florida, Gainesville, USA
  Prof. Dr. S.J. Summers
- Department of Mathematics, Connecticut State University, USA
  Prof. Dr. T. Roman
- Department of Physics, University of South Carolina, USA
  Prof. Dr. P. Mazur
- State University of New York at Stony Brook, USA
  Prof. P. van Nieuwenhuizen
- University of Oregon, USA
  Prof. P.B. Gilkey
- Massachusetts Institute of Technology (MIT), USA
  Dr. A. Iorio, Prof. R. Jackiw
- Institute for Gravitational Physics and Geometry, Penn State University, USA
  Prof. Dr. A. Ashtekar
- University of North Carolina at Chapel Hill, USA
  Prof. em. Dr. J.D. Stasheff

- Universidad de Zacatecas, Mexico
  Prof. D. Ahluwalia-Khalilova, Dr. C. Böhmer
- University of Tasmania, Hobart, Australia
  Prof. Dr. P. Jarvis
- University of Newcastle, Australia
  Prof. Dr. W. Szymanski

12.16 Publications

Journals

D.V. Ahluwalia-Khalilova, D. Grumiller: *Dark matter: A spin one half fermion field with mass dimension one?*, Phys. Rev. D **72**, 067 701 (2005)

D.V. Ahluwalia-Khalilova, D. Grumiller: *Spin half fermions with mass dimension one: Theory, phenomenology, and dark matter*, J. Cosmol. Astropart. Phys. **0507**, 012 (2005)

H. Balasin, C.G. Böhmer, D. Grumiller: *The spherically symmetric standard model with gravity*, Gen. Rel. Grav. **37**, 1435 (2005)

L. Bergamin, D. Grumiller, W. Kummer, D.V. Vassilevich: *Classical and quantum integrability of 2D dilaton gravities in Euclidean space*, Class. Quant. Grav. **22**, 1361 (2005)

M. Bordag: *Reconsidering the quantization of electrodynamics with boundary conditions*, Int. J. Mod. Phys. A **20**, 2505 (2005)

M. Bordag, I.G. Pirozhenko, V.V. Nesterenko: *Spectral analysis of a flat plasma sheet model*, J. Phys. A **38**, 11 027 (2005)

S. Charzynski, J. Kijowski, G. Rudolph, M. Schmidt: *On the stratified classical configuration space of lattice qcd*, J. Geom. Phys. **55**, 137 (2005)

S.P. Eveson, C.J. Fewster, R. Verch: *Quantum inequalities in quantum mechanics*, Ann. Henri Poincaré **6**, 1 (2005)

B. Geyer: *Cohomological Gauge Theories in D > 4 With Special Holonomy Spin(7) and G(2)*, 6. Alexander Friedmann Int. Sem. Grav. Cosmol., Cargese 2004, Int. J. Mod. Phys. A **20**, 2490 (2005)

B. Geyer, G.L. Klimchitskaya, V.M. Mostepanenko: *Thermal Quantum Field Theory and the Casimir Interaction Between Dielectrics*, Phys. Rev. D **72** 085 009 (2005)

B. Geyer, P. Lavrov: *Fedosov Supermanifolds. II. Normal Coordinates*, Int. J. Mod. Phys. A **20**, 2179 (2005)

B. Geyer, D. Robaschik: *Twist-2 Compton Operator and its Hidden Structure: WW-, CG- and Other Relations*, Int. Conference "Light Cone 2004", Amsterdam 2004, Few Body Syst. **36**, 95 (2005)

B. Geyer, D. Robaschik: *The Twist-2 Compton Operator and its Hidden Wandzura-Wilczek and Callan-Gross Relations*, Phys. Rev. D **71**, 054 018 (2005)

B. Geyer, D. Robaschik, J. Eilers: *Target Mass Corrections for Virtual Compton Scattering at Twist-2 and Generalized, Non-Forward Wandzura-Wilczek and Callan-Gross Relations*, Nucl. Phys. B **704**, 279 (2005)

B. Geyer, O. Witzel: *B-Meson Distribution Amplitudes of Geometric Twist vs. Dynamical Twist* Phys. Rev. D **72**, 034 023 (2005)

D. Grumiller: *An action for the exact string black hole*, J. High Energy Phys. **0505**, 028 (2005)

D. Grumiller: *Logarithmic corrections to the entropy of the exact string black hole* Proc. 8th Int. Conf. Path Integrals, Prague, 06.-10.06.2005, ed. by C. Burdik, O. Navratil, S. Posta, Dubna, JINR, 2005

J. Huebschmann: *Singular Poisson-Kähler geometry of Scorza varieties and their secant varieties*, Diff. Geom. Appl. **23**, 79 (2005)

P. Jarvis, J. Kijowski, G. Rudolph: *On the structure of the observable algebra of qcd on the lattice*, J. Phys. A: Math. Gen. **38**, 5359 (2005)

J. Kijowski, G. Rudolph: *Charge superselection sectors for qcd on the lattice*, J. Math. Phys. **46**, 032 303 (2005)

J. Kijowski, G. Rudolph: *The observable algebra of lattice qcd*, Rep. Math. Phys. **55**, 199 (2005)

P. Marecki: *Simulation of decoherence in one-qubit systems*, Archive Inst. Theo. Appl. Informatics Polish Acad. Sci. (IITiS) **17**, 113 (2005)

P. Marecki, N. Szpak: *Spontaneous emission of light from atoms: the model*, Ann. Phys. **14**, 428 (2005)

D. Mülsch, B. Geyer: *Euclidean Super Yang-Mills Theory on a Quaternionic Kähler Manifold*, Int. J. Geom. Meth. Mod. Phys. **2**, 409 (2005)

I.G. Pirozhenko, V.V. Nesterenko, M. Bordag: *Integral equations for heat kernel in compound media*, J. Math. Phys. **46**, 042 305 (2005)

A. Uhlmann: *On Concurrence and Entanglement of Rank Two Channels*, Open Sys. Inf. Dyn. **12**, 93 (2005)

R. Verch, R.F. Werner: *Distillability and positivity of partial transposes in general quantum field systems*, Rev. Math. Phys. **17**, 545 (2005)

in press

V.B. Bezerra, R.S. Decca, E. Fischbach, B. Geyer, G.L. Klimchitskaya, D.E. Krause, D. Lopez, V.M. Mostepanenko, C. Romero: *Comment on 'On the Temperature Dependence of the Casimir Effect'*, Phys. Rev. A; arXiv:quant-ph/0503134

C. Fleischhack: *Kinematical Uniqueness of Loop Quantum Gravity*, in *Quantum Gravity*, Blaubeuren 2005, ed. by B. Fauser, J. Tolksdorf, E. Zeidler (Birkhäuser, Basel)

C. Fleischhack: *Quantengravitation: Keine Experimente, aber Mathematik*, in *Jahrbuch der Max-Planck-Gesellschaft für 2005* (Max-Planck-Gesellschaft)

C. Fleischhack: *Quantization Restrictions for Diffeomorphism Invariant Gauge Theories*, in *Complex Analysis, Operator Theory and Applications to Mathematical Physics*, ed. by F. Haslinger, E. Straube, H. Upmeier, ESI-Preprintreihe, Wien

D. Grumiller: *The volume of 2D black holes*, Proc. 4th Meeting Constr. Dyn. Quant. Grav., Sardinia, September 2005, Journal of Physics: Conference Series

J. Huebschmann: *Quantization in the presence of singularities*, 4th Int. Symp. Quant. Theor. Symm., Varna, 2005, *Quantum Theory and Symmetries IV.*, ed. by V.K. Dobrev (Heron Press, Sofia)

J. Huebschmann: *Singular Poisson-Kähler geometry of certain adjoint quotients*, Proc. "The mathematical legacy of C. Ehresmann", Bedlewo 2005, Banach Center Proceedings

J. Huebschmann: *Kähler quantization and reduction*, J. Reine Angew. Math., arXiv:math.SG/0207166

R. Meyer: *Constraints in two-dimensional dilaton gravity with fermions*, Proc. Int. V.A. Fock School Adv. Phys. (IFSAP 2005), St. Petersburg, November 2005, (University of St. Petersburg Press)

V.M. Mostepanenko, V.B. Bezerra, R.S. Decca, B. Geyer, E. Fischbach, G.L. Klimchitskaya, D.E. Krause, D. Lopez, C. Romero: *Present Status of Controversies Regarding the Thermal Casimir Force*, Phys. Rev. A; arXiv:quant-ph/0512134

Talks

C. Fleischhack: *Stone-von Neumann Theorem in Quantum Geometry*, Loops05 Conf., AEI Potsdam-Golm, October 10 – 14, 2005

C. Fleischhack: *Loop Quantum Gravity*, Int. Symp. Math. Sci., Leipzig, October 6 – 8, 2005

C. Fleischhack: *Stone-von Neumann Theorems in Loop Quantum Gravity*, Workshop Quant. Fields Grav. Non-Commut. Geom., Leipzig, October 3 – 4, 2005

C. Fleischhack: *Stone-von Neumann Theorems in Quantum Geometry*, Mini-Workshop on Quantization, Complex and Harmonic Analysis, Erwin-Schrödinger Institute for Mathematical Physics, Vienna, September 22 – 23, 2005

C. Fleischhack: *Quantengeometrie: Mathematische Physik auf dem Weg zur Quantengravitation*, Selection Committee Meeting of the Emmy-Noether Program of the German National Research Foundation, Frankfurt (Main), September 12, 2005

C. Fleischhack: *Stone-von Neumann Theorem in Quantum Geometry*, 2nd Joint Meeting of AMS, DMV and ÖMG, Mainz, June 16 – 19, 2005

C. Fleischhack: *Quantum Geometry: en route to Quantum Gravity*, CNRS Recruitment Meeting, Paris, May 1 – 4, 2005

C. Fleischhack: *Quantengravitation – ein Versuch mit Schleifchen*, Spring Plenary Meeting of The Young Academy, Lübbenau/Spreewald, March 20 – 22, 2005

C. Fleischhack: *Topologie und Metrik: Geometrie im Großen und im Kleinen*, Einstein-Leibniz Cabinet at the Einstein Salon of the Berlin-Brandenburg Academy of Science, Berlin, January 15, 2005

D. Grumiller: *Path integral quantization of the exact string black hole*, Path Integrals. From Quantum Information to Cosmology, Prague, June 2005

D. Grumiller: *Black Holes and Analogues in Two Dimensions*, Quantum Simulations via Analogues, Dresden, July 2005

D. Grumiller: *Mass and entropy of the exact string black hole*, Fourth Meeting on Constrained Dynamics and Quantum Gravity, Sardinia, September 2005

J. Huebschmann: *Géométrie Poisson-kählérienne des variétés de Scorza et de leurs variétés sécantes*, Colloque de l'Université de Nantes, March 16, 2005

J. Huebschmann: *Stratified Kähler structures on adjoint quotients*, 7th Conf. Geom. Topol. Manif., The Mathematical Legacy of Charles Ehresmann, Bedlewo (Polen), May 12, 2005

J. Huebschmann: *Quantization in the presence of singularities*, IVth Int. Symp. Quant. Theor. Symm., Varna (Bulgaria), August 15 – 21, 2005

J. Huebschmann: *Classical Phase Space Singularities and Quantum Theory*, Workshop Quant. Theor. Latt. Gauge Field Models, Leipzig, October 4, 2005

P. Marecki: *On the backreaction problem for quantum fields in static spacetimes*, 16th Workshop Foundat. Construct. Asp. Quant. Field Theor., MPI-AEI Golm/Potsdam, July 08 – 09, 2005

R. Meyer: *Constraints in two-dimensional dilaton gravity with fermions*, Int. V.A. Fock School Adv. Phys., St. Petersburg, November 2005

G. Rudolph: *Some aspects of lattice qcd*, Int. Symp. Commemor. 25th Anniv. Center Theor. Phys., Polish Acad. Sci., Warsaw, June 11, 2005

G. Rudolph: *On the observable algebra and its representations for lattice qcd* IVth Int. Symp. Quant. Theor. Symm., Varna (Bulgaria), August 15 - 21, 2005

G. Rudolph: *The observable algebra of lattice qcd: general structure*, Workshop Quant. Theor. Latt. Gauge Field Models, Leipzig, October 4, 2005

M. Schmidt: *On the reduced configuration space and the reduced phase space of classical lattice chromodynamics*, 15th Workshop Foundat. Construct. Asp. Quant. Field Theor., Göttingen, January 21 – 22, 2005

M. Schmidt: *On the reduced configuration space and the reduced phase space of classical lattice chromodynamics*, Séminaire Physique Mathématique, Université des Sciences et Technologies Lille I, April 27, 2005

M. Schmidt: *On the reduced configuration space and the reduced phase space of classical lattice chromodynamics*, IVth Int. Symp. Quant. Theor. Symm., Varna (Bulgaria), August 15 – 21, 2005

M. Schmidt: *The reduced classical configuration space of lattice qcd: topology*, Workshop Quant. Theor. Latt. Gauge Field Models, Leipzig, October 4, 2005

A. Uhlmann: *Geometry of State Spaces* (10 h lectures), Int. Summerschool Quant. Information, Dresden, August 29 – September 30, 2005

R. Verch: *Vacuum fluctuations, geometric modular action and relativistic quantum information theory*, 339th WE Heraeus Seminar "Special Relativity: Will It Survive the Next 100 Years?", Potsdam, February 13 – 18, 2005

R. Verch: *Concepts of entanglement in quantum field theory*, Perimeter Institute, Waterloo, Ontario, Canada, June 1, 2005

R. Verch: *Generally covariant quantum field theory*, Perimeter Institute, Waterloo, Ontario, Canada, June 10, 2005

R. Verch: *Quantum field theory in curved spacetime, a grand tour*, Int. Symp. Math. Sci., Leipzig, October 05 – 08, 2005

R. Verch: *Generally covariant quantum field theory*, Loops05 – Int. Conf. Loop Quant. Grav., MPI-AEI Golm/Potsdam, October 10 – 14, 2005

R. Verch: *Lorentzian non-commutative geometries*, Workshop on Hyperbolic operators on Lorentzian manifolds and quantization, Erwin Schrödinger International Institute for Mathematical Physics, Vienna, Austria, November 10 – 12, 2005

W. Weller: *Particle-Hole Excitations in the Quantum Hall System at filling* $\nu = 1/2$, Meeting of the DFG Schwerpunkt "Quantum Hall Systems", Bad Honnef January 27 – 28, 2005

12.17 Graduations

Doctorate

- Alexei Strelchenko
  Polarization of neutral gluons in SU(3) gluodynamics in external field at high temperature
  October 19, 2005

Diploma

- Alexander Hertsch
  C-Algebren erzeugt von unbeschränkten Operatoren*
  January 18, 2005
- Carsten Balleier
  Spinorfeldgleichungen auf Spin^c-Mannigfaltigkeiten
  October 1, 2005

- Hedwig Wilhelm
  Positivität und strenge Positivität der Enveloping-Algebra der Lie-Algebra su(2)
  November 30, 2005

Master

- Nadine Große
  Orbit spaces and invariant theory
  March 31, 2005

12.18 Guests

- Dr. Herbert Balasin
  TU Vienna
  September 21 – 26, 2005 & December 4 – 7, 2005
- Dr. Luzi Bergamin
  TU Wien
  April 13 – 20, 2005
- Szymon Charzynski
  University of Warsaw
  February 19 – March 5, 2005 & September 23 – October 10, 2005
- Prof. Dr. C.J. Fewster
  University of York, England
  September 27 – October 07, 2005
- Prof. Dr. Peter Jarvis
  University of Tasmania, Hobart
  October 1 – November 10, 2005
- Prof. Dr. Jerzy Kijowski
  Center for Theoretical Physics, Polish Academy of Sciences, Warsaw
  October 3 – 7, 2005
- Dr. Ralf Schützhold
  TU Dresden
  April 7 – 8, 2005
- Prof. Dr. Stanislaw L. Woronowicz
  University of Warsaw
  October 3 – 7, 2005

12.19 Awards

Dr. Daniel Grumiller
Erich-Schmid Award by the Austrian Academy of Sciences for excellent contributions to gravity

13

Statistical Physics

13.1 Introduction

We work on the connections of statistical mechanics to quantum field theory, on the mathematical and physical aspects of renormalization group (RG) theory and on its applications to high–energy and condensed matter physics, and on quantum kinetic theory. Our methods range from mathematical proofs to computational techniques.

The RG method applied here is an exact functional transformation of the action of the system, which leads to an infinite hierarchy of equations for the Green functions. Truncations of this hierarchy are used in applications. In a number of nontrivial cases, this truncation can be justified rigorously, so that the method lends itself to mathematical studies. These mathematical aspects are also under investigation.

Another topic we study is the long–time dynamics of large quantum systems, with a view of understanding how dissipative dynamics on the macroscopic scale arises from the microscopically reversible dynamics in interesting scaling limits.

We have ongoing collaborations with the Max–Planck Institute for Solid State Research in Stuttgart, the University of British Columbia, Vancouver, the University of Munich, the University of Würzburg, the University of Mainz, and Harvard University.

Manfred Salmhofer

13.2 Asymptotic Safety in Quantum Einstein Gravity: Nonperturbative Renormalizability and Fractal Spacetime Structure

O. Lauscher, M. Reuter*

*Institut für Physik, Universität Mainz

Recent results obtained within the framework of the renormalization group and its nonperturbative applications indicate that four-dimensional Quantum Einstein Gravity (QEG), the quantum field theory of the spacetime metric, is likely to be an asymptotically safe theory which is applicable at arbitrarily small distance scales. On sub-Planckian distances it predicts that spacetime is a fractal with an effective dimension-

ality of 2. The original argument leading to this result was based upon the anomalous dimension of Newton's constant. Our latest investigations [1, 2] show that also the spectral dimension of asymptotically safe QEG (if indeed it exists) equals 2 microscopically, while it is equal to 4 on macroscopic scales. This result is an exact consequence of asymptotic safety and does not rely on any truncation. Furthermore, the above values for the spectral dimension coincide with those which were recently obtained by Monte Carlo simulations of the causal dynamical triangulation model. While until recently it has been difficult to compare the continuum theory to this discrete approach, the new results suggest that they might be closely related.

[1] O. Lauscher, M. Reuter: J. High Energy Phys. **10**, 050 (2005), arXiv:hep-th/0508202.
[2] O. Lauscher, M. Reuter: arXiv:hep-th/0511260, to appear in the edited volume of the Blaubeuren Workshop 2005 on Mathematical and Physical Aspects of Quantum Gravity.

13.3 Quantum Diffusion

L. Erdös*, M. Salmhofer, H.-T. Yau†

*Mathematisches Institut, Universität München
†Mathematics Department, Harvard University, Cambridge (MA), USA

We study the long-time limit of the time evolution of the Anderson model (quantum Lorentz gas). We prove that, for a weakly coupled system with coupling strength g, the time evolution on timescale t of order g^{-2-a}, $a > 0$, is given by a diffusion equation . This is the first time that a proof about the behaviour of these systems on time scales bigger than g^{-2} is given. It shows how diffusive behaviour emerges from a microscopically reversible dynamics. The essential complication is that the number of collisions that happen on such timescales diverges as an inverse power of g. In [1, 2] we have treated the continuum case. The detailed proof for the lattice case is in preparation.

[1] L. Erdös et al.: arXiv:math-ph/0512014
[2] L. Erdös et al.: arXiv:math-ph/0512015

13.4 Two-Dimensional Fermi Liquids

W. Pedra, M. Salmhofer

The method of posing counterterms in constructive field theoretic studies of two–dimensional fermion systems leads to the inversion problem which has been solved to all orders in perturbation theory [2] but not yet nonperturbatively. We introduce a new RG flow where the Fermi surface is adjusted dynamically in the flow. This allows us to give a nonperturbative construction of two–dimensional Fermi systems with a regular Fermi surface at the temperature above the critical temperature for superconductivity without using counterterms. In the proof we combine the tree expansion of [3] with

the arch expansion of Iagolnitzer and Magnen (see [4]) to extract overlapping loops [1] which are crucial for the regularity properties of the selfenergy [5].

We also use these techniques to prove uniqueness of the KMS states and to determine the low–energy effective action. This action is the natural input for a study of symmetry-broken phases.

[1] J. Feldman et al.: J. Stat. Phys. **84**, 1209 (1996)
[2] J. Feldman et al.: Comm. Pure Appl. Math. **53**, 1350 (2000)
[3] M. Salmhofer, C. Wieczerkowski: J. Stat. Phys. **99**, 557 (2000)
[4] M. Disertori, V. Rivasseau: Comm. Math. Phys. **215**, 251 & 291 (2000)
[5] W. Pedra, M. Salmhofer: Proc. ICMP 2003, and papers to appear

13.5 Competing Ordering Tendencies and the RG

C. Honerkamp*, C. Husemann, O. Lauscher, W. Metzner†, M. Salmhofer

*Institut für Theoretische Physik und Astrophysik, Universität Würzburg
†Abteilung Theorie, Max-Planck-Institut für Festkörperforschung, Stuttgart

The flow to strong coupling observed in many RG studies of interacting fermion systems [1, 2] indicates the occurrence of symmetry breaking. It is also a major technical problem for the attempt to give a more detailed description of the symmetry–broken phases of such models. We have developed a method to continue the fermionic renormalization group flow into phases with broken global symmetry [3]. This method does not require a Hubbard-Stratonovich decoupling of the interaction. Instead an infinitesimally small symmetry-breaking component is inserted into the initial action, as an initial condition for the flow of the self-energy. Its flow is driven by the interaction, and at low scales it saturates at a nonzero value if there is a tendency for spontaneous symmetry breaking in the corresponding channel. For the reduced BCS model, we have shown how a small initial gap amplitude flows to the value given by the exact solution of the model.

In a more general situation with phonons, we have shown how to derive the Eliashberg equations by renormalization group methods [4].

This RG technique is also a powerful tool to investigate competing ordering tendencies. We study the interplay of ferromagnetism and superconductivity in the two–dimensional Hubbard model with hopping amplitudes t between nearest neighbours and t' between next–to–nearest neighbours, in the regime $0.3 < -t'/t < 0.5$, to get an analytical understanding of the quantum phase transition found in [5]. In this situation, the RG technique involves bosons and fermions. The boson fields correspond to composite fields of fermions, e.g. Cooper pairs and magnetic degrees of freedom.

[1] C. Halboth, W. Metzner: Phys. Rev. B **61**, 7364 (2000); Phys. Rev. Lett. **85** 5162 (2000)
[2] C. Honerkamp et al.: Phys. Rev. B **63**, 035 109 (2001)
[3] M. Salmhofer et al.: Prog. Theor. Phys. **112**, 943 (2004)
[4] C. Honerkamp, M. Salmhofer: Prog. Theor. Phys. **113**, 1145 (2005)
[5] C. Honerkamp, M. Salmhofer: Phys. Rev. Lett. **87**, 187 004 (2001); Phys. Rev. B **64**, 184 516 (2001)

13.6 Mathematical Theory of Singular Fermi Surfaces

J. Feldman*, M. Salmhofer

*Mathematics Department, University of British Columbia, Vancouver, Canada

We study the regularity properties of the fermionic self–energy for the case where the Fermi surface of the interacting system has singular points because the gradient of the dispersion relation vanishes (van Hove points). We prove regularity properties to all orders in perturbation theory using RG methods. We also investigate if there is an analogue of the inversion theorem proven in [1] for regular Fermi surfaces, also in this singular case, and its physical consequences [2].

[1] J. Feldman et al.: Comm. Pure Appl. Math. **53**, 1350 (2000)
[2] J. Feldman, M. Salmhofer: in preparation

13.7 Funding

Singular Fermi Surfaces
M. Salmhofer
DFG Sa 1362/1

13.8 Organizational Duties

M. Salmhofer

- Head of the *Fachverband Theoretische und Mathematische Grundlagen der Physik* of the German Physical Society (DPG), until March 31st, 2005.
- Organization of the Mathematical Physics Section at the *DPG–Frühjahrstagung „Physik seit Einstein“*, Berlin, March 7–9, 2005
- Member of the advisory board of the *Andrejewski–Stiftung*.
  Organization of the Andrejewski lectures in Leipzig.
- Referee for Comm. Math. Phys., Phys. Rev. Lett., Phys. Rev. B
- grant review for NSERC of Canada, ANR (France)

13.9 External Cooperations

Academic

- MPI für Festkörperforschung Stuttgart
  W. Metzner
- Universität Würzburg
  C. Honerkamp
- University of British Columbia, Canada
  J. Feldman

- Universität München
  L. Erdös
- Harvard University, USA
  H–T. Yau
- Universität Mainz
  M. Reuter

13.10 Publications

Journals

O. Lauscher, M. Reuter: *Fractal spacetime structure in asymptotically safe gravity*, J. High Electron Phys. **10**, 050 (2005), arXiv:hep-th/0508202.

C. Honerkamp, M. Salmhofer: *Eliashberg equations derived from the functional renormalization group*, Prog. Theor. Phys. **113**, 1145 (2005).

Books

M. Salmhofer: *Renormalization: Statistical Mechanics and Condensed Matter*, in *Encyclopaedia of Mathematical Physics*, Vol. 4, ed. by J.-P. Francoise, G.L. Naber, S.T. Tsou (Elsevier, Oxford 2006) p 407

Talks

O. Lauscher: *RG flows into phases with broken symmetry*, DPG-Frühjahrstagung 2005 in Berlin, March 8, 2005

W. Pedra: *Renormierungsfluss von Fermiflächen*, DPG-Frühjahrstagung 2005 in Berlin, March 8, 2005

W. Pedra: *Zur mathematischen Theorie der Fermiflüssigkeiten bei positiven Temperaturen*. Kolloquium in Rahmen des Promotionsverfahrens. ITP, Universität Leipzig. November 2005.

M. Salmhofer: *Die Renormierungsgruppe, Fermiflüssigkeiten, und ihre Instabilitäten*, Physikalisches Kolloquium, Universität Mainz, January 4, 2005

M. Salmhofer: *The Renormalization Group, Fermi Liquids, and their Instabilities*, Université de Genève, January 18, 2005

M. Salmhofer: *Long-Time Dynamics of Random Schrödinger Operators*, Theoretisch-Physikalisches Kolloquium, Universität Köln, July 1, 2005

13.11 Graduations

Doctorate

- Walter Pedra
  Zur mathematischen Theorie der Fermiflüssigkeiten bei positiven Temperaturen
  November, 2005

13.12 Guests

- C. Honerkamp
  Universität Würzburg
  April 17–20, 2005
- M. Aizenman
  Princeton University
  May 8–13, 2005
- M. Potthoff
  Universität Würzburg
  May 22–23, 2005
- K. Schönhammer
  Universität Göttingen
  May 30–31, 2005
- H.-T. Yau
  Harvard University
  June 13–15, 2005
- C. Wetterich
  Universität Heidelberg
  June 20–21, 2005
- J. Magnen
  Ecole Polytechnique (Paris)
  June 21–23 2005

14

Theory of Condensed Matter

14.1 Introduction

The topics of research in our group are stochasticity and disorder as well as structure formation in soft condensed matter and solids, models of complex biological systems, strongly correlated electron systems, and superconducting materials. Investigations using modern analytic methods and computer applications complement and stimulate each other. We cooperate with mathematicians, theoretical and experimental physicists, biologists and researchers in medicine. There are well established collaborations with groups in France, Germany, Italy, Russia, Switzerland, UK, and USA.

Noise induced phenomena (Behn). Noise induced non-equilibrium phase transitions are studied in coupled arrays of stochastically driven nonlinear systems. The statistics of first passage times and self-organized criticality is investigated in stochastic nonlinear systems with time delay.

Mathematical modeling of the immune system (Behn). Using methods of nonlinear dynamics and statistical physics, we study the architecture and the random evolution of the idiotypic network of the B-cell subsystem and describe the regulation of balance of Th1/Th2-cell subsystems, its relation to allergy and the hyposensitization therapy (Cooperation with the Institute for Clinical Immunology and Transfusion Medicine).

Strongly correlated electron systems (Ihle). The unconventional magnetic properties of transition metal oxides, such as the mixed-valency manganites,are investigated on the basis of correlation models including anisotropic Heisenberg-type exchange interactions. Using Green's function techniques the effects of magnetic short-range order at arbitrary temperatures are studied in comparison with experiments.

Non-equilibrium dynamics of various soft-condensed-matter systems (Kroy). The latter range from desert dunes spontaneously developing as a generic consequence of aeolian sand transport, through non-equilibrium gels of adhesive colloids and proteins, the viscoelastic mechanics of the cytoskeleton, to the non-equilibrium dynamics of single DNA molecules under strong external fields. (Related experimental work is currently in progress at EXP1: PWM, PAF.) A common feature is the presence of strong fluctuations and stochastic dynamics on the micro-scale. The emergence of macroscopic structure and (non-linear) deterministic macroscopic dynamics is to be understood. The applied methods range from analytical studies of stochastic integro-differential equations through liquid-state theories, mode-coupling theory, effective hydrodynamic equations, phenomenological modeling, to numerical simulations.

14.2 Architecture of Randomly Evolving Idiotypic Networks

U. Behn, H. Schmidtchen

The immune system is a hierarchically organized natural adaptive system built by a macroscopic number of constituents which shows a very complex behaviour on several scales of temporal, spatial, and functional organization. It is thus naturally a subject of modeling with methods of statistical physics and nonlinear dynamics, for recent reviews see, e.g., [1, 3, 3]. We investigate models describing the architecture of the idiotypic network [4] formed by the subsystem of B-lymphocytes as the highly organized product of a random temporal evolution.

B-cells express on their surface receptors (antibodies) of a given specificity (idiotype). Crosslinking these receptors by complementary structures (antigen or antibodies) stimulates the lymphocyte to proliferate. Thus even without antigen there is a large functional network of interacting lymphocytes, the idiotypic network. The idiotypes are caricatured by bitstrings. The dynamics of the idiotypic network is driven by the influx of new idiotypes randomly produced in the bone marrow and by the population dynamics of the lymphocytes themself. We model this dynamics by simple cellular automata rules [5].

The vertices of the network can be classified into different groups, which are clearly distinguished, e.g., by the mean life time of the occupied vertices. They include densely connected core groups and peripheral groups of isolated vertices, resembling central and peripheral part of the biological network, cf. Fig. 14.1.

We found the building principles of the observed patterns which allows to calculate analytically size and connectivity of the idiotype groups [6], previously found empiri-

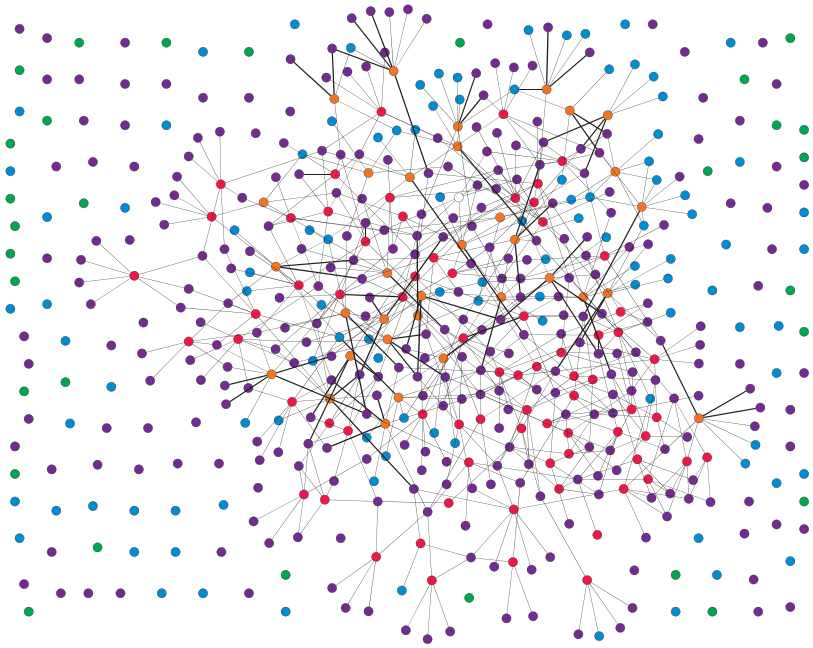

Figure 14.1: Snapshot of the occupied graph of a six-group configuration. The different groups are distinguished by colors. Figure produced using the graph editor yEd-Java™.

cally by statistical methods [5]. The newly achieved microscopic understanding opens the possibility to consider networks of realistic size. Future steps will include to check whether a similar understanding can be reached for more realistic models.

[1] A.S. Perelson, G. Weisbuch: Rev. Mod. Phys. **69** 1219 (1997)
[2] U. Behn et al.: in *Frontiers of Life*, Vol. II, Part Two: *The Immunological System*, ed. by A. Lanzavecchia et al. (Academic Press, London 2001) p 611
[3] U. Behn et al.: in *Function and regulation of cellular systems:Experiments and Models*, ed. by A. Deutsch et al. (Birkhäuser, Basel 2004) p 399
[4] N.K. Jerne: Ann. Inst. Pasteur Immunol. **125C**, 373 (1974)
[5] M. Brede, U. Behn: Phys. Rev. E **64**, 011 908 (2001); ibid. **67**, 031 920 (2003)
[6] H. Schmidtchen, U. Behn: in Proc. ECMTB 2005, ed. by G. de Vries et al. (Birkhäuser, Boston and Basel) in press

14.3 Nonlinear Dynamics of Th1–Th2 Regulation

U. Behn, R. Vogel

T-helper lymphocytes have subtypes which differ in their spectrum of secreted cytokines. These cytokines have autocrine effects on the own subtype and cross-suppressive effects on the other subtype and regulate further the type of immunoglobulines secreted by B-lymphocytes. The balance of Th1- and Th2-cells is perturbed in several diseases. For example, in allergy the response to allergen is Th2-dominated. A widespread and successful therapy consists in the injection of increasing doses of allergen following empirically justified protocols of administration.

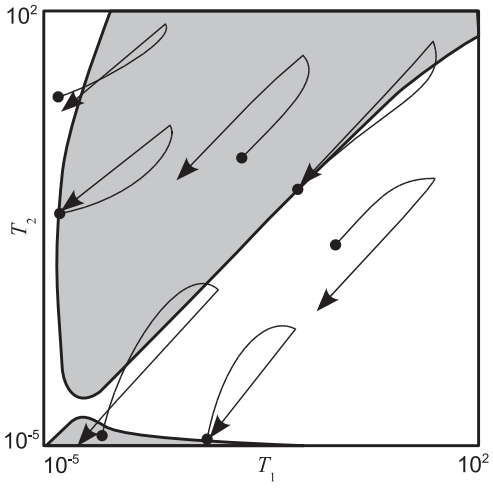

Figure 14.2: Schematic illustration of the concept of dynamical separatrix. The response to the injection of a given dose of allergen is shown in the T_1–T_2 plane for different initial conditions. The trajectories starting from points on the separatrix return to their starting point. The T_1–T_2 plane is divided in regions in which an injection will either improve the ratio T_1/T_2 (*white*) or impair it (*grey*).

A previously in collaboration with Prof. G. Metzner (Institute of Clinical Immunology) developed mathematical model [1, 2] based on a simplified scheme of Th1–Th2 regulation mediated by the cytokine network is closer investigated.

The model provides a theoretical explanation of the switch from a Th2 dominated response to a Th1 dominated response to allergen in allergic individuals as a result of a hyposensitization therapy. The system is driven by proper injections of allergen across a dynamical separatrix towards new attractors, where the response is Th1-dominated as for healthy individuals, cf. Fig. 14.2.

We perform the bifurcation analysis of the fixed points of a stroboscopic map describing the non-autonomous dynamical system driven by periodic allergen injections. The set of unstable fixed points forms the dynamical separatrix between the regions of Th2 dominated response and Th1 dominated response which is crossed during a successful therapy. The maintenance phase of the therapy holds the system near the stable fixed point of the stroboscobic map. Using the tool of stroboscopic maps reduces the complexity of the non-autonomous system allowing a thorough analysis and puts the notion of dynamical separatrix on a firm mathematical ground [3, 4].

[1] U. Behn et al.: in *Dynamical Modeling in Biotechnologies*, ed. by F. Bagnoli et al. (World Scientific, Singapore 2001) p 227
[2] J. Richter et al.: J. Theor. Med. **4**, 119 (2002)
[3] R. Vogel: Diplomarbeit, 2006
[4] R. Vogel, U. Behn: in Proc. ECMTB 2005, ed. by G. de Vries et al. (Birkhäuser, Boston and Basel) in press

14.4 Noise Induced Phenomena in Nonlinear Systems

U. Behn, F. Senf, C. Brettschneider, M. Krieger-Hauwede

We describe non-equilibrium phase transitions [1] in arrays of spatially coupled dynamical systems with different nonlinearities driven by multiplicative Gaussian white noise. Those systems show close analogies to phase transitions in equilibrium. We have determined the phase diagram, the order of the transitions, and the critical behaviour for both global coupling and nearest neighbour coupling on simple cubic lattices comparing analytical results and numerical simulations [2].

The H-theorem [3] for a system of N globally coupled Stratonovich models is found and the convergence to the stationary solution independent of the initial distribution is shown [4]. Due to the effects of multiplicative noise and particle attraction there is no detailed balance and therefore an analytical expression for the steady state distribution is not easily found. Nevertheless, with a sectorization of the state space we are able to show that in the large time limit a stochastic trajectory will be trapped in one of those sectors which have their boundary flows pointing inward, only. These are the ergodic components. In each ergodic component the Kullback entropy is identified as a Lyapunov functional which proves the convergence to the steady state distribution for long times. This result is independent of the system size so that phase transistions associated with the breaking of ergodicity occur already for finite N. The critical exponent of the order parameter depends on all parameters of the Stratonovich model

including the finite system size N, for $N \to \infty$ see [2]. For finite N new analytical results are given in some limit cases.

Our studies of marginally stable stochastically driven systems with delayed time argument are continued. Analogies to the phenomenon of self-organized criticality in spatially extended systems are closer investigated.

[1] J. Garcia-Ojalvo, J.M. Sancho: *Noise in Spatially Extended Systems*, (Springer, New York 1999)
[2] T. Birner et al.: Phys. Rev. E **65**, 046 110 (2002)
[3] T.D. Frank: *Nonlinear Fokker-Planck Equations*, (Springer, Berlin 2005)
[4] F. Senf: Diplomarbeit, 2006; F. Senf, U. Behn: in preparation

14.5 Spin Correlations in Anisotropic Quantum Magnets

D. Ihle, I. Junger, J. Richter*

*Institut für Theoretische Physik, Universität Magdeburg

In the theory of magnetism [1] the interplay of quantum and thermal fluctuations and the effects of spin and spatial anisotropies are of basic interest. For example, in $LaMnO_3$, being a spin $S = 2$ parent compound of the colossal magnetoresistance manganites [2], neutron-scattering experiments [3] yield evidence for a pronounced ferromagnetic short-range order (SRO) in the paramagnetic phase and for a single-ion easy-axis spin anisotropy. Moreover, the study of low-dimensional quantum ferromagnets, also in a magnetic field, was motivated by the progress in the synthesis of new materials. To provide a good description of SRO at arbitrary temperatures, the standard spin-wave approaches cannot be adopted.

In this project low-dimensional anisotropic quantum spin models with arbitrary spin were considered, and the second-order Green-function approaches developed in [4, 5, 6] for $S = 1/2$ were extended to $S \geqslant 1$. For $S \geqslant 1$ ferromagnetic Heisenberg chains with uniaxial single-ion anisotropy, the spin-wave spectra and thermodynamics were investigated performing also exact finite lattice diagonalizations ED [6]. For sufficient large anisotropies, the existence of two maxima in the temperature dependence of the specific heat was shown. For the one-dimensional (1D) and 2D Heisenberg ferromagnets with arbitrary spin in a magnetic field, the thermodynamic properties (magnetization, magnetic susceptibility, specific heat) at arbitrary temperatures and fields were calculated in good agreement with ED data and with the results of quantum Monte-Carlo simulations of the $S = 1/2$ and $S = 1$ models performed in the research group Computer-Oriented Quantum Field Theory (W. Janke, L. Bogacz). The field dependences of the position and height of the maximum in the temperature dependence of the magnetic susceptibility were found to obey power laws. In the 1D case and at very low fields two maxima in the temperature dependence of the specific heat of the $S = 1/2$ and $S = 1$ ferromagnets were found. The appearance of two specific-heat maxima was identified as a distinctive effect of quantum fluctuations. Comparing the theory with magnetization experiments on the 1D copper salt TMCuC, predictions for the occurrence of two specific-heat maxima were made.

For quasi-2D ferro- and antiferromagnets with arbitrary spin the Curie and Néel temperatures and the thermodynamic quantities were calculated in good agreement with exact results in special cases.

[1] U. Schollwöck et al. (Eds.): *Quantum magnetism*, Lecture Notes in Physics **645** (Springer, Berlin 2004)
[2] A.P. Ramirez: J. Phys.: Condens. Matter **9**, 817 (1997); E.L. Nagaev: Phys. Rep. **346**, 387 (2001)
[3] F. Moussa et al.: Phys. Rev. B **54**, 15 149 (1996); K. Hirota et al.: J. Phys. Soc. Jpn. **65**, 3736 (1996)
[4] S. Winterfeldt, D. Ihle: Phys. Rev. B **56**, 5535 (1997); ibid. **59**, 6010 (1999)
[5] D. Ihle et al.: Phys. Rev. B **64**, 054 419 (2001)
[6] I. Junger et al.: Phys. Rev. B **70**, 104 419 (2004)
[7] I. Juhász Junger et al.: Phys. Rev. B **72**, 064 454 (2005)

14.6 Magnetic Systems with Frustration

J. Richter*, D. Schmalfuß*, D. Ihle

*Institut für Theoretische Physik, Universität Magdeburg

In low-dimensional frustrated quantum spin systems [1], such as the spin-half Heisenberg antiferromagnet on the two-dimensional (2D) kagomé lattice [2], the interplay of quantum and frustration effects causes interesting physics. Thereby, the influence of the dimensionality on the stability of the spin-liquid phase and the finite-temperature properties are of particular interest. To describe the magnetic short-range order at arbitrary temperatures, one has to go beyond the usual spin-wave approaches [3]. Previously, it was shown that frustration effects in the two-dimensional Heisenberg model with antiferromagnetic nearest- and next-nearest-neighbor couplings ($J_1 - J_2$ model) may be described successfully by a spin-rotation-invariant Green's-function theory [4, 5]. The role of the interplane coupling in the magnetic behavior of both non-frustrated [6] and frustrated systems [7, 8] was also well described by this theory.

To investigate the influence of the interlayer coupling $J_\perp$ on the quantum phase transitions in the $J_1 - J_2$ model, the second-order Green's-function approaches of [5, 6] were combined. In agreement with known results for the $J_1 - J_2$ model on the square lattice, the phases with magnetic long-range order with small $J_2 < J_{c_1}$ and large $J_2 > J_{c_2}$ were found to be separated by a magnetically disordered (quantum paramagnetic) ground-state phase. Increasing the interlayer coupling $J_\perp > 0$ the parameter region of this phase decreases,and finally the quantum paramagnetic phase disappears for quite small $J_\perp \simeq 0.2 \ldots 0.3 J_1$.

The work is supported by the DFG through the projects RI 615/12-1 and IH 13/7-1.

[1] U. Schollwöck et al. (Eds.): *Quantum magnetism*, Lecture Notes in Physics **645** (Springer, Berlin 2004)
[2] J. Schulenburg et al.: Phys. Rev. Lett. **88**, 167 207 (2002)
[3] A.B. Harris et al.: Phys. Rev. B **64**, 024 436 (2001)

[4] S. Winterfeldt, D. Ihle: Phys. Rev. B **56**, 5535 (1997); ibid. **59**, 6010 (1999)
[5] L. Siurakshina et al.: Phys. Rev. B **64**, 104 406 (2001)
[6] L. Siurakshina et al.: Phys. Rev. B **61**, 14 601 (2000)
[7] D. Schmalfuß et al.: Phys. Rev. B **70**, 184 412 (2004)
[8] D. Schmalfuß et al.: Phys. Rev. B **72**, 224 405 (2005)

14.7 Propagation and Relaxation of Tension in Stiff Polymers

O. Hallatschek, E. Frey*, K. Kroy

*Arnold Sommerfeld Centre, Ludwig-Maximilians-Universität München

Together with Oskar Hallatschek and Erwin Frey we have recently studied tension propagation in polymers, a question that is of interest for single-molecule force spectroscopy and for the problem of force transduction through the cytoskeleton of a cell. An important special case is a strong force suddenly applied or released at one end of a polymer. The basic mechanism is exemplified by the movie.wmv on the group homepage, which shows a thread on a table that is pulled at one end. In contrast to the thread in the movie, where the action of thermal random forces has only been mimicked for establishing a polymer-like initial conformation, thermal noise is active all the time for polymers, and this has to be taken into account. The physics of tension propagation and relaxation turns out to be quite rich, as demonstrated for the mentioned cases of pulling and release in Fig. 14.3.

We have developed a unified theory for the longitudinal dynamic response of a stiff polymer in solution to various external perturbations (mechanical excitations, hydrodynamic flows, electrical fields, temperature quenches, etc.) that can be represented as

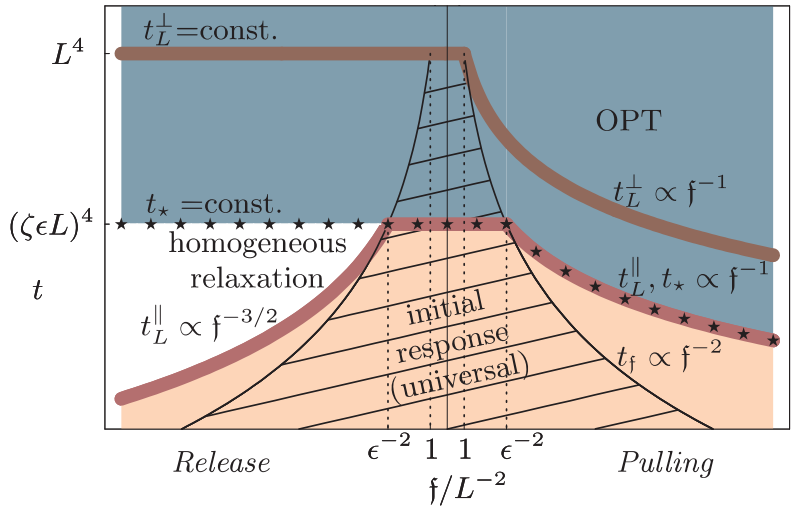

Figure 14.3: The nonlinear dynamics of semiflexible polymers exhibits several intermediate asymptotic regimes as a function of time and external force. The figure displays the tension propagation- and relaxation regimes for pulling forces (*right*) and released prestretching forces (*left*).

sudden changes of ambient/boundary conditions. The theory relies on a comprehensive analysis of the nonequilibrium propagation and relaxation of backbone stresses in a wormlike chain. We recover and substantially extend previous results based on heuristic arguments. New experimental implications are pointed out.

[1] O. Hallatschek et al.: Phys. Rev. Lett. **94**, 077 804 (2005)

14.8 Non-equilibrium Behavior of Sticky Colloidal Particles: Beads, Clusters and Gels

H. Sedgwick*, K. Kroy, A. Salonen*, M.B. Robertson*, S.U. Egelhaaf*, W.C.K. Poon*

*School of Physics, The University of Edinburgh

Acording to equilibrium theory, a large number of identical particles will always crystallize if brought together via external pressure or by mutual attractions. In practice, this is not always easily achieved: A suspension of colloids or proteins "quenched" into the parameter region of fluid-crystal coexistence may undergo a variety of transformations giving rise to a plethora of (metastable) structures (Fig. 14.4). Worst for protein

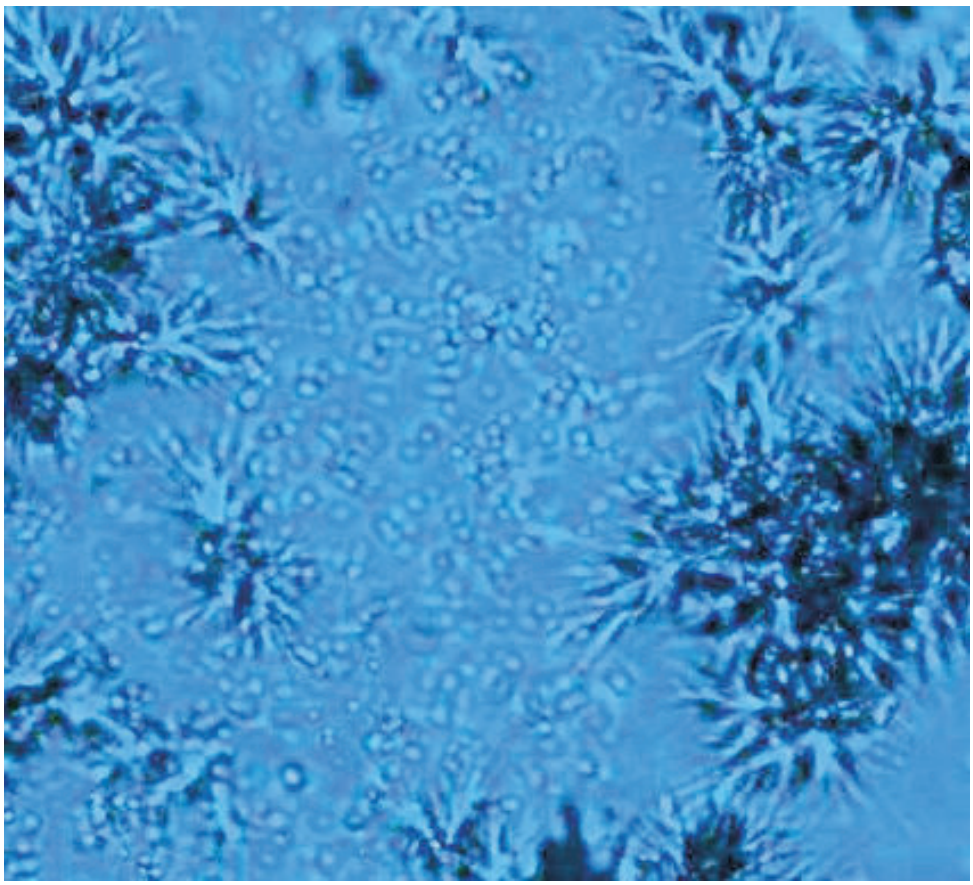

Figure 14.4: Non-equilibrium structure formation in a lysozyme solution. Gel-beads and seaurchin crystals impede the formation of equilibrium protein crystals.

crystalographers is gelation, a non-equilibrium transition into a long-lived amorphous solid state that blocks crystallization. Engineers of food and beauty products rather like such kinetically trapped states. How they arise from a subtle interplay of a meta-stable liqiud-gas phase separation and kinetic arrest has recently been explored in collaboration with the Soft Condensed Matter Group of the University of Edinburgh. We are also interested in gelation under shear.

To understand the non-equilibrium behavior of colloidal particles with short-range attraction, we have recently studied salt-induced aggregation of lysozyme. Optical microscopy revealed four regimes: bicontinuous texture, 'beads', large aggregates, and transient gelation. The interaction of a metastable liquid-liquid binodal and an ergodic to non-ergodic transition boundary inside the equilibrium crystallization region can explain our findings.

[1] H. Sedgwick et al.: Eur. Phys. J. E **16**, 77 (2005)

14.9 The Shape of Barchan Dunes

K. Kroy, S. Fischer, B. Obermayer

In collaboration with H. Herrmann of the University of Stuttgart a minimal model has been formulated which elucidates the basic physical mechanisms underlying dune formation and migration. It predicts non-trivial similarity relations for the shape and dynamics of aeolian and submarine dunes under diverse wind and sand conditions. They reveal a strong universality behind the manifold structures formed by wind-blown sand - based on a subtle interplay of the scale invariance and spontaneous symmetry breaking of the turbulent wind, and the breaking of scale invariance by the grains in motion.

Barchans are crescent-shaped sand dunes forming in arid regions with unidirectional wind and limited sand supply. We obtain analytical and numerical results for dune shapes under different environmental conditions as obtained from the so-called 'minimal model' of aeolian sand dunes. The profiles of longitudinal vertical slices (i.e. along the wind direction) are analysed as a function of wind speed and sand supply. Shape transitions can be induced by changes of mass, wind speed and sand supply. Within a minimal extension of the model to the transverse direction the scale-invariant profile of transverse vertical cuts can be derived analytically.

[1] K. Kroy et al.: J. Phys. Condens. Matter **17**, S1229 (2005)

14.10 Funding

Rotationsinvariante Greenfunktionsmethode für Quantenspingitter
Prof. Dr. J. Richter (Magdeburg), Prof. Dr. D. Ihle
DFG RI 615/12-1, IH13/7-1

14.11 Organizational Duties

U. Behn
- Referee: Phys. Rev. Lett., Phys. Rev. E, J. Phys. A, B. Math. Biol., Adv. Complex Syst.
- Vertrauensdozent für die Nobelpreisträgertagungen in Lindau

D. Ihle
- Referee: Phys. Rev. Lett., Phys. Rev. B, Phys. Stat. Sol.

K. Kroy
- Vice director of the ITP
- Member of the Graduiertenkommission of the University of Leipzig
- Organizer of the NTZ-Workshop *Soft Matters in Biological Physics*, ITP, Universität Leipzig, 20–21 September 2005
- Referee: Phys. Rev. Lett., Phys. Rev. E, Europhys. Lett, J. Theor. Biol., Physica D, J. Geophys. Res.

W. Kolley
- Member of the Promotionsauschuß of the Faculty

14.12 External Cooperations

Academic

- Ludwig-Maximilians-Universität München
  Prof. Dr. E. Frey
- Edinburgh University, UK
  Prof. Dr. W.C.K. Poon
- Institut für Klinische Immunologie, Universität Leipzig
  Prof. Dr. G. Metzner
- Department of Mathematical Physics, University College Dublin, Ireland
  Prof. Dr. Joe Pulé
- Center for Complex Systems Science, CSIRO, Canberra, Australia
  Dr. M. Brede
- Cyprus Institute of Neurology and Genetics, Nicosia, Greece
  Dr. J. Richter
- Program for Evolutionary Dynamics, Harvard University, USA
  Dr. A. Traulsen
- Centre de Physique Theorique, CNRS, Marseille, France
  Prof. Dr. V. Zagrebnov
- Otto-von-Guericke-Universität Magdeburg, Institut für Theoretische Physik
  Prof. Dr. J. Richter
- Ernst-Moritz-Arndt-Universität Greifswald, Institut für Physik
  Prof. Dr. H. Fehske

- JINR Dubna, Bogolyubov Laboratory of Theoretical Physics, Russia
  Prof. Dr. N. M. Plakida
- ETH Zürich, Laboratorium für Festkörperphysik, Switzerland
  Prof. Dr. P. Wachter

14.13 Publications

Journals

E. Frey, K. Kroy: *Brownian motion: a paradigm of soft matter and biological physics*, Ann. Phys. (Leipzig) **14**, 20 (2005)

E. Frey, K. Kroy: *Im Zickzack zwischen Physik und Biologie*, Physik Journal 3/2005, p 61

O. Hallatschek, E. Frey, K. Kroy: *Propagation and Relaxation of Tension in Stiff Polymers*, Phys. Rev. Lett. **94**, 077 804 (2005)

I. Juhász Junger, D. Ihle, J. Richter: *Thermodynamics of $S \geqslant 1$ ferromagnetic Heisenberg chains with uniaxial single-ion anisotropy*, Phys. Rev. B **72**, 064 454 (2005)

K. Kroy, S. Fischer, B. Obermayer: *The shape of barchan dunes*, J. Phys. Condens. Matter **17**, S1229 (2005)

D. Schmalfuß, J. Richter, D. Ihle: *Green's function theory of quasi-two-dimensional spin-half Heisenberg ferromagnets: Stacked square versus stacked kagomé lattices*, Phys. Rev. B **72**, 224 405 (2004)

H. Sedgwick, K. Kroy, A, Salonen, M.B. Robertson, S.U. Egelhaaf, W.C.K. Poon: *Non-equilibrium behavior of sticky colloidal particles: beads, clusters and gels*, Eur. Phys. J. E **16**, 77 (2005)

A.A. Vladimirov, D. Ihle, N.M. Plakida: *Dynamical Spin Susceptibility in the $t-J$ Model: The Memory Function Method*, Theoretical and Mathematical Physics **145**, 1576 (2005)

A. Weiße, H. Fehske, D. Ihle: *Spin-lattice coupling effects in the Holstein double exchange model*, Physica B **359-361**, 702 (2005)

in press

A.R. Bausch, K. Kroy: *A bottom-up approach to cell mechanics*, Nature Phys. (2006)

M.M.A.E. Claessens, R. Tharmann, K. Kroy, A.R. Bausch: *Microstructure and viscoelasticity of confined semiflexible polymer*, Nature Phys. **2**, 186 (2006)

K. Kroy: *Elasticity, dynamics and relaxation in biopolymer networks*, Curr. Op. Coll. Int. Sci. (2006)

H. Schmidtchen, U. Behn: *Architecture of Randomly Evolving Idiotypic Networks*, in Proc. ECMTB 2005, ed. by G. de Vries et al. (Birkhäuser, Boston and Basel)

R. Vogel, U. Behn: *Th1–Th2 Regulation and Allergy: Bifurcation Analysis of the Non-autonomous System*, in Proc. ECMTB 2005, ed. by G. de Vries et al. (Birkhäuser, Boston and Basel)

Talks

U. Behn: *Architecture of randomly evolving idiotypic networks*, Invited Talk, Dept. of Mathematical Physics, University College Dublin, 10.02.2005

U. Behn, J. Przybilla: *Critical behaviour and Universality in stochastically driven nonequilibrium phase transitions*, DPG Jahrestagung, Berlin, 07.03.2005

U. Behn: *Critical behaviour of stochastically driven non-equilibrium phase transitions*, Invited Talk, Seminar Komplexe Systeme und Nichtlineare Dynamik, Institut für Physik, TU Chemnitz, 04.05.2005

U. Behn: *Architecture of randomly evolving idiotypic networks*, Invited Talk, Workshop Complex networks and random graphs: The interplay between structure and function, Bad Honnef, 11.07.2005

U. Behn, M. Brede, H. Schmidtchen: *Architecture of randomly evolving idiotypic networks*, ECMTB 05, Dresden, 20.07.2005

S. Fischer: *Modelling the evolution of aeolian sand dunes*, Invited Talk, TU München, 08.06.2005

J. Glaser: *Molecular Force Microscopy on Graphite*, Mini-Symposium, Hahn-Meitner-Institut Berlin, 15.–16.02.2005

O. Hallatschek: *Anisotropic semiflexible polymer dynamics*, Invited Talk, NTZ-Workshop Soft Matters in Biological Physics, Universität Leipzig, 20.–21.09.2005

K. Kroy: *Shear-driven flocculation of sticky spheres: crossover from kinetic aggregation to anisotropic percolation*, Workshop Dynamical Arrested State of Soft Matter and Colloids, Bad Gatein, 22.–26.01.2005

K. Kroy: *On growth and form of desert dunes*, Invited Talk, North Dakota State University, Fargo, 30.03.2005

K. Kroy: *Scaling concepts in polymer physics*, Mitteldeutsche Physikcombo, Jena, 22.–23.04.2005

K. Kroy: *The Physics of DNA*, Mitteldeutsche Physikcombo, Leipzig, 17.–18.06.2005

K. Kroy: *Tension dynamics in stiff polymers*, Invited Talk, Seminar Mathematische Modellierung Biologischer Systeme, MPI MIS, Leipzig, 22.06.2005

K. Kroy: *Physik der Wanderdünen*, Antrittsvorlesung, Fakultätskolloquium, Leipzig, 19.07.2005

K. Kroy: *How a deterministic response emerges from Brownian polymer dynamics*, Invited Talk, Workshop Brownian Motion: A Paradigm of Soft Matter and Biological Physics, Arnold Sommerfeld Center for Theoretical Physics, München, 26.–28.90.2005

K. Kroy: *On growth and form of desert dunes*, Conference on Traffic and Granular Flow, Humboldt Universität zu Berlin, 10.–12.10.2005

K. Kroy: *Im Zickzack zwischen Physik und Biologie*, Invited after-dinner-lecture, Symposium Naturwissenschaftliche und technische Systeme im Fokus von Fremd- und Selbstorganisation, Arnold Sommerfeld Gesellschaft, Leipzig, 10.-11.11.2005

K. Kroy: *On growth and form of desert dunes*, Invited Talk, Universität Bayreuth, 29.11.2005

B. Obermayer: *Tension Propagation in Semiflexible Polymers*, Mini-Symposium, Hahn-Meitner-Institut Berlin, 15.-16.02.2005

B. Obermayer: *Nonlinear Dynamics of Stiff polymers*, Invited Talk, LMU München, 18.04.2005

D. Rings: *Atomic Force Microscopy: Soft Matter*, Mini-Symposium, Hahn-Meitner-Institut Berlin, 15.-16.02.2005

F. Senf, U. Behn: *H-theorem for interacting systems driven by multiplicative noise*, CompPhys05, 6th NTZ-Workshop on Computational Physics, Leipzig, 02.12.2005

Posters

U. Behn, M. Brede: *Architecture of randomly evolving idiotypic networks*, DPG Jahrestagung, Berlin, 07.03.2005

U. Behn, J. Richter, R. Vogel: *Th1-Th2 Regulation and Allergy: Bifurcation Analysis of the Non-Autonomous System*, ECMTB 05, Dresden, 18.–22.07.2005

J. Glaser: *Hydrodynamic interactions for stiff polymers*, Jülich Soft Matter Days 2005, Gustav-Stresemann-Institut, Bonn, 01.-04.11.2005

B. Obermayer: *Non-linear dynamics of stiff polymers*, DPG Jahrestagung, Berlin, 04.-09.03.2005

B. Obermayer: *Non-linear dynamics of semiflexible polymers*, Jülich Soft Matter Days 2005, Gustav-Stresemann-Institut, Bonn, 01.-04.11.2005

14.14 Graduations

Diploma

- S. Fischer
  Aeolian Sand Transport and Dune Formation
  FU Berlin, 2005

- J. Menche
  Brownsche Teilchen mit inneren Freiheitsgraden
  (prepared at the Institut für Physik, Humboldt-Universität zu Berlin) 2005
- B. Obermayer
  Non-equilibrium Dynamics of Semiflexible Polymers
  FU Berlin, 2005

15

Theory of Elementary Particles

15.1 Introduction

The Particle Physics Group performs basic research in the quantum field theoretic description of elementary particles and in phenomenology. Topics of current interest are conformal symmetry and its breaking in the context of supersymmetric theories, the formulation of models which realize noncommutative geometry, renormalization problems, electroweak matter at finite temperature, the lattice formulation of gauge theories, the derivation of Regge behaviour of scattering amplitudes from Quantum Chromodynamics and the related study of integrable models with and without supersymmetry. Perturbative and non-perturbative methods are applied to answer the respective questions. In perturbation theory the work is essentially analytic using computers only as a helpful tool. Lattice Monte Carlo calculations as one important non-perturbative approach however are based on computers as an indispensable instrument. Correspondingly the respective working groups are organized: in analytical work usually very few people collaborate, in the lattice community rather big collaborations are the rule. Our group is involved in many cooperations on the national and international level (DESY, Munich; France, Russia, Armenia, USA, Japan). Since elementary particles are very tiny (of the order of 10^{-15} m) and for the study of their interactions large accelerators producing enormously high energy are needed, it is clear that results in this direction of research do not have applications in daily life immediately. To clarify the structure of matter is first of all an aim in its own and is not pursued for other reasons. But particle theory has nevertheless a very noticeable impact on many other branches of physics by its power of providing new methodological insight. Similarly for the student specializing in this field the main benefit is her/his training in analysing complex situations and in applying tools which are appropriate for the respective problem. As a rule there will be no standard procedures which have to be learned and then followed, but the student has to develop her/his own skill according to the need that arises. This may be a mathematical topic or a tool in computer application. Jobs which plainly continue these studies are to be found at universities and research institutes only. But the basic knowledge which one acquires in pursuing such a subject opens the way to many fields where analytical thinking is to be combined with application of advanced mathematics. Nowadays this seems to be the case in banks, insurance companies and consulting business.

Klaus Sibold

15.2 Conformal Transformation Properties of the Supercurrent III: Nonabelian Gauge Theories with Local Coupling

K. Sibold, E. Kraus, C. Rupp

We derive the superconformal transformation properties of the supercurrent for $N = 1$ supersymmetric Yang-Mills theory in four dimensions within the superfield formalism. Superconformal Ward identities for Green functions involving insertions of the supercurrent are obtained by coupling the supercurrent to the supergravity field of a classical curved space background. In order to obtain BRS-invariant expressions for the supercurrent and superconfpormal anomalies, we promote the gauge coupling to a chiral superfield.

[1] S. Ferrara, B. Zumino: Nucl. Phys. B **87**, 207 (1975)
[2] O. Piguet, K. Sibold: *Renormalized Supersymmetry. The Perturbation Theory of N=1 Supersymmetric Theories in Flat Space-Time* (Birkhäuser, Boston 1986) p 346
[3] J. Erdmenger et al.: Nucl. Phys. B **530**, 501 (1998)
[4] J. Erdmenger et al.: Nucl. Phys. B **565**, 363 (2000)

15.3 3D Abelian Higgs Model with Singly and Doubly-Charged Matter Fields

A. Schiller

In this project we continue to study properties of coupled gauge-Higgs models in three dimensions using Monte Carlo methods.

In [1, 2] we started to study a three dimensional Abelian Higgs model containing singly- and doubly-charged scalar fields coupled to a compact Abelian gauge field in the London limit. The model attracts interest because of its relevance to high-T_c superconductors with charge 1 holon and charge 2 spinon-pair fields. Its action is defined as

$$S_{\mathrm{A2HM}} = -\beta \sum_P \cos\theta_P - \sum_{Q=1}^{2} \kappa_Q \sum_l \cos(\mathrm{d}\varphi_Q + Q\theta)_l \,, \tag{15.1}$$

where θ_P is the standard lattice plaquette, φ_1 the phase of the singly-charged holon field and and φ_2 the phase of the doubly-charged spinon-pair field. The sums run over plaquettes P and links l, respectively. The model contains two types of vortices carrying magnetic flux and one type of instanton-like monopoles. Using thermodynamic and topological observables we present the phase diagram in the parameter space of the gauge and holon and spinon-pair couplings. The Fermi liquid, the spin gap, the superconductor and the strange metallic phases have been identified in a wide region of parameters. The model may serve as a toy system modelling non-perturbative properties of the Yang-Mills theory.

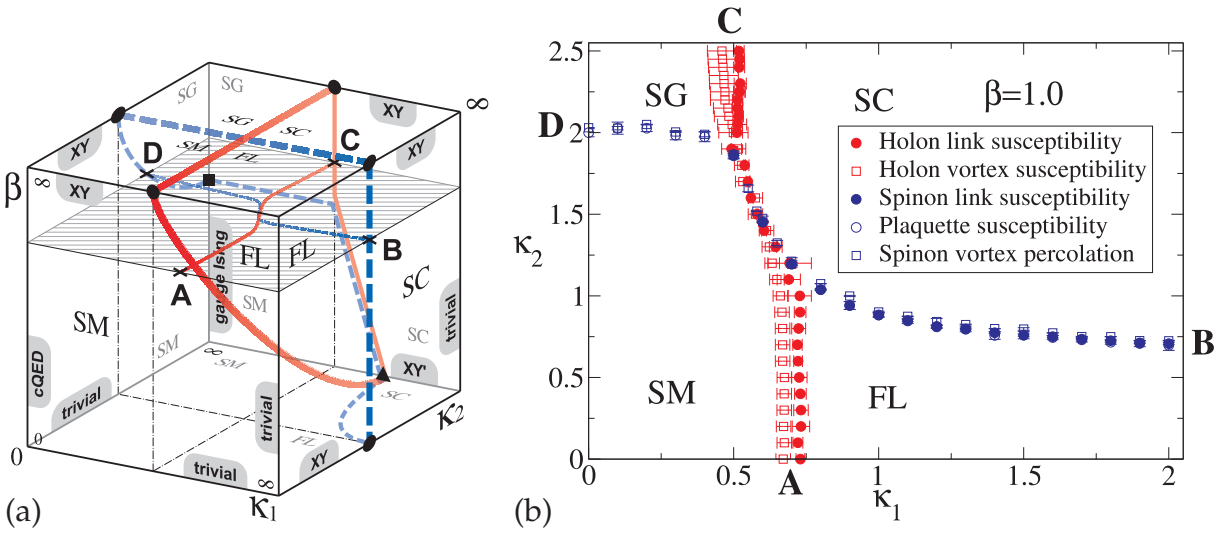

Figure 15.1: (**a**) The qualitative 3*D* phase diagram and (**b**) its numerically obtained 2*D* cross-section at $\beta = 1$.

The structure of the three-dimensional phase diagram of the model (15.1) is quite complicated. However, the faces and edges of the 3*D* phase "cube" (*i.e.* the limiting cases of vanishing or large couplings β and $\kappa_{1,2}$), respectively, can be related to various well-known and sometimes non-trivial systems. These limiting cases are shown schematically on the faces of the 3*D* phase cube, Fig. 15.1a.

The interior of the cube in Fig. 15.1a is our qualitative prediction of the phase structure of the cA2HM. The shaded (κ_1, κ_2) plane agrees with Fig. 15.1b, which represents the result of our numerical investigation for $\beta = 1.0$.

The project is supported by grants RFBR 01-02-17456, DFG 436 RUS 113/73910, RFBR-DFG 03-02-04016, JSPS S04045 and MK-4019.2004.2 and by DFG through the DFG-Forschergruppe "Lattice Hadron Phenomenology" (FOR 465).

[1] M.N. Chernodub et al.: PoS LAT2005, 295 (2005), arXiv:hep-lat/0509088
[2] M.N. Chernodub et al: Phys. Rev. B **73**, 100 506 (2006), arXiv:cond-mat/0512111

15.4 Lattice Perturbation Theory and Renormalisation

H. Perlt, A. Schiller

To obtain continuum results from lattice calculations of hadron matrix elements (three-point correlation functions), the underlying operators have to be renormalised. A perturbative calculation of the corresponding renormalisation constants is always the first step. Parton distributions of the nucleon describe the longitudinal momentum distribution of quarks and gluons. Generalised parton distributions contain information about the interplay of longitudinal momentum and transverse coordinate space, as well as spin and orbital angular momentum degrees of freedom.

During the last years our team in close collaboration with Zeuthen, Regensburg and other members of the QCDSF collaboration has computed lattice renormalisation

constants of local bilinear quark operators for overlap fermions and improved gauge actions. Among the actions we have considered are the Symanzik, Lüscher-Weisz, Iwasaki and DBW2 gauge actions [1] by considering local bilinear quark operators. The calculation have been extended to one-link quark operators [2] and to stout smeared SU(3) links in the fermionic action [3].

Within the framework of lattice QCD we have calculated the non-forward quark matrix elements of operators with two covariant derivatives needed for the renormalisation of the second moment of generalised parton distributions using Wilson fermions [4]. For some representations of the hypercubic group [5] commonly used in simulations we have determined the sets of all possible mixing operators. For those representations the one-loop mixing matrices of renormalisation factors are found. Due to non-vanishing contributions of operators with external ordinary derivatives the number of contributing operators increases compared to forward matrix elements. Recently we extended those calculations to clover fermions [6]. For the first moment we could take over our results [7]. For Wilson and clover fermions mixings with lower dimensional operators appear which have to be subtracted non-perturbatively.

This work is supported by the European Community's Human Potential Program under contract HPRN-CT-2000-00145 Hadrons/Lattice QCD and by DFG under contract FOR 465 (Forschergruppe Gitter-Hadronen-Phänomenologie).

[1] R. Horsley et al: Nucl. Phys. B **693**, 3 (2004) [Erratum-ibid. **713**, 601 (2005)], arXiv:hep-lat/0404007
[2] R. Horsley et al.: Phys. Lett. B **628**, 66 (2005), arXiv:hep-lat/0505015
[3] R. Horsley et al.: PoS LAT2005, 238 (2005), arXiv:hep-lat/0509072
[4] M. Göckeler et al.: Nucl. Phys. B **717**, 304 (2005), arXiv:hep-lat/0410009
[5] M. Göckeler et al.: Phys. Rev. D **54**, 5705 (1996), arXiv:hep-lat/9602029
[6] M. Göckeler et al.: PoS LAT2005, 238 (2005), arXiv:hep-lat/0509072
[7] S. Capitani et al.: Nucl. Phys. B **593**, 183 (2001), arXiv:hep-lat/0007004

15.5 High-Energy Asymptotics and Integrable Quantum Systems

R. Kirschner

The aim of this project is to develop methods for treating the Regge and Bjorken limits in gauge theories like QCD. We rely on the idea of the high-energy effective action [1] which we have shown in recent years to be a useful tool for analyzing the asymptotics of scattering amplitudes. In the Regge case the action describes the scattering by the exchange of reggeized quarks and gluons. The reggeon and parton interactions exhibit remarkable symmetry properties and can be related to integrable quantum systems.

In 2005 we have studied a factorization property of the Yang-Baxter R-opertor in the case of q-deformed $sl(2)$ symmetry and constructed the Baxter's Q-operator for generic representations [2].

The result simplifies the solution of general spin chain dynamics by the method of separation of variables.

Further we have analyzed the conformal symmetry of the interaction of fermionic and gluonic reggeons of perturbative Quantum chromodynamics [3]. The leading interaction has been represented in terms of integral kernels directly related to conformal 4-point functions.

[1] L.N. Lipatov: Nucl. Phys. B **365**, 614 (1991); R. Kirschner et al.: Nucl. Phys. B **452**, 579 (1994); Phys. Rev. D **51**, 838 (1995); L.N. Lipatov: Nucl. Phys. B **452**, 369 (1995); R. Kirschner, L. Szymanowski: Phys. Rev. D **52**, 2333 (1995); Phys. Lett. B **419**, 348 (1998); Phys. Rev. D **58**, 014 004 (1998)
[2] R. Kirschner: Eur. Phys. J. C **41**, 353 (2005), arXiv:hep-ph/0502202
[3] S. Derkachov et al.: Nucl. Phys. B **738**, 368 (2006), arXiv:hep-th/0511024

15.6 Organizational Duties

K. Sibold

- Vice dean of the faculty (until October)
- Director of the ITP (until October)
- Member of the "Forschungskommission" of the university (until October)
- Member of the "Gerätekommission" of the university (until October)
- Member of the board of the International Max-Planck Research School "Mathematics in the Sciences"
- Associated member of the Graduiertenkolleg "Analysis, Geometrie und die Naturwissenschaften"
- Coorganizer of the "Mitteldeutsche Physik-Combo" (joint graduate lecture courses with universities Jena and Halle)
- Member of the "Beirat" of the Fachverband "Mathematische und Theoretische Grundlagen der Physik" (German Physical Society)

A. Schiller

- Referee: Phys. Rev. D

R. Kirschner

- Referee: Eur. Phys. J. A, Eur. Phys. J. C, Phys. Rev. D
- Member of the graduation commission of the faculty

15.7 External Cooperations

Academic

- ITEP, Moscow, Russia
  M.N. Chernodub
- Humboldt Universität Berlin
  E.-M. Ilgenfritz
- Universität Regensburg
  M. Göckeler, A. Schäfer

- Edinburgh University, UK
  R. Horsley
- Dept. Math., Liverpool University, UK
  P.E.L. Rakow
- NIC, Zeuthen & DESY Hamburg
  G. Schierholz
- Nuclear Physics Institute, St. Petersburg, Russia
  Prof. L.N. Lipatov
- St. Petersburg branch of Steklov Mathematical Institute, Russia
  Dr. S.E. Derkachov
- Theory Department, Yerevan Physics Institute, Armenia
  Prof. A. Sedrakyan
- Soltan Institut of Nucl. Studies, Warsaw, Poland & University Liege, Belgium
  Dr. L. Szymanowski
- Sobolev Institut of Mathematics, Novosibirsk, Russia
  Dr. D.Y. Ivanov
- Institut für Theoretische Physik, Universität Hamburg / DESY
  Prof. J. Bartels
- Institut für Theoretische Physik, Universität Regensburg
  Prof. A. Schäfer, Prof. V. Braun
- Ecole Polytechnique, Paris-Palaiseau, France
  Prof. B. Pire

15.8 Publications

Journals

P. Heslop, K. Sibold: *Quantized equations of motion in non-commutative theories*, Eur. Phys. J. C **41**, 545 (2005)

M.N. Chernodub, R. Feldmann, E.-M. Ilgenfritz, A. Schiller: *Monopole chains in a compact Abelian model with Q=2 Higgs field*, Phys. Lett. B **605**, 161 (2005), arXiv:hep-lat/0406015

M. Göckeler, R. Horsley, H. Perlt, P.E.L. Rakow, A. Schäfer, G. Schierholz, A. Schiller: *Perturbative renormalisation of the second moment of generalised parton distributions*, Nucl. Phys. B **717**, 304 (2005), arXiv:hep-lat/0410009

M.N. Chernodub, R. Feldmann, E.-M. Ilgenfritz, A. Schiller: *The compact Q = 2 Abelian Higgs model in the London limit: Vortex-monopole chains and the photon propagator*, Phys. Rev. D **71**, 074 502 (2005), arXiv:hep-lat/0502009

S. Wenzel, E. Bittner, W. Janke, A.M.J. Schakel, A. Schiller: *Kertesz Line in the Three-Dimensional Compact U(1) Lattice Higgs Model*, Phys. Rev. Lett. **95**, 051 601 (2005), arXiv:cond-mat/0503599

R. Horsley, H. Perlt, P.E.L. Rakow, G. Schierholz, A. Schiller: *Renormalisation of one-link quark operators for overlap fermions with Lüscher-Weisz gauge action*, Phys. Lett. B **628**, 66 (2005), arXiv:hep-lat/0505015

A. Sternbeck, E.-M. Ilgenfritz, M. Müller-Preussker, A. Schiller: *Towards the infrared limit in SU(3) Landau gauge lattice gluodynamics*, Phys. Rev. D **72**, 014 507 (2005), arXiv:hep-lat/0506007

S. Derkachov, D. Karakhanyan, R. Kirschner: *Baxter Q-operators of the XXZ chain and R-matrix factorization*, Nucl. Phys. B **738**, 368 (2006), arXiv:hep-th/0511024

R. Kirschner: *Symmetric reggeon interaction in perturbative QCD*, Eur. Phys. J. C **41**, 353 (2005), arXiv:hep-ph/0502202

Talks

M. Göckeler, R. Horsley, H. Perlt, P.E.L. Rakow, A. Schäfer, G. Schierholz, A. Schiller: *One-loop renormalisation for the second moment of GPDs with Wilson fermions*, Nucl. Phys. Proc. Suppl. **140**, 722 (2005), arXiv:hep-lat/0409025

A. Sternbeck, E.-M. Ilgenfritz, M. Müller-Preussker, A. Schiller: *The gluon and ghost propagator and the influence of Gribov copies*, Nucl. Phys. Proc. Suppl. **140**, 653 (2005), arXiv:hep-lat/0409125

M. Gürtler, R. Horsley, V. Linke, H. Perlt, P.E.L. Rakow, G. Schierholz, A. Schiller, T. Streuer: *A lattice determination of g_A and $\langle x \rangle$ from overlap fermions*, Nucl. Phys. Proc. Suppl. **140**, 707 (2005), arXiv:hep-lat/0409164

A. Sternbeck, E.-M. Ilgenfritz, M. Müller-Preussker, A. Schiller: *The influence of Gribov copies on the gluon and ghost propagator*, AIP Conf. Proc. **756**, (2005) 284, arXiv:hep-lat/0412011

R. Horsley, H. Perlt, P.E.L. Rakow, G. Schierholz, A. Schiller: *Perturbative renormalisation of quark bilinear operators for overlap fermions with and without stout links and improved gauge action*, PoS LAT2005, 238 (2005), arXiv:hep-lat/0509072

A. Sternbeck, E.-M. Ilgenfritz, M. Müller-Preussker, A. Schiller: *Studying the infrared region in Landau gauge QCD*, PoS LAT2005, 333 (2005), arXiv:hep-lat/0509090

S. Wenzel, E. Bittner, W. Janke, A.M.J. Schakel, A. Schiller: *Vortex proliferation and the dual superconductor scenario for confinement: The 3D compact U(1) lattice Higgs model*, PoS LAT2005, 248 (2005), arXiv:hep-lat/0510099

R. Kirschner: *Hard diffractive production of vector mesons*, AIP Conf. Proc. **775**, 120 (2005)

Posters

M.N. Chernodub, A. Schiller, E.-M. Ilgenfritz: *An Abelian two-Higgs model and high temperature superconductivity*, PoS LAT2005, 295 (2005), arXiv:hep-lat/0509088

Author Index

E

F

G

H

I

J

K

L

M

N

O

P

Q

R

S

T

U

V

W

X

Y

Z

Marius Grundmann

The Physics of Semiconductors

An Introduction Including Devices and Nanophysics

Springer

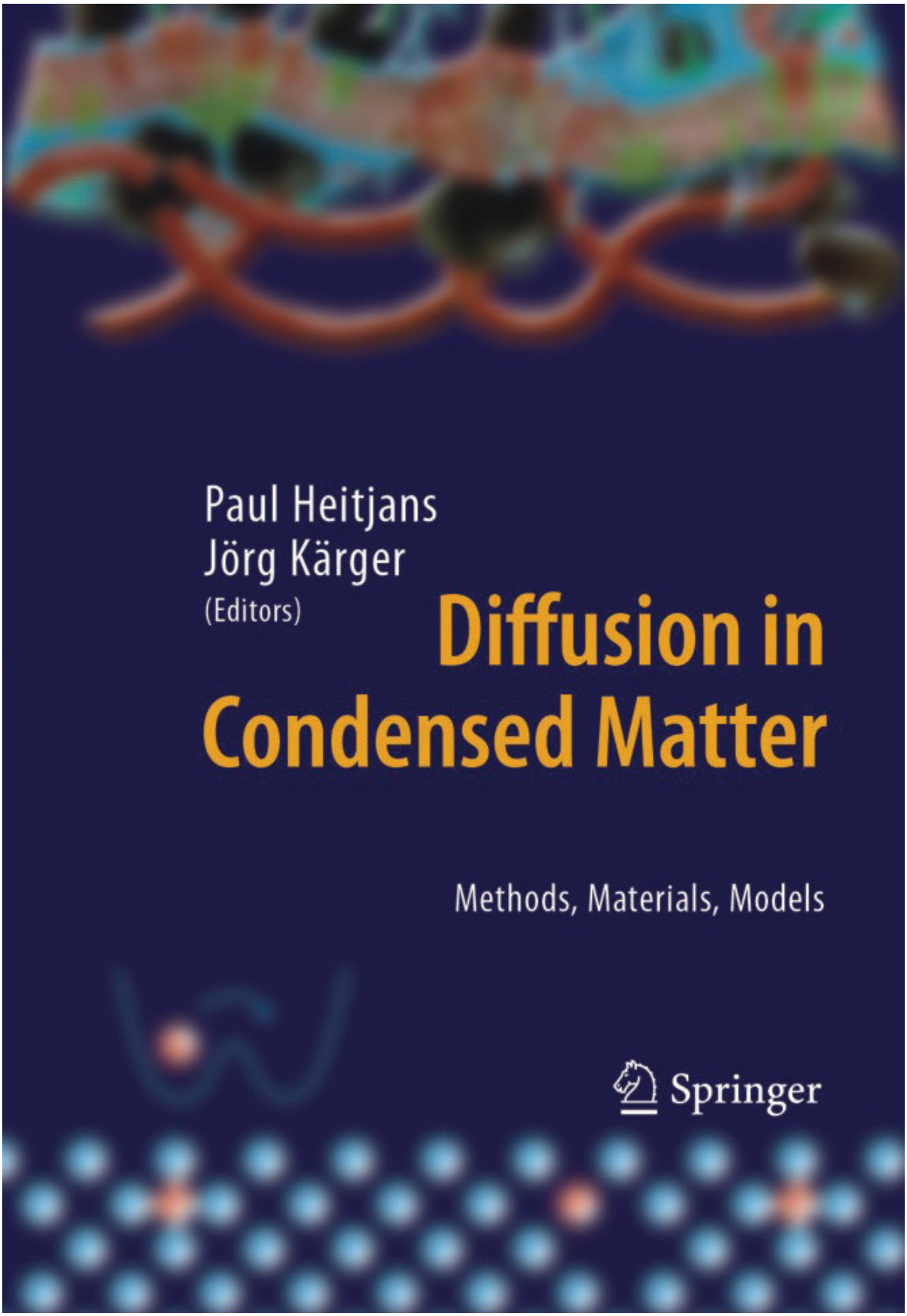

ISBN 3-934178-64-2